University of Nottingham
UK | CHINA | MALAYSIA

Deubiquitination of ELK-1 by USP17 regulates its transcriptional potency and cell proliferation

Charles Bryan Ducker, B.Sc. (Hons)

Thesis submitted to the University of Nottingham for the degree of Doctor of Philosophy

September 2017

BBSRC Doctoral Training Partnerships

Table of Contents

Abstract

The transcription factor ELK-1 is associated with numerous cellular processes, notably in cell proliferation and lineage determination. ELK-1 forms a ternary complex with a dimer of Serum Response Factor at Serum Response Elements associated with immediate-early genes, such as *CFOS.* Following mitogen-stimulated activation of the ERK cascade, ELK-1 is phosphorylated to mediate transcriptional activation of its target genes.

Further to phosphorylation, ELK-1 is covalently modified post-translationally with both monoubiquitin and polyubiquitin chains. This study sought to understand the functional significance and regulation of ELK-1 ubiquitination. Sites of ubiquitination of ELK-1 ectopically expressed in HEK293T cells were mapped and screened for the signature diglycine motif associated with ubiquitinated tryptic peptides using liquid chromatography - tandem mass spectrometry (LC-MS/MS). This revealed that lysine residues within the amino-terminal DNA-binding domain of ELK-1 are monoubiquitinated, including those involved in DNA binding.

Ubiquitination is reversed through the action of deubiquitinating enzymes (DUBs), which are target specific, allowing dynamic control over the protein modification state. USP17, one of several candidate DUBs, was shown to deubiquitinate ELK-1 when ectopically expressed in HEK293T cells. This was

reversed when USP17 expression was knocked down, which also downregulated transcription of ELK-1 responsive genes *CFOS* and *EGR1*. Furthermore, USP17 knock-down in HEK293T cells reduced cell proliferation, an effect that was partially rescued by expression of a hypo-ubiquitinated ELK-1 mutant. Taken together, these results reveal monoubiquitination to be a key regulator of ELK-1 transcriptional potency and mitogen-driven proliferation.

Acknowledgements

Where to begin? First and foremost, I would like to thank my supervisors Professor Robert Layfield and Professor Peter Shaw for encouragement, guidance and support (and countless cups of coffee) throughout my studies, and for constructive feedback and comments on this thesis. I would also like to thank all members from the Layfield and Shaw labs, including Dr. Daniel Scott, Barry Shaw, Lizzie Radley, Dr. Varun Gopala, Emma Burton, Julius Dongdem, Dr. Alice Goode, Dr. Thomas Strahl, Michela Grillo, Sara Quintero Barceinas and Janice Saxton, for helping me along the way. Additionally, people from adjacent labs including Dr. Alex Rathbone, Raquel Mesquita, Clare Martin, Matt Young and Dr. James Cavey added to a great working atmosphere.

Thank you to all my family and friends for supporting me, including everyone from the DTP for providing plenty of laughs and good times throughout. Of those, I also want to thank all members of "The Globe" past and present, and particularly, the continuous tea-making of Tom Wilding-Steele during write-up was most appreciated (and necessary). I would like to extend my gratitude to the Biotechnology and Biological Sciences Research Council for their financial support, without which this work would not has been possible. Lastly, I would like to thank my fellow DTP student and (in)significant other, Harriet Day, for always being there for me, come rain or shine. To quote a famous (fictional) scientist, "Life, uh, finds a way…"

Abbreviations

AMP - Adenosine monophosphate

ANOVA - Analysis of variance

AP-1 - Activator protein 1

APC/C - Anaphase promoting complex/cyclosome

AR - Androgen Receptor

ATG8 - Autophagy-related protein 8

ATP - Adenosine triphosphate

BCA - Bicinchoninic assay

BRcat - Benign-catalytic

BSA - Bovine serum albumin

CBP - CREB binding protein

CD - Cryptic degron

CDC - Cell division cycle

CDK - Cyclin-dependent kinase

cDNA - Complementary DNA

ChIP - Chromatin immunoprecipitation

CHIP - Carboxyl terminus of the Hsc70-interacting protein

Co^{2+}-CMA - Cobalt-carboxylmethylaspartate

Co-IP - Co-Immunoprecipitation

CT - Cycle threshold

DI - Dimerisation interface

DMEM - Dulbecco's Modified Eagle's Medium

DMSO - Dimethyl sulphoxide

DNA - Deoxyribonucleic acid

DNAP - DNA polymerase

dNTPs - Deoxyribonucleotide triphosphates

DTT - Dithiothreitol

DUB- Deubiquitinating enzyme

ECL - Enhanced chemiluminesence

EDTA - Ethylenediaminetetraacetic acid

EGF - Epidermal growth factor

EGFR - Epidermal growth factor receptor

EGR - Early growth response protein

EMT - Epithelial-mesenchymal transition

ERK - Extracellular signal-regulated kinase

ER - Endoplasmic reticulum

ERG - ETS-related gene

ETS - E-twenty-six (E26)

ETV1 - ETS translocation variant 1

FAM - Fat facets in mouse

FBP - F-Box protein

FBS - Foetal bovine serum

FGF - Fibroblast Growth Factor

GABARAP - Gamma-aminobutyric acid receptor-associated protein

GAPDH - Glyceraldehyde 3-phosphate dehydrogenase

GABPA - GA-binding protein alpha chain

GDP - Guanosine diphosphate

GTF - General transcription factor

GTP - Guanosine triphosphate

GRB2 - Growth factor receptor-bound protein 2

HA - Hemagglutinin

HABM - Hyaluronan binding motif

HAND1 - Heart and neural crest derivatives expressed 1

HAS - Hyaluronan synthase

HAT - Histone acetyltransferase

HAUSP - Herpesvirus-associated ubiquitin-specific protease

HBS - HEPES-buffered saline

HDAC - Histone deacetylase

hESC - Human embryonic stem cells

HECT - Homologous to the E6-AP carboxyl-terminus

HNF4 - Hepatocyte nuclear factor 4

IEG - Immediate early gene

IER2 - Immediate early response gene 2

IL - Interleukin

IMAC - Immobilized metal affinity chromatography

IRF1 - Interferon regulatory factor 1

ISG15 - Interferon-stimulated gene 15

JAMM - JAB1/MPN/MOV34 metalloenzyme

KSR - Kinase suppressor of RAS

LC - Liquid chromatography

LC3 - Microtubule-associated protein 1A/1B-light chain 3

LTQ - Linear trap quadrupole

MADS - MCM1, AG, DEFA, and SRF

MAPK - Mitogen-activated protein kinase

MCC - Mitotic checkpoint complex

MCL-1 - Induced myeloid leukaemia cell differentiation protein 1

MCPIP - Monocyte chemotactic protein-induced protein

MDM2 - Mouse double minute 2

MEF - mouse embryonic fibroblast

MEK - MAPK/ERK Kinase

mESC - Mouse embryonic stem cell

MINDY - Motif interacting with ubiquitin-containing novel DUB family

miR - microRNA precursor

MMP - Matrix metalloproteinases

mRNA - messenger RNA

MRTF - Myocardin-related transcription factor

MS/MS - Tandem mass spectrometry

mTORC - Mammalian target of rapamycin complex 1

MTT - 3-(4,5-Dimethylthiazol-2-yl)-2,5-diphenyltetrazolium bromide

N-CoR - Nuclear receptor co-repressor

NF-κB - Nuclear factor kappa-light-chain-enhancer of activated B cells

Ni^{2+}-NTA - Nickel-nitrilotriacetic acid

NRTC - No reverse transcriptase control

NSCLC - Non-small cell lung cancer

NTC - No template control

MW - Molecular weight

OD - Optical density

OPTN - Optineurin

ORF - Open reading frame

OTU - Ovarian tumour protease

PAGE - Polyacrylamide gel electrophoresis

PAI - Plasminogen activator inhibitor

PARP - Poly (ADP-ribose) polymerase

PAX - Paired box

PBS - Phosphate buffered saline

PCNA - Proliferating cell nuclear antigen

PCR - Polymerase chain reaction

PIAS - Protein inhibitor of activated STAT

PIC - Preinitiation complex

PINK1 - PTEN-induced putative kinase 1

PKC - Protein kinase C

PRC - Polycomb repressive complex

P-TEFb - Positive transcription elongation factor b

qRT-PCR - Quantitative real-time polymerase chain reaction

RAF - Rapidly accelerated fibrosarcoma

RAPTOR - Regulatory-associated protein of mTOR

RBR - RING1-BRcat-Rcat

Rcat - Required-for catalysis

RCE - Ras-converting enzyme

RING - Really interesting new gene

RIP - Receptor-interacting serine/threonine-protein kinase

RIPA - Radioimmunoprecipitation assay

RNA - Ribonucleic acid

RNAP - RNA polymerase

ROC1 - RING-box protein 1

SAGA - SPT-ADA-GCN5

SAP1 - SRF accessory protein 1

SAPK - Stress-activated protein kinase

SCF - SKP1/CUL1/FBP

SDS - Sodium dodecyl sulphate

SEM - Standard error of the mean

shRNA - short hairpin RNA

SIRT - Silent mating type information regulation 2

SKP1 - S phase kinase-associated protein 1

SOS - Son of sevenless

SQSTM1 - Sequestosome-1

SRE - Serum Response Element

SRF - Serum Response Factor

STAT - Signal transducer and activator of transcription

SUMO - Small ubiquitin-like modifier

TAD - Transactivation domain

TAE - Tris-acetate EDTA

TBK1 - TANK binding kinase 1

TBS - Tris-buffered saline

TCF - Ternary complex factor

TFA - Trifluoroacetic acid

TGF - Transforming growth factor

TLS - Translesion synthesis

TPA - 12-O-tetradecanoylphorbol-13-acetate

TRAF - TNF-receptor-associated factor

UAS - Upstream activating sequence

UBA - Ubiquitin-associated domain

UBD - Ubiquitin-binding domain

UBP- Ubiquitin binding protein

UBQ - Ubiquitin

UBM - Ubiquitin-binding motif

UBZ - Ubiquitin-binding ZnF

UCH - Ubiquitin carboxyl-terminal hydrolase

uPA - Urokinase-type plasminogen activator

UPS - Ubiquitin-proteasome system

USP - Ubiquitin-specific protease

WT - Wild type

ZnF - Zinc finger

1 Introduction

1.1 ELK-1

1.1.1 Overview and historical perspective

Cell growth, proliferation and differentiation are complex, concerted processes that rely on carefully controlled regulation of gene expression. Control over gene expression is maintained through signalling pathways that respond to external cellular stimuli, such as mitogens, prompting expression profiles commensurate for diverse cellular outcomes, such as cell division. Downstream effectors of these signalling pathways are transcription factors; a generic term used to describe a broad range of proteins that act to alter gene expression patterns by either activating or repressing specific target genes. This is achieved through recognition of DNA and protein binding motifs, varying between transcription factor families, which can recruit other proteins to aid transcriptional repression or activation (known as co-repressors and co-activators respectively) (Lemon & Tjian, 2000).

ELK-1 is an E-twenty-six (E26 - ETS) domain family member transcription factor, named for the conserved DNA-binding ETS domain that it shares with the first discovered member of the family, ETS-1 (de Taisne et al., 1984; Watson et al., 1985; Karim et al., 1990). ETS genes were originally discovered through the *v-ets* oncogene within the leukaemia-causing avian retrovirus E26, which was

found to have been transduced from homologous genes in the chicken genome (*c-ets-1* and *c-ets-2*) to encode part of a hybrid viral protein (Nunn et al., 1983; Leprince et al., 1983; Ghysdael et al., 1986; Boulukos et al., 1988). This led to the discovery of human ETS genes (*ETS-1*, *ETS-2*, and later *ERG*) and the proteins encoded by these genes (de Taisne et al., 1984; Watson et al., 1985; Reddy et al., 1987; Rao et al., 1987; Watson et al., 1988). ELK-1 is the founding member of the ternary complex factor (TCF) subfamily of ETS transcription factors, comprising two additional members, ELK-3 (Net) (Giovane et al., 1994) and ELK-4 (SAP1) (Dalton & Treisman, 1992). The name derives from the ternary complex that TCFs form with a dimer of Serum Response Factor (SRF) at the Serum Response Element (SRE) in target genes. ELK-1 was discovered in complex with SRF at the proto-oncogene *CFOS* SRE, and was originally named p62 due to an apparent molecular weight of 62 kDa (Shaw et al., 1989). It later transpired that this protein was identical to the gene product of *ELK-1*, which had also been isolated on the basis of its homology to the oncogene *v-ets* (Rao et al., 1989; Hipskind et al., 1991).

ELK-1 activity is stimulated through phosphorylation by the Mitogen-Activated Protein Kinase (MAPK)/ Extracellular signal-Regulated Kinase (ERK) cascade following mitogen stimulation, which potentiates ELK-1 DNA binding and transactivation (Gille et al., 1992; Janknecht et al., 1993; Marais et al., 1993; Gille et al., 1995). The canonical target gene for ELK-1 mediated transcription is the immediate early gene (IEG) *CFOS*, which is rapidly-induced following ERK

stimulation by growth factors (Greenberg & Ziff, 1984; Müller et al., 1984; Gille et al., 1992). ELK-1 can form dimers, which may contribute to protein stability in the cytoplasm, but nuclear ELK-1 appears to undergo DNA interactions as a monomer (Drewett et al., 2000; Evans et al., 2011).

1.1.2 Functional domain organisation

ELK-1 has several functional domains that, running from amino- to carboxyl-terminus, are named the ETS (A), B, R, D, C and F(XFP) domains. These are involved in DNA-binding (ETS), SRF interaction (B), SUMOylation and transcriptional repression (R), MAPK/ERK docking (D/F) and phosphorylation and transcriptional activation (C). These are outlined in Figure 1-1. ELK-1 also contains a nuclear export signal (NES) and two nuclear localisation signals (NLS) that can promote ELK-1 nuclear export or import respectively.

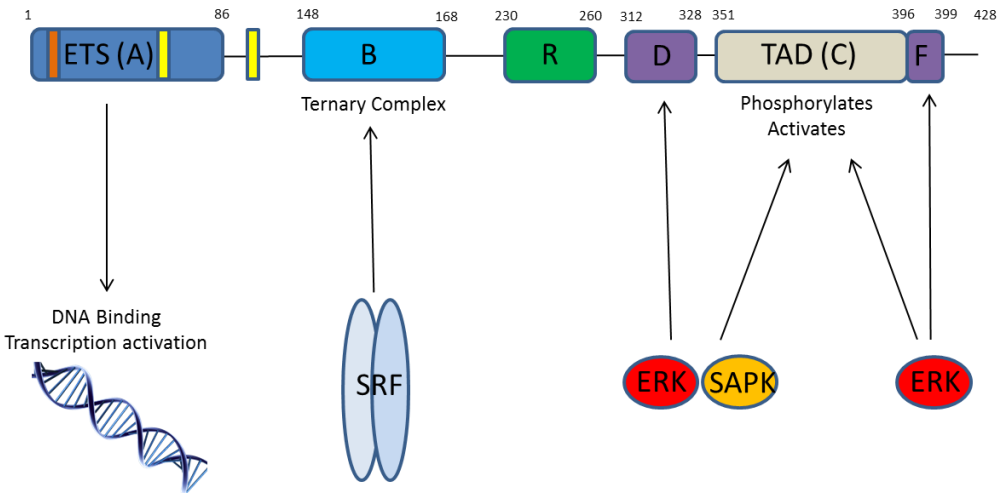

Figure 1-1: Schematic of ELK-1 with functional domains labelled. ETS (A) - DNA-binding, B - SRF binding, R - SUMOylation and repression, D/F - MAP kinase docking, C - Phosphorylation and transactivation. Highlighted in orange in the ETS domain is the NES and in yellow are the NLS sequences.

1.1.3 DNA binding – The ETS (A) domain

The ETS, or A domain, as previously mentioned, is the region of ELK-1 that contacts DNA and is highly conserved across ETS transcription factors. It binds to purine-rich DNA sequences with a GGA core sequence (Karim et al., 1990; Fisher et al., 1991). A particularly high affinity site for ETS-domain binding (including that of ELK-1) is the E74 site (5'-ACCGGAAGT-3'), first characterised as a target for the ETS domain protein E74 in *Drosophila* (Urness & Thummel, 1990). Structural studies on the ELK-1 ETS domain bound to the E74 DNA site showed that the ETS domain adopts a winged helix-turn-helix conformation

(Mo et al., 2000). ETS domains contain three α-helices and four β-sheets, running in the order α1-β1-β2-α2-α3-β3-β4, where α3 is the DNA-binding helix (Figure 1-2).

When compared with the closely related ELK-4 (for which an E74-bound ETS-domain structure is also available), both complexes are very similar, perhaps unsurprising given that the ELK-1 and ELK-4 ETS domains are 80% identical (Mo et al., 1998; Mo et al., 2000). However, despite 100% conservation in the α3 helix, there is significant variation in amino acids distal to the DNA-contacting residues. Particularly, a conserved tyrosine residue in the α3 helix that is oriented towards the DNA major groove in ELK-4 (Y65) is directed away from the central GGA DNA motif in ELK-1 (Y66), leading to around a third of α3-E74 DNA interactions differing between the two transcription factors (Mo et al., 2000). A notable difference between the ELK-1 and ELK-4 ETS domains in their affinity for DNA is that ELK-4 exhibits more relaxed binding, permitted by two amino acid differences (ELK-1/ELK-4 - D38/Q37 and D69/V68), allowing more promiscuity in DNA-binding target selection (Shore & Sharrocks, 1995; Shore et al., 1996). As a more permissive DNA-interactor, the ELK-4 ETS domain is capable of binding the relatively poor *CFOS* SRE ETS-binding site directly (Masutani et al., 1997), whereas ELK-1 is incapable of binding in the absence of SRF (Shaw et al., 1989). The ETS domain is also implicated in mediating transcriptional repression, recruiting the histone deacetylase (HDAC)-mSIN3A corepressor complex to target promoters, which is temporally delayed post-

ERK activation. This limits transcriptional output and reverts target genes such as *CFOS* to an inactive state, preventing sustained gene activation following mitogen stimulation (S. Yang et al., 2001).

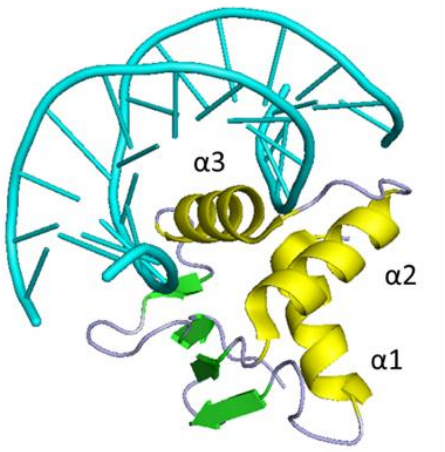

MDPSVTLWQFLLQLLREQGNGHIISWTSRDGGEFKLVDAEEVARLWG

LRKNKTNMNYDKLSRALRYYYDKNIIRKVSGQKFVYKFVSYPEVAGC

Figure 1-2: Cartoon representation of ETS domain of ELK-1 (human) bound to E74 high affinity DNA site (residues 5-90), Primary sequence of the ETS domain is shown below and α-helices and β-sheets highlighted. Structure taken from (Mo et al., 2000) – PDB 1DUX – re-rendered with PyMOL..

1.1.4 SRF interaction

SRF is the founding member of the MADS domain-containing transcription factor family, named for the first discovered members (MCM1, AG, DEFA, and SRF) which share this conserved DNA-binding domain (Norman et al., 1988; Schwarz-Sommer et al., 1990). The MADS box binds the target DNA sequence CC(A/T_6)GG known as a CArG box, to which SRF binds as a homodimer (Minty & Kedes, 1986; Norman et al., 1988). CArG boxes are present downstream of ETS binding sites at SREs (Shaw, 1992). ELK-1 interaction with SRF occurs *via* the B-box domain, allowing protein-protein interactions that complement ETS domain DNA-binding at the SRE (Figure 1-3). The B-box was discovered through deletion of sections in ELK-1 and assaying for the ability to form a ternary complex, which revealed that amino acids 137-169 were indispensable for this (Janknecht & Nordheim, 1992).

ELK-1 and SRF can interact in the absence of DNA-binding, where the ELK-1 B-domain and the carboxyl-terminal half of the minimal SRF DNA-binding domain (termed the core^{SRF}) are necessary for this interaction with or without the SRE (Mueller & Nordheim, 1991; Shore & Sharrocks, 1994). Alanine scanning in ELK-1 identified five residues that were key to this interaction (Y153, S156, Y159, F162 and I164), which were initially thought to form an α-helical hydrophobic region that binds a surface-exposed hydrophobic patch in SRF (Ling et al., 1997; Ling et al., 1998). Although no structure currently exists for the ELK-1-SRF

interaction, there is a structure available for ELK-4 (ETS+B domains) bound to core^{SRF} dimer at the SRE. This revealed that the B-domain adopts an atypical 3^{10}-helix/β-strand/3^{10}-helix conformation (two partial α-helices flanking a β-sheet) (Hassler & Richmond, 2001) rather than the α-helix that was previously predicted (Ling et al., 1997). The ETS domain and the B-domain were shown to be connected by an unstructured flexible linker (Hassler & Richmond, 2001), consistent with the observation that the spacing between the ETS binding site and CArG box in the SRE did not affect ternary complex formation, nor did the length of the flexible linker (Treisman et al., 1992).

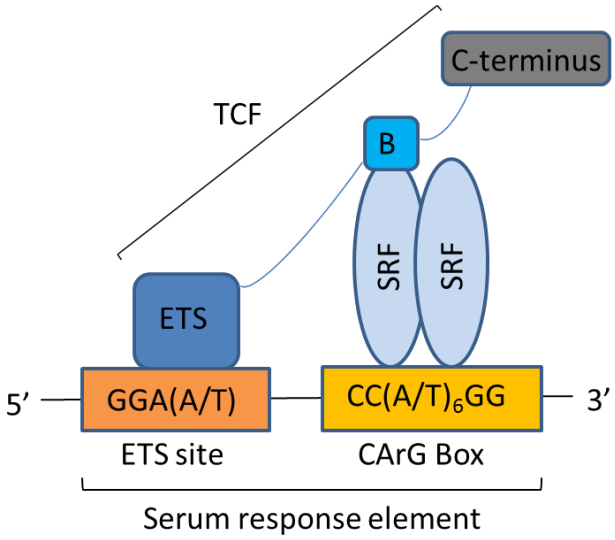

Figure 1-3: Schematic representation of a TCF bound to the SRE as part of a ternary complex. The ETS domain is shown bound to an ETS site, with B-domain forming contacts with a dimer of SRF, bound to a CArG box.

1.1.5 Transactivation (C) domain

Transactivation domains (TADs) are regions of transcription factors that mediate transcriptional activation, often by acting as scaffolds for binding of transcriptional coregulators. STAT family transcription factors are an example of this, whose carboxyl-terminal TADs directly bind and recruit the histone acetyltransferase (HAT) p300 to target promoters (Bhattacharya et al., 1996; Paulson et al., 1999). TADs are modular in nature and do not generally mediate target specificity, as their fusion to DNA-binding domains of different transcription factors can still yield transcriptional activation at gene targets of the DNA-binding domain. This is the case for a chimera consisting of the DNA-binding domain from the yeast transcription factor Gal4 and the TAD of the herpes simplex virus transcription factor VP16 (Gal4-VP16), which activates target genes with promoters containing Gal4-consensus sites (UAS motifs) (Sadowski et al., 1988).

The ELK-1 TAD (C-domain), as with other TADs, is critical for its transcriptional activation (Marais et al., 1993; Janknecht et al., 1993). This is controlled *via* multiple MAP kinase phosphorylation sites in the carboxyl-terminal-localised TAD, generally acting to promote activity (S383/9), although some sites are also reported as temporal repressors (T337, T418 and S423) (1.1.7.1, 1.1.7.2) (Gille et al., 1992; Marais et al., 1993; Janknecht et al., 1993; Gille et al., 1995A; Mylona et al., 2016). The ELK-1 TAD was discovered following experiments

showing that upon stimulation with growth factors, the electrophoretic mobility of the ELK-1-SRF ternary complex was markedly reduced (*via* electrophoretic mobility shift assay), which was mediated by the ELK-1 carboxyl-terminus (Marais et al., 1993; Janknecht et al., 1993). This was thought to be due to a conformational change in ELK-1 elicited by phosphorylation in the ELK-1 carboxyl-terminus (Marais et al., 1993; Janknecht et al., 1993). Furthermore, when fused to the Gal4 DNA-binding domain, the ELK-1 carboxyl-terminus (amino acids 307-428) was sufficient to activate Gal4-target gene transcription by reporter assay in NIH3T3 cells in response to various growth factors. This was also phosphorylation-dependent (particularly S383), confirming this region of ELK-1 as a TAD (Marais et al., 1993; Janknecht et al., 1993). It was later clarified that amino acids 376-404 represent the minimal region of ELK-1 required for transactivation, while flanking regions of the TAD act to enhance this (Janknecht et al., 1994). Phosphorylation had also been shown to potentiate ELK-1 ternary complex formation at the SRE (Gille et al., 1992), and SRF-independent autonomous DNA binding (Sharrocks, 1995).

Subsequently, the mechanism behind these observations was realised when the hypothesized conformational change in ELK-1 following TAD phosphorylation was confirmed, which also involved cooperation of the B-box in a switch from inactive (closed) to active (open) ELK-1 states. In the unphosphorylated, closed conformation, both the B-domain and TAD inhibit DNA binding by making contacts with the ETS domain. Phosphorylation triggers

allostery in ELK-1, relieving and opening its structure, promoting DNA binding and ternary complex formation (S. Yang et al., 1999) (Figure 1-4). As with other TADs, the ELK-1 TAD can also act as an adaptor to directly interact with co-activators, such as p300, which can occur in the absence of phosphorylation (Li et al., 2003).

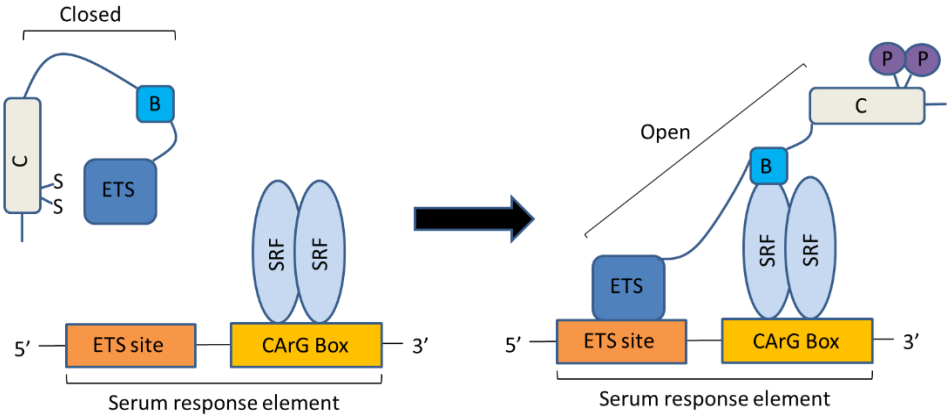

Figure 1-4: Schematic showing the effects of phosphorylation at S383/9 on ELK-1. In the unphosphorylated, closed form, ELK-1 is inhibited from DNA-binding and ternary complex formation through contacts made between the ETS domain, the TAD and the B-domain. Following phosphorylation by MAP kinases, the ELK-1 structure becomes more open, releasing the ETS domain to bind DNA and the B-domain to contact SRF at the CArG box in target genes, promoting transcriptional activation. Adapted with reference to (Sharrocks, 1995; S. Yang et al., 1999).

1.1.6 Functional cooperation with Mediator

The transmission of regulatory signals from DNA-bound transcription factors to RNA polymerase II (RNAPII), which prompts the recruitment of general transcription factors (GTFs) and assembly of the preinitiation complex (PIC) to gene promoters, is critical in promoting transcription. Mediator, a multiprotein complex, communicates these signals through a "molecular bridge", constituting diverse protein-protein interactions that relay signalling information between the Mediator, transcription factors and RNAPII (Allen & Taatjes, 2015). With regard to ELK-1, functional cooperation with Mediator subunit MED23 (Sur2) is required for transcriptional activation following ELK-1 phosphorylation. *Med23* knockout in mouse embryonic stem cells (mESCs) prevented a Gal4 DNA-binding domain-Elk-1 TAD fusion protein from driving transcription (in the presence of activated Mek), which could be rescued with addition of human MED23 (Stevens, 2002). Further exploration of this relationship found that the same phosphorylated Gal4-Elk-1 construct was only capable of recruiting GTFs and RnapII to immobilised DNA (containing Gal4-binding sites) and initiating transcription in the presence of Med23, which was not the case for a Gal4-VP16 fusion, ruling out Mediator inactivation *per se* (Cantin et al., 2003).

Another study using mESCs found that RNAPII recruitment to the Elk-1 target gene *Egr1* was roughly three-fold higher in serum-treated wild-type cells than

Med23 knockout cells, while histone acetylation at the *Egr1* promoter was unaffected. Despite this, the roughly ~13-fold greater induction of *Egr1* in wild-type against mutant cells could not be explained by this alone, leading the authors to conclude that the presence of Med23 at the *Egr1* promoter also positively regulated the rate of transcription initiation (W. Wang et al., 2005).

In the absence of serum stimulation, basal transcription levels of *Egr1* are maintained by the Med23-Elk-1 interaction not through recruitment of RnapII and GTFs, but through recruitment of the elongation factor P-tefb *via* Cdk9, prompting RnapII phosphorylation and entry into the elongation stage of transcription (W. Wang et al., 2013). ELK-1 also has functional associations with Mediator through the MED14 subunit, which is phosphorylated by ERK recruited by ELK-1 to target gene promoters. The importance of this relationship is suggested by the downregulation of *CFOS* and *EGR1* in HeLa cells following MED14 depletion, while leaving *MCL1* expression unaffected (which is not ELK-1-responsive in this cell line), although pleiotropic effects on Mediator function from MED14 knockdown may also have contributed to this effect (Galbraith et al., 2013).

1.1.7 Post-translational modifications

1.1.7.1 Phosphorylation driven transactivation

The ERK pathway is a signal transducing phosphorylation cascade pivotal in cellular processes including proliferation and differentiation, which is classically stimulated following the recognition of extracellular mitogenic growth factors and cytokines by transmembrane receptors (Wortzel & Seger, 2011). A paradigmatic example of this is the receptor tyrosine kinase epidermal growth factor receptor (EGFR), which auto-phosphorylates following recognition of members of the epidermal growth factor (EGF) family of protein ligands (Wells, 1999) (Figure 1-5). Growth signals are transmitted through the GRB2 adaptor and the GTP/GDP exchange factor SOS to the small GTPase RAS (H-RAS/K-RAS/N-RAS), which switches from an inactive GDP-bound state to an active GTP-bound state (Chardin et al., 1993; Margolis & Skolnik, 1994). Following this, RAS recruits RAF (A-RAF/B-RAF/C-RAF) to the cell membrane, which is activated in a multistage process involving dimerisation and phosphorylation (Wellbrock et al., 2004; Garnett et al., 2005). Successive phosphorylation events activate a MAP kinase cascade in the order RAF-MEK(1/2)-ERK(1/2), facilitated through scaffold proteins such as kinase suppressor of RAS (KSR) (Therrien et al., 1995; A. Nguyen et al., 2002; Wortzel & Seger, 2011). MEK1/2 are dual-specificity kinases that phosphorylate both threonine and tyrosine residues in their only known substrates, ERK1/2 (p44/p42 MAP kinase) (Roskoski, 2012). ERK1/2 then either form homodimers and phosphorylate

downstream cytoplasmic targets, or translocate to the nucleus and phosphorylate nuclear targets, such as ELK-1, which is thought to be dimerisation-independent (Gille et al., 1992; Khokhlatchev et al., 1998; Casar et al., 2008; Lidke et al., 2010).

Phosphorylation of ELK-1 within its TAD by ERK following mitogen stimulation potentiates ternary complex formation and transcriptional activation at the *CFOS* SRE (Gille et al., 1992; Janknecht et al., 1993; Marais et al., 1993; Gille et al., 1995A). This can also be mediated following cellular stress through alternative MAP kinase pathways culminating in ELK-1 phosphorylation by either SAPK (Gille, et al., 1995B; Cavigelli et al., 1995; Whitmarsh et al., 1995) or p38 kinases (Raingeaud et al., 1996). Phosphorylation can occur at multiple sites in the carboxyl-terminal TAD of ELK-1, although S383 and S389 are the most functionally important phosphate acceptors, as their mutation to alanine reduced ternary complex formation and abrogated transcription from the *CFOS* promoter region (Janknecht et al., 1993; Marais et al., 1993; Gille et al., 1995A). As previously mentioned, phosphorylation by MAP kinases has several effects on ELK-1, including increased DNA binding and ternary complex formation, whereby the ELK-1 ETS domain shifts from being closed and inaccessible to a more open structure (Gille et al., 1992; Sharrocks, 1995; S. Yang et al., 1999). It should be noted, however, that unphosphorylated ELK-1 is still capable of binding DNA, albeit less efficiently (Sharrocks, 1995).

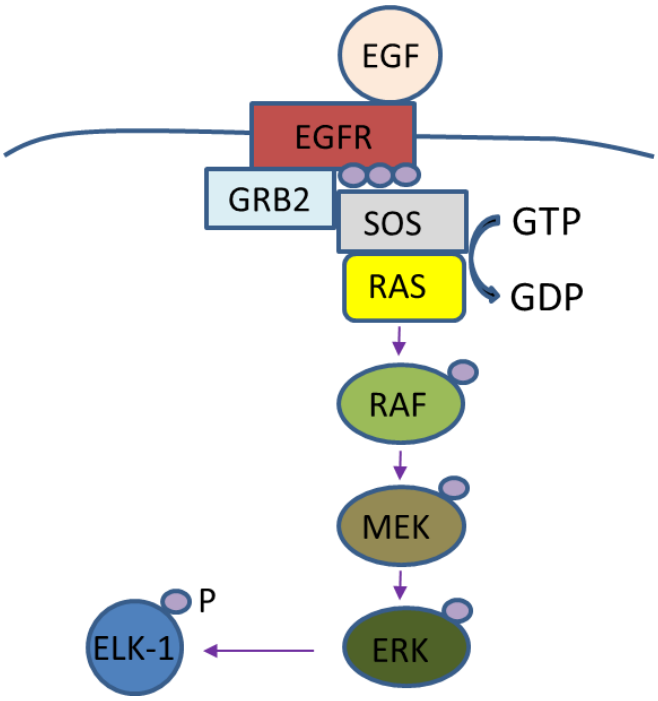

Figure 1-5: The ERK cascade in EGF signalling. EGF recognition by EGFR causes its autophosphorylation (purple circles) and recruitment of GRB2 and SOS. RAS is recruited to the plasma membrane, and is activated through GDP exchange for GTP mediated by SOS. RAF is subsequently recruited to the plasma membrane and is phosphorylated and activated, proceeding to phosphorylate and activate MEK. ERK is then phosphorylated and activated by MEK, and phosphorylates downstream targets such as ELK-1.

1.1.7.2 Influence of phosphorylation on co-activator and co-repressor recruitment

ELK-1 phosphorylation can also be repressive, as T337, T418 and S423 have been characterised as slowly modified sites (compared with fast sites S383/9 in the centre of the TAD) that negatively regulate ELK-1-driven transcription, proposed to provide a self-limiting feedback loop through ERK phosphorylation (Mylona et al., 2016). This work re-assessed earlier conclusions that TAD phosphorylation sites exhibit stoichiometrically similar modification kinetics following ERK cascade induction (Cruzalegui et al., 1999). Besides this, phosphorylation also influences the functional association of ELK-1 with transcriptional co-activators, such as the HATs CBP (Janknecht & Nordheim, 1996; Nissen et al., 2001) and p300 (Q. Li et al., 2003). For p300, ELK-1 phosphorylation is not required for recruitment to gene promoters *per se*, but rather allosteric changes enhance binding affinities (between both ELK-1 ETS-DNA and ELK-1 TAD-p300) and drive HAT activity, relieving transcriptional repression (Q. Li et al., 2003). Similarly, CBP (which instead binds ELK-1 through its amino-terminus) is thought to be constitutively bound to ELK-1 at the SRE, and phosphorylation of ELK-1 and CBP triggers conformational changes in CBP, prompting recruitment of the basal transcriptional machinery and initiating transcription (Nissen et al., 2001). As previously mentioned, ELK-1 phosphorylation also promotes functional cooperation with other co-activator proteins important in RNAPII recruitment and transcription initiation and

elongation, such as Mediator (Stevens, 2002; Galbraith et al., 2013). Conversely, it has been shown that ELK-1 phosphorylation can prompt the recruitment of co-repressors such as the mSIN3A HDAC 1/2 complex, possibly temporally delayed until after transcription initiation to self-limit gene expression (S. Yang et al., 2001).

Diverse changes in histone modification patterns driving transcriptional activation are dependent on ELK-1 phosphorylation, exemplified by the multitude of acetylation, methylation and phosphorylation events that are targeted to histones following activation of the ERK cascade. These have been shown to proceed in an ordered fashion in mouse embryonic fibroblasts (MEFs), whereby histone modifications orchestrated following Erk induction correlated positively with increased transcription from associated genes (Esnault et al., 2017). This progresses temporally, with histone H3 phosphorylation and acetylation preceding other modifications, culminating in an increase in in H3K4-trimethylation at transcribed sites (Esnault et al., 2017). At SRF-TCF target genes, all of these histone modifications require upstream TCF phosphorylation to proceed, and with the exception of H3 phosphorylation, all other modifications also require TCF-mediated recruitment of transcriptional machinery (Esnault et al., 2017).

1.1.7.3 MAP kinase docking sites

MAP kinase docking is mediated *via* the ELK-1 D-domain and FXFP motif. The D-domain resides at the amino-terminal side of the transactivation-domain, and is required for effective phosphorylation by both ERK (S. Yang et al., 1998A) and SAPK (S. Yang et al., 1998B). ERK can also be transiently recruited to target gene promoters by active ELK-1 primarily through the D-domain, from where it presumably phosphorylates other targets (H. Zhang et al., 2008). The FXFP motif (FQFP in ELK-1) specifically acts as a docking site for ERK, which is situated at the carboxyl-terminal side of the TAD, and is conserved among several ERK substrate proteins. It acts independently of the D-domain, although the two sites combine additively to increase the binding affinity of ELK-1 for ERK (Jacobs et al., 1999). Phosphorylation of the primary transactivation site S383 by ERK is mediated mostly through the FXFP motif (Fantz et al., 2001; H. Zhang et al., 2008).

The D-domain and FXFP are also both docking sites for Androgen Receptor (AR), which ELK-1 binds and recruits as a co-activator to target genes, a process which does not require ERK docking or TAD phosphorylation, and is probably restricted to prostate cancer cells (Patki et al., 2013; Rosati et al., 2016). This was shown to be independent of SRF which actually interfered with ELK-1 binding to AR (shown by two-hybrid assay in recombinant HeLa cells), suggesting that SRF depletion may free docked ELK-1 from IEGs for interaction

with AR, supported by evidence that AR is not involved in IEG regulation (Patki et al., 2013; Rosati et al., 2016). Additionally, the presence of ERK appeared to disrupt ELK-AR interaction, which, coupled with the convergence of ERK and AR binding sites in ELK-1, suggests that they may compete with each other for ELK-1-recruitment to transcriptional targets (Galbraith et al., 2013; Rosati et al., 2016).

1.1.7.4 SUMOylation

ELK-1 contains a repression domain (R) which acts to dampen basal transcriptional activation, and unlike the ETS, B, C and D domains, is not conserved in ELK-3 or ELK-4 (S. Yang et al., 2002). Repression is mediated through ELK-1 modification by small ubiquitin-like modifier (SUMO) at KXE consensus motifs (where X is a hydrophobic amino acid), which directly represses ELK-1 transcriptional activation and antagonises the ERK pathway. A double SUMOylation site mutant (K230/249R) showed increased activity at the *CFOS* and *EGR-1* promoters compared to wild-type ELK-1 (S. Yang et al., 2003). Repression is achieved through recruitment of HDAC-2 by SUMOylated ELK-1 to gene targets (S. Yang & Sharrocks, 2004), perhaps complementing the recruitment of mSIN3A HDAC 1/2 complex by the ETS domain in catalysing deacetylation and downregulating gene activation (S. Yang et al., 2001). Interestingly, ELK-1 de-repression is mediated by the SUMO E3 ligase PIASxα, which positively regulates p300 co-activator activity while prompting the

removal of co-repressor HDAC2 from ELK-1-targeted gene promoters, having little to no effect on ELK-1 SUMOylation or phosphorylation (S. Yang & Sharrocks, 2005).

ELK-1 SUMOylation has further roles in subcellular localisation. In experiments involving fusion of Balb/C mouse fibroblasts to HeLa cells stably expressing SUMO1/2 and transfected with ELK-1, wild-type ELK-1 exhibited HeLa nuclear retention, whereas a version of ELK-1 with all three SUMO modification sites mutated (K230/249/254R) readily shuttled to mouse nuclei (Salinas et al., 2004). This showed that, aside from transcriptional repression, SUMOylation is also key to the nuclear presence of ELK-1, which can display fluid movement between nuclear and cytoplasmic compartments of the cell (Salinas et al., 2004; Evans et al., 2011).

1.1.7.5 Ubiquitination of ELK-1

Currently, there are only three publications evaluating ELK-1 ubiquitination. It was previously found that bacterially-expressed and purified His-tagged ELK-1 was readily polyubiquitinated in an *in vitro* ubiquitination assay when incubated with rabbit reticulocyte lysate (S. Fuchs et al., 1997). This occurred independently of SAPK, which can phosphorylate and activate ELK-1 in response to cell stress such as UV irradiation, and had been shown to target its canonical substrate C-JUN for polyubiquitination (Cavigelli et al., 1995; S. Fuchs

et al., 1997). The shorter neuronal-specific isoform of ELK-1 (sELK-1) is missing the first 54 amino-terminal residues, and is far less stable than full-length ELK-1, partially due to its polyubiquitination and degradation by the 26S proteasome (1.2.7.2). This is thought to be due to a dimerisation interface (DI) in the ETS domain, whose absence in sELK-1 reveals a cryptic degron (CD) next to the B-domain that promotes the rapid turnover of dimerisation-defective ELK-1 (Evans et al., 2011). Within the ELK-1 DI is the NES, a leucine-rich motif which mediates ELK-1 transport to the cytoplasm through recognition by CRM1 (Exportin), which sELK-1 also lacks, and hence is exclusively nuclear (Vanhoutte et al., 2001). Interestingly, a version of sELK-1 missing all lysine residues was still inherently unstable, which suggests that proteasomal degradation is not the only route of sELK-1 turnover (Janice Saxton, unpublished data). A schematic of the domain structure of ELK-1 is shown in Figure 1-6, with DI and CD labelled.

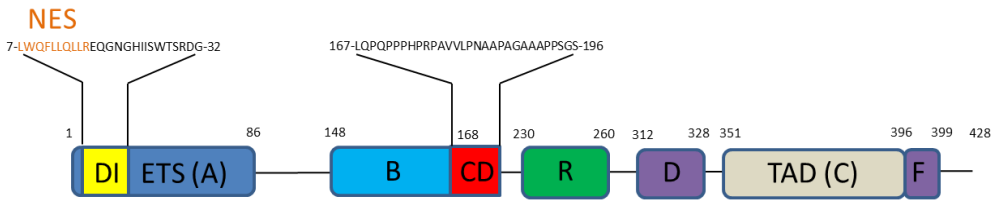

Figure 1-6: Schematic of ELK-1 with functional domains labelled. Highlighted are the DI (yellow), and the CD (red) which is revealed in dimerisation-deficient ELK-1 for turnover by the proteasome (CD – red). Within the DI, highlighted in orange is the NES. Made with reference to (Vanhoutte et al., 2001; Evans et al., 2011).

Most recently, FBXO25 was reported to serve as an E3 ligase responsible for ELK-1 polyubiquitination. FBXO25 complexes with S phase kinase-associated protein 1 (SKP1), Cullin1 (CUL1) and RING-box protein 1 (ROC1) forming an active RING E3 ligase (1.2.4.1), which has been shown to polyubiquitinate ELK-1 and promote its degradation by the 26S proteasome, impairing ELK-1 target gene transcription (Teixeira et al., 2013). This E3 ligase has also been linked to ERK cascade regulation *via* the inhibition of ERK phosphorylation (Teixeira et al., 2017). Aside from polyubiquitination, previous experiments have identified a pool of monoubiquitinated ELK-1 in human cells. Based on analysis of lysine substitution mutants, this monoubiquitination appeared to be targeted to the ETS domain of ELK-1, and was diminished upon ERK cascade induction by serum/TPA (Chow, PhD thesis, University of Nottingham, 2010). This, coupled with the increased transactivation of a hypo-ubiquitinated ELK-1 mutant against wild-type ELK-1 at the SRE, suggests that monoubiquitination negatively regulates ELK-1 activity (Janice Saxton, unpublished data). One of the main aims of this thesis was to clarify the sites of ubiquitin modification in ELK-1, to expand upon the understanding of both mono- and polyubiquitination and how each regulate ELK-1 function.

1.1.8 ELK-1 target genes

1.1.8.1 Classic targets - Immediate Early Genes

As mentioned previously (1.1.1), the signature target gene of ELK-1 is the IEG *CFOS*, where it binds with SRF to an ETS site at the SRE in the promoter, and this has served as a paradigm for the study of transcriptional activation through mitogen signalling cascades. *CFOS* expresses the C-FOS protein, which is itself a transcription factor that forms a heterodimer with C-JUN, producing the activator protein 1 (AP-1) complex. The AP-1 complex has many roles in cell growth and proliferation, including regulating the expression of *CCND1* during cell cycle re-entry, and hence ELK-1 is classically associated with these processes (Angel & Karin, 1991; Burch et al., 2004). However, the SRE is common among IEGs, meaning that ELK-1 has been implicated in the transcriptional activation of many of these genes. Other *bona fide* IEG ELK-1 targets include *EGR1, EGR-2* (*KROX20*) and *JUNB*, whose expression can be inhibited by disruption of the ERK cascade (Hipskind et al., 1994; Hodge et al., 1998; G. Wang et al., 2005). *EGR1* and *EGR2* expression is particularly reliant on ELK-1-MED23 functional cooperation (Stevens, 2002; G. Wang et al., 2005), possibly due to the multiple SRE sites resident within the promoters of these genes (Christy & Nathans, 1989; Chavrier et al., 1989). *IER2* (*PIP92*) is a further example of an ELK-1-responsive IEG, but differs from the *CFOS* SRE in that ELK-1 is capable of binding to it individually, as well as part of a ternary complex (Latinkić & Lau, 1994)

Recent global studies in MEFs identified that acute ERK activation following stimulation with the protein kinase C (PKC) activator 12-O-tetradecanoylphorbol 13-acetate (TPA), led to the induction of over 3000 genes, and promoted histone modification at more than 2000 transcription start sites within 30 minutes, which correlated positively with transcription (Gualdrini et al., 2016; Esnault et al., 2017). When using TCF-knockout MEFs (lacking *Elk-1*, *Elk-3* and *Elk-4*), reintroduction of wild-type human ELK-1, but not transcriptionally inactive mutants, rescued transcription at approximately 50% of direct and indirect TCF targets (1016/2142), illustrating the size and scope of the ELK-1-SRF gene regulatory network (Gualdrini et al., 2016). Furthermore, using this same approach, it was found that wild-type ELK-1 expression (but not inactive mutants) was sufficient for the reconstitution of the hierarchical histone modifications required for transcription at *bona fide* ELK-1 targets in TCF-null MEFs, including *Fos*, *Egr1*, *Egr2* and *Ier2* (Esnault et al., 2017).

The *MCL-1* gene is induced in monocytes by TPA treatment, which also proceeds through the ERK-ELK-1 activation axis (Townsend et al., 1999). However, this is not the case in either HeLa or HEK293T cells, where *MCL-1* expression is independent of ELK-1, illustrating the inherent variation in expression profiles in different cell lines and tissues (Galbraith et al., 2013; Janice Saxton, unpublished data). IEG gene expression can occur in response to ERK signalling, although this is not always the case. Stress signals can potentiate

C*FOS* induction *via* ELK-1 through SAPK (Gille et al., 1995B) or p38 MAP kinase signalling (Raingeaud et al., 1996). Similarly, *IER2* can be expressed through either ERK-dependent or independent mechanisms, and its upregulation in response to anisomycin-induced cell death is driven by either SAPK or p38 phosphorylation of ELK-1 (Chung et al., 1998; Chung et al., 2000).

1.1.8.2 Involvement in other gene regulation pathways

Aside from IEGs, ELK-1 can also target other genes, including *ZC3H12A* (encoding the RNAse MCPIP), which is up-regulated following IL-1-dependent ERK cascade induction (Kasza et al., 2010). Several matrix metalloproteinases (MMPs) have been identified as ELK-1 target genes, with high *MMP-2* and *MMP-9* expression co-occurring with hyper-phosphorylation of ELK-1 in gastric cancer cell lines (Choi et al., 2011). This is a complex relationship, as ELK-1 has also been implicated in the transcriptional repression of *Mmp-2* in response to 17β-estradiol signalling in rat cardiac fibroblasts, highlighting the importance of signalling, cellular and organismal context on transcriptional regulation (Mahmoodzadeh et al., 2010). *MMP-13* expression in cartilage chondrocytes is positively regulated by ELK-1 both directly through promoter-binding-potentiated transcription, and indirectly as a mediator of the NFκB pathway following FGF-2 induction (Muddasani et al., 2007). Transcription of *MMP* genes *per se* is also regulated by the AP-1 complex, meaning ELK-1 can also influence this process indirectly through regulation of *CFOS* expression (Auble

& Brinckerhoff, 1991; Crowe & Brown, 1999; Pan et al., 2008). Gene targets of the liver-specific transcription factor HNF4α have been linked to ELK-1, with many of these also containing ETS binding sites, and ELK-1 depletion decreased HNF4α target gene promoter occupation (Z. Wang et al., 2011). As previously mentioned (1.1.7.3), in prostate cancer ELK-1 recruitment of AR to gene promoters is required for regulation of AR target gene expression, adding to the growing list of ELK-1-responsive genes (Patki et al., 2013).

Evidence from experiments on human embryonic stem cells (hESCs) suggests that ELK-1 has a dual role in transcriptional activation and repression through co-localisation with ERK2 and Polycomb repressive complexes (PRC) (Goke et al., 2013). Furthermore, despite the consensus view that ELK-1 forms a ternary complex factor when contacting DNA, this is not always the case. There is evidence to suggest that ELK-1 can bind some target genes in an autonomous, SRF-independent manner, albeit with a great deal of functional redundancy at these gene promoters with other ETS-domain transcription factors (Boros et al., 2009A; Boros et al., 2009B). For example, EGF signalling in MCF7 breast cancer cells promoted the transcriptional activation of *PAI-1* through ELK-1, which occurred without ternary complex formation (Wyrzykowska et al., 2010). Interestingly, ELK-3 is an inhibitor of PAI-1 expression (although in MEFs rather than human breast cancer cells), which could indicate opposing functions of TCFs (Buchwalter et al., 2005). A chromatin immunoprecipitation (ChIP)-chip study found that 78% of endogenous ELK-1 targets in serum-starved HeLa cells

were SRF-independent (821/1053), although these autonomous ELK-1 targets showed considerable overlap with those identified in a similar study in Jurkat cells for another ETS-protein, GABPA (445/821 – 54%) (Valouev et al., 2008; Boros et al., 2009A). Additionally, in the aforementioned CHIP-seq dataset produced in TPA-stimulated TCF-null MEFs, reintroduction of human ELK-1 predominantly reconstituted transcription through SRF (Gualdrini et al., 2016). This study also confirmed that TCFs indirectly negatively regulate Myocardin-related transcription factor (MRTF) activity through competition for SRF-binding in response to growth stimulus, which had previously been reported in smooth muscle cells (Z Wang et al., 2004; Gualdrini et al., 2016).

1.1.8.3 Short ELK-1 – Neuronal specific isoform

Differential gene regulation is also mediated in neuronal cells by a truncated isoform of ELK-1, sELK-1. Due to missing a section from the ETS domain, sELK-1 DNA-binding and ternary complex formation at the SRE is impaired, while it is exclusively localised in the nucleus because it lacks an amino-terminal NES (Vanhoutte et al., 2001). The role of sELK-1 appears to be in opposition of full-length ELK-1 function, as its presence drives ELK-1 to re-localise to the cytoplasm, whereas in non-neuronal cell lines it is usually almost entirely nuclear (Janknecht et al., 1994; Sgambato et al., 1998; Vanhoutte et al., 2001). This grants further complexity to ELK-1 transcriptional control in the brain (Vanhoutte et al., 2001).

1.1.9 Biological function

1.1.9.1 Effects on pluripotency and differentiation

ETS domain-transcription factors are widespread throughout metazoans, but absent from plant, fungi and protozoans (Degnan et al., 1993). Primordial *Elk* genes appear to have arisen in early deuterostomes, such as the sea urchin (*Strongylocentrotus purpuratus*) and acorn worm (*Saccoglossus kowalevskii*). These early ELK proteins possess functional ETS domains and phosphorylatable ERK-responsive TADs, but lack the domain necessary for ternary complex formation, which appears to have evolved with the advent of the mesoderm germ layer (Saxton et al., 2016). Despite the conservation and evolution of ELK-1 as a TCF, much speculation has surrounded its conserved biological role, and suggestions of redundancy with other TCFs are supported by the overlap in TCF target genes (Boros et al., 2009B), biological examples of functional equivalency between TCFs (Costello et al., 2010), and the lack of any phenotypic changes in mouse following *Elk-1* gene deletion (Cesari et al., 2004).

However, ELK-1 loss-of-function hampers the embryonic development of *Xenopus* mesoderm (Nentwich et al., 2009). Furthermore, In hESCs, ELK-1 contributes to the maintenance of pluripotency through the occupation and repression of genes involved in differentiation, where it co-localises with PRC1/2 (Goke et al., 2013). This implies that ELK-1 function is important in maintaining stemness and regulating lineage commitment. Interestingly, ELK-1

has a dual repressor-activator role in hESCs, as it is also important in self-renewal, where it associates with gene promoters alongside ERK2 and mediates proliferation and cell-cycle progression as a transcriptional activator (Goke et al., 2013). An example of ELK-1 involvement in differentiation can be seen in neuronal PC12 cells, which exhibit neurite extension following nerve growth factor treatment mediated through sELK-1, in opposition to full-length ELK-1 (Vanhoutte et al., 2001). Insulin-driven adipogenesis is also critically regulated through Elk-1 *via* Med23, as depletion of either partner abrogated adipocyte differentiation in mouse fibroblasts (W. Wang et al., 2009).

1.1.9.2 Cancer growth and metastasis

ELK-1 activation through mitogens is most commonly associated with cell cycle entry and proliferation (Gille et al., 1992; Vickers et al., 2004). In agreement with this, TCF-deficient MEFs exhibit impaired proliferation (Gualdrini et al., 2016). Therefore, ELK-1 activity aligns with the progression of a variety of cancers. Protein kinase C-η mediated glioblastoma cell proliferation proceeds through ERK and ELK-1 activation (Uht et al., 2007). Moreover, high ELK-1 expression promoted bladder cancer cell growth and tumour formation, which required activated AR (Kawahara et al., 2015). Similarly, ELK-1 is required for hormone-independent growth in prostate cancer, which is also orchestrated through co-operation with AR (Patki et al., 2013; Rosati et al., 2016). ELK-1-MED23 cooperation was found to be critical in cell-cycle progression and

proliferation of hyperactive K-RAS-driven lung cancer, further illustrating the importance of ELK-1 in carcinogenesis (X. Yang et al., 2012).

ELK-1 is also involved in cell migration, and through this has further associations with malignancy. The metastatic gastric cancer cell line SNU638 displayed high levels of invasion and migration due to high *MMP2* and *MMP9* expression, which could be reconstituted in the non-metastatic cell line SNU484 by ELK-1-driven transcription of these genes following secretory leukocyte protease inhibitor treatment (Choi et al., 2011). Depletion of ELK-1 in bladder cancer cells impaired MMP-2 and MMP-9 expression and activity, leading to reduced migration, which, in contrast to ELK-1 effects on proliferation, was AR-independent (Kawahara et al., 2015). High PAI-1 protein levels relate to metastasis and low survival rates in breast cancer (Leissner et al., 2006), due to its ability to detach cells from extracellular matrices by binding uPA and disrupting tethering cell-surface complexes involving uPA receptor, vitronectin and integrins (Czekay et al., 2003). Hence, involvement in *PAI-1* transcription further links the ELK-1 to cancer invasiveness (Wyrzykowska et al., 2010). It has recently emerged that ELK-1 appears to have important roles in both proliferation and migration in the promotion of cervical cancer. The microRNA miR-326 displayed low expression levels in cervical cancer, and its introduction into cervical cancer cell lines CaSki and HeLa inhibited cell growth and migration. This was shown to be due to ELK-1 knockdown, and could be reversed by rescued ELK-1 expression (P. Zhang et al., 2017). However, TCF

activity can also negatively regulate cell motility through competition for SRF binding with MRTFs, as TCF-impaired MEFs increased the invasiveness of 4T1 breast carcinoma cells significantly against wild-type MEFs in organotypic co-culture (Gualdrini et al., 2016).

1.1.9.3 Apoptosis, cell survival and inflammation

The introduction of a dominant-negative ELK-1 mutant into EcR293 cells under the control of the ponasterone A promoter caused apoptosis (Vickers et al., 2004). This was shown to be due to downregulation of the anti-apoptotic gene *MCL-1*, whose activation is mediated through a TCF-SRF mechanism in certain cell lines such as monocytes (Townsend et al., 1999; Vickers et al., 2004). This is also relevant in the context of cancer, as EGF expression can drive *MCL-1* expression and cell survival in MCF7 and SK-BR-3 cells, which could be blocked by dampening of the ERK pathway or ELK-1 knockdown (Booy et al., 2011). Moreover, ELK-1 phosphorylation correlated positively with levels of MCL-1 protein in human breast tumour tissue (Booy et al., 2011). However, overexpression of ELK-1 in both rat and human cells has also been shown to accelerate apoptosis following calcium ionophore treatment (Shao et al., 1998). There is also some evidence of ELK-1 involvement in inflammatory responses through bacterial lipopolysaccharide-mediated induction of monocytes (Guha et al., 2001) and the IL-1β-driven induction of the endoribonuclease MCPIP, which has important functions in both inflammation

and cardiovascular disease (L. Zhou et al., 2006; Kasza et al., 2010). Overall, ELK-1 is involved in a range of dynamic cellular processes and its dysregulation is directly or indirectly implicated in many disease pathologies, particularly in the proliferation and invasiveness of a range of cancers.

1.2 Ubiquitination

1.2.1 Overview and historical perspective

Ubiquitin is a protein with numerous regulatory functions in eukaryotes. Its covalent linkage to other proteins is a common post-translational modification, known as ubiquitination (or ubiquitylation), which promotes a multitude of downstream signalling effects. It was originally discovered as an 8.5 kDa polypeptide isolated from bovine thymus, and was named ubiquitous immunopoietic polypeptide due to its apparent presence in all forms of life and supposed hormonal activity (Goldstein et al., 1975; Schlesinger et al., 1975). This was later amended when it was found that ubiquitin was specific to eukaryotes and was not, in fact, a thymic hormone (Low & Goldstein, 1979). Subsequently, a series of "cell-free" experiments using rabbit reticulocyte lysates revealed that chains of a heat stable polypeptide, ATP-dependent proteolysis factor 1, were found to be covalently linked to proteins (in an ATP-driven process) and prompted the degradation of target proteins (Ciehanover et al., 1978; Ciechanover et al., 1980A; Hershko et al., 1980). This was subsequently found to be ubiquitin (Ciechanover et al., 1980B). As this was the

first shown function of ubiquitin, mediating protein degradation is generally considered to be its canonical role in the cell, although ubiquitin modifications of target proteins have many effects other than proteolytic (Komander, 2009).

1.2.2 Types and complexity of ubiquitination

Ubiquitin is usually conjugated to target proteins *via* lysine residues. Atypically, this can also occur at serine, threonine, cysteine and (amino-terminal) methionine residues in target proteins (Ciechanover & Ben-Saadon, 2004; X. Wang et al., 2007; X. Wang et al., 2012). Beyond monoubiquitination, proteins can also be both multi-monoubiquitinated (more than one ubiquitin monomer ligated at multiple lysines) and polyubiquitinated (chain of ubiquitin linked to a single lysine) of which links can be formed between any of the seven lysines residing within ubiquitin (K6, K11, K27, K29, K33, K48 and K63), as well as at the amino-terminal methionine (producing a peptide linkage) (Figure 1-7) (Figure 1-8) (Komander, 2009). These polyubiquitin chains in turn can vary greatly in length and can be homogeneous with respect to the linkages or heterogeneous (mixed), where the lysine involved in ubiquitin-ubiquitin linkage remains constant or is variable respectively (Komander, 2009). Beyond this, polyubiquitin chains can be branched, whereby multiple chains originate from the same ubiquitin, forming a fork-like conformation (Komander, 2009; H. Meyer & Rape, 2014). Moreover, polyubiquitin chains can be conjugated to target proteins, or free, in which case they are termed unanchored (Strachan

et al., 2012). Despite being a post-translational modification in itself, it has recently emerged that ubiquitin can also be post-translationally modified, such as through acetylation and phosphorylation, adding further possible signalling complexity (Koyano et al., 2014; Ohtake et al., 2015; Matsuda, 2016).

The vast array of modifications possible can signal for a wide range of effects on modified proteins, including (but not limited to) degradation, altered subcellular localisation, and changes in activity. K48- and K63- linked polyubiquitin chains are the most studied and well-characterised linkage types, generally associated with protein degradation and cell signalling pathways, respectively (Komander, 2009). Different polyubiquitin chain topologies exhibit variable structural conformations. For example, K48-linked chains adopt closed and compacted conformations owing to extensive hydrophobic interactions between ubiquitin moieties, whereas K68-linked and linear chains are much more open, allowing more flexibility around the isopeptide/peptide bond (Eddins et al., 2007; Komander et al., 2009A). This contributes to the recognition of different chain types leading to different downstream effects on target proteins. Understanding the information imparted by a ubiquitination event and how it is read (and hence unravelling the 'ubiquitin code'), is incredibly complex due to the variety and dynamic nature of this elegant system of control. The network giving rise to the ubiquitin code consists of *writers* (ubiquitination enzymes- E1, E2 and E3s), *readers* (proteins capable of

recognising ubiquitin marks) and *erasers* (deubiquitinating enzymes), which together afford considerable signalling complexity (Komander & Rape, 2012).

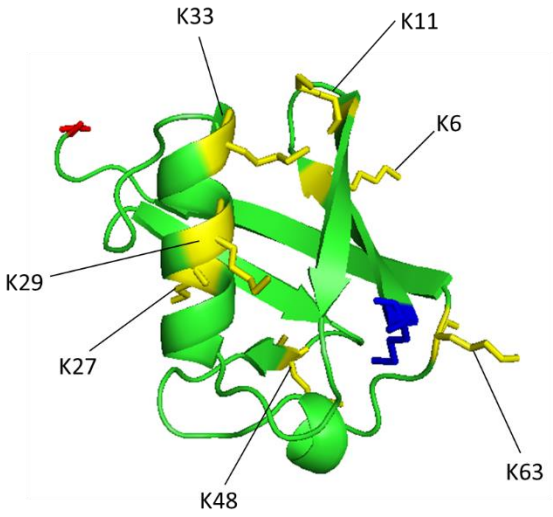

Figure 1-7: Structure of ubiquitin (human), with all lysine residues and termini labelled. Lysine = yellow, amino-terminus (M) = blue, carboxyl-terminus (G) = red. Structure taken from (Vijaykumar et al., 1987) - PDB 1UBQ – re-rendered with PyMOL.

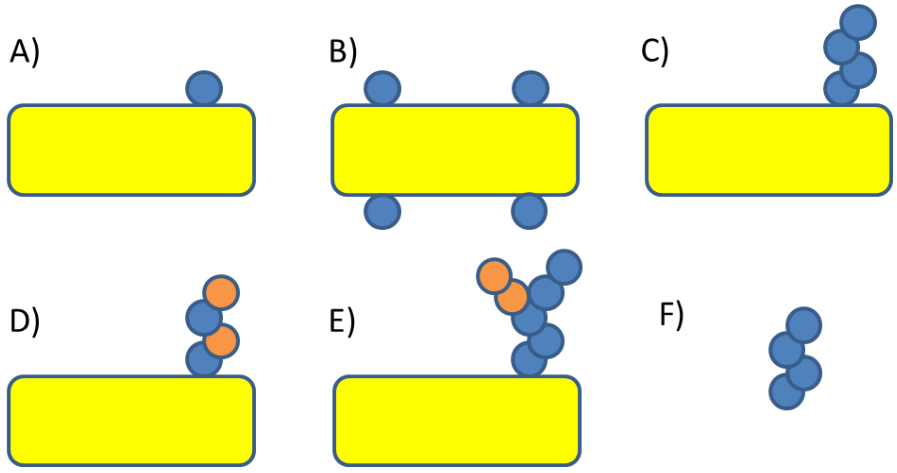

Figure 1-8: Examples of possible ubiquitin modifications to target proteins. Yellow box indicates target protein, blue/orange circles represent ubiquitin. A) Monoubiquitination is the covalent attachment of one ubiquitin unit. B) Multi-monoubiquitination is several individual ubiquitin units bound at multiple lysines in the target protein. C) Homogenous polyubiquitin chains are chains of ubiquitin linked together *via* the same lysine residue e.g. K48-linked polyubiquitin chains. D) Heterogenous (mixed) polyubiquitin chains are chains of ubiquitin linked together *via* variable lysine residues e.g. K11 (orange) and K48-linked (blue) polyubiquitin chains. E) Branched polyubiquitin chains occur when two ubiquitin chains branch out from a ubiquitin moiety. F) Unanchored polyubiquitin chains are not conjugated to a target protein. Produced with reference to (Komander, 2009).

1.2.3 The mechanism of ubiquitination

Ubiquitination typically involves three coordinated enzymatic activities acting sequentially, carried out by proteins termed E1 ubiquitin-activating, E2 ubiquitin-conjugating and E3 ubiquitin ligases (Hershko et al., 1983). E1 enzymes activate free ubiquitin through an ATP-driven, two-step process; proceeding firstly through acyl-adenylation of the ubiquitin carboxyl-terminus, followed by covalent linkage of a catalytic cysteine within the enzyme to ubiquitin with concomitant release of AMP. E2 enzymes then bind both the activated ubiquitin and the E1 and enable the transfer of ubiquitin to an E2 active site cysteine by catalysing a trans thioesterification reaction (Hershko et al., 1983). This is followed by ligation of the ubiquitin to the target protein through the action of an E3 ligase, usually forming an isopeptide bond between the carboxyl-terminal glycine of ubiquitin and a selected target protein lysine residue (Pickart & Eddins, 2004). In humans, there are two E1 activating enzymes, around 40 E2 conjugating enzymes, and approximately 600 E3 ligases. Together they form the *writers* of the ubiquitin code (Komander & Rape, 2012). Adding complexity to this is E4 ligase activity, where ubiquitin moieties attached to target proteins by E3 ligases can be extended into longer chains through E4 activity (in conjunction with E1, E2 and E3 enzymes), usually prompting proteasomal degradation (Koegl et al., 1999).

1.2.4 E3 ligases

There are several subfamilies of E3 ligases, most of which belong to the Really Interesting New Gene (RING) ligases. Other families include the Homologous to E6-associated protein Carboxyl-Terminus (HECT) and RING1-BRcat-Rcat (RBR) ligases. RING ligases work by aligning the target protein with an ubiquitinated E2-thioester and encouraging ubiquitin transfer, in a manner whereby ubiquitin is transferred directly from E2 to target lysine. HECT ligases act by catalysing substrate ubiquitination through a thioester intermediate, coordinated through a carboxyl-terminal HECT domain containing a catalytic cysteine residue (Metzger et al., 2012). RBR ligases are multidomain complexes that adopt a ubiquitin-transfer mechanism encompassing features of both HECT and RING ligases, in that catalysis is mediated both by a RING domain for binding E2-ubiquitin and a catalytic cysteine residue to mediate thioester intermediate transfer from E3 to target protein (as per HECT). The RING domain transfers ubiquitin from E2 to a carboxy-terminal required-for catalysis (Rcat) domain which contains the catalytic cysteine residue, downstream of a benign-catalytic (BRcat) domain, which is structurally identical to Rcat, but lacks the cysteine residue (Spratt et al., 2014). These mechanisms are illustrated in Figure 1-9.

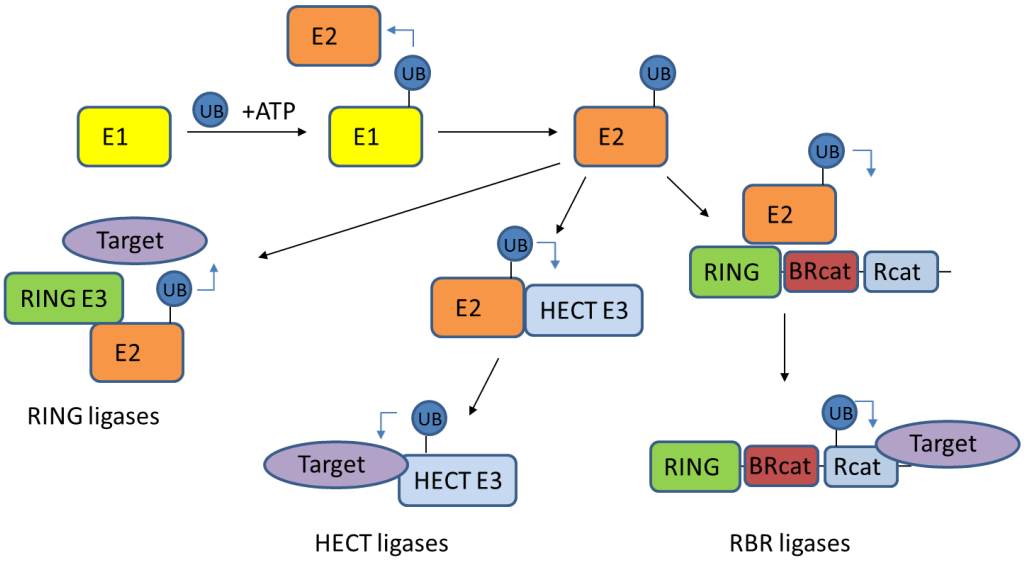

Figure 1-9: Schematic representation of RING, HECT and RBR E3 ligase mechanisms of action. An E1-activating enzyme activates ubiquitin *via* ATP hydrolysis, followed by transfer to an E2 conjugating enzyme. Ring ligases act to orient an E2-ubiquitin to promote ubiquitin transfer to the target protein. HECT ligases form a thioester intermediate with ubiquitin before subsequent transfer to target protein. RBR ligases combine RING and HECT-like mechanisms, where a RING domain transfers ubiquitin from E2 to Rcat domain, with subsequent transfer of ubiquitin to target protein. Made with reference to (Spratt et al., 2014).

1.2.4.1 Cullin-RING ligases

The largest group of E3s are the cullin-RING ligases, which act as multimeric complexes, consisting of a cullin backbone, a RING domain, a substrate recognition module and an adaptor. SCF (SKP1/CUL1/FBP) ligases represent a subset of this family, of which FBXO25 is an example of an F-Box protein (FBP) substrate recognition protein. CUL1 acts as a scaffold protein, ROC1 contains the RING domain for ubiquitin transfer and SKP1 acts as an adaptor and binds the FBXO25 F-box motif, forming a molecular bridge between CUL1 and FBXO25. CUL1 also recruits the E2 CDC34 to the complex, and FBXO25 mediates specificity by recruiting a target protein for ubiquitination (Craig & Tyers, 1999).

SCF activity is often regulated by phosphorylation, and particularly, phosphorylation often precedes ubiquitination of a target substrate (Willems et al., 1999). Degrons are motifs within target proteins that allow E3 recognition, binding and polyubiquitination, resulting in degradation by the proteasome (Varshavsky, 1991). Internal degrons are often localised to PEST sequences within target proteins, which are stretches of polypeptide rich in proline (P), glutamic acid (E), serine (S) and threonine (T) that commonly act as proteolytic signals (Rechsteiner & Rogers, 1996). Phosphorylation at serine and threonine residues in PEST sequences can act as a phosphodegron, prompting recognition by FBPs and ubiquitination by SCF complexes (Yada et al., 2004; R. Meyer et al., 2011). With regard to FBXO25, the mitochondrial antiapoptotic

protein HAX-1 is recognised by the F-Box protein following phosphorylation by protein kinase Cδ (Baumann et al., 2014). Interestingly, the binding and ubiquitination of HAX-1 also requires FBXO25 phosphorylation, and both mapping of the FBXO25 binding region and phosphorylation sites in HAX-1 indicated that this process is not directed through a previously characterised HAX-1 PEST sequence (B. Li et al., 2012; Baumann et al., 2014).

1.2.5 Ubiquitin-binding domains

Ubiquitin-binding domains (UBDs) are modular regions of proteins capable of reading ubiquitin marks, which are found in adaptors and enzymes of the ubiquitin system. These commonly target a hydrophobic region of ubiquitin centred around an isoleucine residue (I44), or an acidic region including an aspartate residue (D58) (Heride et al., 2014). They form the *readers* of the ubiquitin code, acting to recognise ubiquitin marks and transmit information to enact molecular and cellular changes (Komander & Rape, 2012). The majority of UBDs adopt an α-helical structure, all of which target the I44 patch (Hurley et al., 2006). Ubiquitin-associated (UBA) domains are prime examples of this, which primarily bind polyubiquitin chains (Hofmann & Bucher, 1996). An example of UBDs showing specificity in binding is in Rad23 (from yeast), whose UBA domain can preferentially bind K48-linked polyubiquitin chains (Raasi & Pickart, 2003). Unanchored polyubiquitin chains can also be recognised by Zinc finger-ubiquitin binding protein (ZnF-UBP) domains, which binds the free

carboxyl-terminus of unconjugated ubiquitin with high affinity (Reyes-Turcu et al., 2006). An example of the functional importance of UBDs can be seen in translesion synthesis, where ubiquitin-binding motif (UBM) and ubiquitin-Binding ZnF (UBZ) domains are critical in recognition of monoubiquitinated PCNA by Y-family polymerases in replication foci, although uncharacteristically for most UBDs, UBM domains actually target a leucine residue in ubiquitin (L8) rather than I44 (Bienko et al., 2005).

1.2.6 Monoubiqutination

Monoubiquitination of target proteins usually signals for non-proteolytic effects on the target protein. The most widespread and consequently comprehensively studied examples of monoubiquitination are of epigenetic histone modifications of lysine residues 119 and 120 (in humans) respectively in histone H2A (H2AK119ub) and H2B (H2BK120ub). The dynamic cross-talk and regulation of gene expression *via* signals imparted by the addition and removal of histone modifications is known as the histone code, of which some specific modifications are well characterised as transcriptional activators (such as H3K14ac) and others transcriptional repressors (such as H3K27me3) (Y. Zhang, 2003) (Figure 1-10). H2A monoubiquitination is usually associated with transcriptional repression. It is a mark commonly laid down by the PRC1, which acts to silence developmental homeobox (HOX) genes (Chan et al., 1994). PRC1 is a complex of proteins with E3 activity, and it is thought to work in tandem

with the methylation activity of PRC2 (H3K27me3). PRC2 first acts to lay down the trimethyl mark, which is then recognised by the chromo-domain of PRC1, facilitating its binding and prompting the enzymatic histone monoubiquitination enacted by the RING1a and 1b E3 domains (Cao et al., 2002; Fischle et al., 2003). However, recently this relationship has been brought into question, as a study in *Arabidopsis thaliana* found that despite commonly co-localising with H3K27me3 marks, H2Aub ubiquitination appeared to be independent of PRC2 activity (Y. Zhou et al., 2017). Histone H2B is generally considered a positive mark for gene transcription and has been shown to influence many processes, including gene transcription, DNA repair and mRNA processing (Bonnet et al., 2014).

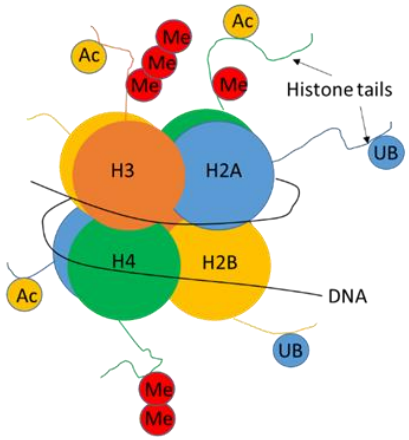

Figure 1-10: Representation of a nucleosome. DNA wraps around the octamer of histone proteins. The histone tails orient outwards and are open to modification.

Aside from histones, many other proteins, including transcription factors, are open to modification by monoubiquitination, leading to wide-ranging effects including disrupting or promoting interactions and altering subcellular localisation. For example, Proliferating cell nuclear antigen (PCNA) is monoubiquitinated. This has important functions on the promotion of translesion synthesis (TLS), where DNA damage requires a switch from replicative DNA polymerases to Y-family DNA polymerase η (DNAPη) in order to overcome blocks during DNA replication. Upon monoubiquitination by the E2-E3 complex RAD6(UBE2A)-RAD18 (at K164), PCNA interacts with and promotes recruitment of DNAPη, mediating incorporation of nucleotides across DNA-damaged lesions, in a process conserved from yeast to human (Hoege et al., 2002; Kannouche et al., 2004). This has been shown to be regulated by K164 modification by other ubiquitin-like proteins such as SUMO (in *Saccharomyces cerevisiae*) (Pfander et al., 2005) and NEDD8 (in human cells), the latter of which also proceeds through RAD18 activity, and acts to antagonise ubiquitination and blocks DNAPη interaction (Guan et al., 2017). Hence, monoubiquitination can promote protein-protein interactions, and PCNA illustrates the importance of crosstalk between different post-translational modifications in effectuating molecular signalling.

Conversely, Y-polymerases can also be monoubiquitinated (Bienko et al., 2005), but DNAPη monoubiquitination masks its PCNA-binding region, inhibiting TLS progression (Bienko et al., 2010). In yeast, the E2-E3 complex

Ubc13–Mms2–Rad5 can extend monoubiquitination into K63 polyubiquitination of PCNA, also occurring in humans through Rad5 homologues HLTF and SHPRH, which preserves genomic stability through disengaging PCNA from DNAPη, promoting template switching (Chiu et al., 2006; Motegi et al., 2008; Parker & Ulrich, 2009).

Monoubiquitination can also inhibit protein-protein interactions. A prime example of this is SMAD4, a protein which associates with the receptor-mediated SMAD2/3 (R-SMADs) to form an active transcriptional complex following TGF-β signalling, a process key in the maintenance of proliferative homeostasis. When monoubiquitinated by RING-ligase Ectodermin/Tif1γ, SMAD4 interaction with R-SMADs is destabilised, inhibiting TGF-β-SMAD signalling. The inability of monoubiquitinated SMAD4 to form complexes with R-SMADS results in its ejection from the nucleus, which is also the case following SMAD2/3 depletion (Dupont et al., 2009). The presence of Ectodermin/Tif1γ is required for this relocalisation to the cytoplasm, suggesting that through abrogation of R-SMAD-SMAD4 binding, monoubiquitination also indirectly affects SMAD4 subcellular localisation, as complex formation is required to maintain SMAD4 in the nucleus (De Bosscher et al., 2004; Dupont et al., 2005). It should be noted that Ectodermin/Tif1γ has also been shown to promote the degradation of SMAD4 (Dupont et al., 2005). This could be due to the E3 ligase having the capability of polyubiquitinating SMAD4 for proteasomal degradation, or the increased monoubiquitination

could allow another E3 ligase to extend chains to signal for proteolysis, as other E3 ligases have been implicated in SMAD4 turnover (Wan et al., 2004). Alternatively, monoubiquitin has also been shown to drive proteasomal degradation in some circumstances (Livneh et al., 2017).

The tumour suppressor p53 is a critical regulator of the cell cycle whose mutation is associated with a vast array of human carcinomas (Joerger & Fersht, 2007). It is a nuclear transcription factor that controls checkpoints for transitions from both G1-S and G2-M and can act to promote apoptosis (Agarwal et al., 1995; Fridman & Lowe, 2003). Both monoubiquitination and polyubiquitination of p53 is carried out by the RING ligase MDM2, which mediates its nuclear export and proteasomal degradation respectively (M. Li et al., 2003). Through this, p53 activity is downregulated, through either removal from the nucleus or through proteolysis. Ubiquitination events reduce the affinity of p53 for MDM2 binding while also revealing an otherwise concealed NES, causing disassociation of MDM2 and cytoplasmic transport of p53 (Carter et al., 2007). It has been further demonstrated that monoubiquitinated p53 can be trafficked to mitochondria under cell stress where it can trigger mitochondrial apoptosis (Marchenko et al., 2007).

Monoubiquitination can also promote proteasomal degradation. Cyclin B1 can be degraded in the absence of polyubiquitin chains, requiring only multi-monoubiquitination for degradation by the proteasome (Dimova et al., 2012).

Similarly, the myogenesis regulator PAX3 was found to be degraded by the proteasome, which was mediated through monoubiquitination, with no evidence of polyubiquitin chain formation. Unlike cyclin B1, however, PAX3 degradation required only a single monoubiquitin moiety conjugated to the target protein for proteolytic processing (Boutet et al., 2007).

1.2.7 Protein degradation

1.2.7.1 Autophagy

Two major intracellular pathways mediate the degradation of proteins and recycling of amino acids – the Ubiquitin-Proteasome System (UPS) and autophagy (macroautophagy). Generally, the UPS is responsible for proteolysis of short lived, misfolded/denatured/truncated and regulated proteins, whereas autophagy handles long-lived and aggregated proteins in addition to organelles (Lilienbaum, 2013). Both involve ubiquitination of targets, which is very-well established with regard to the UPS, but is less well understood for autophagy. Autophagy proceeds through lysosomal double-membraned vesicles named autophagosomes, whereby target cargoes are recognised by autophagy receptors which bind ATG8/LC3/GABARAP-like proteins at the phagophore to be engulfed and processed (Khaminets et al., 2016). This can be targeted through ubiquitination of cargo, allowing recognition of ubiquitin marks by autophagy receptors containing UBDs such as p62/SQSTM1 (Pankiv et al., 2007), NDP52 (Thurston et al., 2009) and optineurin (OPTN) (Wild et al.,

2011). This can also be regulated through phosphorylation, such as through TBK-1 phosphorylation of OPTN, which enhances LC3-binding (Wild et al., 2011). Moreover, autophagy receptors NDP52 and OPTN can recognise phospho-ubiquitin, which is important in the degradation of mitochondria (mitophagy) following ubiquitination of mitochondrial proteins by PARKIN (an RBR E3 ligase) and the phosphorylation of ubiquitin at S65 (and PARKIN) by PINK1 kinase (Koyano et al., 2014; Lazarou et al., 2015; Matsuda, 2016).

1.2.7.2 26S proteasome

Ubiquitination of proteins often leads to targeted degradation *via* the UPS. The UPS operates through polyubiquitination (classically K48-linked) enacted by an E3 ligase docked onto a degradation signal (degron) residing within the target protein, which targets it for proteolysis (Muratani & Tansey, 2003). The proteasome itself is a large 26S complex composed of one 20S unit flanked at either end by two 19S complexes. The 19S caps are responsible for substrate recognition, deubiquitination (allowing recycling of ubiquitin) and delivery of denatured polypeptide into the proteolytic 20S container where targets are sequestered and degraded (Glickman & Ciechanover, 2002). Both E3 ligases and deubiquitinating enzymes (DUBs) associate with the proteasome, maintaining a balance of polyubiquitin chain extension and removal (Crosas et al., 2006). The three deubiquitinating enzymes, RPN11, USP14 and UCH37, associate with the proteasome and act to remove and recycle ubiquitin from

target proteins, preceding their entry into the proteolytic chamber (Figure 1.11) (Leggett et al., 2002; Hu et al., 2005; Al-Shami et al., 2010). Additionally, USP14 can rescue substrates from degradation, regulating proteasomal processivity (Lee et al., 2010).

Despite the most common mark for UPS processing being K48-linked ubiquitin chains, this is not always the case, and in fact all other chains topologies (excluding K63-linked) can mediate proteolysis of the target protein (P. Xu et al., 2009). Often, truncated or misfolded proteins are removed by the proteasome, although the proteasomal degradation of proteins is also a method of regulating steady-state levels and activity of "normal" proteins. As previously mentioned, E3 ligases mediate ubiquitination to target proteins to the proteasome, often by docking to target proteins through degrons, such as destabilising internal PEST sequences (Varshavsky, 1991; Rechsteiner & Rogers, 1996). Another common degron recognised by E3 ligases are N-degrons, which are located at the amino-terminus of target proteins, and signal for degradation by the N-end rule pathway, whereby protein half-life is determined by destabilising amino-terminal amino acid residues (Bachmair et al., 1986; Varshavsky, 2011). This can proceed either through the Arg/N-end rule pathway, where amino-terminal arginylation precedes E3 (termed N-recognin) recognition (Bachmair et al., 1986), or the Ac/N-end rule pathway, where the amino-terminus is instead acetylated (Hwang et al., 2010).

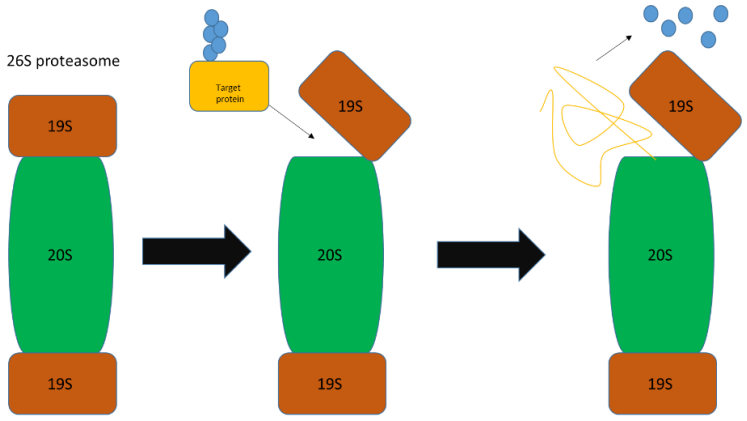

Figure 1-11: The 26S proteasome. Polyubiquitinated proteins are recognised by the 19S subunit, deubiquitinated, unfolded and passed through to the 20S proteolytic subunit which carries out their degradation. Ubiquitin is recycled in the process (blue circle).

1.2.7.3 Proteasomal control of transcription factors

Proteolysis of active transcription factors is required to maintain balance of transcriptional activity and fine-tuned control of cellular homeostasis. The 26S proteasome is resident within both the cytoplasm and the nucleus, and recruitment of sub-complexes of the proteasome to actively transcribed genes has been documented (Reits et al., 1997). One model proposes a system whereby active transcription factors stimulate E3 ligase recruitment to gene promoters, which proceed to ubiquitinate active targets that are rapidly turned over by the nuclear-resident UPS; halting further transcription while facilitating the successful elongation of already active transcripts (Muratani & Tansey,

2003). In some circumstances inhibiting the proteasome can prevent the transcriptional activation of certain transcription factors, such as Gcn4, whose polyubiquitination (following phosphorylation) and degradation enhances its activity, in a process termed “activation by destruction” (*in Saccharomyces cerevisiae*) (Lipford et al., 2005). Through this, transcription factors can be activated and ubiquitinated, promoting transcription of target genes before being removed for proteolysis and replaced by a newly synthesised transcription factor at gene promoters.

As previously mentioned, ELK-1 contains a cryptic degron (amino acids 167-196) (1.1.6.5), which is possibly presented to an E3 ligase in the misfolded or monomeric state for polyubiquitination (Evans et al., 2011). Another example of degron-mediated proteolysis within ETS-domain transcription factors is that of the proto-oncogenic ETV1 of the PEA3 family. It has been shown that COP1 is the E3 ligase that acts on ETV1, together with its binding partner DET1. Amino-terminal truncations in ETV1 resembling those seen in prostate cancer that are lack two COP1 degrons are not degraded by the UPS, leading to their accumulation and overabundance in the disease state and further implicating COP1 as a negative regulator of ETV-1 (Vitari et al., 2011).

Aside from degrading proteins in their entirety, the UPS can also partially process substrates. This is the case for NF-κB, a protein implicated in a multitude of cellular processes, including both innate and adaptive immunity

and inflammatory responses (Kaltschmidt et al., 2000; Lawrence, 2009). It is retained in an inactive state in the cytosol as a complex composed of two subunits known as NF-κB1 (p50) and RELA (p65), whose nuclear localisation sequences are obscured by the bound inhibitor of NF-κB (IκBα) (Baeuerle & Baltimoire, 1988; Ghosh et al., 1990; Nolan et al., 1991). As an added level of complexity, p50 is actually expressed as a protein of size 105 kDa (p105), with the amino-terminal region encoding the active p50 and the carboxy-terminus resembling IκBα, and as such is inactive (Fan & Maniatis, 1991). Hence, the cytoplasm consists of both ternary complexes with an inhibitor (p50, p65 and IκBα) and heterodimers with an inactive subunit (p65 and p105) that each requires processing for activity. Both of these processing events are achieved through ubiquitination and incomplete proteasomal processing of either IκBα or the amino-terminus of p105, giving rise to active heterodimers that translocate to the nucleus and enact alterations in gene expression (Palombella et al., 1994). Both IκBα and p105 also require phosphorylation, which precedes their ubiquitination, and IκBα is in fact processed while still in complex (Miyamotot et al., 1994; MacKichan et al., 1996). The FBP FBW1 recognises the phosphodegron that is present in IκBα, and promotes its proteolysis through the UPS (Hatakeyama et al., 1999). Interestingly, multi-monoubiquitination of p105 can also prompt its recognition by the proteasome, rather than polyubiquitination (Kravtsova-Ivantsiv et al., 2010). Lastly, SUMOylation of IκBα further stimulates UPS activity, through promotion of polyubiquitin chain formation (Aillet et al., 2012).

IRF1 is a transcription factor that is a known tumour suppressor whose activation commonly stimulates induction of apoptosis, but conversely in some circumstances can also suppress it (Chapman et al., 2000; P. Kim et al., 2004; Bouker et al., 2005). It can be degraded by the UPS, the E3 of which in this case is CHIP, which binds within an unstructured region of IRF1 known as the Mf2 domain (Narayan et al., 2011). Further to this, all lysines identified as ubiquitination targets are resident within the DNA-binding domain of IRF1, and as such cannot be ubiquitinated when actively bound to DNA due to CHIP's inability to access and dock at its specific target sequence, preventing degradation while active (Landré et al., 2013). MDM2 can also act as an ubiquitin ligase for IRF-1 *via* Mf2 docking, showing the promiscuity of this domain as a ligase recognition sequence, and illustrating that multiple E3s can target the same protein (Landré et al., 2013).

As previously mentioned, p53 can be monoubiquitinated and polyubiquitinated by MDM2 (M. Li et al., 2003). Activity of p53 under normal (unstressed) conditions is kept under control by rapid degradation driven by the E3 ligase MDM2, whereby p53 actually upregulates *MDM-2* transcription in a negative feedback loop, actively promoting its own proteolysis (X. Wu et al., 1993). MDM2 was shown to promote p53 ubiquitination and degradation through a heterodimeric RING–RING interactions with its homolog MDMX, which functionally depend on each other for p53 inhibition (Gu et al., 2002). It can also be degraded following action of other E3 ligases. COP-1 and CHIP are

notable examples, whereby *COP1* expression is upregulated by p53 (as for *MDM-2*) whereas CHIP triggers mutant p53 degradation transiently through a chaperone-associated process (Dornan et al., 2004; Esser et al., 2005). p53 is also open to chain elongation by an E4-ligase mechanism, through activity of E4 factors p300/CBP (Shi et al., 2009), which can also regulate p53 by acetylation (Ito et al., 2001).

1.2.8 Deubiquitinating enzymes

Ubiquitination is reversible, as deubiquitinating enzymes (DUBs) can remove the mark from target proteins. Together they make up the *erasers* of the ubiquitin code (Komander & Rape, 2012). There are approximately 100 DUBs in the human genome, organised into six families. These families are ubiquitin-specific proteases (USPs), ubiquitin carboxyl-terminal hydrolases (UCHs), ovarian tumour proteases (OTUs), Josephins, JABI/MPN/MOV34 metalloenzymes (JAMMs) and the most recently discovered – motif interacting with ubiquitin-containing novel DUB family (MINDY) DUBs (Komander et al., 2009B; Abdul Rehman et al., 2016). All DUB families are cysteine proteases, except for JAMMs, which are zinc metalloproteases. DUB activity is critical for nearly all cellular functions, such is the importance of control over ubiquitination events, and as such they often represent oncogenes and tumour suppressors in cancer development (Hussain et al., 2009).

Some DUBs show little discrimination between different forms of ubiquitination, whereas others exhibit specificity towards particular polyubiquitin chain topologies. For example, AMSH and AMSH-LP are JAMM metalloproteases that show specificity towards K63-linked ubiquitin chains, while being incapable of cleaving K48-linked or linear chains (Sato et al., 2008). Substrate specificity can be determined by UBDs within DUBs, such as the characteristic ZnF-UBP domain in USP5, which binds carboxyl-terminal glycine residues (G75 and G76) in free ubiquitin granting it affinity for unanchored polyubiquitin chains and allowing their disassembly (Wilkinson et al., 1995; Reyes-Turcu et al., 2006).

Aside from polyubiquitin chain topology, DUBs can also specifically bind target proteins. An example is the inhibitor of NF-κB signalling and dual-function enzyme A20, which has amino-terminal DUB activity against K63-linked polyubiquitin chains on TRAF6 and RIP, while its carboxyl terminus has E3 ligase activity which polyubiquitinates RIP for proteasomal degradation (Wertz et al., 2004). The A20 amino-terminus shows specificity for target protein rather than polyubiquitin chain topology, removing polyubiquitin from TRAF6 and RIP without dissembling chains (S. Lin et al., 2008). Tight control over DUB activity and stability is achieved through a variety of means, including phosphorylation (Khoronenkova et al., 2012; Liu et al., 2017), allostery through ubiquitination (Faggiano et al., 2015), competition for adaptor protein/complex binding

(Atanassov et al., 2016) and cell-cycle dependent regulation of DUB expression (McFarlane et al., 2010).

1.2.8.1 Ubiquitin specific proteases

Ubiquitin specific proteases (USPs) represent the largest family of DUBs, comprising over half of the known DUBs in humans. They are defined by a USP domain, which contains a conserved catalytic triad of cysteine, histidine and aspartate (or asparagine) (Komander et al., 2009B). As is standard for cysteine proteases, the catalytic histidine acts to deprotonate the catalytic cysteine (promoted by hydrogen-bonding with aspartate/asparagine), which exerts nucleophilic attack on the (iso)-peptide bond and forms a thioester intermediate, and is subsequently hydrolysed (Verma et al., 2016).

The USP domain adopts a conserved structure consisting of three domains – an array of β-sheets known as the fingers, a β-sheet core termed the palm and an α-helical thumb domain, which together create a binding pocked for ubiquitin between the palm and thumb regions and at the tip of the fingers, first shown in USP7 (HAUSP) (Figure 1-12) (Hu et al., 2002). USP domains contain six conserved regions (termed boxes) that define them, which are interspersed by insertions in loop regions that lead to a wide range of USP domain sizes, while not affecting regions of secondary structure. Box 1 and 2 form the thumb, box 3 and box 4 form the fingers, and box 5 and box 6 form the palm (Ye et al.,

2009). Specificity can be controlled entirely through the core USP domain, as is the case for USP18, which despite its relatively small size, and lack of any other functional domains, specifically recognises its substrate ISG15 (a ubiquitin-like protein). This is achieved through ISG15-binding *via* a key hydrophobic patch in an ISG15-binding box that forms contacts with a hydrophobic region specific to ISG15 (Basters et al., 2017). USPs also often contain ubiquitin-like-domains (UBLs), which resemble ubiquitin, and can have various functions. USP14 associates with the proteasome through its UBL (M. Hu et al., 2005). UBLs can also have effects on catalysis such as in the case of USP7, which contains five consecutive UBL domains, the last two units of which promote ubiquitin-binding and catalysis through interaction with the catalytic domain, switching USP7 from an inactive to active state (Faesen et al., 2011).

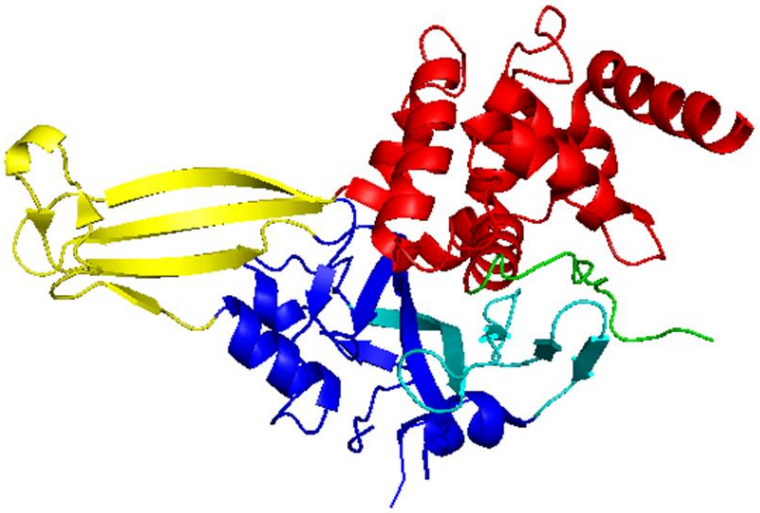

Figure 1-12: Crystal structure of USP7 USP domain (207-553). Consists of several subdomains - the thumb (red), the fingers (yellow), the palm (blue) and the catalytic cleft, consisting of Cys box (green) and His box (cyan). A cleft running through the palm and thumb permits ubiquitin docking and isopeptide bond hydrolysis. Structure taken from (M. Hu et al., 2002) - PDB 1NB8 – re-rendered with PyMOL.

1.3 Possible DUB candidates for ELK-1 deubiquitination

During this study, work was carried out to identify the DUB responsible for deubiquitinating ELK-1. Preceding experimental work, an extensive manual review of the literature identified several possible DUBs that could act on ELK-1 (Peter Shaw, personal communication). Candidate DUBs were selected based on overlapping tissue expression profiles and subcellular localisation with that

of ELK-1, and particularly functional implications in cell cycle progression and proliferation. Through this, five DUBs were selected for analysis experimentally, all of which belonged to the USP family of DUBs. These were USP7, USP9X, USP17, USP22 and USP44. Through experimental work, USP17 was found to be a DUB for ELK-1 (6.1). The following is a brief overview of each of the selected DUBs, followed by a more detailed section outlining USP17.

1.3.1 USP7

USP7, or herpesvirus-associated ubiquitin-specific protease (HAUSP), is a nuclear-residing protein (Fernández-Montalván et al., 2007) that controls levels of p53 by forming a complex with the E3 ligase MDM2, preventing its auto-polyubiquitination and turnover by the proteasome (Fang et al., 2000; Meulmeester et al., 2005). This is achieved by a specific isoform of USP7 (USP7S), that is stabilised by phosphorylation by CK2 (Khoronenkova et al., 2012). MDM2 polyubiquitinates and degrades p53 (Kubbutat et al., 1997) so USP7 depletion allows stabilisation of p53, leading to cell cycle arrest (Cummins & Vogelstein, 2004). It has also been suggested that USP7 overexpression promotes cell proliferation in small cell lung cancer by deubiquitinating and stabilising the nuclear protein Ki-67 (C. Zhang et al., 2016). USP7 is implicated in the DNA damage response by deubiquitinating and stabilising the E3 ligase RNF168, which polyubiquitinates histone H2A with K63 chains and recruits TP53BP1 and BRCA1 at sites of single/double strand DNA

breaks (Doil et al., 2009; Q. Zhu et al., 2015). Through this, USP7 also promotes cell-cycle arrest, rather than proliferation.

1.3.2 USP9X

The X-linked DUB USP9X (or fat facets in mouse (FAM)) is important in neuronal cells, where it localises to the axonal growth cones. In addition, its truncation/mutation has been associated with intellectual disability through reduced axonal growth and neuronal cell migration (Tarpey et al., 2009; Homan et al., 2014). Knockdown of USP9X in human neural progenitor cells caused cell cycle arrest in G0. This was found to be due to a decrease in mTORC1 signalling, as USP9X stabilises the mTORC1 protein RAPTOR by deubiquitination of polyubiquitin chains, and in doing so promotes cell cycle progression by increasing mTORC1 signalling (Bridges et al., 2017). USP9X has been shown to influence TGF-β signalling by removing monoubiquitin from SMAD4, with USP9X depletion abrogating TGF-β-induced cell growth arrest and metastatic breast cancer cell line motility (Dupont et al., 2009). Another target for USP9X is the anti-apoptotic protein MCL1, which is deubiquitinated of polyubiquitin chains and protected from proteasomal degradation by USP9X activity, promoting cell survival (Schwickart et al., 2010). Furthermore - and most relevantly with regard to ELK-1 - USP9X has previously been shown to deubiquitinate polyubiquitin chains and prevent proteasomal degradation of the ETS family transcription factor ETS-1, driving its induction of N-RAS

expression and promoting cell proliferation and melanoma growth (Potu et al., 2017). In fact, USP9X has also been shown to stabilise another ETS protein, ERG, in a similar manner, linking the DUB to prostate cancer progression (S. Wang et al., 2014).

1.3.3 USP22

USP22 is localised to the nucleus (Xiong et al., 2014), and is present within the transcriptional co-activator SPT-ADA-GCN5 (SAGA) complex, where it catalyses the deubiquitination of monoubiquitinated histones H2A and H2B and contributes to chromatin remodelling, regulation of gene activation and cell-cycle progression (Joo et al., 2007; Y. Zhao et al., 2008). Activity of USP22 is limited by its access to coactivator proteins ATXN7L3 and ENY2, which it competes for with two non-SAGA associated DUBs, USP27X and USP51 (Atanassov et al., 2016). The proto-oncogene MYC recruits USP22 to target gene promoters and is required for its transcriptional activity, with USP22 knockdown resulting in both inhibition of MYC-induced malignant cell transformation and cell cycle arrest in G1 (X. Zhang et al., 2008). The HDAC SIRT1 is stabilised by USP22 deubiquitination of polyubiquitin chains, allowing deacetylation activity on p53 and antagonising its transcriptional activity and downstream apoptosis induction, linking USP22 function directly to cell cycle progression (Z. Lin et al., 2012). USP22 also removes K63-linked polyubiquitin chains from FBP1, allowing it to bind and repress target genes such as the cell-

cycle inhibitor *p21*, further associating USP22 with cell proliferation (Atanassov & Dent, 2011).

1.3.4 USP44

USP44 is a predominantly nuclear DUB whose stability is cell cycle regulated when ectopically expressed in MEFs, with highest protein levels during G1/S, declining *via* degradation by the proteasome through to mitosis (Y. Zhang et al., 2011). USP44 acts as an inhibitor of the anaphase promoting complex/cyclosome (APC/C), causing stabilisation of cyclin B1 and reinforcing the mitotic checkpoint by promoting complex formation between the spindle checkpoint protein MAD2 (a component of the mitotic checkpoint complex (MCC)) and CDC20 (Y. Zhang et al., 2011). This control over anaphase entry had previously been attributed to CDC20 deubiquitination by USP44 preserving its interaction with the MCC and preventing premature mitotic progression (Stegmeier et al., 2007), although this has been brought into question by evidence showing that a lysine-less mutant of CDC20 could nonetheless activate the APC/C and mitosis (Nilsson et al., 2008). Like USP22, USP44 functions as part of a complex, the nuclear receptor co-repressor (N-CoR) complex, and also deubiquitinates histone H2B of monoubiquitin (G. Fuchs et al., 2012; Lan et al., 2016). Unlike USP22 and the SAGA complex, however, USP44 deubiquitination of H2B is associated with target gene repression through N-CoR recruitment of HDACs (Ishizuka & Lazar, 2003). USP44 depletion

led to an increase in H2B monoubiquitination levels and abrogated breast cancer cell line MDA-MB-231 invasiveness (Lan et al., 2016).

1.3.5 USP17/DUB3

1.3.5.1 Overview and historical perspective

USP17, or DUB3, describes a multigene family of very similar proteins consisting of multiple copies in blocks of tandem repeats, which are highly copy-number variable (Alkan et al., 2009; Burrows et al., 2010). USP17/DUB genes were first discovered in mice and named *Dub1*, *Dub1a, Dub2* and *Dub2A*, and their expression was found to be induced in response to cytokines such as IL-2 and IL-3 (Y. Zhu et al., 1996; Y. Zhu et al., 1997; Baek et al., 2001; Baek et al., 2004). All of these, and other members identified as part of the DUB subfamily are localised to chromosome 7 in mice, thought to be as a result of tandem duplication events (Y. Zhu et al., 1997; Burrows et al., 2010). A tandemly repeated megasatellite sequence (named RS447) on human chromosome 4 was found to harbour an open reading frame (ORF) with high homology to both murine *Dub1* and *Dub2* (Gondo et al., 1998). This was later found to be an intron-less gene encoding an active deubiquitinating enzyme that was named USP17 (Saitoh et al., 2000).

Discovery of multiple genomic sequences on human chromosomes 4 and 8 with homology to the murine DUB genes led to the cloning of a deubiquitinating

enzyme with similar cytokine inducibility, that was named DUB3 (Burrows et al., 2004). Both DUB3 and USP17 reside within RS447, which has a copy number varying from 20-103, mostly on chromosome 4 with some minor sequences also present on chromosome 8 (Okada et al., 2002). Multiple other USP17-like genes were later identified spread across chromosomes 4 and 8 as part of this highly polymorphic megasatellite repeat (Burrows et al., 2005). It has since been shown that some USP17-like repeats on chromosome 8 exist in the copy number variable beta-defensin gene cluster, which is likely to influence the variation in RS447 (and hence USP17-like genes) copy number in addition to any tandem duplication events (Burrows et al., 2010). The ancestral sequence of *DUB3/USP17* has gone through independent duplication events in all species it has been studied in (including human, mouse, rat, dog, cow and chimpanzee), probably due to it originating in an inherently unstable genomic region prior to species divergence, although some duplication events in humans and chimpanzees appear to have occurred before their divergence (Burrows et al., 2010). Next-generation sequencing of three human genomes gave a *USP17/DUB3* copy number of between 122-186, highlighting the genetic variability and complexity of these genes (Alkan et al., 2009).

1.3.5.2 Domain structure

Due to their high sequence similarity, USP17-like proteins will be referred to collectively as USP17. USP17 possesses the characteristic USP domain that defines this family of DUBs. However, USP17 lacks obvious UBDs common to USPs, such as UBL and UBA domains (Komander et al., 2009B). The USP domain contains the catalytic triad of cysteine (C89), histidine (H334) and aspartate (D350) separated into a Cys box (C89) and His box (H334 and D350) respectively (Hjortland & Mesecar, 2016). Human USP17 possesses carboxyl-terminal hyaluronan binding motifs (HABMs)(R/K)X7(R/K), which are not present in the murine DUB family members (Figure 1-13). Hyaluronan is a non-sulphated glycosaminoglycan that is a component of the extracellular matrix, but can also be intracellular (Evanko & Wight, 1999). USP17 HABMs have been implicated in the induction of apoptosis through interaction with intracellular hyaluronan (Shin et al., 2006). The apparent nucleolar localisation of full length USP17 matches that of hyaluronan within cells (Evanko & Wight, 1999; Shin et al., 2006). Endogenous USP17 has also been shown to be distributed throughout HeLa cells, and to co-localise with its substrate RCE1 at the endoplasmic reticulum (ER) (Burrows et al., 2009). USP17 distribution throughout HeLa cells with particular abundance in the nucleus was also observed in another study (Ramakrishna et al., 2011).

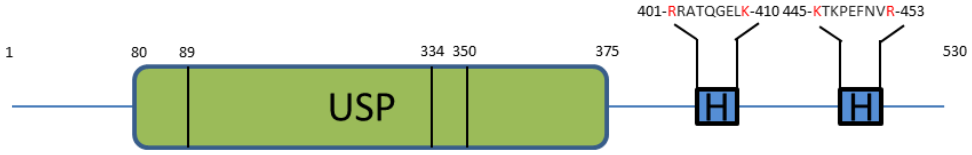

Figure 1-13: Schematic of USP17 domain structure (human). USP domain contains catalytic triad C89, H334 and D350. Hyaluronan binding sites are highlighted (H), with arginine and lysine residues key to interaction highlighted in red. Produced with reference to (Hjortland & Mesecar, 2016).

1.3.5.3 Polyubiquitin chain topology specificity of USP17

Thus far, USP17 has been shown to mostly hydrolyse polyubiquitin chains, with no established specificity over chain topology *in vivo*. Most commonly, USP17 is associated with protecting targets from proteasomal degradation by disassembling attached K48-linked polyubiquitin chains (Pereg et al., 2010; C. Song et al., 2017), but it has also been shown to target non-proteolytic K63-linked polyubiquitin chains (Burrows et al., 2009; Ramakrishna et al., 2011). The cytokine and transcription factor IL-33 is cleaved of both K48 and K63-linked polyubiquitin chains through USP17 activity (Ni et al., 2015), which is also the case for the hyaluronan synthesizing enzyme HAS2 (Mehić et al., 2017). USP17 was also shown to remove monoubiquitin from histone H2AX (Delgado-Diaz et al., 2014). *In vitro* deubiquitination assays have found that USP17 effectively cleaves various di-ubiquitin (K11, K33, K48 and K63) and tetra-ubiquitin chains

(K11, K48 and K63), while only partially processing other di-ubiquitin substrates (K6, K27 and K29), and having no effect on linear di-ubiquitin. This study also found that USP17 exhibits high catalytic efficiency and activity, and clarified that the DUB is monomeric in solution (Hjortland & Mesecar, 2016). Recently, it was discovered that USP17 activity is partially regulated through phosphorylation by CDK4/6. Phosphorylation at S41 appears to be important for USP17 catalytic activity, as S41A mutation impaired substrate deubiquitination (Liu et al., 2017).

1.3.5.4 Cell cycle regulator

Expression of USP17 is induced by cytokines IL-4 and IL-6, and constitutive overexpression of the DUB inhibits cell proliferation (Burrows et al., 2004), although this also true of its endogenous depletion (McFarlane et al., 2010). USP17 expression is cell-cycle regulated, being highly expressed during G1-S transition, and its depletion impairs RAS and RHOA activation, preventing cells from transitioning from G1-S phase (McFarlane et al., 2010). Control over RAS activation was shown to be due to the deubiquitination of K63-linked polyubiquitin chains from RAS-converting enzyme 1 (RCE1) by USP17, independent of the UPS (Figure 1-14) (Burrows et al., 2009). Prior to plasma membrane translocation, RAS must be modified by a farnesyl lipid moiety in its carboxyl-terminus CAAX (C= modified cysteine) motif at the ER, in a process termed prenylation (Casey et al., 1989). Following this, the -AAX following the

prenylated cysteine is removed through proteolysis, carried out by RCE1, before methylation of the carboxyl group of the modified cysteine and trafficking to the membrane (Boyartchuk, 1997; Otto et al., 1999; Choy et al., 1999). When overexpressed, USP17 abrogated RCE1 catalytic activity through deubiquitination, preventing RAS localisation to the plasma membrane and inhibiting ERK signalling (Burrows et al., 2009). This affected both H-RAS and N-RAS, but not K-RAS (De La Vega et al., 2010). However, paradoxically, USP17 depletion also impaired RAS translocation to the plasma membrane, suggesting that USP17 is also a requirement for ERK activation (McFarlane et al., 2010).

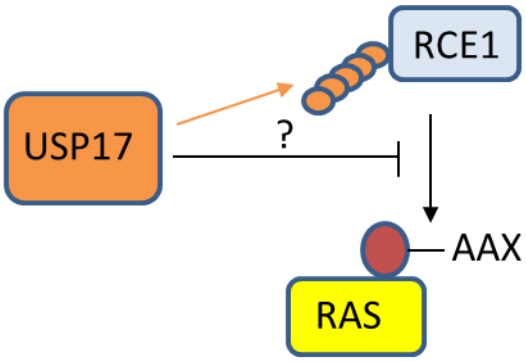

Figure 1-14: At the ER, RAS is prenylated (dark red circle) at its carboxyl-terminal CAAX box (C= cysteine, A= aliphatic amino acid, X= any amino acid). The AAX is cleaved by RCE1, before the prenylcysteine carboxyl group is methylated, and RAS is trafficked to the plasma membrane. RCE1 is ubiquitinated by K63-linked polyubiquitin chains (orange circles), and ectopic USP17 expression negatively regulates RCE1 activity (through deubiquitination- orange arrow) and RAS localisation to the plasma membrane. However, USP17 depletion also negatively regulates RAS localisation to the plasma membrane.

USP17 also regulates SDS3, a critical subunit of the SIN3A-HDAC 1/2 co-repressor complex, binding to SDS3 through its carboxyl-terminal region. Through K63-linked polyubiquitin chain removal, USP17 negatively regulates SDS3-associated HDAC activity, leading to disrupted proliferation and apoptotic induction in HeLa cells overexpressing USP17, which could be partially rescued with concomitant SDS3 depletion (Ramakrishna et al., 2011). USP17 is further implicated in regulation of HDAC activity, through the protection of HDAC2 from UPS processing through removal of K48-linked polyubiquitin chains (H. Song et al., 2015).

Due to its involvement in the cell-cycle, USP17 is upregulated in a range of cancers (McFarlane et al., 2010). The mitotic-inducing phosphatase CDC25A is deubiquitinated and stabilised by USP17, allowing CDC25A to dephosphorylate CDK1 and activate the CDK1-cyclinB complex to drive forward the cell cycle. Hence, USP17 expression correlates positively with that of CDC25A in primary human breast tumours (Pereg et al., 2010). SMAD4 has also recently been shown to be a target of USP17, which was protected from proteasomal degradation by USP17 deubiquitination, promoting the invasiveness and proliferation of osteosarcoma (C. Song et al., 2017). However, low USP17 expression has also been linked to increased glioma tumorigenesis, where overexpression of USP17 led to reduced protein levels of RAS and MYC and attenuated cell proliferation, whereas low USP17 expression was more likely to present in high grade (stage III and IV) tumours (Hu et al., 2016).

1.3.5.5 Cell migration

USP17 has also been shown to have important functions in cell migration. Through this USP17 is also associated with cancer metastasis, as non-small cell lung cancer (NSCLC) cell lines were found to express *USP17* mRNA to high levels, and its depletion resulted in a reduction of MMP3 and MMP9 protein levels along with reduced invasiveness (McFarlane et al., 2013; S. Zhang et al., 2016). NSCLC progression has also been linked to USP17 through its deubiquitination and stabilisation of HAS2 (Mehić et al., 2017). Regulation of several motility-associated GTPases is also mediated through USP17. As well as RHOA, both CDC42 and RAC are also mis-localised following USP17 knockdown, and this also inhibits both amoeboid and mesenchymal cellular migration through impaired cytoskeletal rearrangements of actin and tubulin polymerisation (de la Vega et al., 2011). USP17 also promotes breast cancer metastasis through its stabilisation of the transcription factor SNAIL1, a key driver of epithelial-mesenchymal transition (EMT) (Liu et al., 2017; Y. Wu et al., 2017). Epithelial cells going through EMT lose cell polarity and cell-cell adhesion and become migratory mesenchymal cells, and USP17 promotes this process through SNAIL1, exemplified by the high protein levels of USP17 and SNAIL1 in tissue samples from metastatic breast cancers (Y. Wu et al., 2017). This could relate to the stabilisation of HAS2 by USP17, as high hyaluronan production can also positively regulate EMT through *SNAIL1* induction (Chanmee et al., 2014; Mehić et al., 2017).

1.3.6 Studying ubiquitination using mass spectrometry

The challenge of studying potentially very small populations of transiently ubiquitinated protein is a considerable one, which justifies the overexpression of substrates and ubiquitin in order to study these modifications. However, more tools are being developed for enriching ubiquitinated proteins and polyubiquitin chains, such as the engineering of UBDs for ubiquitin purification, and the availability of commercially-available specific polyubiquitin chain topology antibodies, making study of such populations more amenable (Hjerpe et al., 2009; Strachan et al., 2012; Scott et al., 2015). As mass spectrometry becomes a more and more powerful tool for quantifying ubiquitination events, far more information can be gleaned on the nature of these modified species (G. Xu et al., 2010; Olsen & Mann, 2013).

A prominent MS/MS method for studying ubiquitination sites and polyubiquitin chain linkages is through bottom-up, data-dependent shotgun proteomic analyses. During ubiquitination, the carboxyl-terminal glycine of ubiquitin covalently attaches to a target lysine. Upon trypsin digestion, peptides with a characteristic di-glycine stub are produced, as an arginine residue in ubiquitin (R74) precedes the caboxyl-terminal glycines (G75, G76) covalently attached to the digested target protein. The ubiquitinated lysine is itself refractory to trypsinisation, leaving a GG moiety that can be identified through MS/MS on digested peptides due to the mass difference of 114 Daltons, allowing

identification of ubiquitination sites (G. Xu et al., 2010)(Figure 1-15). MS/MS employs two mass spectrometers, whereby ion formation precedes mass-to-charge ratio separation by the first mass spectrometer, followed by fragment ion production from selected precursor (parent) ions. The resulting fragment (daughter) ions are then separated and detected in a second mass spectrometer, allowing an appraisal of chemical composition, and in this case diglycine modification sites.

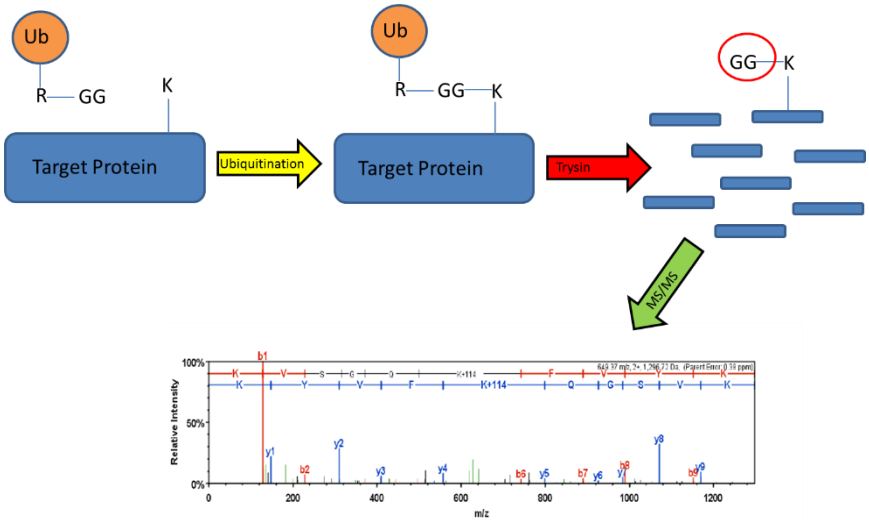

Figure 1-15: Trypsin digested protein yields peptides. At sites of ubiquitination a signature GlyGly moiety remains., which can be identified by MS/MS. This also applied to polyubiquitin chains.

1.4 Research aims and objectives

Previous work had shown that ELK-1 was both monoubiquitinated (Chow, PhD thesis, University of Nottingham, 2010) and polyubiquitinated (S. Fuchs et al., 1997; Chow, PhD thesis, University of Nottingham, 2010; Evans et al., 2011; Teixeira et al., 2013). The aim of this project was to develop a greater understanding of the molecular mechanisms underpinning these post-translational modifications on ELK-1, and how they impinged on ELK-1 transcriptional activity. This was achieved through proteomic approaches to clarify sites of ubiquitination in ELK-1 (Chapter 4), followed by experiments to determine the effects of mitogens on monoubiquitination and how this relates to ELK-1 phosphorylation (Chapter 5). Experimental work was carried out on the regulation of ubiquitinated ELK-1 disassembly, leading to the identification of the DUB responsible for removal of both monoubiquitin and polyubiquitin chains from ELK-1 (Chapter 6). Lastly, the effects of ELK-1 monoubiquitination were observed in a cellular context, considering the influence of this post-translational modification on ELK-1 target gene expression and cellular proliferation (Chapter 7).

2 Materials

2.1 Antibodies

Table 2-1: Antibodies used. For source, R = rabbit, M = mouse, r = rat, P = pig

Antibody (Source)	**Code**	**Provider**
ELK-1 (R)	H160 (SC-22804)	Santa Cruz
ELK-1 (R)	I20	Santa Cruz
ELK-1 (R)	9182	Cell Signalling
ELK-1 (R)	ELKC	*In house*
ELK-1 (R)	E277	Abcam
phospho-ELK-1 (S383) (R)	9181	Cell Signalling
ERK2 (R)	C14 (SC-154)	Santa Cruz
phospho-ERK (T202/Y204) (M)	9106S	Cell Signalling
H-RAS (M)	R02120	BD Biosciences
C-RAF (M)	R19120	BD Biosciences
HA-HRP (r)	3F10 (11867423001)	Roche
His (M)	MCA1396GA	ADB Serotec
V5 (R)	AB3792	Millipore
MYC (M)	SC-40	Santa Cruz
FLAG (M)	M2	Sigma Aldrich
USP7 (R)	A300-033A	Bethyl
USP17L2/DUB-3 (R)	PA5-44961	Invitrogen
USP17 (R)	SAB1306139	Sigma Aldrich
USP17L24 (R)	AP5491b	Abgent
FBXO25 (M)	AB57051	Abcam
Actin (M)	AC-15	Sigma Aldrich
PARP (R)	550429	BD Biosciences
Tubulin (M)	SC-8035	Santa Cruz
Ubiquitin (M)	VU1	Life Sensors
K48-polyubiquitin chains (R)	APU2	Millipore
K63-polyubiquitin chains (M)	HWA4C4	Enzo Life Sciences
Mouse-HRP (R)	P0260	Dako
Rabbit-HRP (P)	P0217	Dako

2.2 Mammalian expression/knockdown vectors

Table 2-2 Plasmids used in this study. All plasmids contain ampicillin resistance cassettes

Target	**Vector**	**Source**
His-ELK-1	pCMV5	*In house*
HA-ELK-1	pCMV5L	*In house*
HA-ELK-1 ΔD/ FXLA	pCMV5L	*In house*
HA-ELK-1 S383/389A	pCMV5L	*In house*
HA-ELK-1	pcDNA3	Bob Hipskind, Montpellier
HA-ELK-1 K35R	pcDNA3	*In house*
ELK-1	pCMV5	*In house*
HA-ELK-3	pCMV5L	*In house*
HA-ELK-4	pCMV5L	*In house*
HA-ubiquitin	pCMV5	Simon Dawson, Nottingham
His-Tyg-ubiquitin	pcDNA3	Gu Wei, New York
His-Tyg-ubiquitin K0	pcDNA3	*In house*
V12 H-RAS	pCMV5	Melanie Cobb, Dallas TX
C-RAF259D	pCMV5	Walter Kölch, Dublin
USP7 (WT + C>S)	pcI	Roger Everett, Glasgow
Flag-USP9x (WT + C>S)	pCMV TnT	Ralf Kittler, Dallas TX
Myc-USP17 (WT + C>S)	pcDNA3	Daniele Guardavaccaro, Utrecht
Flag-USP17 (WT + C>S)	pME18S	James Burrows, Belfast
V5-USP22 (WT + C>S)	pcDNA3.1	Sharon Dent, Smithville TX
HA-USP44 (WT + C>A)	pcDNA4	Neils Mailand, Copenhagen
His-HAND1	pcDNA3.1	This work (Appendix A)
MYC-FBX025	pCMV5	*In house*
psh#1 USP17	pSUPER	Daniele Guardavaccaro, Utrecht
psh#2 USP17	pSUPER	Daniele Guardavaccaro, Utrecht
psh#1 ELK-1	pSUPER	This work (Appendix B)
psh#2 ELK-1	pSUPER	This work (Appendix C)

2.3 shRNA target sequences

Table 2-3: Gene targets used for shRNA knockdown in this study

Name	**NCBI ref**	**Target (5'-3')**
psh#1 USP17	NM_201402.2	GCAGGAAGATGCCCATGAA
psh#2 USP17	NM_201402.2	GAATGTGCAATATCCTGAG
psh#1 ELK-1	NM_001114132.2	GGCCTTGCGGTACTACTAT
psh#2 ELK-1	NM_001114132.2	GCTTCCTACGCATACATTG

2.4 RT-PCR Probes and Primers

Table 2-4: TaqMan primers and probes used in this study

Gene	**Forward primer (5'-3')**	**Reverse primer (5'-3')**	**Taqman Probe (5'-3')**
CFOS	ACTACCACTCACCCGCAGAC	GTGGGAATGAAGTTGGCACT	CCTGTCAACGCGCAGGACTTCTG
EGR1	CAGCACCTTCAACCCTCAG	CAGCACCTTCTCGTTGTTCA	CTACGAGCACCTGACCGCAGAGTCTT
GAPDH	CTGCACCACCAACTGCTTAG	ACAGTCTTCTGGGTGGCAGT	CCCTGGCCAAGGTCATCCATG

2.5 Buffers and solutions

Table 2-5: Buffers and solutions used in this study. All were prepared in Milli-Q water unless otherwise specified. All chemicals were obtained from Sigma Aldrich unless otherwise specified.

Buffer	**Composition**
1. Buffer A (for SDS-PAGE)	1.1 M Tris, 0.1% (w/v) SDS, 30% (v/v) glycerol (pH 8.8)
2. Buffer B (for SDS-PAGE)	1.1 M Tris, 0.1% (w/v) SDS (pH8.8)
3. Co-IP buffer	40 mM HEPES, 1% (v/v) NP-40, 150 mM KCl, 5mM $MgCl_2$, 0.5 mM EDTA, 0.5 mM DTT (pH 7.9)
4. Coomassie destain	10% (v/v) methanol, 10% (v/v) glacial acetic acid
5. Coomassie stain	50% (v/v) methanol, 20% (v/v) glacial acetic acid, 0.12% (w/v) Coomassie Brilliant Blue R-250
5. Digestion buffer	0.1 M ammonium bicarbonate, 2 M urea, 5% (v/v) acetonitrile (pH8.0)
6. DNA loading dye (6X)	0.25% bromophenol blue, 0.25% (w/v) xylene cyanol FF, 15% (w/v) Ficoll
7. Electrode buffer	0.025 M Tris, 0.19 M glycine, 0.1% (w/v) SDS
8. Gel-loading buffer (2X) (SDS-PAGE)	0.15 M Tris, 8 M urea, 2.5% (w/v) SDS, 20% (v/v) glycerol, 10% (v/v) 2-mercaptoethanol, 3% (w/v) DTT, 0.1% (w/v) bromophenol blue (pH 6.8)
9. Gel-loading buffer (2X) (On-bead IMAC-samples)	0.12 M Tris, 4% (w/v) SDS, 20% (v/v) glycerol, 5% (v/v) 2-mercaptoethanol, 0.1% (w/v) bromophenol blue, 200 mM imidazole (pH 6.8)
10. HBS (2X)	50 mM HEPES 280 mM NaCl, 1.5 mM Na_2HPO_4 (pH 7.1)

Buffer (continued)	**Composition (continued)**
11. High salt buffer	20 mM HEPES, 420 mM NaCl, 20% (v/v) glycerol, (pH 7.9)
12. Hypotonic buffer (2X)	40 mM HEPES (pH 7.9)
13. Immunoblot blocking buffer	5% (w/v) Marvel milk powder/BSA, TBS-Tween (0.05% v/v)
14. Inoue transformation buffer	10 mM PIPES, 55 mM $MnCl_2.4H_2O$, 15 mM $CaCl_2.2H_2O$, 250 mM KCl, (pH 6.7)
15. LB agar	10 g/L tryptone, 5 g/L yeast extract, 10 g/L NaCl, 15 g/L agar, 2.5 g/L select agar
16. LB broth	10 g/L tryptone, 5 g/L yeast extract, 10 g/L NaCl
17. MTT solution	0.5% (w/v) thiazolyl blue tetrazolium bromide in sterile PBS
18. MTT solvent	4 mM HCl, 0.1% NP-40 (v/v) in isopropanol
19. Ponceau S	0.1% (w/v) Ponceau S, 10% (v/v) glacial acetic acid
20. RIPA buffer	50 mM Tris, 150 mM NaCl, 1% (v/v) Triton x-100, 0.5% (w/v) sodium deoxycholate, 0.1% SDS, 1 mM EDTA, (pH 8.0)
21. Stacking buffer	0.14 M Tris, 0.1% (w/v) SDS (pH 6.8)
22. TAE buffer	40 mM Tris-acetate, 1 mM EDTA (pH 8.0)
23. TBS	20 mM Tris, 150 mM NaCl (pH 7.5)
24. Ubiquitination assay lysis/ wash buffer 1	0.01 M Tris, 0.1 M Na_2HPO_4/NaH_2PO_4, 6 M guanidinium-HCl, 10 mM imidazole, 10 mM β-mercaptoethanol (add fresh)(pH 8.0)

Buffer (continued)	**Composition (continued)**
25. Ubiquitination assay wash buffer 2	0.01 M Tris, 0.1 M Na_2HPO_4/NaH_2PO_4, 8 M urea, 10 mM β-mercaptoethanol (add fresh)(pH 8.0)
26. Ubiquitination assay wash buffer 3	0.01 M Tris, 0.1 M Na_2HPO_4/NaH_2PO_4, 8 M urea, 10 mM β-mercaptoethanol (add fresh)(pH6.3)
27. Western transfer buffer	25 mM Tris, 192 mM glycine, 20% (v/v) methanol

3 Methods

3.1 DNA techniques

3.1.1 Polymerase chain reaction

The polymerase chain reaction (PCR) was used to amplify plasmid DNA for cloning purposes. This was carried out in a 50 µl reaction containing:

- 10 µl 5X Q5 reaction buffer
- 1 µl 10 mM dNTPs
- 2.5 µl 10 µM forward primer
- 2.5 µl 10 µM reverse primer
- 100 ng template plasmid DNA
- 0.5 µl Q5 high fidelity DNA polymerase (New England Biolabs)
- 10 µl 5x Q5 high GC enhancer
- Nuclease-free water to 50 µl

A typical thermal cycling program for a small PCR amplicon (<1 kb) is shown below, carried out using a Sensoquest thermocycler (Geneflow):

1. Initial Denaturation - 98^{o}C for 30 secs
2. Denaturation - 98^{o}C for 10 secs
3. Annealing - 60^{o}C for 30 secs
4. Extension - 72^{o}C for 10 secs
5. Final extension – 72^{o}C for 2 minutes

25x cycles for step 2-4

3.1.2 Taq polymerase tailing

For TA cloning, Taq polymerase tailing (adding an Adenine residue) of PCR products was necessary. To the PCR product was added 1 ul Taq polymerase and incubated at 72^{o}C for 10 minutes. TA cloning was carried out using a TA cloning kit (Thermo Fisher Scientific).

3.1.3 Restriction digests

Between 0.5 µg-1 µg plasmid DNA was digested using 2.5-5U of each restriction enzyme in either a single or double digestion, including a 10X reaction buffer

optimum for the enzymes used in a total volume of 10-25 µl. Reactions were incubated in a water bath at 37^{o}C for 1-2 hours.

3.1.4 Agarose gel electrophoresis

Agarose gels containing 1-2% agarose (either electrophoresis grade or cloning grade depending on application) dissolved in TAE buffer (22) were used to resolve DNA. Samples were supplemented with 6X DNA loading dye (6), which were loaded onto the gel alongside ƛ (564-21,226 bp) and/or pUC8 (80-586 bp) DNA ladders (New England Biolabs). Samples were resolved at 100 V until the dye front reached the bottom of the gel, and the gel was post-stained by incubation in 0.5 µg/ml ethidium bromide for 10 minutes. Stained DNA was visualised using a UV imager (Syngene).

3.1.5 Gel excision and extraction

DNA bands were excised from agarose gels on a UV transilluminator with a clean scalpel. Gel extraction was carried out with a QIAquick Gel Extraction (Quiagen) according to the manufacturer's protocol, with final elution in 30 µl elution buffer. Quantity and quality of DNA was assessed by Nanodrop 2000c UV/IV spectrophotometer (Thermo Fisher Scientific).

3.1.6 DNA Ligations

DNA ligations were set up in a total volume of 25 µl including 1U T4 ligase (New England Biolabs), 2.5 µl 10X buffer, 50 ng vector DNA and sufficient insert DNA to give a 3:1 insert to vector molar ratio (calculated using NEBioCalculator v1.6.0 (New England Biolabs). Ligations were incubated overnight at 4^{o}C.

3.2 Bacterial techniques

All microbiological techniques were carried out using *Escherichia coli* NM522 or XL-10 Gold.

3.2.1 Bacterial Transformation

3.2.1.1 Plasmid DNA

For plasmid transformation into bacteria, 80 µl home-made competent NM522 cells were added to 1 µg of desired plasmid, followed by incubation on ice for 20 minutes. Cells were then heat shocked at 42^{o}C for 45 seconds, before addition of 900 µl LB (16) and incubation at 37^{o}C with shaking for 30 minutes. 10% of resultant cell suspension was plated onto LB agar (15) with ampicillin (100 µg/ml) and incubated at 37^{o}C overnight.

3.2.1.2 Ligation reactions

From a 25 µl ligation reaction, 10 µl was transformed into either NM522 or XL-10 Gold *Escherichia coli* ultra-competent cells. XL-10 Gold were used when NM522 were insufficiently competent to produce clonal colonies. Method was otherwise identical to (3.2.1.1) except entire cell suspension (rather than 10%) was grown on LB agar (15) with ampicillin (100 µg/ml).

3.2.2 Plasmid purification

3.2.2.1 Small-scale (Miniprep)

The day before plasmid purification, 10 ml LB (16, containing 100 µg/ml ampicillin) was inoculated with NM522 *Escherichia coli* containing the construct of interest (either from an individual colony on an LB-agar plate or a glycerol stock) and grown with shaking at 37^{o}C overnight. The following morning plasmid preparations were carried out using a QIAprep Spin Mini-prep kit (Qiagen) as per manufacturer's recommendations, with DNA quantity and quality assessed by Nanodrop 2000c UV/IV spectrophotometer (Thermo Fisher Scientific).

3.2.2.2 Large scale (Maxiprep)

The day before purification, 200 ml LB (16, containing 200 µg/ml ampicillin) was inoculated with NM522 *Escherichia coli* containing the construct of interest (either from colony on LB-agar plate or glycerol stock) and grown with shaking at 37^{o}C overnight. The following morning plasmid preparations were carried out using a Nucleobond AX PC500 kit (Macharey-Nagel) kit as per manufacturer's recommendations, with DNA quantity and quality assessed by Nanodrop 2000c UV/IV spectrophotometer (Thermo Fisher Scientific).

3.2.3 Glycerol stock preparation

Glycerol stocks were prepared by taking 500 µl of an overnight culture in LB - ampicillin (100 µg/ml) of NM522 or XL-10 Gold *Escherichia coli* carrying the plasmid of interest and combining this with 500 µl of 30% v/v glycerol (filter sterilised) in a cryo-vial. These were then suitable for long-term storage at -80^{o}C.

3.2.4 Inoue method – Competent cell preparation

Ultra-competent XL-10 gold *Escherichia coli* were prepared using the Inoue method, with all centrifugation steps carried out at 2500xg for 10 minutes at 4^{o}C. LB (25 ml) was inoculated with 50 µl X-10 gold stock cells and grown for 6

hours at 37°C with shaking, after which 3 x 250 ml LB (16) were inoculated with 2, 4 and 10 ml from this starter culture respectively and grown with shaking at 18°C overnight. The following morning, OD_{600} of each culture was read on a spectrophotometer every 30 minutes until a culture reached 0.55. This was then incubated in an ice water bath for 10 minutes, and at this point the other two cultures were discarded. Cells were harvested by centrifugation, medium was discarded and the centrifuge tube was up-ended on a paper towel for 2 minutes to remove residual medium. Cells were resuspended in 80 ml ice-cold Inoue transformation buffer (14, filter sterilised) by swirling, harvested by centrifugation and dried on paper towels as before. Cells were then resuspended in 20 ml ice-cold Inoue buffer by swirling, 1.5 ml DMSO was added and mixed and cells were left on ice for 10 minutes. Cells were then aliquoted into Eppendorf tubes (500 µl), snap frozen in liquid nitrogen and stored at -80°C.

3.3 Eukaryotic cell culture

3.3.1 Thawing cells

Human cell lines (stored at either -80°C or in liquid nitrogen) were thawed as quickly as possible in a 37°C water bath, and transferred to a 10 cm dish containing 10 ml pre-warmed growth medium. After cells had adhered to the dish (usually after an hour), the medium was exchanged for fresh medium.

3.3.2 Freezing cells for long term storage

When freezing down stocks to be stored at -80°C or in liquid nitrogen, a subconfluent dish (~80-90%) was trypsinised as normal for that cell line and resuspended in 10 ml of full medium. Cells were collected by centrifugation at 1000rpm for 5 minutes, the medium was removed and cells were resuspended in 1 ml 5% v/v DMSO in foetal bovine serum (FBS). Cells were then placed in an insulated box at -80°C overnight, and either stored at -80°C or transferred to liquid nitrogen the following day.

3.3.3 Cell starving and mitogen stimulation

Some experiments required cells to be starved and/or stimulated with mitogens. Starving consisted of keeping cells in growth medium supplemented with 0.5% v/v FBS (all cell lines used were grown in 10% FBS under normal circumstances) for 24 hours. In order to stimulate post-starvation, cells were treated with 15% v/v FBS and 100 ng/ml 12-*O*-tetradecanoylphorbol-13-acetate (TPA) for between 30 minutes and 2 hours before harvesting.

3.3.4 HEK293T cells

3.3.4.1 Maintenance

HEK293T cells were passaged every 3-4 days to a ratio of 1/10 in Dulbecco's modified Eagle's medium (DMEM), supplemented with 10% FBS, 100 U/ml penicillin and 100 µg/ml streptomycin. Cells were grown at 37^{o}C in 7.5% CO_2. When passaged, cells were washed in 10 cm dish with 2x 5ml sterile PBS, very briefly washed with 1 ml 0.5x trypsin/EDTA and left at 37^{o}C for 5 minutes to allow cells to detach.

3.3.4.2 Transient transfection

Transient transfections were carried out using calcium phosphate co-precipitation and DNA prepared by maxiprep procedure (3.2.2.2). The day before transfection, 10 cm dishes of 80-90% confluent cells were passaged to a ratio of 1/8. On the day of transfection, 4 hours beforehand, media was changed for fresh full medium. A total of 10 µg DNA was required for each transfection. Added to this was 500 µl of 0.25 M calcium chloride (filter sterilised) with incubation on ice for 10 minutes, before 550 µl 2 x HBS (10, filter sterilised) was added dropwise with low speed vortexing, followed by a further a 20-minute incubation on ice. The entire mixture was pipetted onto plates, mixed, and returned to the incubator overnight. The following day, medium was removed, cells were washed twice with warm DMEM and replenished with

fresh full or starving medium, depending on experiment. Approximately 48 hours post-transfection, cells were harvested *via* scraping in ice cold PBS.

3.3.5 HeLa cells

3.3.5.1 Maintenance

HeLa cells were passaged every 3-4 days to a ratio of 1/12 in DMEM supplemented with 10% FBS, 100 U/ml penicillin and 100 µg/ml streptomycin. Cells were grown at 37^{o}C in 5% CO_2. When passaged, cells were washed with 2x 5 ml sterile PBS in 10 cm dish, trypsinised with 1 ml 0.5x trypsin/EDTA for 1 minute and left at 37^{o}C for 5 minutes to allow cells to detach.

3.3.5.2 Transient transfection

HeLa cells were passaged to 3x10^{5} cells/well in a 6-well dish post-trypsinisation (with the use of a Haemocytometer), 24 hours prior to transfection with TransIT-LT1 reagent (Mirus Bio). Transfection was carried out with 2.5 µg plasmid DNA as per manufacturer's instructions.

3.3.6 MTT assay

Twenty-four hours post-transfection HEK293T/HeLa cells were trypsinised, counted (using a Haemocytometer) and re-seeded into multiple 96-well plates

at a density of $2x10^3$ cells per well (4 wells per condition). Cell proliferation was monitored daily using MTT assay over 4 days. Each day, 20 µl of 3-(4,5-dimethylthiazol-2-yl)-2,5-diphenyltetrazolium bromide (MTT) solution (17, filter sterilised) was added to each well, and the cells were returned to the 37°C incubator for 3 hours. Following this, media was removed and cells were resuspended in 150 µl MTT solvent (18), incubated for 15 minutes at room temperature with agitation and mixed by pipetting, before absorbance was read (OD_{595}) using a Multiskan FC Microplate Photometer (Thermo Fisher Scientific).

3.3.7 Cell counting assay

Twenty-four hours post-transfection HEK293T cells were re-seeded into 24-well plates at a density of $1x10^4$ cells per well (using a Haemocytometer) and counted after 4 days using the Moxi Z Mini Automated Cell Counter (Orflo).

3.4 RNA techniques

All RNA solutions were made using DEPC-treated water

3.4.1 Total RNA extraction – TRIzol

HEK293T cells were harvested by scraping in 1 ml PBS on a 10cm dish, followed by centrifugation at 10,000rpm for 1 minute at 4^{o}C with supernatant discarded. To extract total RNA, 1 ml of TRIzol reagent (Thermo Fisher Scientific) was added to cell pellets and resuspended until dissolved, before 200 µl chloroform was added, mixed by shaking and centrifuged at 12,000xg for 15 minutes at 4^{o}C. The top, clear aqueous layer (500 µl) was transferred to a fresh Eppendorf tube (the interface and lower red organic layer were discarded) and 500 µl isopropanol was added, mixed and incubated for 10 minutes at room temperature, then centrifuged at 12,000xg for 10 minutes at 4^{o}C. The supernatant was discarded and pellets were washed with 1 ml 75% ethanol, before briefly mixing using a vortex, and centrifuging at 7,500xg for 5 minutes at 4^{o}C. Supernatants were removed and pellets were air dried for 10 minutes.

Pellets were resuspended in 30 µl of water and incubated on a heating block at 55^{o}C for 10 minutes. To this was added 2.5 µl RNase free DNase and 10 µl 10X reaction buffer, made up to 100 µl with water, and incubated for 10 minutes at room temperature. This was then supplemented with water to 400 µl, before

an equal volume of phenol/chloroform/isoamyl alcohol was added, thoroughly mixed and centrifuged at 10,000xg for 10 minutes at 4°C. The upper aqueous layer (350 µl) was transferred to a fresh Eppendorf tube and supplemented with 35 µl 3M sodium acetate (pH 5.2) and 700 µl absolute ethanol. Samples were incubated for 20 minutes at -20°C, before centrifuging at 14,000xg for 10 minutes at 4°C. The supernatant was discarded and the pellet was washed with 1 ml 75% ethanol and centrifuged again at 14,000xg for 10 minutes at 4°C. The Eppendorf tube was left open for 5 minutes to partially air dry before the sample was dissolved in 30 µl water. RNA quality and quantity were assessed by Nanodrop 2000c UV/IV spectrophotometer (Thermo Fisher Scientific).

3.4.2 mRNA enrichment

A sample of TRIzol extracted total RNA (2 µg) was supplemented with water to 20 µl, before being heated to 65°C for 2 minutes and then briefly kept on ice. mRNA enrichment was carried out using Dynabeads mRNA purification kit (Ambion) as per manufacturer's instructions, with a final elution volume of 14 µl.

3.4.3 First strand DNA synthesis

To the 14 µl mRNA sample obtained from Dynabeads were added 3 µl random primers (0.1 µg/µl stock), 1 µl 10 mM dNTPs and 2 µl water, which was then

incubated at 65^{o}C for 5 minutes followed by 1 minute on ice. Added to this (with mixing) was 4 ul 5X first strand buffer, 1 µl 0.1 M DTT, 1 µl RNase OUT and 1 µl superscript III reverse transcriptase (total volume ~27 µl)(Thermo Fisher Scientific). This was incubated sequentially at 25^{o}C for 5 minutes, 50^{o}C for 60 minutes and 70^{o}C for 15 minutes on a Sensoquest thermocycler (Geneflow).

3.4.4 Quantitative real-time polymerase chain reaction (qRT-PCR)

TaqMan probes were used for qRT-PCR, labelled with fluorophore 5'FAM and quencher 3'TAMRA (Thermo Fisher Scientific), where probes were targeted to a specific gene target sequence between a forward and reverse primer giving a total product of ~130 bp. A series of cDNA standards were prepared from all experimental samples, pooling 5µl of each sample together (SUPERNEAT) and diluting 1/4 to give the NEAT, before serial dilution of this to give 1/16, 1/64 and 1/256. cDNA unknowns were diluted 1/8 to fall within the standard curve from above standards, with 3 µl template required for each PCR reaction (carried out in triplicate) in a total volume of 13 µl containing:

- 6.5 µl TaqMan Fast Universal PCR Master Mix (2X) (Thermo Fisher Scientific)
- 0.375 µl 10 µM forward primer
- 0.375 µl 10 µM reverse primer
- 0.25 µl 10 mM probe
- 2.5 µl water
- (3 µl cDNA sample)

PCR master mixes were prepared (minus cDNA) and 10 µl aliquots were pipetted into 96 well plates, with cDNA subsequently added. Plates consisted of standards, cDNA unknowns, no template controls (NTC) and no reverse transcriptase controls (NRT) for each target gene – where NTC included water instead of cDNA and NRT included a sample from first strand synthesis including no superscript III reverse transcriptase. A typical plate setup is shown below with three unknown samples and two target genes (Table 3-1):

	1	2	3	4	5	6	7	8	9	10	11	12
A	Neat	Neat	Neat	1/4	1/4	1/4	1/16	1/16	1/16	1/64	1/64	1/64
B	1/256	1/256	1/256	NTC	NTC	NTC	NRT	NRT	NRT	U1	U1	U1
C	U2	U2	U2	U3	U3	U3						
D												
E	Neat	Neat	Neat	1/4	1/4	1/4	1/16	1/16	1/16	1/64	1/64	1/64
F	1/256	1/256	1/256	NTC	NTC	NTC	NRT	NRT	NRT	U1	U1	U1
G	U2	U2	U2	U3	U3	U3						
H												

Table 3-1: Typical plate setup for a qRT-PCR experiment, with two target genes (yellow and green). NTC = No template control, NRT = No reverse transcriptase control, U = Unknown

Samples were run on a StepOnePlus thermocycler (Applied Biosystems) on fast (40 minute) setting under the following cycling conditions:

1. Denaturation – 95^{o}C for 20 seconds
2. Annealing – 95^{o}C for 1 second
3. Extension – 60^{o}C for 20 seconds

50X cycles of step 2-3

By plotting log_{10} quantity for standards (where NEAT =1, 1/4 = 0.25 etc) against cycle threshold (CT), a standard curve was produced (relative standard curve method). This allowed the relative quantitation of unknown samples from their CT values, which were normalised against the housekeeping gene GAPDH.

3.5 Protein and proteomic techniques

3.5.1 Total protein extraction and quantification

Depending on size of pellet, cells were lysed in 200-500 µl RIPA buffer (20, filter sterilised and supplemented with 0.1% v/v mammalian phosphatase and protease inhibitor cocktails [Sigma Aldrich]) and rotated at 4^{o}C for 1 hour, before being centrifuged at 14,000rpm for 15 minutes at 4^{o}C, with the supernatant retained. For evaluation of protein concentration, the Bicinchoninic assay (BCA) (Pierce) was used according to the manufacturer's

instructions. OD_{595} was measured on a Multiskan FC Microplate Photometer (Thermo Fisher Scientific), giving a relative measurement of protein concentration when compared against a BSA standard curve.

3.5.2 SDS-PAGE and Immunoblot (Western blot)

Proteins were resolved by size through Sodium Dodecyl Sulphate Polyacrylamide Electrophoresis (SDS-PAGE), on gradient gels ranging from 5%-20% polyacrylamide (5% and 20% gels produced using buffer B (2) and A (1) respectively). Samples were resuspended in an equal volume of 2X SDS-PAGE gel-loading buffer (8), heated at 100^{o}C for 5 minutes, loaded onto SDS-PAGE gel alongside 3 µl BLUeye prestained protein ladder (Sigma Aldrich) and resolved at 80mA until the dye front reached the bottom of the gel. For qualitative evaluations of total protein content on gels, either Coomassie stain (5) followed by destaining was used (4), or silver stain through use of a PlusOne Silver staining kit (GE Healthcare) as per the manufacturer's guidelines.

For immunoblot, proteins were transferred to Amersham Protran nitrocellulose membrane (GE Healthcare) overnight *via* wet transfer in Western transfer buffer (27) at 40 mA. To confirm protein transfer was successful, Ponceau S (19) was used, after which membranes were blocked in immunoblot blocking buffer (13) for 1 hour, and following this were incubated in primary antibody (1/1000-1/50,000 in blocking buffer) for a minimum of 1 hour at room

temperature and a maximum of overnight at 4°C. Membranes were then washed 3X 6 minutes with TBS Tween (0.05% v/v) and incubated in 1/3000 secondary antibody in blocking buffer for 1 hour at room temperature, followed by a further 3 washes. Immunoblots were visualised on High performance chemiluminescence film (GE Healthcare) following a 1-minute incubation with Western Lightning Plus-ECL enhanced chemiluminesence (ECL) reagent (PerkinElmer) consisting a 1:1 ratio of luminol to peroxide.

3.5.3 ELK-1 ubiquitination assay – Immobilised Metal Affinity Chromatography (IMAC)

ELK-1 ubiquitination assays were carried out on HEK293T cells 48 hours post-calcium phosphate transfection. After cell harvesting, each plate of cells was resuspended in 1 ml of ice-cold PBS and separated into 20% (200 µl) and 80% (800µl) fractions. Cells were centrifuged at 10,000rpm for 1 minute at 4°C and PBS was discarded, before the 20% fraction was lysed in 200 µl RIPA buffer (20, filter sterilised and supplemented with 0.1% v/v phosphatase and protease inhibitor cocktails [Sigma Aldrich]) and protein content was assessed with BCA assay (Pierce). The 20% fraction was used as input lysate for immunoblot.

The 80% pellet was lysed in 800 µl lysis buffer (24) on rotator at 4°C for 1 hour, before twice sonicating (Jencons) for 10 seconds at amplitude 25 Hz and 80% power output. Lysates were then centrifuged at 14,000rpm 4°C for 15 minutes,

retaining supernatant. Ni-NTA Agarose beads (150 µl 50:50 suspension per sample) (Thermo Fisher Scientific) were washed once with an equal volume of PBS and twice with lysis buffer (24), and equilibrated with lysis buffer for 1 hour on rotator at 4^{o}C. To bead sample was added 500-100 µg total protein from lysed 80% pellet supernatant (deduced from previous BCA assay on 20% pellet) and rotated at room temperature for 2 hours.

Beads were then centrifuged at 2000rpm for 2 minutes, with the supernatant aspirated and discarded, and sequentially washed (with 5 minutes on rotor at room temperature) with 1 ml wash buffer 1 (24), wash buffer 2 (25), wash buffer 3 (26), wash buffer 4 (wash buffer 3 plus 0.2% Triton X-100) and wash buffer 5 (wash buffer 3 plus 0.1% Triton X-100). If experiment was a prelude to mass spectrometry, 30% of beads were resuspended in 50 µl 2X IMAC SDS-PAGE gel-loading buffer (9) for SDS-PAGE and 70% were retained for mass spectrometry. If experiment was purely for immunoblotting, all beads were resuspended in 50 µl 2X IMAC SDS-PAGE gel-loading buffer (9).

3.5.4 ELK-1 ubiquitination assay- Nuclear/cytoplasmic extracts

HEK293T cell nuclear and cytoplasmic extracts were produced by first washing cells with 5 ml ice-cold PBS, before a further wash with 1 ml hypotonic buffer (12, filter sterilised) and brief lysis on plate with 0.5 ml hypotonic buffer supplemented with 0.2% v/v NP-40 and 0.1% v/v mammalian phosphatase and

protease inhibitor cocktails (Sigma Aldrich) with scraping. Lysates were transferred to Eppendorf tube and quickly centrifuged at 14,000rpm at 4^{o}C for 20 seconds, with supernatant (cytosolic fraction) and pellet (nuclear fraction) separated and both retained. The cytosolic fraction was supplemented with NaCl to 120 mM, centrifuged at 14,000rpm at 4^{o}C for 15 minutes, with 10% taken for immunoblot input lysate and added to an equal volume of 2x SDS-PAGE gel-loading buffer (8), and the rest was retained for IMAC. Nuclear pellets were resuspended in 150 µl high salt buffer (11), rotated for 30 minutes at 4^{o}C and centrifuged at 14,000rpm at 4^{o}C for 15 minutes. An aliquot (10%) was taken for immunoblot input lysate and added to an equal volume of 2X SDS-PAGE gel-loading buffer (8).

For IMAC, entire nuclear and cytoplasmic extracts were resuspended in ubiquitination assay lysis buffer up to 1.5 ml (24), rotated at 4^{o}C for 30 minutes and sonicated (Jencons) twice for 10 seconds at amplitude 25 Hz and 80% power output. They were then transferred to Polypropylene columns (Quiagen) and 10 ml lysis buffer (24) was added. Nickel-Agarose beads were prepared as for (3.5.3) and added, and samples were rotated at room temperature for 2 hours. Columns were allowed to flow-through, and beads were transferred to Eppendorf tube with lysis buffer. Wash steps were then carried out as (3.5.3) and beads were resuspended in 50 µl 2X IMAC SDS-PAGE gel-loading buffer (9)

3.5.5 Tryptic digestion and tandem mass spectrometry

All steps of "on-bead" tryptic digestions of IMAC samples were carried out in digestion buffer (5, until peptide extraction) in Amicon Ultra centrifugal filters with a 10 kDa molecular weight cut off (Sigma Aldrich). Following resuspension of beads in 100 µl digestion buffer, samples were centrifuged for 5 minutes at 14,000rpm with flow-through discarded, and this process was repeated with a 400 µl wash of beads. To the samples was added 100 µl of 5 mM DTT and they were incubated in the dark for 30 minutes at 37^{o}C, before another centrifugation step as before. Following this, 100 µl 100 mM chloroacetamide was added and again incubated in the dark at 37^{o}C for 30 minutes and centrifuged. A further wash of 400 µl was then carried out, and samples were tryptically digested 3 times with 100 µl 0.02 mg/ml sequencing grade trypsin (Pierce) for a minimum of 4 hours per digestion at 37^{o}C. Peptides were extracted with successive washes of 300 µl 0.1% v/v TFA (in water) and 0.1% v/v TFA in 70% v/v acetonitrile, with 20 minutes incubation at 37^{o}C, followed by centrifugation with the flow-through retained.

Samples were evaporated to dryness on a vacuum centrifuge at 2000rpm overnight before being submitted to bottom-up MS/MS on a Linear Trap Quadrupole (LTQ)-Orbitrap-Velos spectrometer with nano-flow liquid chromatography (LC) (Thermo Fisher Scientific) (in collaboration with the University of Leicester PNACL). Identification of peptides was conducted in

data-dependent mode. The raw data file obtained from each LC-MS/MS acquisition was run against the UniProt human database. Data was analysed and GlyGly (+114, lysine), phosphoryl (+80, serine, threonine and tyrosine) and acetyl (+42, lysine) moieties were identified as variable modifications using Scaffold (Proteome Software), combining Mascot (Matrix Science) and X! (The GPM) tandem search engines to validate assigned spectra.

3.5.6 Co-immunoprecitation

Co-immunoprecipitation (Co-IP) experiments were carried out using HEK293T cells 48 hours post-calcium phosphate transfection. Cells were lysed on-plate with 1 ml Co-IP buffer (3, filter sterilised and supplemented with 0.1% v/v mammalian phosphatase and protease inhibitor cocktails [Sigma Aldrich]) followed rotation at 4^{o}C for 1 hour. They were then twice sonicated (Jencons) for 10 seconds at amplitude 25 Hz and 80% power output followed by centrifugation at 14,000rpm at 4^{o}C for 15 minutes, retaining supernatant. At this point 50 µl was resuspended in an equal volume of 2X SDS-PAGE gel loading buffer (8) for immunoblot input lysate. To the remainder was added 20 µl Protein A/G PLUS-Agarose (Santa Cruz Biotechnology) for preclearing, and samples were rotated at 4^{o}C for 2 hours. Beads were pelleted at 2000rpm at 4^{o}C for 2 minutes, with supernatant lysate retained and transferred to a fresh Eppendorf. Either 2 µg (10 µl) primary antibody or control IgG was added to samples and they were returned to rotator at 4^{o}C overnight.

The following morning, 20 µl Protein A/G PLUS-Agarose was added to samples, which were rotated at 4^{o}C for 2 hours. Beads were centrifuged at 4^{o}C for 2 minutes, with supernatant discarded, before being washed with 1 ml Co-IP buffer and returned to rotator at 4^{o}C for 10 minutes. Beads were again centrifuged, with supernatant discarded and washing step was repeated until samples had received 4 washes. Following removal of the final wash, beads were resuspended in 30 µl 2X SDS-PAGE gel loading buffer (8).

3.6 Statistical analyses

qRT-PCR, MTT and cell counting data are expressed as mean -/+ standard error of the mean (SEM). Figure legends identify statistical tests used to analyse data, carried out using GraphPad Prism 7 (GraphPad Software). Significance is reported in Figures by *p<0.05, **p<0.01, ***p<0.001 and ****p<0.0001.

4 Mapping of ubiquitination sites in ELK-1 by tandem mass spectrometry

4.1 ELK-1 is monoubiquitinated and polyubiquitinated *in cellulo*

It has previously been reported that ELK-1 can be polyubiquitinated and degraded by the 26S proteasome (Evans et al., 2011), and other work has also demonstrated a pool of monoubiquitinated ELK-1 in cells (Chow, PhD Thesis, University of Nottingham, 2010). Evidence of this post-translational modification was first documented *via* ubiquitination assays in HEK293T cells. To reproduce these results and study the different pools of ubiquitin-modified ELK-1, alternate assays were devised to visualise either mono or polyubiquitination.

The "polyubiquitination assay" involved co-transfecting His-tagged ELK-1 and HA-tagged ubiquitin into HEK293T cells, and enriching for the His-tagged ELK-1 *via* IMAC under denaturing conditions - to abrogate protein-protein interactions while preserving covalent modifications, and hence ubiquitination (Figure 4-1). Samples obtained from IMAC were then resolved by SDS-PAGE and immunoblotted for the HA-tagged ubiquitin. By blotting for HA-ubiquitin, longer polyubiquitin chain topologies are preferentially detected, as these longer chains contain more ubiquitin moieties, which are in turn recognised by greater numbers of HA-epitope antibodies, leading to stronger

chemiluminescent signal. Put simply, a single polyubiquitin chain of HA-ubiquitin will produce a much greater signal intensity to that of a single monoubiquitin attached to the target protein. Polyubiquitination of transfected His-ELK-1 can be seen following IMAC (Figure 4-2A, top panel), with high molecular weight HA-ubiquitin chains of increasing length. Also included in the experiment was treatment of transfected cells with the proteasome inhibitor MG132, which had a minimal effect on transfected ELK-1 polyubiquitination (Figure 4-2A, lane 6), possibly due to the high background level of polyubiquitination even without this inhibitor.

The “monoubiquitination assay” employs a similar experimental setup, with the exception that ubiquitin is instead His-tagged and ELK-1 is HA-tagged (Figure 4-1). Through this, ubiquitin is enriched for by IMAC and ELK-1 is probed for by immunoblot, allowing for a more representative display of ubiquitinated ELK-1 populations – as signal intensity is not influenced by the number of ubiquitin moieties conjugated to the target protein. Transfected HA-ELK-1 was ubiquitinated in HEK293T cells (Figure 4-2B, top panel) by His-tagged ubiquitin, shown by distinct bands separated by ~8 kDa, which could either equate to monoubiquitination dispersed over multiple sites or short polyubiquitin chains conjugated to a single lysine. These modifications were not enhanced by treatment of cells with the MG132, and in fact seem reduced in comparison to untreated cells (Figure 4-2B, compare lanes 3 and 6). This suggests the function of ELK-1 monoubiquitination is not primarily as a signal for protein turnover by

the 26S proteasome. To sum up, altering the protein with the His-tag gives rise to distinct ubiquitination patterns by blot, due to detection sensitivity varying when selecting for ELK-1 or ubiquitin. Notably, the majority of transfected ELK-1 remains unmodified, while smaller sub-populations of ELK-1 are polyubiquitinated and monoubiquitinated.

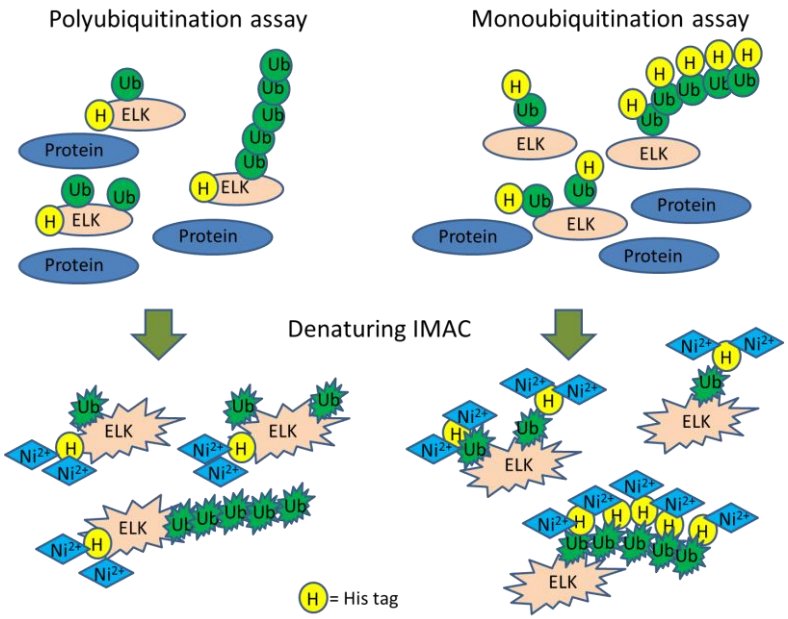

Figure 4-1: Cartoon depiction of monoubiquitination and polyubiquitination assays. Constructs encoding either His-tagged ELK-1 and HA-tagged ubiquitin (polyubiquitination assay) or HA-tagged ELK-1 and His-tagged ubiquitin (monoubiquitination assay) were transfected to HEK293T cells, and the His-tagged protein was enriched by denaturing IMAC. Samples were then resolved by SDS-PAGE and HA-tagged proteins were then probed for by immunoblotting to visualise ubiquitin conjugates.

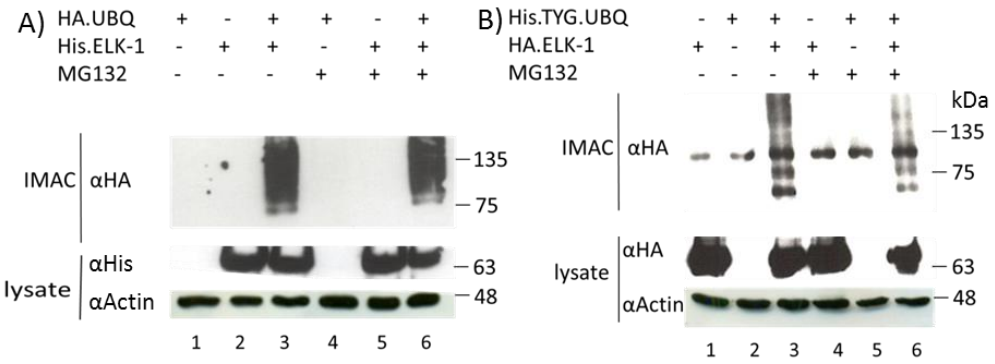

Figure 4-2: A) ELK-1 polyubiquitination assay. HEK293T cells were transfected with His-ELK-1 and HA-ubiquitin (UBQ) for 48 hours before either leaving untreated or treating with 20 μM proteasome inhibitor MG132 for six hours followed by harvesting. Top panel displays immunoblot for HA-tagged ubiquitin following denaturing IMAC for His-ELK-1. Bottom panels display input lysate with β-actin as a loading control. B) ELK-1 monoubiquitination assay. Same experimental setup as A) except HEK293T cells are transfected with HA-ELK-1 and His-TYG-ubiquitin. Top panel displays immunoblot for HA-tagged ELK-1 following denaturing IMAC for His-ubiquitin. Bottom panel as A).

4.2 Major ELK-1 ubiquitination populations constitute monoubiquitination and short polyubiquitin chains

Following on from the monoubiquitination assay, experiments were carried out to elucidate whether the ladder of ubiquitin moieties seen in this experiment were due to multiple monoubiquitination events at separate lysine acceptor sites within transfected ELK-1 or short polyubiquitin chains. To this end, the assay was repeated, but with a lysine-less ubiquitin (K0-UBQ) which cannot support polyubiquitin chain formation, other than in the form of linear chains *via* its amino-terminal methionine. A comparison of wild-type versus K0 ubiquitin can be seen in Figure 4-3 (compare lane 3 against lane 5). K0 ubiquitin produced a single band at the same molecular weight as a band produced with wild-type ubiquitin, indicating that this indeed represents a single ubiquitin modification. However, higher molecular weight species above this were only present with wild-type ubiquitin, showing that these equate to short polyubiquitin chains rather than multiple monoubiquitination.

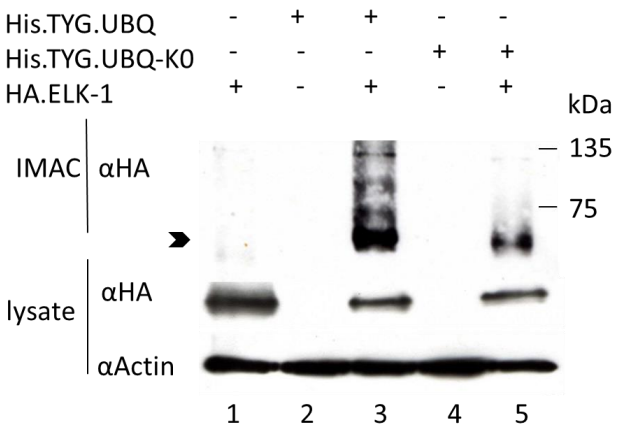

Figure 4-3: HEK293T cells were transfected with HA-ELK-1 and either His-TYG-ubiquitin (UBQ) or lysine-less HIS-TYG-ubiquitin (UBQ-K0) for 48 hours before harvesting. Top panel displays immunoblot for HA-tagged ELK-1 following denaturing IMAC for His-TYG-ubiquitin. Bottom panels display input lysate with β-actin as a loading control. Arrowhead denotes band corresponding to monoubiquitinated ELK-1.

4.3 ELK-1 polyubiquitin chain topology is consistent with targeting for proteasomal degradation

Different polyubiquitin chain topologies give rise to different downstream outcomes on target proteins. Identifying which internal ubiquitin lysine polyubiquitin chains form from is hence imperative in understanding functional significance, and as such antibodies targeted to specific polyubiquitin linkages are now commercially available. To further scrutinise the polyubiquitin chains

on ELK-1 by immunoblot, antibodies raised against K48 and K63-linked polyubiquitin chains were utilised. These antibodies were first tested against polyubiquitin ladders comprising only K48 and K63 linkages. As can be seen in Figure 4-4, K48 and K63 chain antibodies only recognised their specific ubiquitin ladders, whereas a generic antibody against ubiquitin recognised both chain types. It should be noted that the K63 antibody showed a reduced sensitivity compared to the generic ubiquitin antibody (compare lanes 2 and 6), and did not recognise higher molecular weight polyubiquitin chains. This experiment confirmed the specificity of these antibodies, at least in a simple homogenous sample.

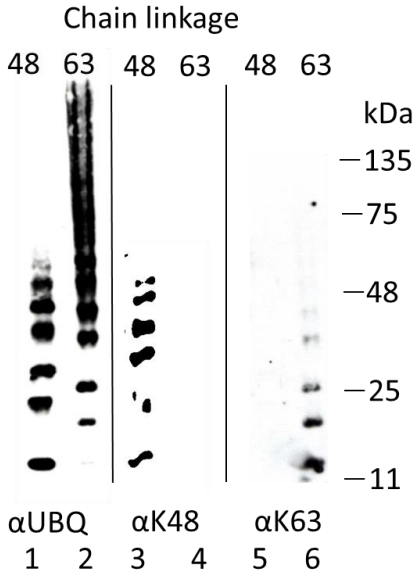

Figure 4-4: Polyubiquitin chain antibodies recognise their specific chain topology. 50 ng K48 or K63-linked ubiquitin ladders were resolved by SDS-PAGE and immunoblotted with either a generic ubiquitin antibody (UBQ) or a K48/K63 chain specific antibody.

These antibodies were tested on IMAC enriched His-tagged ELK-1 in the polyubiquitination assay (with HA-ubiquitin), to interrogate the polyubiquitin chain types present. This was carried out in the absence and presence of proteasome inhibition (MG132), and also included was the shorter isoform of ELK-1 (sELK). This isoform is missing the first 54 amino-terminal residues, and is significantly less stable and more readily turned over by the proteasome than full-length ELK-1 (Evans et al., 2011). As expected, proteasome inhibition effectively stabilised sELK-1 while having a minimal effect on full-length ELK-1 (Figure 4-5 – lysate αHis panel).

Immunoblot of samples post-IMAC show that K48 chains associated with both isoforms of ELK-1 increased in abundance post-proteasome inhibition. As K48-chains are classically associated with protein turnover by the proteasome (Grice & Nathan, 2016), this corroborates data pointing to ELK-1 as a target of the proteasome (Evans et al., 2011). Additionally, a faint ubiquitin trace can be seen with K63-chain antibody associated with full-length ELK-1, also increasing post-MG132 treatment. This is an unexpected result, as K63 polyubiquitin chains are not considered a signal for proteasomal processing, although this weak signal could be a sign of non-specific antibody binding in a highly ubiquitinated sample. Regardless, evidence points to ELK-1 as a proteasome target, despite the full-length protein's apparent stability. After it was confirmed that ELK-1 was both monoubiquitinated and polyubiquitinated, the next step was to map modification sites using MS/MS.

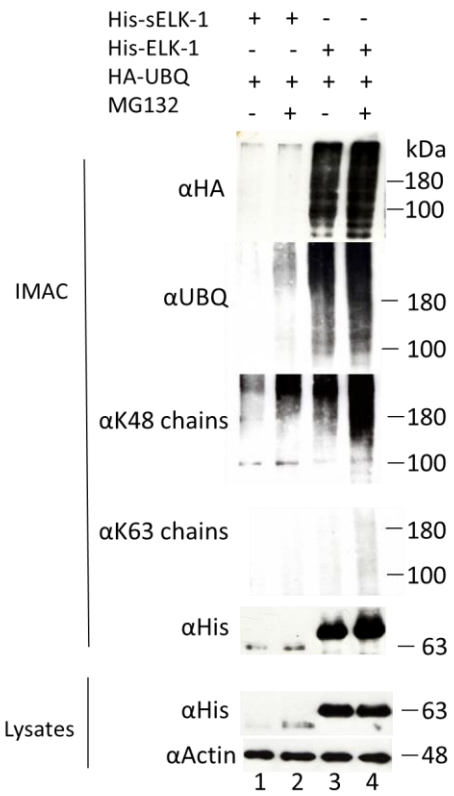

Figure 4-5: ELK-1 K48-linked polyubiquitin chain topology is consistent with proteasomal targeting. HEK293T cells were transfected with HA-ubiquitin (UBQ) and either His-ELK or His-sELK for 48 hours before either leaving untreated or treating with 20 μM proteasome inhibitor MG132 for six hours, followed by harvesting. Top panel displays immunoblot for HA-tagged ubiquitin (HA, UBQ, K48-chain and K63 chain antibodies) and His-ELK-1 following denaturing IMAC. Bottom panels display input lysate with β-actin as a loading control.

4.4 HAND1 as a positive control for MS/MS analyses

Heart and neural crest derivatives expressed 1 (HAND1) is a transcription factor with important roles in cardiac morphogenesis and cardiomyocyte differentiation in the developing heart (McFadden, 2004). When overexpressed with a His-tag in HEK293T cells, it was noted that HAND1 was expressed to high levels, and purified well by denaturing IMAC, possibly aided by an internal span of seven histidines in its amino-terminal primary structure in addition to the carboxyl-terminal His-tag (Figure 4-6). In addition, HAND1 appeared to be stably monoubiquitinated post-IMAC (Figure 4-7). This was *via* endogenous ubiquitination, rather than the ectopic ubiquitination seen in the previously shown ELK-1 assays, as it occurred without co-transfection of ubiquitin. This was a serendipitous discovery, as the His-HAND1 clone was intended for use as a positive control for an E3 ligase (8.5.1), but as this modification was so clear, this provided an ideal model for identifying ubiquitination sites by MS/MS, with a view to mapping sites in ELK-1.

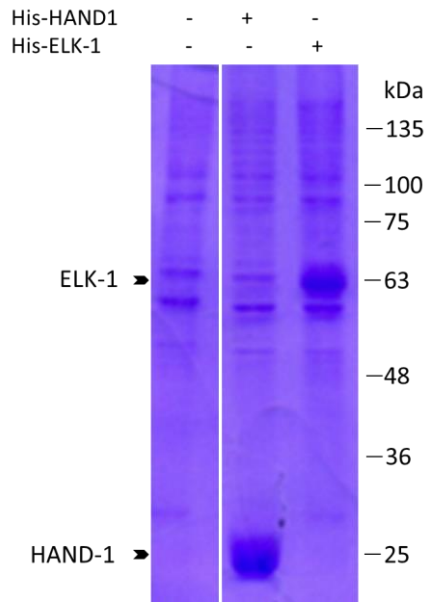

Figure 4-6: His-HAND1 or His-ELK-1 were transfected into HEK293T cells for 48 hours before harvesting and submitted to denaturing IMAC. Purified His-HAND1 and His-ELK-1 are identified by arrowhead on Coomassie stain from Nickel beads loaded onto SDS-PAGE gels.

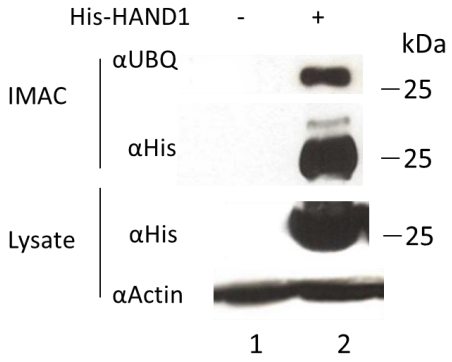

Figure 4-7: HAND1 is monoubiquitinated *in cellulo.* His-HAND1 was transfected into HEK293T cells for 48 hours before harvesting. Top panels display immunoblot for endogenous ubiquitin and His-HAND1 following denaturing IMAC. Bottom panels display input lysate with β-actin as a loading control.

4.5 MS/MS identifies HAND1 ubiquitin modification site as K163

At sites of ubiquitination, the carboxyl-terminal glycine of ubiquitin is conjugated to target lysines, and tryptic digestion at these sites result in a missed cleavage site at the lysine involved in isopeptide bond formation. This yields a signature peptide with a diglycine stub derived from the carboxyl-terminus of ubiquitin (preceding this is an arginine in ubiquitin which is cleaved), allowing for screening for ubiquitination targets and sites (1.4). On-bead tryptic digests were carried out on IMAC purified His-HAND1 samples (and control samples with no ectopic His-tagged protein), and they were submitted to MS/MS on an LTQ-Orbitrap-Velos spectrometer with nano-flow LC, screening for the presence of these diglycine remnants (in collaboration with the University of Leicester Proteomics facility).

Using this methodology, lysine 163 was identified as a site of ubiquitination in HAND1 (Figure 4-8). Interestingly, polyubiquitin-chain linkage peptides pertaining to both K48 and K63 chains were also found in His-HAND1 enriched samples (but not in control samples), suggesting that HAND-1 was also polyubiquitinated. Evidence has previously pointed to HAND1 being degraded by the proteasome through the action of the E3 ligase FBXO25 (Jang et al., 2011). Phosphorylation can also be assessed by MS/MS in a similar manner to ubiquitination, and this was also used to map sites in HAND1, with four sites being identified. Of these, T107 and S109 have already been well characterised

as phosphorylation sites through phosphopeptide mapping, with double mutants shown to reduce heterodimer formation with E-protein, a requirement for transcriptional activity (Firulli et al., 2003). Furthermore, both hypo and hyper-phosphorylation of these sites in mice led to cardiomyocyte hypertrophy and fibrosis through pathological heart remodelling (Lu et al., 2011). This validates the use of this methodology for studying post-translational modifications, with modification sites identified agreeing with published data.

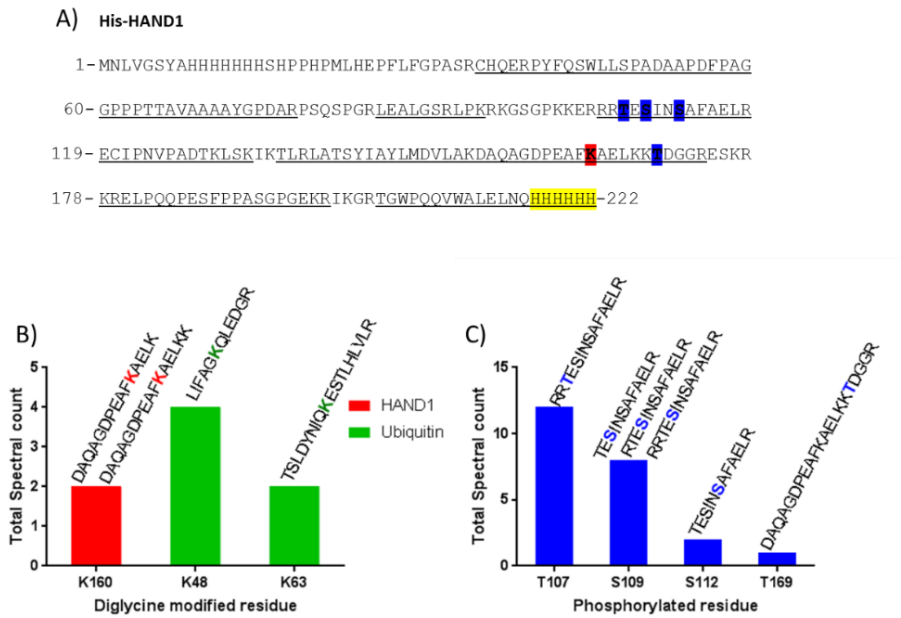

Figure 4-8: HAND1 ubiquitination and phosphorylation sites identified by qualitative MS/MS. A) Primary structure of His-HAND1 clone, with underlined regions representing coverage by MS/MS (73% coverage). Modified residues and His-tag are highlighted. K = Ubiquitination site, S/T= Phosphorylation site, HHHHHH= His-tag. B) Lysine residues identified as ubiquitination sites in HAND1 and sites of chain formation in ubiquitin, with the total number of spectral counts for each (from a single MS/MS run). Tryptic peptide is labelled above graph, with modification site highlighted. C) Serine/Threonine residues identified as phosphorylation sites in HAND1, with the total number of spectral counts for each. Tryptic peptide is labelled above graph, with modification site highlighted (N=1).

4.6 IMAC optimisation for purification of transfected His-ELK-1

Before generating ELK-1 samples for MS/MS analysis, the purification procedure was optimised. Maximising purity of target proteins improves the chances of identifying small pools of ubiquitin-modified populations, which are more likely to be missed in more complex mixtures by shotgun proteomic analyses. Previous IMAC experiments had been carried out using nickel-nitrilotriacetic acid (Ni^{2+}-NTA) agarose beads. Cobalt-carboxylmethylaspartate (Co^{2+}-CMA) agarose beads offer an alternative matrix through which to purify hexa-histidine tags. Both systems possess a similar protein binding capacity (5-10 mg/ml beads), whereby nickel has a higher affinity for the His-tag while cobalt has the advantage of reduced non-specific binding (Bornhorst & Falke, 2000). Non-specific binding can be a problem with IMAC, as proteins with short spans of internal histidines can also be enriched, one example being Non-POU domain-containing octamer-binding protein (Dong et al., 1993), which was consistently identified in MS datasets from IMAC-enriched samples (data not shown).

A side by side comparison of nickel versus cobalt beads used in purification of His-ELK-1 under denaturing conditions is shown in Figure 4-9A. In four separate samples, nickel was shown to be more effective at capturing transfected His-ELK-1, confirmed by densitometry of band intensity in immunoblots (Figure 4-9B). This may be explained by the lower affinity of cobalt for hexa-histidine as

compared with nickel, and under the harsh denaturing protocol involving multiple washes with 6 M guanidinium-HCl/ 8 M urea, more His-ELK-1 may have been lost. For this reason, nickel-NTA beads were retained for use in further IMAC experiments.

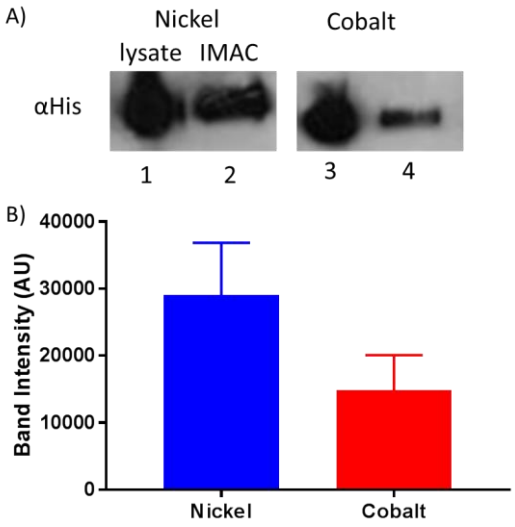

Figure 4-9: Nickel-NTA beads are more effective for purification of His-ELK-1 than cobalt-CMA beads. A) Representative immunoblot for His-ELK-1 post-denaturing IMAC, displaying nickel versus cobalt resin performance in assay. B) Densitometry of immunoblot band intensity of purified His-ELK-1 using ImageJ. Error bars represent +/- SEM (N=4).

The next step for improvement of IMAC was to optimise the concentration of imidazole in the lysis/binding buffer. Imidazole binds nickel with high affinity, helping to displace non-specifically bound proteins. Deducing the ideal imidazole content in IMAC binding buffers is ultimately a compromise between

purity and yield, as low imidazole concentrations do not adequately eliminate non-specific binding, while high concentrations result in reduced binding of target His-tagged protein (Bornhorst & Falke, 2000). Purifications had previously been carried out with 5 mM imidazole in lysis buffer, so a range between 5-100 mM was trialled. Post-IMAC, samples were submitted to SDS-PAGE and Coomassie stain, silver stain or immunoblot (Figure 4-10). From Coomassie stain, 10 mM imidazole gave a clean His-ELK-1 band of highest intensity, with higher concentrations reducing the yield as His-tagged protein was out-competed by imidazole (Figure 4-10B). Silver stain suggested that 5 mM gave the most intense band by densitometry (Figure 4-10C); although this could be due to higher background from nonspecific protein binding in this more sensitive stain. Moreover, by immunoblot of IMAC/input protein, 10 mM imidazole was found to be the optimum concentration for purifying His-ELK-1 (Figure 4-10D). This concentration was selected for use in further IMAC experiments.

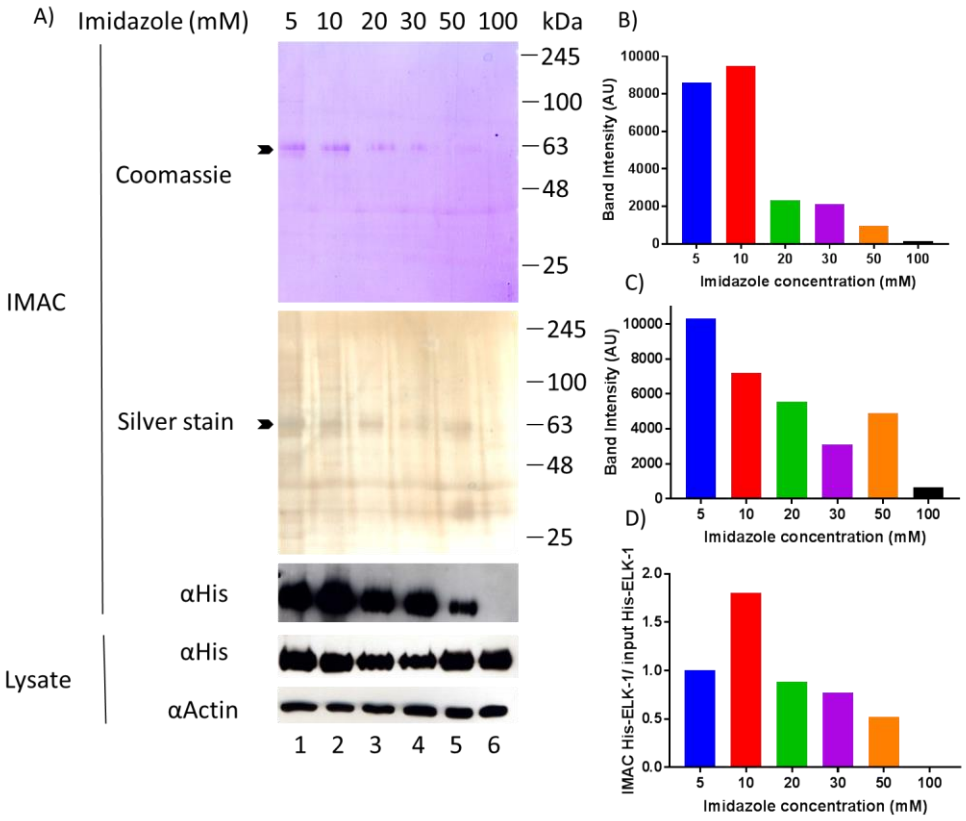

Figure 4-10: Optimisation of imidazole concentration in IMAC lysis/binding buffer. A) IMAC was carried out with imidazole concentrations varying between 5-100 mM on lysates from His-ELK-1 transfected HEK293T cells. Top panel to bottom displays Coomassie stain, silver stain (purified His-ELK-1 band indicated by arrowheads) and immunoblot for His-tag of post-IMAC samples, and below this immunoblot for input lysate. B) Densitometry of His-ELK-1 band intensity from Coomassie stain C) Densitometry of His-ELK-1 band intensity from silver stain D) Densitometry of His-ELK-1 band from immunoblot normalised to input protein in ImageJ (N=1).

4.7 His-ELK-1 is endogenously polyubiquitinated post-serum/TPA stimulation

After testing MS/MS methodologies on HAND1 as a positive control, and making efforts to improve the IMAC protocol, ubiquitinated ELK-1 samples were generated for MS/MS. Ubiquitination assays had confirmed that ectopically expressed ELK-1 was modified by ectopically expressed ubiquitin in HEK293T cells (Figures 4-2, 4-3 and 4-5), but what had not been clarified was whether endogenous ubiquitin could modify ELK-1 in the same manner. It had previously been shown that serum-starved HEK293T and HeLa cells showed increased monoubiquitination, which dissipated on activation of the ERK cascade (Chow, PhD Thesis, Univeristy of Nottingham, 2010). This was also the case in HEK293T cells (5.2). To better understand the relationship between ELK-1 activity and its ubiquitination, HEK293T cells were transfected with His-ELK-1, serum starved for 24 hours and left either untreated or stimulated with serum and TPA for either 30 or 60 minutes before harvesting. TPA is a potent activator of protein kinase C, which activates the ERK pathway – and hence ELK-1 – through RAF (but independent of RAS) (Ueda et al., 1996). Harvested cells were submitted to IMAC and immunoblotted with ubiquitin antibodies.

Figure 4-11 shows that polyubiquitination of ELK-1 with endogenous ubiquitin increased 30 minutes post-stimulation and declined after 60 minutes, which was particularly evident when probing for K48-linked chains. This suggests that

activation (by phosphorylation) of ELK-1 could prompt its degradation by the 26S proteasome, possibly through a phosphodegron (motifs within target proteins that promote E3 ligase recognition and UPS processing following phosphorylation) as a self-limiting mechanism of transcriptional activity (Lipford et al., 2005; Cheng et al., 2016). However, it should be noted that the generic ubiquitin antibody gave a strong signal in control samples with no transfected ELK-1 (lanes 1-3), although this was not present with the K48-linked polyubiquitin chain-targeting antibody. Additionally, serum-starved cells reduced ERK activity (P-ERK immunoblot, lanes 1 and 4) but failed to completely block phosphorylation of ectopically expressed ELK-1 (P-ELK-1 immunoblot, lane 4). This could be due to phosphorylation by an alternative MAP kinase, such as SAPK (Gille et al., 1995B) or p38 MAP kinase (Raingeaud et al., 1996). Nonetheless, mitogen starvation versus stimulation appeared to have distinct effects on ELK-1 ubiquitination patterns, and hence IMAC-enriched His-ELK-1 samples pertaining to serum-starvation or serum-starvation followed by 30 minutes TPA/serum stimulation were generated for further study. It should be noted that an increase in polyubiquitination post-ERK activation is the opposite of what is seen with monoubiquitination, where mitogens promoted the removal of this modification (Chow, PhD Thesis, Univeristy of Nottingham, 2010) (5.2).

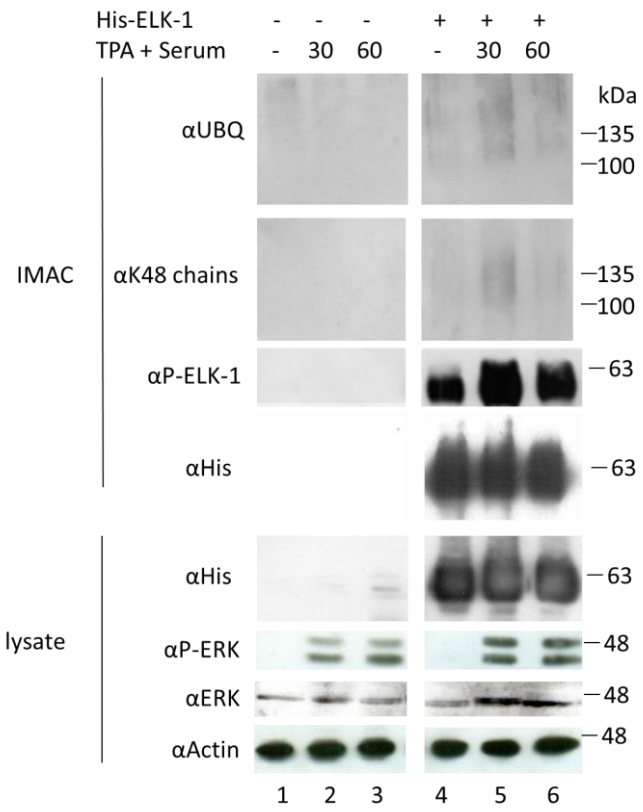

Figure 4-11: His-ELK-1 is polyubiquitinated post-TPA/ serum stimulation. HEK293T cells were transfected with His-ELK-1 for 24 hours, followed by serum-starvation (0.5% v/v serum) for 24 hours. This was followed by either leaving untreated or treating with 100ng/ml TPA/ 10% v/v serum for either 30 or 60 minutes before harvesting. Top panels display immunoblot for endogenous ubiquitin (conjugated to ELK-1) and His-ELK-1 following denaturing IMAC. Phospho-ELK-1 (P383) blot is indicative of ELK-1 activation. Bottom panels display input lysate with β-actin as a loading control. Phospho-ERK (T202/Y204) blot is indicative of ERK1/2 activity.

4.8 MS/MS mapping identifies that lysine residues in DNA-binding ETS domain are targets of ubiquitination in ELK-1

IMAC enriched His-ELK-1 samples from serum-starved or TPA/serum stimulated (harvested 30 minutes post-treatment) HEK293T cells (as well as control samples with no ectopic ELK-1) were prepared for MS/MS. “On-bead” samples were reduced with DTT and alkylated with chloroacetamide, to remove cysteine-cysteine disulphide bonds and prevent their reformation respectively. Chloroacetamide was chosen as an alkylating agent rather than the more commonly used iodoacetamide as the latter can form two molecule covalent adducts with lysine residues, matching the exact mass of a diglycine adduct (114 Da) and hence leading to erroneous assigning of ubiquitination sites (Nielsen et al., 2008). Samples were then tryptically digested and screened by MS/MS for diglycine remnants (3.5.5), with the UniProt protein library used for sequence validation and assignment, looking for sites of modification by endogenous ubiquitin. Per experiment, peptides for between 281-854 proteins (two peptides minimum per protein) were identified. This illustrates the sensitivity of mass spectrometry, in that even after purifying by denaturing IMAC, a large range of non-specifically bound proteins apparently persisted through binding to the nickel beads and were hence identified. Daughter ions pertaining to diglycine-modified peptides originating from the ELK-1 primary sequence were found in all six samples submitted (three starved, three

serum/TPA stimulated). Collectively, sequence coverage for ELK-1 was very high (95%), although, in general, the carboxyl-terminus was less well covered than the amino-terminus between samples. It should be noted that the MS methodologies used were not quantitative, so provided no information on the abundance of a particular modified peptide.

Lysine residues within the DNA-binding amino-terminal ETS domain were found to be sites of ubiquitination (Figure 4-12). These were K35, K52 and K59, and agreed with previous mutational studies that suggested these residues – particularly K35 – were likely ubiquitin acceptor sites. There was however ambiguity around K52R and K59R mutations, as these also drastically reduced DNA-binding (Chow, PhD Thesis, Univeristy of Nottingham, 2010). The MS data presented here represents endogenous ubiquitin, but when compared with the aforementioned mutational screening experiments (with transfected, tagged ubiquitin), both methodologies identified K35 as a ubiquitination site. K35, K52 and K59 were all found to be modified by ubiquitin under both starved and stimulated conditions, with K35 the most consistently identified (found in 2/3 starved and 2/3 stimulated samples). In comparison, K52 and K59 diglycine peptides were both found in 1/3 of starved and 1/3 stimulated samples. More ubiquitinated peptides were found in serum-stimulated samples than starved, although as the methodologies used were purely qualitative and sensitive to

different ionisation abilities of different peptides, variations in abundances of modified populations due to cell treatment cannot be inferred from this.

Ubiquitin sequences were also present in all MS/MS samples (including control samples without His-ELK-1), and, further to this, diglycine peptides indicative of polyubiquitin chains, which were not present in control samples. Signature peptides indicative of K48-polyubiqutin chains were also found in both starved and stimulated samples (1/3 and 3/3 respectively). However, K48-linked polyubiquitin chains were found in all three serum/ TPA stimulated cells, compared to a solitary diglycine peptide in one of the starved samples. This, allied with immunoblot data (Figure 4-11), further suggests that phosphorylation and activation of ELK-1 could prompt its degradation by the proteasome. One peptide indicative of K63-linked polyubiquitin chains was also found in one of the starved samples, although this was not replicated in any other sample, suggesting this may be an artefact.

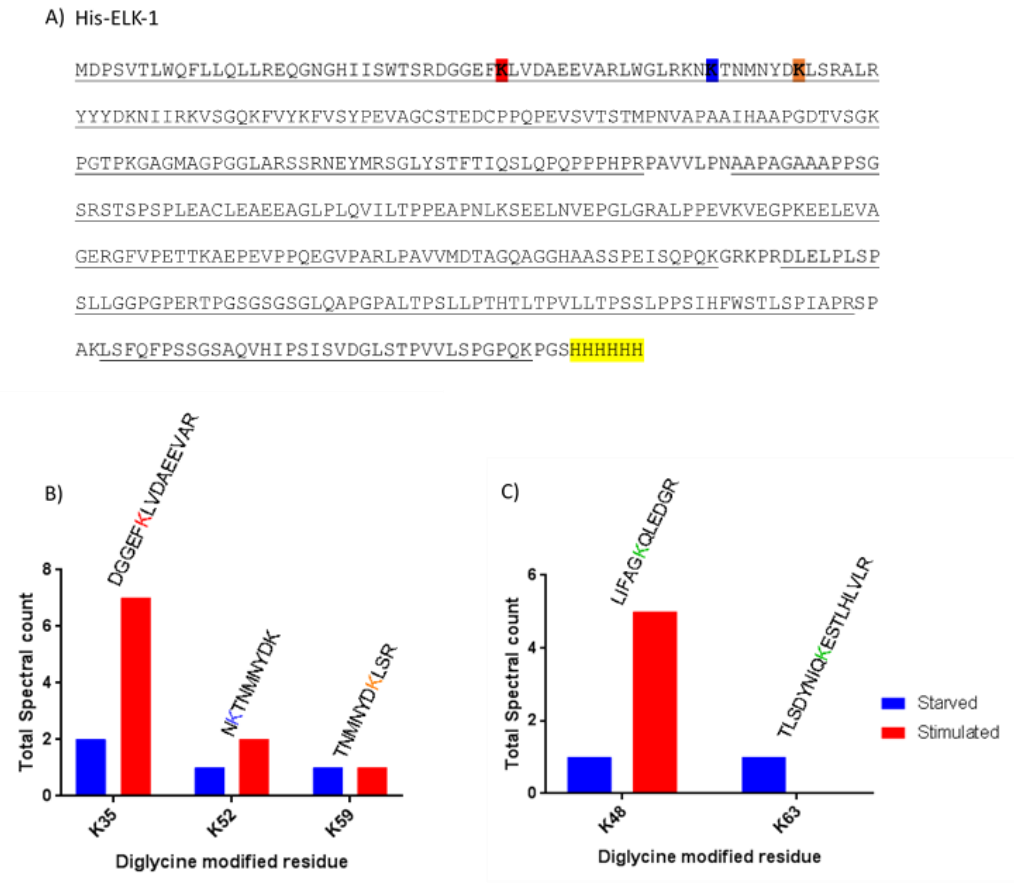

Figure 4-12: ELK-1 is ubiquitinated in the amino-terminal ETS domain A) Primary structure of His-ELK-1 clone, with underlined regions representing coverage by qualitative MS/MS (95% coverage). Diglycine modified residues and His-tag are highlighted. HHHHHH= His-tag. B) Lysine residues identified as ubiquitination sites in ELK-1 with the total number of spectral counts for each in starved and serum/ TPA stimulated samples. Tryptic peptide is labelled above graph, with modification site highlighted. C) Same as for B) but with sites of chain formation in ubiquitin. (N=3, 3 starved, 3 stimulated).

The structure of the ELK-1 ETS domain has been characterised and consists of a winged helix-turn-helix conformation with 3 α-helices and 4 β-sheets, running in the order α1-β1-β2-α2-α3-β3-β4, where α3 is the DNA-binding helix (Mo et al., 2000) (Figure 4-13). K35 resides in β2, with K52 in between α2 and α3 and K59 in α3. Both K52 and K59 are important in ELK-1 DNA binding – K52 associating with DNA backbone 3' thymidine phosphate through an ionic salt bridge, and K59 forming hydrogen bonds with DNA. K35, on the other hand, does not directly contact DNA.

It is not currently known whether K35, K52 or 59 are sites of monoubiquitination, polyubiquitination or both. One possible explanation, based on the increase in K35-associated diglycine-containing peptides post-TPA/serum stimulation, is that K35 is a site for polyubiquitination and proteasomal degradation in response to mitogens. However, K>R mutational screening in ELK-1 pointed to K35 as the only clear candidate for monoubiquitination (Chow, PhD Thesis, Univeristy of Nottingham, 2010). Furthermore, these assays suggested carboxyl-terminal lysine residues rather than amino-terminal ones contribute more to stabilising ELK-1, and K35R mutation did not influence this (Chow, PhD Thesis, Univeristy of Nottingham, 2010). This, coupled with the generally poor coverage of the carboxyl-terminal end of ELK-1 by MS/MS, suggests that other ubiquitination sites that could be implicated in protein turnover may have been missed. Regardless, the fact that ubiquitination is targeted to the DNA binding domain, and residues involved in

DNA binding – suggests that ubiquitination may have an influence on DNA binding and transcriptional activity of ELK-1.

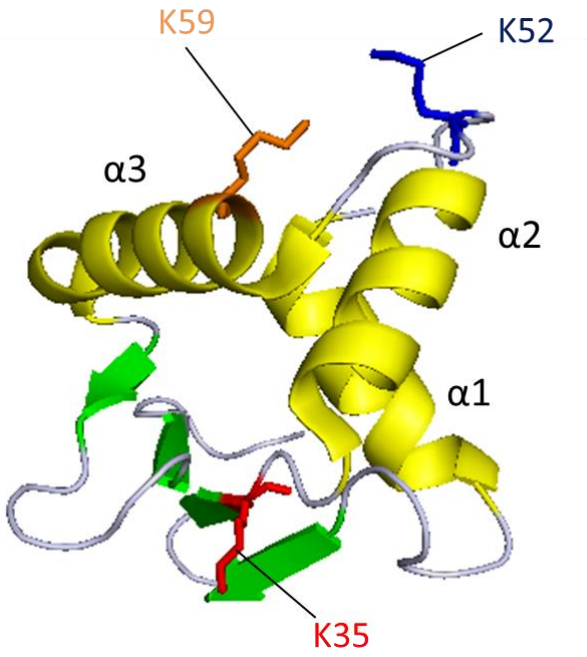

MDPSVTLWQFLLQLLREQGNGHIISWTSRDGGEFKLVDAEEVARLW

GLRKNKTNMNYDKLSRALRYYYDKNIIRKVSGQKFVYKFVSYPEVAGC

Figure 4-13: Cartoon representation of ETS domain of ELK-1 (residues 5-90) (human), with targets of ubiquitination highlighted in stick format- K35, K52 and K59. Primary sequence of the ETS domain is shown below with sites of ubiquitination highlighted and α-helices and β-sheets highlighted. Structure taken from (Mo et al., 2000) – PDB 1DUX – re-rendered with PyMOL.

4.9 Monoubiquitination assay confirms K35 as primary ubiquitin modification site of ELK-1

K35 was the most consistently identified ubiquitination site of His-ELK-1 by MS/MS. Hence, a monoubiquitination assay was subsequently carried out with ELK-1 constructs containing K35R mutation, to test the effect of this on ubiquitinated pools of ELK-1. Figure 4-14 shows that this mutation abrogated modification of ELK-1, agreeing with previous data and further confirming this site as a major ubiquitination target (Chow, PhD Thesis, Univeristy of Nottingham, 2010).

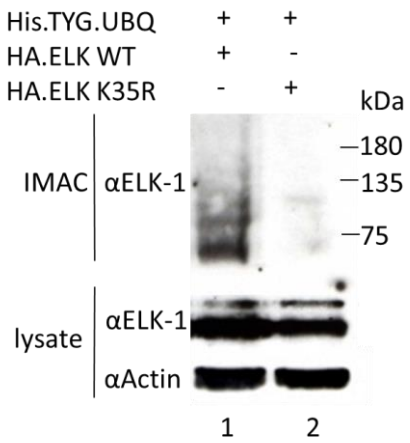

Figure 4-14: K35R mutation abrogates ELK-1 monoubiquitination. HEK293T cells were transfected with His-TYG-ubiquitin (UBQ) and either wildtype HA-ELK-1 or K35R mutant for 48 hours before harvesting. Top panel displays immunoblot for HA-tagged ELK-1 following denaturing IMAC. Bottom panels display input lysate with β-actin as a loading control.

4.10 Sites of other post-translational modifications in ELK-1

MS/MS can be used to identify other post-translational modifications in a similar manner as ubiquitin- with phosphorylation giving peptides with an extra mass of 80 Daltons through the phosphate group (attached to serine, threonine or tyrosine) and acetylation 42 Daltons through the acetyl group (added to lysine or protein amino-terminus). Phosphorylation has been well-established as an activation mark for ELK-1, with ERK phosphorylation at S383 and S389 promoting ternary complex formation and transcriptional activity (Janknecht et al., 1993; Marais et al., 1993; Gille et al., 1995A). Screening LC-MS/MS data of starved and stimulated His-ELK-1 samples (from HEK293T cells) for phosphorylation yielded multiple sites (eight in total- Figure 4-15), although neither S383 nor S389 were identified. This is despite immunoblot data with phospho-specific antibody suggesting ample phosphorylation at S383 (Figure 4-11), and probably reflects the relatively poor coverage of ELK-1 carboxyl-terminus by MS/MS.

Of the phosphorylation sites identified, several have been reported in previous large-scale mass spectrometry datasets according to PhosphoSitePlus (S166, S303, S304, and S326) (Dephoure et al., 2008; Grosstessner-Hain et al., 2011), while S324 has been previously characterised as an ERK target and is associated with transcriptionally active ELK-1, despite apparently making no contribution to ternary complex formation (Gille et al., 1995A). The presence of S324

phosphopeptide in both starved and stimulated samples perhaps illustrates further the inefficiency of transcriptionally silencing ectopic His-ELK-1 in HEK293T cells by serum starvation. S202, T222 and T293 have not previously been reported as phosphorylation sites – it remains to be seen whether these are biologically relevant modification targets or artefactual "noise".

Unlike phosphorylation, acetylation of ELK-1 has not been studied extensively. Interestingly, MS/MS analysis found lysine sites targeted by other post-translational modifications to also be targets for acetylation. K35 – confirmed as a ubiquitination site (Figure 4-12) – was also found to have associated acetyl-peptides under both starved and stimulated conditions. Additionally, K254 – a *bona fide* SUMOylation site implicated in transcriptional repression and nuclear-cytoplasmic shuttling – was also found to be an acetylation site under both starved and stimulated conditions (Salinas et al., 2004). Lysine residues targeted for multiple post-translational modifications could potentially indicate antagonistic effects, such as in the case of HIC1, where SUMOylation and acetylation compete for a specific lysine residue to promote or dampen its transcriptional repression activity respectively (Stankovic-Valentin et al., 2007).

Equally, direct competition between ubiquitination and acetylation of the same lysine residues has been documented before, such as for p53, where acetylation promotes stability, whereas ubiquitination at these residues promotes protein turnover (Ito et al., 2002). K271 – a lysine residue with no

known functional significance in ELK-1 - was also found to be acetylated, although only in stimulated samples, possibly suggesting this modification was prompted by ELK-1 activation. This could indicate that acetylation is a positive marker for ELK-1 transcriptional activity, and fits with evidence for K254 – where nine acetylated peptides were found in stimulated samples compared with a single peptide in starved samples – perhaps due to acetylation out-competing the repressive SUMOylation mark post-stimulation and potentiating the transcriptional activation of ELK-1. This is, however, unproven and is not further evaluated experimentally in this study. Regardless, MS/MS has indicated modification sites that agree with mutational analysis (phosphorylation and ubiquitination), phosphopeptide mapping (phosphorylation) and previous mass spectrometry datasets (phosphorylation) while also suggesting new modification sites and post-translational modifications.

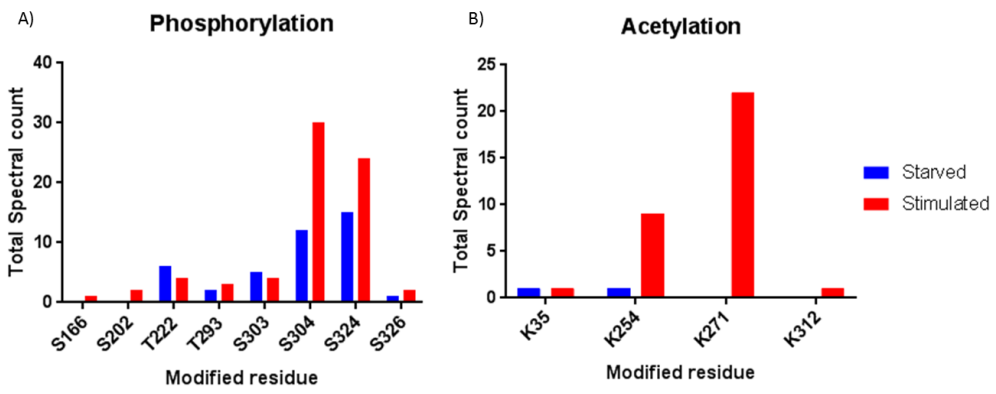

Figure 4-15: Qualitative MS/MS maps sites of other post-translational modifications in His-ELK-1 in HEK293T cells. A) Serine/threonine residues identified as phosphorylation sites in ELK-1 with the total number of spectral counts for each in starved and serum/ TPA stimulated samples. (N=2, 2 starved, 2 stimulated). B) Same as A) but for lysine residues identified as acetylation sites. (N=1, 1 starved, 1 stimulated).

To conclude, LC-MS/MS confirmed that K35 is a major site of ubiquitination, while ubiquitination assays suggested that modified ELK-1 is mostly monoubiquitinated. However, ELK-1 was also modified by K48-linked polyubiquitin chains, suggesting it can be targeted for proteasomal degradation. LC-MS/MS data also identified multiple phosphorylation sites in ELK-1, some of which had been previously identified (S166, S303, S304, S324 and S326), and some of which had not (S202, T222 and T293). Lastly, both ubiquitination sites (K35) and SUMOylation sites (K254) in ELK-1 were found to also be modified by acetylation, highlighting the possibility of competition and

cross-talk between ELK-1 post-translational modifications. Further work was required to elucidate the functional significance and regulatory network behind ELK-1 ubiquitination.

5 Determining the subcellular localisation of ubiquitinated ELK-1 and its response to mitogens

5.1 The majority of both mono- and polyubiquitinated ELK-1 is cytosolic

After mapping sites of ubiquitination in ELK-1 (4.8), attempts were made to identify how this modification is controlled and whether it is functionally important. Firstly, experiments were designed to clarify the subcellular localisation of ubiquitinated ELK-1. Post-translational modifications can affect the cellular distribution of target proteins, such as is the case with ELK-1 SUMOylation (Salinas et al., 2004). Monoubiquitination and polyubiquitination assays were carried out on subcellular extracts of transfected HEK293T. Nuclear and cytoplasmic fractions were IMAC-purified and resolved by SDS-PAGE and immunoblotting.

It can be seen from Figure 5-1 that the majority of mono- and polyubiquitinated ELK-1 is cytoplasmic. Monoubiquitinated ELK-1 was also present in the nuclear fraction. Blots for PARP and tubulin were included as controls for fraction purity for the nucleus and cytoplasm respectively, and Ponceau S stain showed the total protein load from the lysate. Equivalent percentages of cytosolic and nuclear extract obtained from fractionation were loaded, and the Ponceau S highlights that proportionally there was a much higher protein load in the cytoplasm. Despite this, there was a roughly equal abundance of ectopic ELK-1

in both the cytoplasm and nucleus – with slightly more in the nucleus (for both His and HA-tagged ubiquitin). This contrasts with endogenous ELK-1, which is largely (although not exclusively) nuclear in non-neuronal cells (Janknecht et al., 1994)

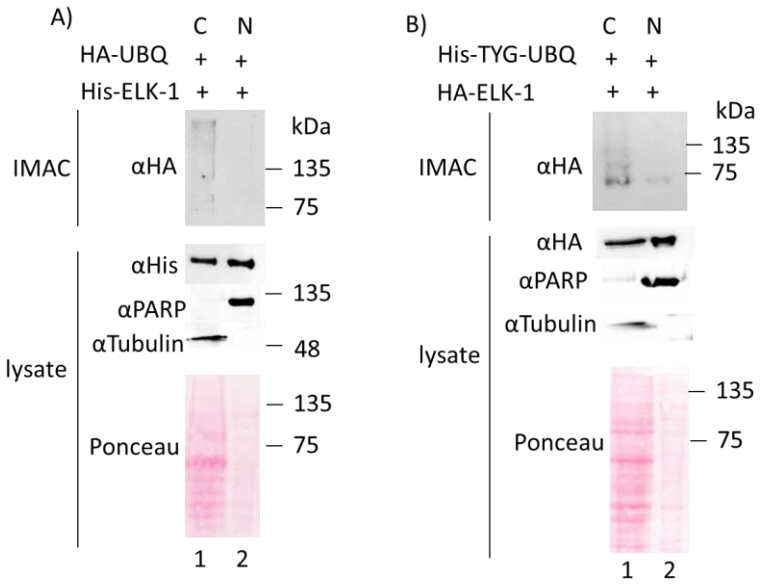

Figure 5-1: Ubiquitinated ELK-1 is mostly cytosolic. A) Polyubiquitination assay. HEK293T cells were transfected with HA-ubiquitin (UBQ) and His-tagged ELK-1 for 48 hours before harvesting and cytosolic/nuclear fractionation. Top panel displays immunoblot for HA-tagged ubiquitin following denaturing IMAC for His-ELK-1. Bottom panels display input lysate with PARP and tubulin as nuclear and cytosolic loading controls respectively and Ponceau stain as a total protein loading control. B) Monoubiquitination assay. Same experimental setup as A) except HEK293T cells are transfected with HA-ELK-1 and His-TYG-ubiquitin. Top panel displays immunoblot for HA-tagged ELK-1 following denaturing IMAC for His-ubiquitin. Bottom panel as A). C= Cytoplasm, N= Nucleus.

5.2 Chronic activation of the ERK cascade diminishes ELK-1 monoubiquitination

Previous experiments had shown that acute activation of the ERK cascade by serum/TPA stimulation diminished ELK-1 monoubiquitination (Chow, PhD thesis, University of Nottingham, 2010). This was further examined by introducing constitutively active isoforms of C-RAF and H-RAS into HEK293T cells along with HA-tagged ELK-1 and His-tagged ubiquitin and examining ELK-1 monoubiquitination status. RAF S259D mutation stimulates the activation of ERK without promoting tumorigenicity (Dhillon et al., 2003). V12 RAS is an oncogenic form of RAS, which is in a constantly active GTP-bound form rather than the inactive GDP-bound form and also constitutively activates the ERK cascade (Leevers & Marshall, 1992). The transfection of either of these into HEK293T cells greatly increased ERK and ELK-1 phosphorylation, and hence activation (Figure 5-2, bottom panel, lanes 4 and 5 from both A) and B)). This also impacted ELK-1 monoubiquitination, reducing the level of this modification (top panel, compare lanes 3 and 5 from both A) and B)). ERK activation (by mitogens) therefore promoted the deubiquitination of ELK-1 with concomitant phosphorylation and transcriptional activation.

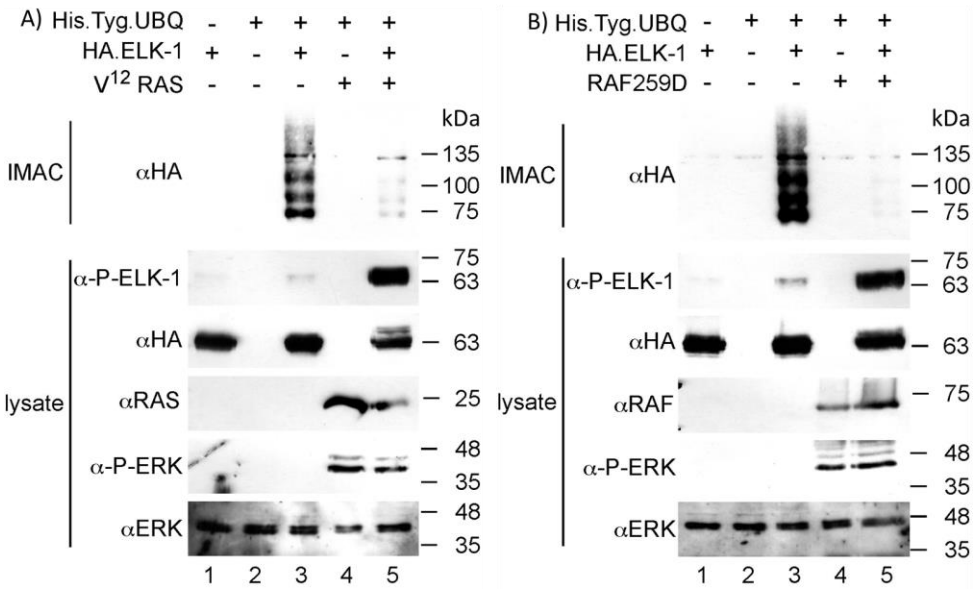

Figure 5-2: ERK cascade activation diminishes ELK-1 monoubiquitination. A) HEK293T cells were transfected with His-TYG-ubiquitin (UBQ), HA-ELK-1 and oncogenic RAS (V12 RAS) for 48 hours before harvesting. Top panel displays immunoblot for HA-tagged ELK-1 following denaturing IMAC for His-TYG-ubiquitin. Bottom panels display input lysate with ERK as a loading control. B) Same as A) but with constitutively active RAF (RAF259D) replacing V12 RAS. Phospho-ELK-1 (P383) and phospho-ERK (Y204) blots are indicative of ELK-1 and ERK1/2 activation respectively.

5.3 Monoubiquitinated ELK-1 can also be phosphorylated

Mitogens stimulate the ERK pathway, which in turn promotes the phosphorylation and activation of ELK-1 (Gille et al., 1992; Marais et al., 1993; Janknecht et al., 1993; Gille et al., 1995A). Experiments with constitutively active RAS and RAF forms (Figure 5-2), and acute stimulation by TPA/serum (Chow, PhD thesis, University of Nottingham, 2010) showed that as well as resulting in phosphorylation of ELK-1, deubiquitination also occurred. The question remained, however, whether ubiquitin was removed from ELK-1 before phosphorylation, and whether phosphorylation of ELK-1 prompted this removal. Probing ubiquitinated ELK-1 populations from HEK293T cells produced in monoubiquitination assays with phospho-ELK-1 antibody (S383) showed that ELK-1 was modified by both ubiquitin and phosphorylation at the same time, due to the presence of coincident immunoreactive bands (Figure 5-3). Hence, monoubiquitination of ELK-1 does not need to be removed before phosphorylation occurs.

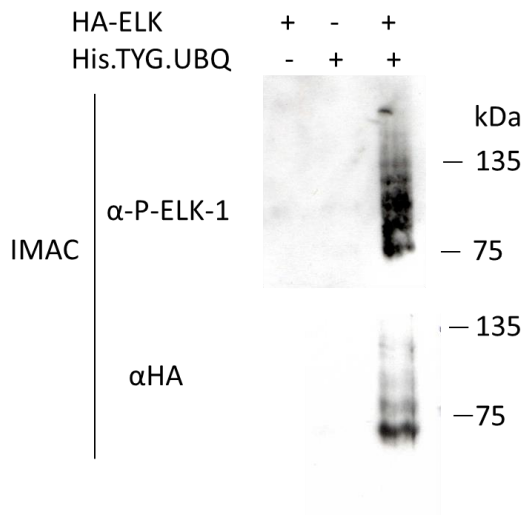

Figure 5-3: ELK-1 can be both ubiquitinated and phosphorylated at the same time. HEK293T cells were transfected with His-TYG-ubiquitin (UBQ) and HA-ELK-1 for 48 hours before harvesting. Panels display immunoblot for HA-tagged ELK-1 and phosphorylated ELK-1 (S383) following denaturing IMAC for His-TYG-ubiquitin from transfected HEK293T cells (kept in DMEM, 10% v/v serum).

5.4 Deubiquitination of ELK-1 in response to mitogens is independent of phosphorylation

The removal of monoubiquitin from ELK-1 correlated with ERK activation and ELK-1 phosphorylation (Figure 5-2). Although ubiquitin was not necessarily removed from ELK-1 prior to its phosphorylation (Figure 5-3), it was unclear whether phosphorylation of ELK-1 was the driving factor behind its subsequent deubiquitination. To identify whether this was the case, phosphorylation-defective mutants of ELK-1 were used in monoubiquitination assays with the

addition of the previously used constitutively active forms of RAF (259D) and V12-RAS (V12). ELK-1 S383/389A mutation removes two key phosphorylation targets for ERK-mediated ELK-1 transactivation (Marais et al., 1993; Janknecht et al., 1993; Gille et al., 1995A), while ELK-1 ΔD/FXLA removes both MAP kinase docking sites, preventing ERK from binding and phosphorylating ELK-1 (H. Zhang et al., 2008).

Monoubiquitination assays carried out with these phosphorylation defective forms of ELK-1 are shown in Figure 5-4. Phospho-ELK-1 immunoblot (S383) confirmed that ELK-1 S383/389A was not phosphorylated due to acceptor sites being removed (lanes 5 and 6), and that ELK-1 ΔD/FXLA phosphorylation was depleted compared to wild-type ELK-1 due to hindered MAP kinase docking (compare lanes 8 and 9 against lanes 2 and 3). Both forms of phosphorylation-deficient ELK-1 were monoubiquitinated (lanes 4 and 7), and were both deubiquitinated upon ERK cascade activation by RAF S259D and V12 RAS (lanes 5, 6, 8 and 9). This showed that the deubiquitination of ELK-1 after stimulation occurs independently of phosphorylation.

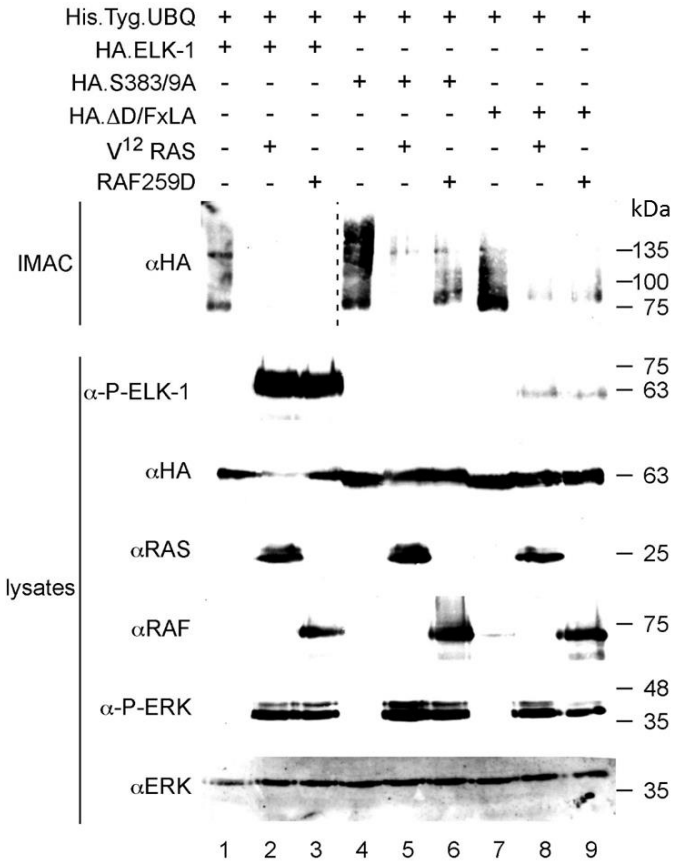

Figure 5-4: Deubiquitination of ELK-1 in response to mitogens is independent of phosphorylation. HEK293T cells were transfected with His-TYG-ubiquitin (UBQ) and constitutively active RAS (V12 RAS) or RAF (RAF259D), alongside either wild-type HA-ELK-1 or phosphorylation defective mutants ELK-1 S383/389 or ELK-1 ΔD/FXLA for 48 hours before harvesting. Top panel displays immunoblot for HA-tagged ELK-1 following denaturing IMAC for His-TYG-ubiquitin. Bottom panels display input lysate with ERK as a loading control. Phospho-ELK-1 (P383) and phospho-ERK (Y204) blots are indicative of ELK-1 and ERK1/2 activation respectively. Dotted line indicates different hyperfilm exposures.

These experiments gave some molecular insight into the localisation and removal of ubiquitinated ELK-1. It appears that ubiquitinated ELK-1 is mostly cytosolic, possibly due the inability of ELK-1 to bind DNA when ubiquitinated in the ETS domain, preventing it from being retained in the nucleus. Furthermore, chronic ERK cascade activation led to a reduction in ELK-1 monoubiquitination, in contrast to the increase in polyubiquitination seen on acute ERK activation (4.7). Whether this occurred due to monoubiquitin conversion into polyubiquitin by chain elongation, or whether monoubiquitin was removed and polyubiquitin later added to an alternate lysine acceptor is unclear. Monoubiquitin removal appears to not be linked to ELK-1 phosphorylation directly, as phosphorylation was dispensable in prompting the deubiquitination of ELK-1 post-ERK stimulation. Alternatively, ERK cascade activation could drive the expression or activation of a DUB that acts on ELK-1. The next step was to identify the enzyme responsible for this.

6 Identification of the deubiquitinating enzyme for ELK-1

6.1 DUB enzyme screen identifies that USP17 is capable of deubiquitinating ELK-1

Identifying which of the approximately 100 human DUBs had deubiquitinating activity towards ubiquitin-modified ELK-1 was important in understanding the functional significance and regulation of the modification. An extensive review of the literature identified several possible DUBs that could act on ELK-1 (Peter Shaw, personal communication). Criteria for selection included overlapping subcellular localisation and tissue expression profiles with that of ELK-1 (such as in the brain) and involvement in cell cycle progression and proliferation. Through this, five DUBs were selected for analysis experimentally, all of which belonged to the largest family of DUBs – the USPs. These were USP7, USP9X, USP17, USP22 and USP44 (Table 6-1) (1.3).

DUB	Subcellular localisation	Tissue expression	Involvement in cell cycle
USP7	Nuclear	Haematopoietic system, Reproductive system	-Deletion causes cell-cycle arrest -Promotes p53 degradation by interaction with MDM2
USP9x	Cytoplasm, axonal growth cones (neurons)	Brain, Reproductive system	-Knockdown causes cell-cycle arrest in G0 -Promotes mTORC signalling by RAPTOR stabilisation -Prevents ETS-1 degradation, driving NRAS expression
USP17	Nuclear, ER, Cytoplasm	Heart, Skeletal muscle, Kidney, Liver	-Expression is cell-cycle regulated -Knockdown impairs G1-S transition and RAS localisation -Promotes cell-cycle progression by stabilising CDC25A
USP22	Nuclear	Brain	-Knockdown causes cell-cycle arrest in G1 -Stabilises SIRT1, antagonising p53 transcriptional activity -Required for transcriptional activity of MYC targets -Positively regulates FBP1 repression of p21 expression
USP44	Nuclear	Reproductive system	-Stability regulated through the cell-cycle -Reinforces the mitotic checkpoint by promoting MCC and CDC20 complex formation

Table 6-1: Candidate DUBs for ELK-1 deubiquitination. Brief overview of subcellular localisation, tissue expression profiles and some examples of evidence pointing to DUB involvement in the cell cycle. Produced with reference to (Clague et al., 2013) (1.3).

Mammalian DUB expression vectors were obtained from the following: Roger Everett (Glasgow, USP7), Ralf Kittler (Dallas TX, FLAG-USP9X), Daniele Guardavaccaro (Utrecht, MYC-USP17), Sharon Dent (Smithville TX, V5-USP22) and Neils Mailand (Copenhagen, HA-USP44). To deduce whether any of these selected DUBs had deubiquitinating activity on ELK-1, they were screened in monoubiquitination assays in HEK293T cells (Figures 6-1 and 6-2). Both wild-type and catalytically inactive mutants (C>S/A) were screened by co-expression in assay, to ensure that any changes in ELK-1 ubiquitination status were due to DUB enzyme activity. As can be seen from Figure 6-1, wild-type USP17 substantially deubiquitinated monoubiquitinated ELK-1, while USP17C>S mutant and all other DUBs had a negligible effect. As USP7 was untagged, a USP7 antibody was used to confirm expression, which also detected endogenous USP7, although signal was appreciably higher when USP7 was overexpressed (lanes 4 and 5).

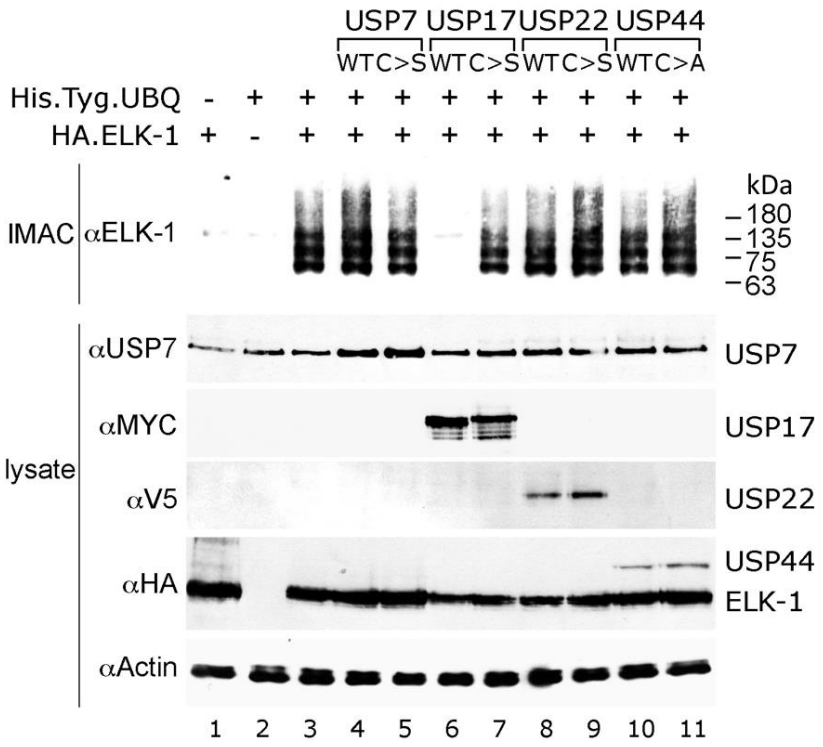

Figure 6-1: DUB screening assay points to USP17 as an enzyme responsible for deubiquitinating ELK-1 of monoubiquitin. HEK293T cells were transfected with HA-ELK-1, His-TYG-ubiquitin (UBQ) and either wild-type or catalytically inactive (C>S/A) DUBs for 48 hours before harvesting. Top panel displays immunoblot for HA-tagged ELK-1 following denaturing IMAC for His-TYG-ubiquitin. Bottom panels display input lysate with β-actin as a loading control.

USP17 encompasses a multitude of very similar genes which are highly copy-number variable (Alkan et al., 2009). They code for proteins approximately 60 kDa in size (530aa) that share between 90-100% sequence identity, with most variability occurring within the carboxyl-terminus. Some are confirmed pseudogenes (*USP17L6P* and *USP17L9P*), while several are considered probable pseudogenes, as despite possessing intact ORFs, they are not thought to produce transcripts (based on the NCBI database - *USP17L3*, *USP17L4*, *USP17L8*). Ultimately, it is unclear which of these genes are active and which, if any, are dormant. USP17 expression is both cell cycle regulated (McFarlane et al., 2010) and induced by cytokines (Burrows et al., 2004), so it is tempting to speculate that different *USP17* genes could be expressed at different points of the cell cycle and in response to different signalling molecules. Table 6-2 outlines the *USP17*-like genes that are not considered pseudogenes (based on the NCBI database) and hence could encode protein. The MYC-tagged clone used in the assay most closely resembles USP17L11 (524/530 amino acid matches), 17 (525), 20 (524) and 22 (524), all of which reside on chromosome 4.

Gene	Chromosome	ID	NCBI Ref Seq
USP17L1	8	401447	NM_001256873.1
USP17L2	8	377630	NM_201402.2
USP17L5	4	728386	NM_001242329.1
USP17L7	8	392197	NM_001256869.1
USP17L10	4	100287144	NM_001256852.1
USP17L11	4	100287178	NM_001256854.1
USP17L12	4	100287205	NM_001256853.1
USP17L13	4	100287238	NM_001256855.1
USP17L15	4	100288520	NM_001256894.1
USP17L17	4	100287327	NM_001256857.1
USP17L18	4	100287364	NM_001256859.1
USP17L19	4	100287404	NM_001256860.1
USP17L20	4	100287441	NM_001256861.1
USP17L21	4	100287478	NM_001256862.1
USP17L22	4	100287513	NM_001256863.1
USP17L24	4	728369	NM_001242327.1
USP17L25	4	728373	NM_001242326.1
USP17L26	4	728379	NM_001242328.1
USP17L27	4	728393	NM_001242330.1
USP17L28	4	728400	NM_001242331.1
USP17L29	4	728405	NM_001242332.1
USP17L30	4	728419	NM_001256867.1

Table 6-2: *USP17*-like genes in the NCBI database that could encode protein. Several genes have been eliminated, including several confirmed pseudogenes (*USP17L6P*, *USP17L9P*) and genes that are thought to be pseudogenes (*USP17L3*, *USP17L4*, *USP17L8*). *USP17L7* is inactive catalytically (C89F mutation); the *USP17L15* gene codes for a product ~4 kDa longer than all others due to a carboxyl-terminal extension.

Experiments were designed to further validate USP17 as a *bona fide* DUB of ELK-1. Firstly, a second FLAG-tagged USP17 expression clone, equating to USP17L24, 25, 26, 27, 28, 29 and 30 (all encoding an identical protein), was trialled in a monoubiquitination assay, alongside a FLAG-USP9X expression clone, which was considered a candidate DUB for ELK-1 deubiquitination but had not been tested. This was to assess whether the MYC-tag from the previous assay had any influence on USP17 activity, and to identify whether multiple USP17-like proteins are capable of deubiquitinating ELK-1. As can be seen from Figure 6-2, catalytically-active USP17 once again proved able to deubiquitinate ELK-1, with USP9X having no effect (compare lanes 4 and 6). This both reinforces the evidence that ELK-1 is a target for USP17, and that different USP17-like proteins generally target the same proteins, unsurprising given their very high sequence identity.

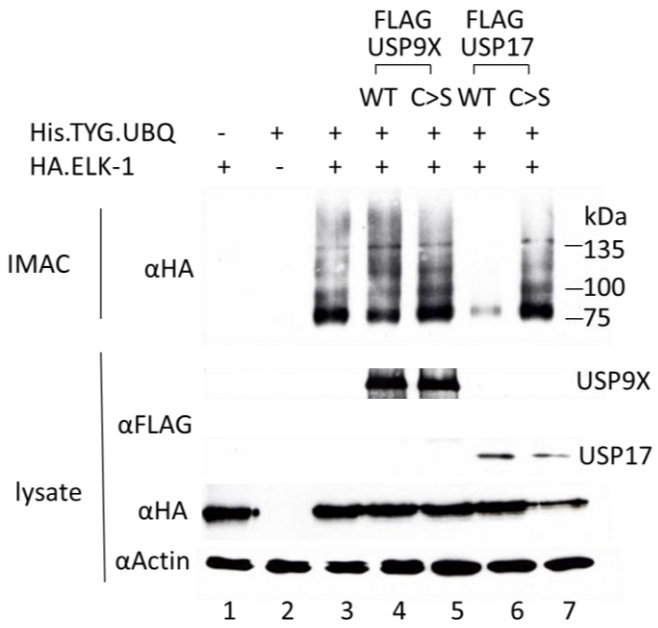

Figure 6-2: Second USP17 overexpression clone also deubiquitinates ELK-1. HEK293T cells were transfected with HA-ELK-1, His-TYG-ubiquitin (UBQ) and either wild-type or catalytically inactive (C>S) DUBs for 48 hours before harvesting. Top panel displays immunoblot for HA-tagged ELK-1 following denaturing IMAC for His-TYG-ubiquitin. Bottom panels display input lysate with β-actin as a loading control.

Before finally concluding that ectopic USP17 deubiquitinates ELK-1, the assay was repeated with untagged ELK-1, to ensure that the HA-tag from previous assays was not influencing the result. As can be seen from Figure 6-3, untagged ELK-1 was still deubiquitinated by USP17, showing that the HA-tag was not a confounding issue (lane 2). A band of low intensity corresponding to monoubiquitinated ELK-1 remained (as was the case in Figure 6-2), due to this

being the largest ubiquitinated population of ELK-1, and therefore was not entirely removed by USP17 catalysis.

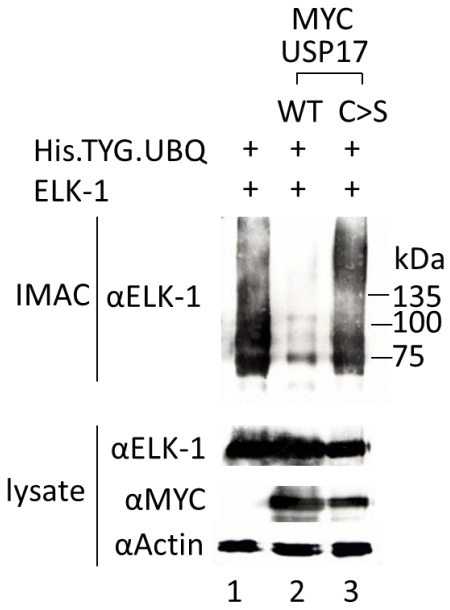

Figure 6-3: HA-tag does not influence ELK-1 deubiquitination. HEK293T cells were transfected with untagged ELK-1, His-TYG-ubiquitin (UBQ) and either wild-type or catalytically inactive (C>S/A) USP17 for 48 hours before harvesting. Top panel displays immunoblot for ELK-1 following denaturing IMAC for His-TYG-ubiquitin. Bottom panels display input lysate with β-actin as a loading control.

The previous assays showed that ELK-1 monoubiquitination was removed by USP17, but higher molecular weight ubiquitin conjugates also detected on the blot appeared to be removed. To clarify whether USP17 was able to remove polyubiquitin chains, a polyubiquitination assay was carried out including

USP17, alongside USP7 as a negative control. Figure 6-4 shows that USP17 does indeed disassemble polyubiquitin chains (lane 5), while USP7 and catalytically inactive USP17 did not. Therefore, USP17 appears to remove all ubiquitin conjugates from ELK-1, rather than selecting specifically for either monoubiquitin or polyubiquitin.

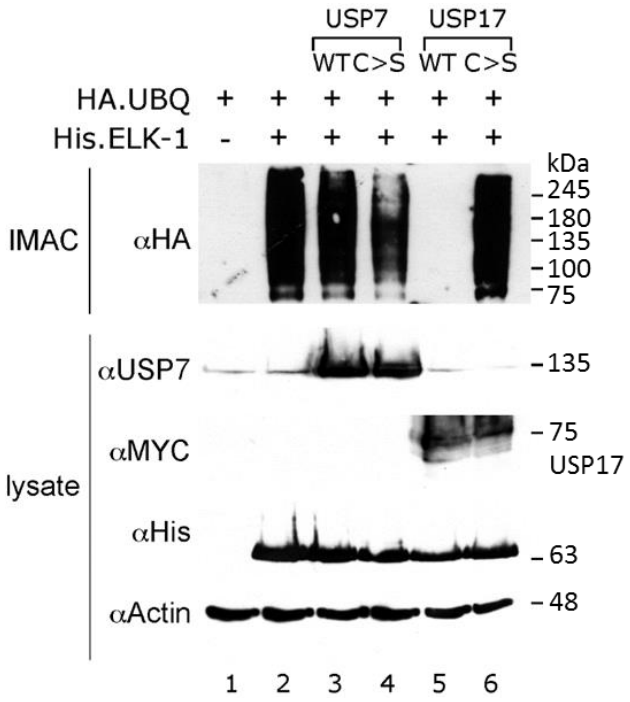

Figure 6-4: USP17 removes polyubiquitin chains from ELK-1. HEK293T cells were transfected with His-ELK-1, HA-ubiquitin (UBQ) and either wild-type or catalytically inactive (C>S) DUB for 48 hours before harvesting. Top panel displays immunoblot for HA-tagged ubiquitin following denaturing IMAC for His-ELK-1. Bottom panels display input lysate with β-actin as a loading control.

6.2 USP17 knockdown increases ELK-1 ubiquitination

Having shown that overexpressed USP17 could deubiquitinate ELK-1, experiments were carried out to assess whether the opposite held true - that knocking down endogenous USP17 expression increased ELK-1 ubiquitination. To achieve this, it was necessary to immunoblot for endogenous USP17. Previous reports suggested that this could prove challenging, with some resorting to ectopic expression of USP17 with concomitant USP17 shRNA to show knockdown efficacy indirectly (Hernández-Pérez et al., 2017), and others requiring immunoprecipitation enrichment prior to immunoblotting to visualise endogenous USP17 (McFarlane et al., 2010; Mehić et al., 2017). From three commercial antibodies tested, two failed to detect endogenous USP17 in HEK293T cells (Sigma Aldrich USP17 SAB1306139 and Abgent USP17L24 AP5491b) (data not shown). The third antibody was reported to detect endogenous USP17 in HEK293T cells (Invitrogen USP17L2 Cat#PA-5-44961) (H. Nguyen et al., 2017).

Immunoblot optimisations using this antibody were carried out on 50 µg HEK293T lysates (Figure 6-5). The membrane blocking agent proved to be the most important variable - when nitrocellulose membrane was blocked in 5% w/v Marvel milk powder, only a non-specific band was detected, whereas using 5% w/v BSA gave a band equating to endogenous USP17 (compare lanes 1 and 2 against 3 and 4). TBS-Tween (0.05% v/v) wash steps also gave a band of

greater intensity than PBS-Tween (0.05% v/v) (compare lanes 3 and 4), so 5% w/v BSA-TBS-Tween blocking followed by TBS-Tween washes were the conditions selected for USP17 immunoblotting.

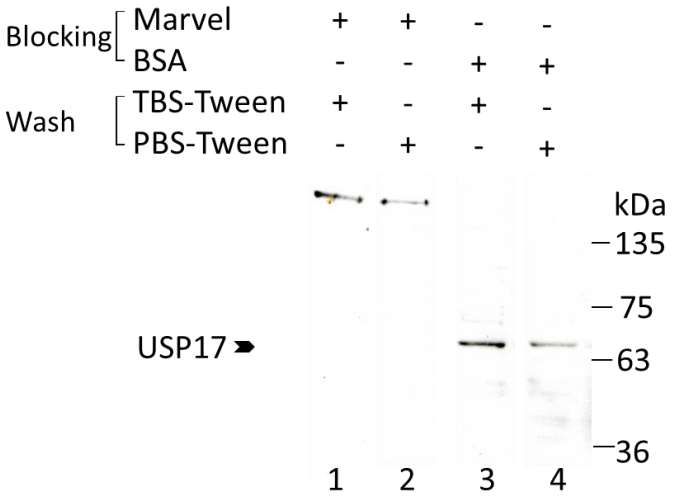

Figure 6-5: Immunoblot optimisation for USP17. USP17L2 antibody (Invitrogen Cat#PA-5-44961) was trialled in immunoblot, varying blocking agent (5% w/v Marvel vs 5% w/v BSA) and wash reagent (TBS-Tween (0.05% v/v) vs PBS-Tween (0.05% v/v)) on 50 µg HEK293T lysate. Arrowheads indicate endogenous USP17.

USP17-like protein coverage by the selected antibody was assessed by comparing sequence identity of the synthetic peptide used in the generation of antibody (amino acids 496-524) against the USP17-like proteins in the NCBI database. Table 6-3 shows that the antibody matches 100% with 19/28 USP17-

like proteins, showing one or two amino acid mismatches with the other nine and suggesting good general coverage.

Protein	USP17L2/DUB3 Antibody
USP17L1	1
USP17L1X1	1
USP17L2	X
USP17L3	1
USP17L3X1	1
USP17L4	2
USP17L5	X
USP17L7	2
USP17L8	2
USP17L10	1
USP17L11	X
USP17L12	X
USP17L12X1	X
USP17L13	X
USP17L15	X
USP17L17	X
USP17L18	1
USP17L19	X
USP17L20	X
USP17L21	X
USP17L22	X
USP17L24	X
USP17L25	X
USP17L26	X
USP17L27	X
USP17L28	X
USP17L29	X
USP17L30	X

Table 6-3: Sequence comparison of synthetic peptide used in the generation of USP17L2 antibody (Invitrogen Cat#PA-5-44961- amino acids 496-524) against the USP17-like proteins in the NCBI database. 100% matches are represented by crosses (X), and where this is not the case, numbers denote the number of amino acid mismatches.

Knocking down endogenous expression of *USP17* was complicated by the fact that multiple *USP17*-like genes could be being expressed at any point in the cell-cycle. Short hairpin RNA (shRNA) targeting *USP17* had previously been designed and shown to be effective, utilising the pSUPER plasmid which encodes the shRNA of interest (J. Kim et al., 2014). Regions of *USP17* targeted by these two shRNAs (USP17 sh#1 and sh#2) are shown in Figure 6-6. *USP17*-like gene coverage by these hairpin RNAs was assessed by comparing sequence identity against the *USP17*-like genes in the NCBI database. Table 6-4 shows that both USP17 sh#1 and sh#2 match 100% with the majority of *USP17*-like genes, and several of the single-base mismatches for sh#1 are in probable pseudogenes (*USP17L3*, *USP17L3X1*, *USP17L4*). Both plasmids fail to target *USP17L7*, which if expressed would be inactive due to a catalytic cysteine mutation (C89F). Overall, both knockdown vectors have generally good coverage over potential *USP17* transcripts.

NM_201402.2
Homo sapiens ubiquitin specific peptidase 17-like family member 2 (USP17L2)

```
   1- ATGGAGGACGACTCACTCTACTTGGGAGGTGAGTGGCAGTTCAACCACTTTTCAAAACTCACATCTTCTC
  71- GGCCAGATGCAGCTTTTGCTGAAATCCAGCGGACTTCTCTCCCTGAGAAGTCACCACTCTCATCTGAGGC
 141- CCGTGTCGACCTCTGTGATGATTTGGCTCCTGTGGCAAGACAGCTTGCTCCCAGGAAGAAGCTTCCTCTG
 211- AGTAGCAGGAGACCTGCTGCGGTGGGGGCTGGGCTCCAGAATATGGGAAATACCTGCTACGAGAACGCTT
 281- CCCTGCAGTGCCTGACATACACACCGCCCCTTGCCAACTACATGCTGTCCCGGGAGCACTCTCAAACATG
 351- TCAGCGTCCCAAGTGCTGCATGCTCTGTACTATGCAAGCTCACATCACATGGGCCCTCCACAGTCCTGGT
 421- CATGTCATCCAGCCCTCACAGGCATTGGCTGCTGGCTTCCATAGAGGCAAGCAGGAAGATGCCCATGAAT
 491- TTCTCATGTTCACTGTGGATGCCATGAAAAAGGCATGCCTTCCCGGCCACAAGCAGGTAGATCATCACTC
 561- TAAGGACACCACCCTCATCCACCAAATATTTGGAGGCTGCTGGAGATCTCAAATCAAGTGTCTCCACTGC
 631- CACGGGATTTCAGACACTTTTGACCCTTACCTGGACATCGCCCTGGATATCCAGGCAGCTCAGAGTGTCA
 701- AGCAAGCTTTGGAACAGTTGGTGAAGCCCGAAGAACTCAATGGAGAGAATGCCTATCATTGCGGTCTTTG
 771- TCTCCAGAGGGCGCCGGCCTCCAAGACGTTAACTTTACACACTTCTGCCAAGGTCCTCATCCTTGTCTTG
 841- AAGAGATTCTCCGATGTCACAGGCAACAAACTTGCCAAGAATGTGCAATATCCTGAGTGCCTTGACATGC
 911- AGCCATACATGTCTCAGCAGAACACAGGACCTCTTGTCTATGTCCTCTATGCTGTGCTGGTCCACGCTGG
 981- GTGGAGTTGTCACGACGGACATTACTTCTCTTATGTCAAAGCTCAAGAAGGCCAGTGGTATAAAATGGAT
1051- GATGCCAAGGTCACTGCCTGTAGCATCACTTCTGTCCTGAGTCAACAGGCCTATGTCCTCTTTTACATCC
1121- AGAAGAGTGAATGGGAAAGACACAGTGAGAGTGTGTCAAGAGGCAGGGAACCAAGAGCCCTCGGCGCTGA
1191- AGACACAGACAGGCGAGCAACGCAAGGAGAGCTCAAGAGAGACCACCCCTGCCTCCAGGCACCCGAGTTG
1261- GACGAGCGCTTGGTGGAAAGAGCCACTCAGGAAAGCACCTTAGACCACTGGAAATTCCCCCAAGAGCAAA
1331- ACAAAACGAAGCCTGAGTTCAACGTCAGAAAAGTCGAAGGTACCCTGCCTCCCAACGTACTTGTGATTCA
1401- TCAATCGAAATACAAGTGTGGGATGAAAAACCATCATCCTGAACAGCAAAGCTCCCTGCTAAACCTCTCT
1471- TCGACGACCCGGACAGATCAGGAGTCCGTGAACACTGGCACCCTCGCTTCTCTGCAAGGGAGGACCAGGA
1541- GATCCAAAGGGAAGAACAAACACAGCAAGAGGGCTCTGCTTGTGTGCCAGTGA-1593
```

Figure 6-6: Human *USP17* cDNA sequence and knockdown targets. Coding region of *USP17L2* gene, with sh#1 and sh#2 target regions highlighted (5' to 3').

Gene	USP17 sh#1	USP17 sh#2
USP17L1	1	X
USP17L1X1	1	X
USP17L2	X	X
USP17L3	1	X
USP17L3X1	1	X
USP17L4	1	X
USP17L5	X	X
USP17L7	1	3
USP17L8	X	X
USP17L10	X	X
USP17L11	X	X
USP17L12	X	X
USP17L12X1	X	X
USP17L13	X	X
USP17L15	X	X
USP17L17	X	X
USP17L18	X	X
USP17L19	X	X
USP17L20	X	X
USP17L21	X	X
USP17L22	X	X
USP17L24	X	X
USP17L25	X	X
USP17L26	X	X
USP17L27	X	X
USP17L28	X	X
USP17L29	X	X
USP17L30	X	X

Table 6-4: Sequence identity matches of *USP17* pSUPER shRNA (sh#1/sh#2) vector targets with *USP17*-like genes. 100% matches are represented by crosses (X), and where this is not the case, numbers denote the number of base mismatches against a transcript. *USP17L3*, *USP17L3X* and *USP17L8* are considered pseudogenes. *USP17L1X*, *USP17L3X* and *USP17L12X* are possible transcript variants of *USP17L1*, *USP17L3* and *USP17L12* respectively.

Before assessing whether pSUPER sh#1 and sh#2 effectively knocked down endogenous USP17, overexpression of MYC-USP17 with concomitant pSUPER transfection in HEK293T cells was carried out. Figure 6-7 shows that both short RNA knockdown vectors successfully depleted ectopic expression of MYC-USP17, shown using both MYC and USP17 antibodies.

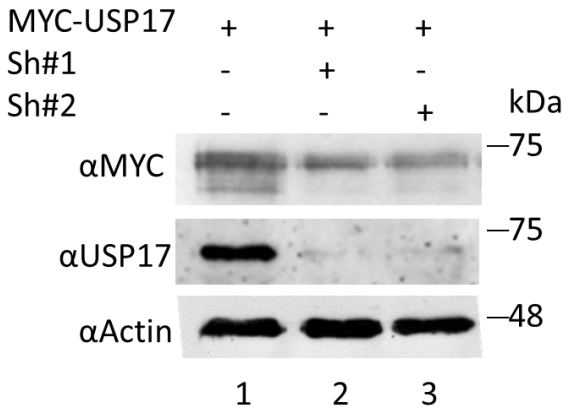

Figure 6-7: USP17 knockdown vectors successfully deplete USP17 overexpression. HEK293T cells were transfected with MYC-USP17 and pSUPER USP17 knockdown vectors sh#1 and sh#2. Cell lysate (20 µg) was loaded onto SDS-PAGE, transferred and submitted to immunoblotting for USP17 (MYC/USP17) and β-actin as loading control.

Transfections were then carried out with pSUPER sh#1 and sh#2 on HEK293T cells, and cell lysates were produced. Immunoblot for USP17 showed that both vectors successfully depleted endogenous USP17 (Figure 6-8). Hence, immunoblotting for USP17 and knocking down its expression had both proven successful and further experiments could be performed.

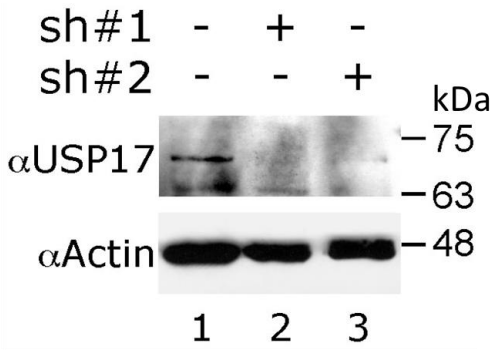

Figure 6-8: pSUPER sh#1 and sh#2 depleted endogenous USP17 expression. HEK293T cells were transfected with pSUPER USP17 knockdown vectors sh#1 or sh#2. Cell lysate (50 μg) was loaded onto SDS-PAGE and subjected to immunoblotting for USP17 and β-actin as loading control.

To investigate whether USP17 knockdown impacted on ELK-1 ubiquitination, monoubiquitination assays were carried out with the additional co-transfection of pSUPER sh#1 and sh#2 into HEK293T cells. Figure 6-9 shows that transfection of both knockdown vectors led to an increase in ELK-1 ubiquitination. This appeared to affect ubiquitination of ELK-1 in general, rather than specifically mono- or polyubiquitinated ELK-1 forms, with signal intensity increasing in knockdown samples at both low molecular weight conjugates and high molecular weight polyubiquitin species. This fits with previous evidence that USP17 appears to remove both mono- and polyubiquitin chains from ELK-1 (Figures 6-1, 6-2, 6-3 and 6-4). Importantly, this experiment showed that endogenous USP17 regulates ELK-1 ubiquitination, rather than just overexpressed USP17.

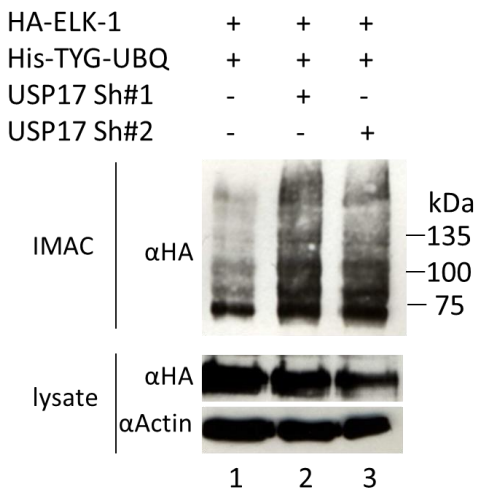

Figure 6-9: USP17 depletion resulted in increased ELK-1 ubiquitination. HEK293T cells were transfected with HA-ELK-1 and His-TYG-ubiquitin with or without USP17 sh#1 or sh#2 for 48 hours, before harvesting. Top panel displays immunoblot for HA-tagged ELK-1 following denaturing IMAC for His-TYG-ubiquitin. Bottom panels display input lysate with β-actin as a loading control.

Reduction in ELK-1 monoubiquitination has previously been noted post-induction with TPA/serum stimulation (Chow, PhD thesis, University of Nottingham, 2010). To assess the effect of ERK-cascade induction on ubiquitination status following USP17 depletion, various pre-assay cell treatments were trialled in a monoubiquitination assay while including USP17 sh#1 and sh#2 knockdown vector transfection. Twenty-four hours post-transfection, HEK293T cells were either serum-starved (24 hours), kept in full medium (24 hours), or serum-starved (22 hours) followed by TPA/serum stimulation (2 hours). IMAC and immunoblotting showed that under all

conditions, USP17 depletion increased ELK-1 ubiquitination (Figure 6-10). Notably, the lowest molecular weight HA-ELK post-IMAC immunoblot band (corresponding to monoubiquitinated ELK-1) was depleted post-TPA/serum stimulation (induced) against serum-starved cells (starved) and cells kept in full medium (normal), but was rescued by USP17 knockdown (top panel, compare lane 5 and 6). Equally, under all conditions, high molecular weight ubiquitin conjugates also increased in abundance after USP17 knockdown. This further shows that USP17 deubiquitinates both mono- and polyubiquitinated ELK-1. It should be noted that there was very little difference between serum-starved cells and cells kept in full medium, owing to high basal ectopic ELK-1 phosphorylation regardless of serum withdrawal, as was seen in previous experiments (4.7).

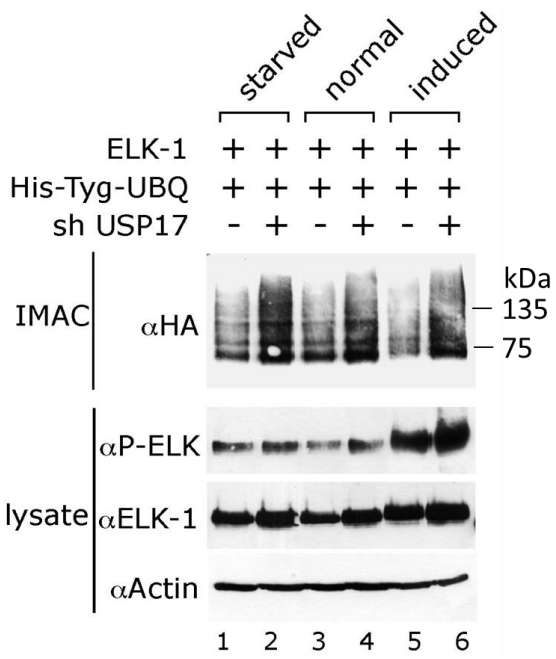

Figure 6-10: USP17 depletion increases both mono- and polyubiquitination of ELK-1 under various conditions. HEK293T cells were transfected with HA-ELK-1, His-TYG-ubiquitin and either pSUPER (empty vector) or a combination of pSUPER sh#1 and sh#2 (sh USP17). Twenty-four hours post-transfection cells were either serum-starved (starved), kept in full medium (normal), or serum-starved followed by TPA/serum stimulation (induced). Top panel displays immunoblot for HA-tagged ELK-1 following denaturing IMAC for His-TYG-ubiquitin. Bottom panels display input lysate with β-actin as a loading control.

6.3 USP17 and ELK-1 co-immunoprecipitate

Having shown that USP17 influences ELK-1 ubiquitination through both ectopic expression and endogenous depletion of the DUB, Co-IP experiments were carried out to identify whether there is a physical interaction between the two proteins, to clarify whether USP17 targets ELK-1 specifically (including unmodified ELK-1) or associates only with ubiquitin conjugates attached to ELK-1. HA-ELK and MYC-USP17C/S were transfected into HEK293T cells, which was followed by an IP using either ELK-1 or MYC antibody. Samples were then resolved by SDS-PAGE and immunoblotted for the reciprocal protein through HA(ELK-1) or MYC(USP17) antibody. When enriching for HA-ELK-1, MYC-USP17C/S was pulled down alongside it (Figure 6-11A, top panel, lane 2), but not in control lanes (lane 1 and 3). Equally, when enriching for MYC-USP17C/S, HA-ELK-1 co-immunoprecipitated (Figure 6-11B, top panel, lane 2).

These experiments showed that USP17 can interact with ELK-1. MYC-USP17C/S rather than wild-type USP17 was chosen for the assay as it was reasoned that catalytically inactive USP17 may bind with higher affinity than catalytically active USP17, due to its inability to hydrolyse ubiquitin conjugates and hence remain associated with ELK-1. However, when the same Co-IP experiment was carried using wild-type MYC-USP17, both proteins were still found to co-immunoprecipitate (data not shown). Hence, this strongly suggests that USP17 interacts with ELK-1, rather than associating with ubiquitin conjugates

independent of the target protein. Despite this, the possibility of ELK-1 and USP17 interacting indirectly through an intermediary protein cannot be ruled out on this data alone.

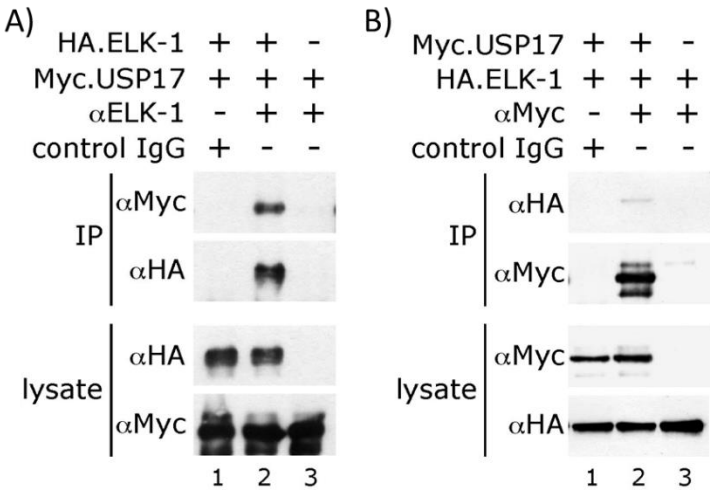

Figure 6-11: USP17 and ELK-1 co-immunoprecipitate. A) HEK293T cells were transfected with HA-ELK-1 and MYC-USP17C/S for 48 hours, and then submitted to immunoprecipitation (IP) with ELK-antibody (H-160). Top panels display post-IP immunoblot for HA-ELK and MYC-USP17C/S. Bottom panels display input protein. B) Same as A) but IP carried out using MYC antibody.

6.4 USP17 also deubiquitinates other TCFs in addition to ELK-1

ELK-1 is one of three TCFs in human cells. The others are ELK-3 and ELK-4. All three TCFs are expressed to similar relative levels across similar tissue profiles, and have conserved domains for interaction with the *CFOS* SRE *via* SRF and carboxyl-terminal TADs for ERK phosphorylation (Price et al., 1995). Functional redundancy between the TCFs in promoter occupancy and transcriptional activation has been reported (Boros et al., 2009B). All three TCFs have also previously been shown to be ubiquitinated (Chow, PhD thesis, University of Nottingham, 2010), and as USP17 had been shown to deubiquitinate ELK-1, experiments were carried out to determine whether it had a similar effect on ELK-3 and ELK-4. A monoubiquitination assay was carried out in HEK293T cells transfected with HA-tagged ELK-1, ELK-3 and ELK-4, and His-TYG-ubiquitin with or without MYC-USP17. All three TCFs were substantially deubiquitinated by USP17 (Figure 6-12, lanes 2, 4 and 6 for ELK-1, ELK-3 and ELK-4 respectively). This shows that as well as being a *bona fide* DUB for ELK-1, USP17 can also deubiquitinate the other TCFs, suggesting any functional regulation through USP17 activity is likely conserved across ELK-1, ELK-3 and ELK-4. It also seems likely that ELK-3 and ELK-4 may be modified in the ETS domain, as the ELK-1 modification sites (K35, K52 and K59) are conserved across all three TCFs (Figure 6-13).

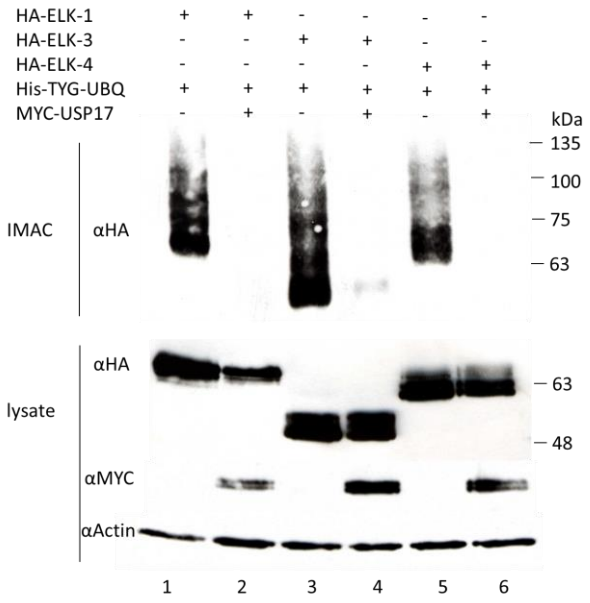

Figure 6-12: USP17 can deubiquitinate other TCFs. HEK293T cells were transfected with HA-ELK-1, ELK-3 or ELK-4, and His-TYG-ubiquitin with or without MYC-USP17 for 48 hours before harvesting. Top panel displays immunoblot for HA-tagged TCF following denaturing IMAC for His-TYG-ubiquitin. Bottom panels display input lysate with β-actin as a loading control.

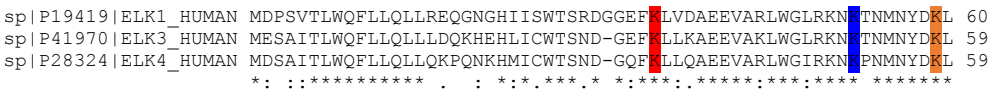

Figure 6-13. Lysine residues targeted for ubiquitination in ELK-1 are conserved across the TCFs. Amino-terminal primary sequences of ELK-1, ELK-3 and ELK-4 (Human) aligned using Clustal Omega, with ELK-1 lysines targeted for ubiquitination labelled (K35, K52 and K59). * (asterisk) = single, fully conserved residue, : (colon) = conservation between groups of strongly similar properties, . (period) = conservation between groups of weakly similar properties.

To conclude, USP17 was shown to deubiquitinate ELK-1, removing both monoubiquitin and polyubiquitin chains. This was the case for both ectopic and endogenous USP17, with both impacting on ELK-1 ubiquitination status. ELK-1 and USP17 also co-immunoprecipitated, suggesting that they can interact. Lastly, USP17 could also deubiquitinate ELK-3 and ELK-4, possibly by removing ubiquitin from the conserved ETS domain lysine residues in the TCFs. However, the impact of ubiquitination on ELK-1 function and its deubiquitination by USP17 required further investigation.

7 USP17 regulates ELK-1 transcriptional potency and cell proliferation

7.1 USP17 depletion impairs *CFOS* and *EGR1* expression

Experimental evidence in the previous chapter has shown that USP17 interacts with and deubiquitinates ELK-1. However, the effects on ELK-1 function had yet to be elucidated. To explore the effects of USP17 expression on ELK-1 target gene transcription, qRT-PCR experiments were carried out. Overexpression of USP17 led to the upregulation of several ELK-1 targets, including *CFOS*, *EGR1*, *EGR2*, *IER2* and downstream *CCND1* (Janice Saxton, unpublished data). A reciprocal experiment was carried out using pSUPER USP17 sh#1 and sh#2, which had already been shown to deplete USP17 expression effectively (Figures 6-7 and 6-8). These were transfected into HEK293T cells, after which RNA was extracted and cDNA prepared for qRT-PCR, and *CFOS* and *EGR1* expression levels were assessed with TaqMan probes (3.4.4). USP17 depletion led to a significant decrease in *CFOS* and *EGR1* expression against control transfected cells (empty pSUPER) (Figure 7-1). This shows that USP17 knockdown reduces the transcription of ELK-1 target genes and, allied with the USP17-overexpression data, suggests that ELK-1 driven transcription is increased in the presence of USP17. This could be due to either USP17 deubiquitination of ELK-1 de-repressing ELK-1 and potentiating its activation, or alternatively the deubiquitination could stabilise ELK-1, preventing its

proteasomal degradation and hence leaving more ELK-1 to promote transcription.

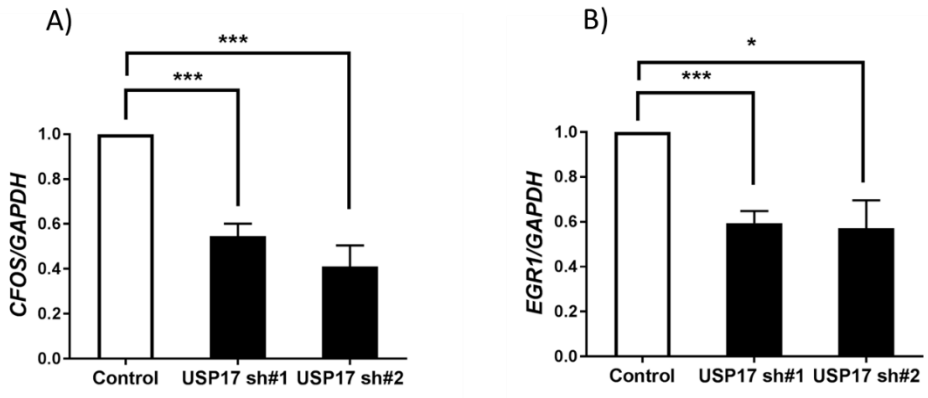

Figure 7-1: USP17 depletion impairs *CFOS* and *EGR1* expression. A) HEK293T cells were transfected with pSUPER-USP17 knockdown vectors (sh#1 and sh#2) or pSUPER empty vector (Control) for 48 hours before harvesting. RNA was extracted and used to make cDNA, and qRT-PCR experiments were carried out using TaqMan probes designed against *CFOS* and *GAPDH* (housekeeping control gene). Data is expressed as *CFOS*/*GAPDH* fold change, with Control normalised to 1. B) Same as A) but looking at *EGR1* expression. Statistical analyses were performed using Student's t test (N=4, -/+ SEM, **p*<0.05 ****p*<0.001).

7.2 USP17 does not appear to protect ELK-1 from proteasomal degradation

USP17 removes polyubiquitin chains from ELK-1 (6.1). Polyubiquitin chains associated with ELK-1 appear to be K48-linked; a canonical signature for proteasomal degradation (4.3, 4.7). Therefore, it is possible that USP17 may stabilise ELK-1 by removing these polyubiquitin chains and preventing ELK-1 from being recognised as a substrate by the 26S proteasome. However, previous ubiquitination experiments gave no indication that ectopically expressed USP17 increased the stability of ectopically expressed ELK-1 (6.1). To resolve this, experiments involving transfecting USP17 and assessing changes in steady-state levels of endogenous ELK-1 were devised. To carry these out, reliable immunoblotting for endogenous ELK-1 was required. Previously, αH-160 had been considered the most reliable ELK-1 antibody for immunoblotting, and had also been used for immunoprecipitation experiments (6.3). However, its discontinuation by Santa Cruz Biotechnology required its replacement with a suitable alternative antibody. Five ELK-1 antibodies were trialled in immunoblot on cell lysates from HeLa, HEK293T and MCF7 cells. These were αI20 (Santa Cruz, rabbit polyclonal), αH160 (Santa Cruz, rabbit polyclonal), α9182 (Cell Signalling, rabbit polyclonal), αELKC (Shaw lab "*in-house*", rabbit polyclonal) and αE277 (Abcam, rabbit monoclonal). Figure 7-2 compares immunoblots with each antibody. All antibodies detected a band of approximately 63 kDa corresponding to (unmodified) ELK-1 (indicated by

arrowhead) except for α9182, and nonspecific bands were seen with all antibodies apart from αE277. Notably, αE277 gave a clean ELK-1 band for all three cell lines, including MCF7, showing higher specificity and sensitivity than all other antibodies. Hence, this was the antibody chosen for immunoblotting for endogenous ELK-1.

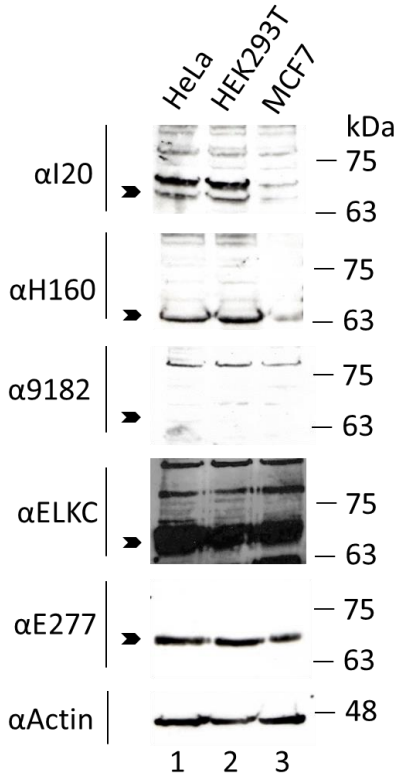

Figure 7-2: Antibody αE277 is most suitable for immunoblotting for endogenous ELK-1. HeLa, HEK293T and MCF7 cell lysates (50 µg) were resolved by SDS-PAGE and immunoblotted with following antibodies: αI20, αH160, α9182, αELKC, αE277 and β-actin for loading control. Arrowhead denotes band corresponding to ELK-1.

Having selected an appropriate ELK-1 antibody, experiments assessing the effects of USP17 overexpression on endogenous ELK-1 stability could be carried out. HEK293T cells were transfected with expression vectors for wild-type USP17 and catalytically inactive mutant (C>S), and 48 hours later either left untreated or treated with 20 μM proteasome inhibitor MG132 for six hours. Immunoblots were carried out on cell lysates produced after treatment, probing for endogenous ELK-1 and β-actin, with the ratio of ELK-1/actin used to determine relative levels of ELK-1. Figure 7-3 shows a representative set of blots (A), with densitometry for three replicate experiments shown below (B).

The data suggests there was a slight increase in stability of ELK-1 when USP17 was overexpressed (compare lanes 1 and 2), although this was also the case with catalytically inactive DUB (lane 3). In agreement with evidence that ELK-1 is a substrate of the proteasome, MG132 treatment lead to a significant accumulation of ELK-1 (Evans et al., 2011). There was also a significant difference between MG132 treated cells when transfected with empty vector (control) versus USP17C/S (compare lanes 4 and 6). This was a surprising result, as it is unclear how catalytically inactive USP17 (and to a lesser extent, wild-type USP17) could reduce the level of ELK-1 in the presence of MG132. The 26S proteasome is the only mechanism linked to ELK-1 degradation so far, and the autophagy inhibitor bafilomycin did not influence ELK-1 stability (Evans et al., 2011), so it does not seem likely that ELK-1 could be degraded through this pathway. Regardless, there is no evidence to support USP17 catalytic activity

protecting ELK-1 from proteasomal degradation, as ELK-1 was only significantly stabilised by MG132 treatment. Hence, an alternative mechanism for the decrease in transcription of ELK-1 target genes post-knockdown of USP17 expression (Figure 7-1) seemed likely.

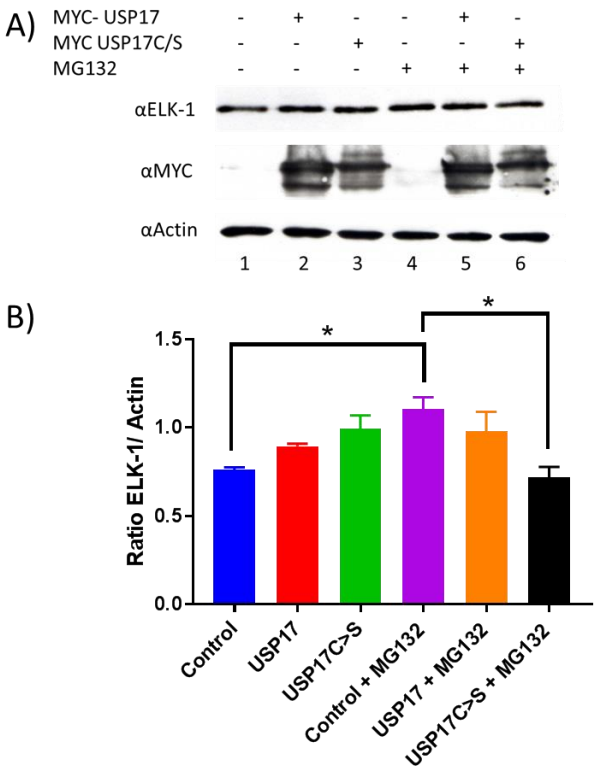

Figure 7-3: USP17 does not significantly affect ELK-1 stability. A) HEK293T cells were transfected with wild-type or catalytically inactive (C>S) USP17 for 48 hours, followed by either leaving untreated or treating with 20 µM proteasome inhibitor MG132 for six hours. Whole cell lysates were produced and 50 µg was resolved by SDS-PAGE and immunoblotted for endogenous ELK-1 (αE277), MYC (USP17) and β-actin as loading control. B) Plots of ELK-1/actin from densitometry quantified with ImageJ. Statistical analyses were carried out using one-way ANOVA with post-hoc analysis using Tukey's multiple comparisons test. (N=3, -/+ SEM, *p<0.05).

7.3 USP17 depletion inhibits cell proliferation in HeLa cells

The MTT assay is a colorimetric assay for assessing cell metabolic activity, based on NAD(P)H-dependent oxidoreductase enzyme reduction of 3-(4,5-dimethylthiazol-2-yl)-2,5-diphenyltetrazolium bromide (MTT reagent), producing a purple colour (3.3.6). This can also be used to assess relative proliferation rates by measuring absorbance, where an increase of proliferating cells gives a stronger colouration (Mosmann, 1983). It had previously been shown by MTT assay that USP17 knockdown (using pSUPER USP17 sh#1) blocked proliferation and growth in HeLa cells (McFarlane et al., 2010). Replicate experiments were carried out to reproduce this data and further study the functional significance of USP17 on cell growth. HeLa cells were transfected with either empty pSUPER vector, USP17 sh#1 or sh#2, and after 24 hours were trypsinised and re-seeded into 96 well plates, before being assessed by MTT assay over four days. Both USP17 sh#1 and sh#2 significantly reduced cell proliferation in HeLa cells (Figure 7-4).

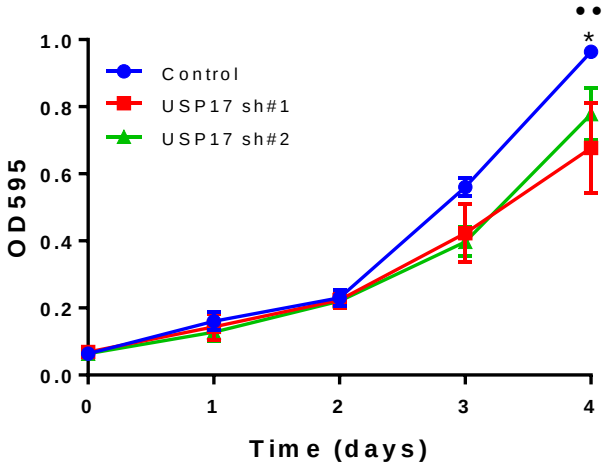

Figure 7-4: USP17 depletion inhibits proliferation in HeLa cells. Cells were transfected with either empty pSUPER vector, USP17 sh#1 or sh#2, and after 24 hours were trypsinised and re-seeded into 96 well plates, before being assessed by MTT assay over four days. Post-hoc analyses were conducted using Tukey's multiple comparisons test for repeated measures ANOVA. * = Control vs USP17 sh#2. • = Control vs USP17 sh#2 (N=3, -/+ SEM, *p<0.05, **p<0.01).

7.4 ELK-1 and USP17 depletion inhibits HEK293T cell proliferation

Functionally, ELK-1 is most commonly associated with regulating cell proliferation (Vickers et al., 2004), and its depletion has been shown to retard growth in bladder cancer cell lines (Kawahara et al., 2015). To explore the effects of ELK-1 on proliferation, knockdown shRNAs for ELK-1 were designed

to assess how ELK-1 depletion affected cell growth, using pSUPER plasmid derivatives as with USP17. Targets in the coding region of the *ELK-1* gene are shown in Figure 7-5 for ELK sh#1 and sh#2. These were tested by transfection into HEK293T cells, followed by immunoblot for ELK-1. ELK sh#1 knocked down expression of ELK-1, whereas ELK sh#2 failed to achieve this (Figure 7-6).

NM_001114123.2
Homo sapiens ELK1, ETS transcription factor (ELK1), transcript variant 1

```
   1- ATGGACCCATCTGTGACGCTGTGGCAGTTTCTGCTGCAGCTGCTGAGAGAGCAAGGCAATGGCCACATCATCTCCTGGACT
  82- TCACGGGATGGTGGTGAATTCAAGCTGGTGGATGCAGAGGAGGTGGCCCGGCTGTGGGGGCTACGCAAGAACAAGACCAAC
 163- ATGAATTACGACAAGCTCAGCCGGGCCTTGCGGTACTACTATGACAAGAACATCATCCGCAAGGTGAGCGGCCAGAAGTTC
 244- GTCTACAAGTTTGTGTCCTACCCTGAGGTCGCAGGGTGCTCCACTGAGGACTGCCCGCCCCAGCCAGAGGTGTCTGTTACC
 325- TCCACCATGCCAAATGTGGCCCCTGCTGCTATACATGCCGCCCCAGGGGACACTGTCTCTGGAAAGCCAGGCACACCCAAG
 406- GGTGCAGGAATGGCAGGCCCAGGCGGTTTGGCACGCAGCAGCCGGAACGAGTACATGCGCTCGGGCCTCTATTCCACCTTC
 487- ACCATCCAGTCTCTGCAGCCGCAGCCACCCCCTCATCCTCGGCCTGCTGTGGTGCTCCCCAGTGCAGCTCCTGCAGGGGCA
 568- GCAGCGCCCCCCTCGGGGAGCAGGAGCACCAGTCCAAGCCCCTTGGAGGCCTGTCTGGAGGCTGAAGAGGCCGGCTTGCCT
 649- CTGCAGGTCATCCTGACCCCGCCCGAGGCCCCAAACCTGAAATCGGAAGAGCTTAATGTGGAGCCGGGTTTGGGCCGGGCT
 730- TTGCCCCCAGAAGTGAAAGTAGAAGGGCCCAAGGAAGAGTTGGAAGTTGCGGGGGAGAGAGGGTTTGTGCCAGAAACCACC
 811- AAGGCCGAGCCAGAAGTCCCTCCACAGGAGGGCGTGCCAGCCCGGCTGCCCGCGGTTGTTATGGACACCGCAGGGCAGGCG
 892- GGCGGCCATGCGGCTTCCAGCCCTGAGATCTCCCAGCCGCAGAAGGGCCGGAAGCCCCGGGACCTAGAGCTTCCACTCAGC
 973- CCGAGCCTGCTAGGTGGGCCGGGACCCGAACGGACCCCAGGATCGGGAAGTGGCTCCGGCCTCCAGGCTCCGGGGCCGGCG
1054- CTGACCCCATCCCTGCTTCCTACGCATACATTGACCCCGGTGCTGCTGACACCCAGCTCGCTGCCTCCTAGCATTCACTTC
1135- TGGAGCACCCTGAGTCCCATTGCGCCCCGTAGCCCGGCCAAGCTCTCCTTCCAGTTTCCATCCAGTGGCAGCGCCCAGGTG
1216- CACATCCCTTCTATCAGCGTGGATGGCCTCTCGACCCCCGTGGTGCTCTCCCCAGGGCCCCAGAAGCCATGA -1287
```

Figure 7-5: ELK-1 cDNA sequence (human) and knockdown targets. Coding region of *ELK-1* gene, with sh#1 and sh#2 target regions highlighted.

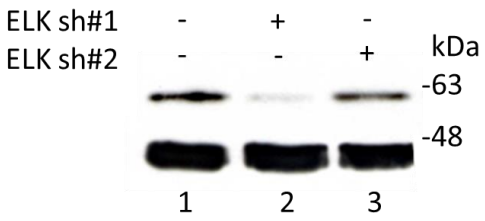

Figure 7-6: pSUPER ELK sh#1 knocks down endogenous ELK-1 expression, whilst ELK sh#2 has no effect. HEK293T cells were transfected with pSUPER ELK-1 knockdown vectors sh#1 or sh#2. Cell lysate was loaded onto SDS-PAGE (50 µg) and immunoblotted for ELK-1 (αE277) and β-actin as loading control.

Both shRNAs were used in an MTT assay to assess ELK-1 effects on cell proliferation. As ELK sh#2 had no effect on ELK-1 protein levels, this was included as a negative control. HEK293T cells were transfected with empty pSUPER vector or either of the ELK shRNAs and MTT assays were carried over four days. HEK293T cells were chosen to replace HeLa cells for the MTT assay as they were more reproducibly transfected to high levels, and HEK293T cells had been used in all previous experiments. Figure 7-7 shows that ELK-1 knockdown with ELK sh#1 retarded cell growth significantly when compared against both the control and ELK sh#2 shRNA. ELK sh#2 had no effect, and cells transfected with this plasmid grew equivalently to the control. As ELK sh#2 had already been shown to have no effect on ELK-1 expression, this validated the robustness of the MTT assay and the pSUPER shRNA transfection system, with the empty vector and an ineffective shRNA both having a comparable lack of effect on cell proliferation. The inhibitory effect on proliferation after transfection with ELK sh#1 showed that ELK-1 has an important role in HEK293T cell proliferation.

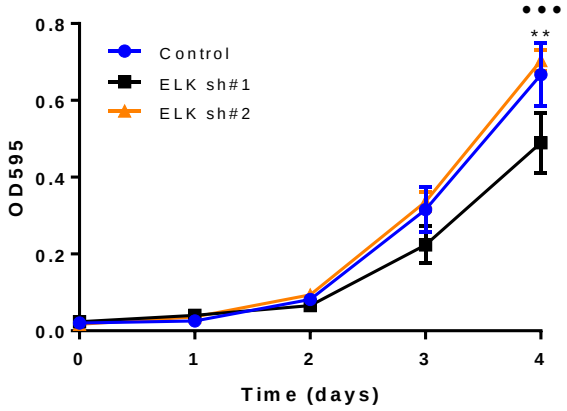

Figure 7-7: HEK293T cells were transfected with either empty pSUPER vector, ELK sh#1 or sh#2, and after 24 hours were trypsinised and re-seeded into 96 well plates (2000 cells/well), before being assessed by MTT assay over four days. Post-hoc analyses were conducted using Tukey's multiple comparisons test for repeated measures ANOVA. * = Control vs ELK sh#1. • = ELK sh#1 vs ELK sh#2 (N=5, -/+ SEM, *p<0.05, **p<0.01).

Having shown that both USP17 and ELK-1 knockdown affected cell growth, further MTT assays were carried out on HEK293T cells after knocking down USP17 and ELK-1 expression, both individually and concomitantly. This was to assess whether USP17 knockdown influenced HEK293T cell growth (in addition to HeLa cells), and to understand whether there were any additive effects on growth inhibition when knocking down both USP17 and ELK-1 expression. Alongside MTT assays, direct counting assays were carried out after four days transfection (using an automated MOXI cell counter) to provide further

assurance that the differences seen in MTT assay were due to cell proliferation and growth changes rather than alterations in cell metabolism. Figure 7-8 shows that ELK sh#1 and USP17 sh#1 significantly reduced cell growth individually against the control (by both MTT and cell counting), and this was also the case when used in combination. However, this effect was not additive, as there was no significant difference between the combinatorial shRNA transfection against transfecting them individually. This is perhaps not surprising, because if USP17 and ELK-1 were linked functionally in driving cell proliferation, then depletion of either could affect cell growth equally. Hence, knocking expression of both down would have no further effect, as reduced expression of just one would blunt the effect of the other.

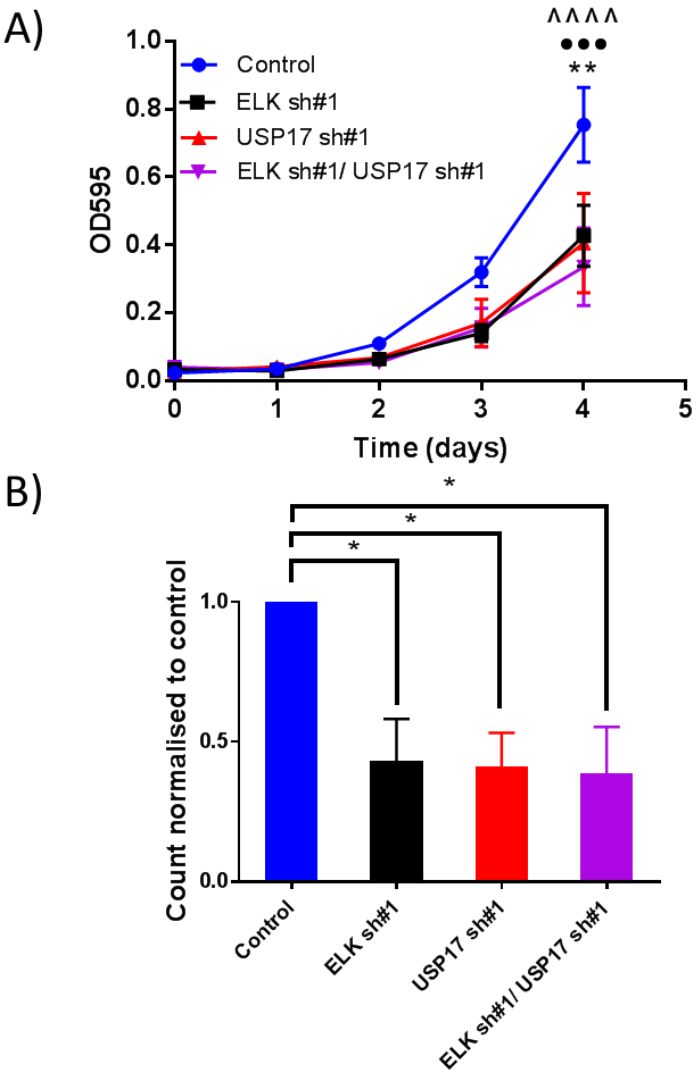

(Figure legend overleaf)

Figure 7-8: ELK-1 and USP17 depletion inhibits HEK293T cell proliferation. A) HEK293T cells were transfected with either empty pSUPER vector, USP17 sh#1, ELK sh#1, or USP17 sh#1 and ELK sh#1, and after 24 hours were trypsinised and re-seeded into 96 well plates (2000 cells/well), before being assessed by MTT assay over four days. Post-hoc analyses were conducted using Tukey's multiple comparisons test for repeated measures ANOVA. * = Control vs ELK sh#1. • = Control vs USP17 sh#1 ^ = Control vs ELK sh#1/ USP17 sh#1 (N=4, -/+ SEM, *p<0.05, **p<0.01, ***p<0.001). B) Same as A), but 24 hours post-transfection cells were instead re-seeded into 24-well plates (10,000 cells/well) and counted after four days using a MOXI Z mini automated cell counter. Counts are normalised against the control (set as 1). Post-hoc analyses were conducted using Tukey's multiple comparisons test for one-way ANOVA. (N=4, -/+ SEM, *p<0.05).

7.5 ELK-1 K35R mutation increases cell proliferation

To deduce whether ELK-1 ubiquitination had a direct effect on cell proliferation, MTT assays were carried out on HEK293T cells transfected with either empty vector (control), wild-type ELK-1 or K35R mutation (R being similarly charged but unable to accept ubiquitin). K35 had been shown to be the main monoubiquitin acceptor site in ELK-1 such that its mutation (K>R) resulted in hypo-ubiquitinated ELK-1 (4.9), and unlike the other identified ubiquitination sites (K52 and K59), this had only a minor effect on ELK-1-SRF

mediated DNA-binding (Chow, PhD thesis, University of Nottingham, 2010). Figure 7-9 shows that ELK-1 K35R transfected cells grew significantly faster than wild-type transfected cells. Therefore, circumventing or preventing ELK-1 monoubiquitination increased cell proliferation, possibly by increasing ELK-1 target gene activation (7.1). This would point to USP17 acting as a major driver of cell-cycle progression and proliferation through ELK-1 deubiquitination. However, this presumed causal link between USP17 and ELK-1 required further investigation. It should be noted that control cells also grew faster than ELK-1 wild-type-transfected cells. This suggests that an excess of ELK-1 could either slow cell growth or promote cell death, possibly through apoptosis as has been reported before (Shao et al., 1998). Furthermore, this repression of cell growth appears to be mediated through ELK-1 monoubiquitination, as K35R has been shown to be the major monoubiquitin acceptor site (Chow, PhD thesis, University of Nottingham, 2010) (4.8, 4.9).

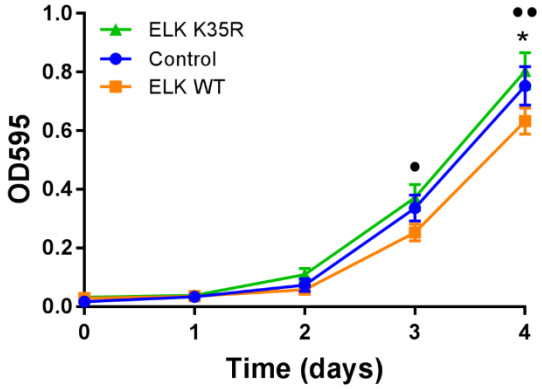

Figure 7-9: ELK-1 K35R mutation increases cell proliferation. HEK293T cells were transfected with either empty pcDNA3 vector (Control), wild-type ELK-1 (ELK WT), or ELK-1 K35R (ELK K35R) and after 24 hours were trypsinised and re-seeded into 96 well plates (2000 cells/well), before being assessed by MTT assay over four days. Post-hoc analyses were conducted using Tukey's multiple comparisons test for repeated measures ANOVA. * = Control vs ELK WT. • = ELK K35R vs ELK WT (N=3, -/+ SEM, *p<0.05, **p<0.01).

7.6 ELK-1 K35R rescues cell proliferation after USP17 depletion

To determine whether the impact of ELK-1 on cell proliferation was regulated by USP17, further MTT and cell counting assays were carried out in HEK293T cells. USP17 depletion had been shown to reduce cell growth (Figures 7-4 and 7-8), and hypo-ubiquitinated ELK-1 K35R mutant had been shown to increase growth against wild-type ELK-1 (Figure 7-9). HEK293T cells were transfected

with either empty vector (control), ELK-1 K35R, USP17 sh#1 or both ELK K35R and USP17 sh#1 combined. Growth was again assessed by MTT assay and cell counting to deduce whether ELK-1 K35R could rescue cell proliferation after USP17 knockdown. This was found to be the case, as ELK-1 K35R/USP17 sh#1 transfected cells grew significantly faster than USP17 sh#1 alone, in both cell counting assays and MTT assay (Figure 7-10). Cells transfected with ELK-1 K35R alone also appeared to show faster growth by MTT assay against control cells, although this was not corroborated by cell counting or previous experiments (Figure 7-9).

The ELK-1 K35R-mediated recovery from USP17 knockdown was only partial, as control cells showed significantly higher MTT readings and cell counts than ELK-1 K35R-rescued USP17-depleted cells. This may be the case because USP17 has other regulatory roles in cell cycle progression, including targets upstream of ELK-1 such as RCE1, which is crucial for RAS localisation to the plasma membrane (Burrows et al., 2009). Another target of USP17 is CDC25A, which is stabilised by USP17-mediated deubiquitination and can promote cell cycle progression by activating cyclin-dependent kinases (Pereg et al., 2010). Regardless, the experimental evidence points to USP17 as a positive regulator of ELK-1 transcriptional activity, thereby driving cell cycle progression and proliferation.

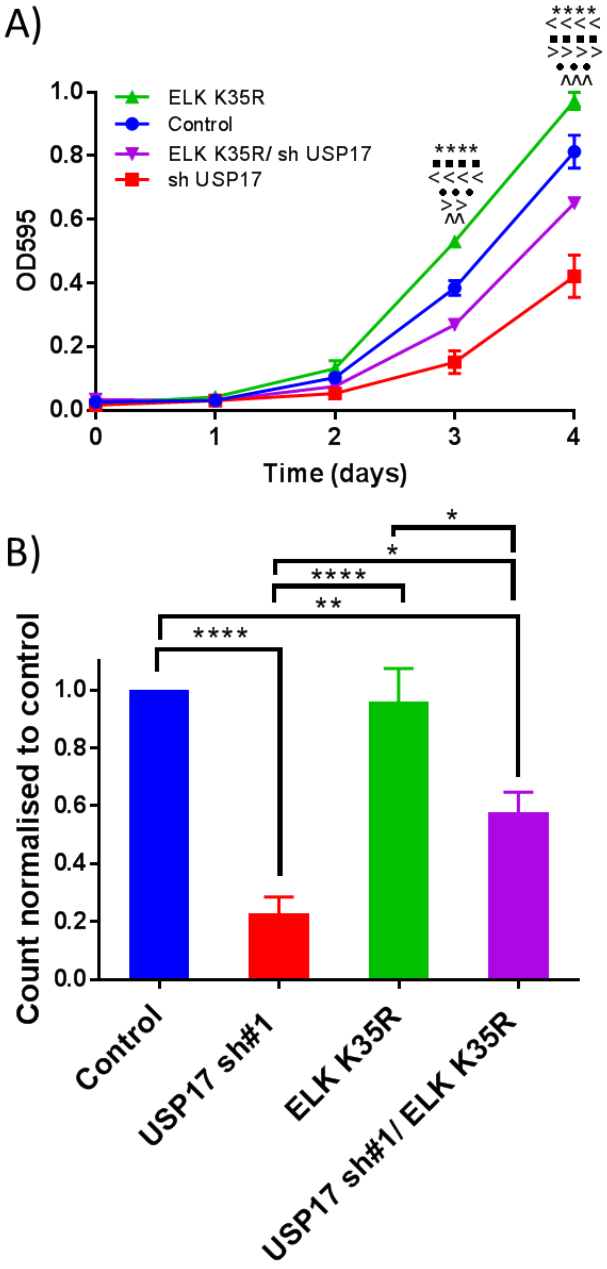

(Figure legend overleaf)

Figure 7-10: ELK-1 K35R rescues cell proliferation after USP17 depletion. A) HEK293T cells were transfected with empty pcDNA3 vector (Control), pSUPER-USP17 sh#1, wild-type pcDNA3-ELK-1 (ELK WT) and pcDNA3-ELK-1 K35R (ELK K35R) and after 24 hours were trypsinised and re-seeded into 96 well plates (2000 cells/well), before being assessed by MTT assay over four days. Post-hoc analyses were conducted using Tukey's multiple comparisons test for repeated measures ANOVA. * = Control vs USP17 sh#1, < = USP17 sh#1 vs ELK K35R, ■ = ELK K35R vs ELK K35R/ USP17 sh#1, > = USP17 sh#1 vs ELK K35R/ USP17 sh#1, • = Control vs ELK K35R, ^ = Control vs ELK K35R/ USP17 sh#1 (N=3, -/+ SEM, **p<0.01, ***p<0.001 ****p<0.0001). B) Same as A), but 24 hours post-transfection cells were instead re-seeded into 24-well plates (10,000 cells/well) and counted after four days using a MOXI Z mini automated cell counter. Counts are normalised against the control (set as 1). Post-hoc analyses were conducted using Tukey's multiple comparisons test for one-way ANOVA. (N=4, -/+ SEM, *p<0.05, **p<0.01, ***p<0.001 ****p<0.0001).

7.7 Ectopic expression of USP17 increases ERK2 phosphorylation in the absence of mitogens

Having shown that USP17 and ELK-1 are linked functionally in driving cell cycle progression, focus was turned towards the ERK cascade, upstream of ELK-1 (1.1.7.1). Ectopic expression of USP17 had previously been found to block RAS localisation and activation, resulting in impaired ERK phosphorylation. This was shown to be due to removal of K63-linked polyubiquitin chains from RCE1, negatively regulating its proteolytic processing of the carboxyl-terminal amino acids of RAS at the ER, which is required for RAS trafficking to the plasma membrane (Burrows et al., 2009). Additionally, overexpressing USP17 inhibited cell proliferation in both IL-3-dependent Ba/F3 cells and NIH3T3 cells (Burrows et al., 2004). However, depletion of USP17 also dysregulated RAS (and RHOA) localisation and activation, showing that USP17 is required for ERK signalling (McFarlane et al., 2010). High USP17 expression has also been documented in various cancers, suggesting it may positively regulate growth signalling (McFarlane et al., 2010; McFarlane et al., 2013; C. Song et al., 2017). Previous data in this chapter agrees with sources citing USP17 as an important regulator of the cell cycle (McFarlane et al., 2010; Pereg et al., 2010).

To investigate further the effect of USP17 on the ERK cascade, HEK293T cells were transfected with empty vector, MYC-USP17 or MYC-USP17 C/S, serum-starved and then either left untreated or stimulated with TPA/serum for 30

minutes before harvesting. Lysates were immunoblotted with ERK and phospho-ERK antibodies to assess the presence of active pools of ERK. Figure 7-11 shows that wild-type USP17 expression increased the basal level of ERK2 phosphorylation in serum-starved cells, while C/S mutated USP17 did not (compare lanes 3 and 5), illustrating that USP17 catalytic activity was important in this change. There were no discernible differences between phospho-ERK levels in any of the TPA/serum stimulated samples, regardless of USP17 expression (lanes 2, 4 and 6), possibly due to the high level of induction of both ERK1 and ERK2 by this treatment, rendering any differences less obvious. Alternatively, this could be due to TPA acting independently of RAS (Ueda et al., 1996), which seems a likely point of ERK cascade regulation by USP17 due to the involvement of USP17 in RAS subcellular localisation and activity (Burrows et al., 2009).

Ultimately, although USP17 expression did increase basal levels of ERK phosphorylation, it did not markedly affect mitogen-induction of the ERK cascade, so on this basis it appears not to be the likely route to increased ELK-1 activity. It should be noted that samples were also immunoblotted for phospho-ELK-1, but failed to give any signal in any experimental sample, probably due to poor antibody sensitivity when probing for endogenous ELK-1. Further work is needed to clarify whether USP17 regulates ERK pathway constituents other than RAS, and how its ectopic expression increased basal

ERK2 phosphorylation in these experiments, as opposed to the decrease seen in active RAS and ERK in previous studies (Burrows et al., 2009).

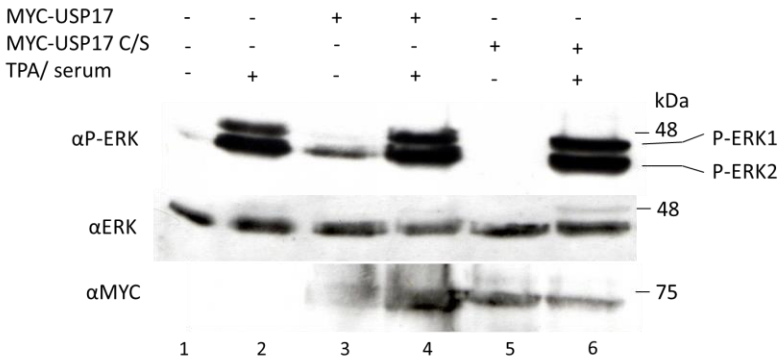

Figure 7-11: Ectopic expression of USP17 increases ERK2 phosphorylation in the absence of mitogens. HEK293T cells were transfected with empty vector, MYC-USP17 or MYC-USP17 C/S for 24 hours, followed by serum-starvation for 24 hours and then either left untreated or stimulated with 100 ng/ml TPA/ 10% serum for 30 minutes before harvesting. Cell lysates (50 μg) were probed for phospho-ERK, ERK and MYC antibodies by immunoblot. Phospho-ERK (T202, Y204) blot is indicative of ERK1/2 activity.

To conclude, USP17 depletion was shown to impair ELK-1 target gene expression and cell proliferation. This correlated with an increase in ELK-1 monoubiquitination, preventing target gene expression, in a process independent of the proteasome. This could be partially rescued by mutation of the major monoubiquitin acceptor site in ELK-1, providing direct evidence that deubiquitination of ELK-1 by USP17 positively regulates cell cycle progression

and proliferation. Furthermore, USP17 was shown to increase basal ERK phosphorylation upstream of ELK-1, suggesting that USP17 could potentially regulate the MEK/ERK/ELK-1 axis at multiple points, but disagreeing with previous suggestions that constitutive expression of USP17 inhibits the ERK cascade (Burrows et al., 2009). Overall, the data indicates a complex system of control over the cell cycle and cellular responses to mitogens with USP17 at its heart.

8 Discussion

The phosphorylation and activation of ELK-1, and ternary complex formation at the SRE prompting transcriptional activation of IEGs, is a well-studied process that has proved to be a paradigm for the signal-relayed induction of eukaryotic gene expression. The post-translational phosphorylation and SUMOylation modification sites and function of these modifications in ELK-1 have previously been characterised, being associated with the activation and repression of ELK-1 respectively (Marais et al., 1993; Janknecht et al., 1993; Gille et al., 1995A; S. Yang & Sharrocks, 2004). However, despite the polyubiquitination of ELK-1 being known about for some time, it remains a poorly understood modification (S. Fuchs et al., 1997). Furthermore, ELK-1 has also been shown to be monoubiquitinated (Chow, PhD thesis, University of Nottingham, 2010). This thesis sought to gain an understanding of monoubiquitination and polyubiquitination *per se* and the consequences of their covalent conjugation to ELK-1. Several key experimental findings have revealed ubiquitination sites and effects on ELK-1 activity. Furthermore, USP17 has been identified as a DUB enzyme responsible for ELK-1 deubiquitination, and that in doing so it regulates the expression of ELK-1-responsive genes. These represent novel discoveries that expand on previous knowledge of ELK-1-driven transcription and cell proliferation.

8.1 ETS domain as site of ubiquitination in ELK-1

Mutational screening of lysine residues had previously shown that the ETS domain was the major site of monoubiquitination in ELK-1, with K35 found to be the most likely candidate as monoubiquitin acceptor. In these experiments, a double lysine mutant (K50R, K52R) and a single mutant (K59R) were also found to be refractory for monoubiquitination. However, mutational screening of DNA-binding lysine residues as ubiquitination sites was ambiguous, as SRE DNA-binding defective versions of ELK-1 with a full complement of lysine residues were also not monoubiquitinated (Chow, PhD thesis, University of Nottingham, 2010). K52 resides in a loop region between α2 and α3 (the DNA-binding helix), and engages DNA through formation of a salt bridge. K59 is a key DNA-binding residue in the α3 helix, which forms hydrogen bonds with the GGA core in ETS binding sites (Mo et al., 2000) (Figure 8-1). Hence, K52 and K59 could not be assigned as monoubiquitination sites on this data alone. MS/MS data confirmed K35, K52 and K59 as sites of ubiquitination in HEK293T cells (4.8). In contrast to K52 and K59, K35 is distal to the DNA-binding helix and forms no contacts with DNA, although it does form part of the ETS domain secondary structure as part of β2 (Mo et al., 2000). However, K35 appears to be the major site of monoubiquitination, as it was the most frequently identified diglycine-containing peptide seen in MS/MS datasets.

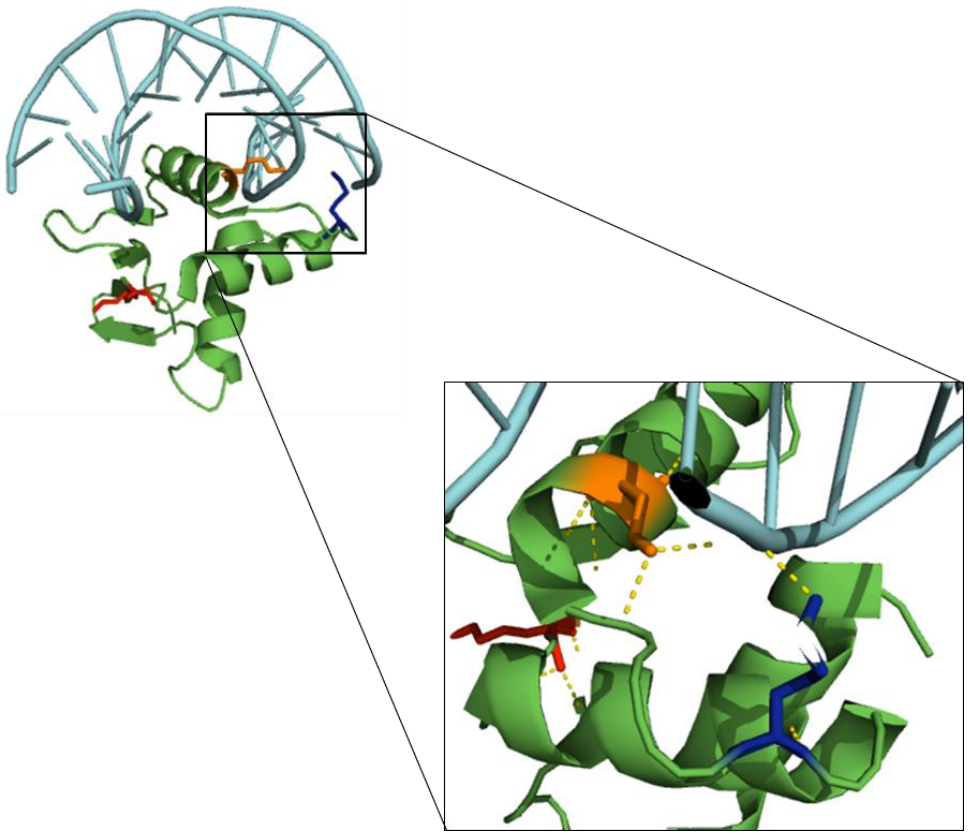

Figure 8-1: Structure of ELK-1 ETS domain (residues 5-90) (human) bound to E74-high affinity site DNA. Sites of ubiquitination are highlighted (K35, K52 and K59) in stick format. Close-up view shows polar contacts within complex (yellow dashes) with focus on K52 and K59 interactions with DNA. Structure taken from (Mo et al., 2000) - PDB 1DUX – re-rendered with PyMOL.

The assignment of DNA-binding residues as ubiquitination sites, coupled with the inability of ELK-1 to be modified by monoubiquitin unless able to bind DNA at the SRE, raises some interesting questions. Is the modification added to ELK-1 while DNA-bound? This seems unlikely with regard to K52 and K59, which will likely be inaccessible when in contact with DNA, such as is the case for IRF1,

which when DNA-bound cannot be ubiquitinated (Landré et al., 2013). It is likely that K35 is the only site that would be accessible to E3 ligases when ELK-1 is bound to DNA. Is ubiquitinated ELK-1 able to bind DNA? Again, for K52 and K59, this seems unlikely, as an 8.5 kDa protein adduct would be expected to impair interaction with DNA. This is not as clear for K35, although it seems highly plausible that the addition of a ubiquitin moiety could impact on DNA binding, either through direct steric interference or through inducing allosteric changes in the ETS domain (Figure 8-2).

Is DNA-binding defective ELK-1 not monoubiquitinated due to its expulsion from the nucleus? It has previously been suggested that the continued presence of ELK-1 in the nucleus is partially dictated through DNA-interactions, as ELK-1 DNA-binding mutants shuttle between the nucleus and cytoplasm more readily than wild-type ELK-1 (Evans et al., 2011). Therefore, a possible reason for ELK-1 DNA-binding mutants being refractory for monoubiquitination could be their rapid removal from the nucleus. For this to be true, monoubiquitination of ELK-1 would have to occur in the nucleus. *In vitro* ubiquitination assays involving incubation of recombinant ELK-1 with E1, E2, ubiquitin, DUB inhibitor ubiquitin aldehyde and HeLa nuclear extract had previously shown that this was sufficient for wild-type ELK-1 monoubiquitination, while an ELK-1 mutant lacking lysine residues in the ETS domain was refractory to modification (Jurgen Handwerger, unpublished data). Therefore, the E3 ligase responsible for monoubiquitination is present in the

nuclear compartment, which was provided by HeLa nuclear extract in the assay, and rapid nuclear exclusion remains a possible explanation for DNA-binding defective ELK-1 also resisting monoubiquitination. Building on from these experiments, it was also found that addition of an SRE oligonucleotide duplex to the *in vitro* ubiquitination reactions (relying on endogenous SRF in nuclear extract for ternary complex formation) increased ELK-1 monoubiquitination (Jurgen Handwerger, unpublished data). A possible explanation for this result is that DNA-binding is a prerequisite for monoubiquitination (at least for K35), suggesting that the ELK-1 E3 ligase either only recognises or can only access ELK-1 when DNA-bound. Together, these experiments show that ELK-1 is monoubiquitinated in the nucleus, which is dependent on ternary complex formation at the SRE.

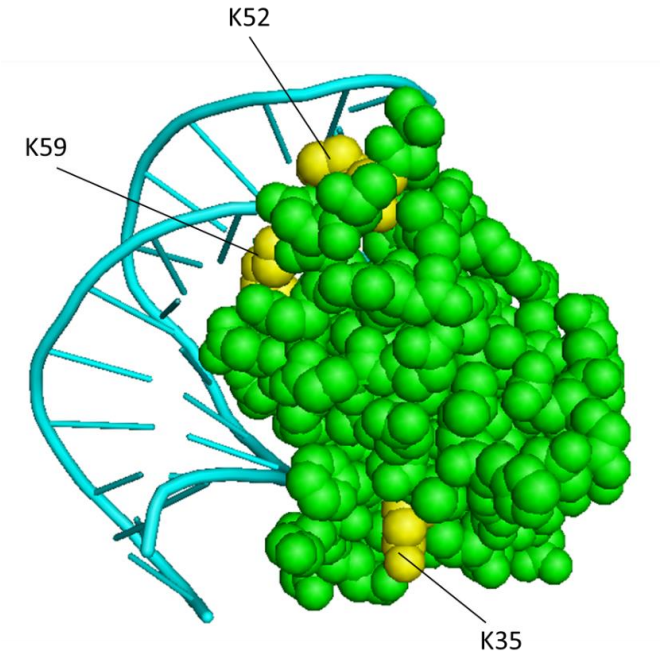

Figure 8-2: Structure of ELK-1 ETS domain (residues 5-90) (human) bound to E74-high affinity site DNA in sphere format. Sites of ubiquitination are highlighted in yellow (K35, K52 and K59). Structure taken from (Mo et al., 2000) - PDB 1DUX – re-rendered with PyMOL.

8.2 Monoubiquitination versus Polyubiquitination of ELK-1

ELK-1 is both monoubiquitinated and polyubiquitinated, with the latter appearing to be through K48-linked polyubiquitin chains. This was confirmed by immunoblotting following polyubiquitination assay, where K48-linked polyubiquitin chains were found associated with His-ELK-1 (transfected into HEK293T cells) following denaturing IMAC, which was the case with or without additional ectopic HA-tagged ubiquitin (4.1, 4.3, 4.7). K48-linked polyubiquitin chains are the canonical signal for turnover by the 26S proteasome, which

agrees with previous studies that indicate ELK-1 can be degraded *via* the UPS (Evans et al., 2011; Teixeira et al., 2013). MS/MS data also confirmed that ELK-1 is modified by K48-linked polyubiquitin chains, as diglycine peptides corresponding to these linkages were identified in His-ELK-1 IMAC samples (from transfected HEK293T cells), while being absent in control samples (HEK293T cells transfected with empty vector) (4.8). What is unclear, however, is whether monoubiquitination and polyubiquitination are functionally linked. Looking at the MS/MS data in isolation, it appears that K35, K52 and K59 could represent monoubiquitination and polyubiquitination sites, and that monoubiquitination merely acts as a primer for polyubiquitin chain extension. There are precedents for this, such as in the cooperation of the E2-E3 pairs Rad6-Rad18 and Ubc13–Mma2–Rad5 in the monoubiquitination and subsequent polyubiquitination of PCNA respectively (in *Saccharomyces cerevisiae*) (Parker & Ulrich, 2009). In support of this, monoubiquitination assays including ubiquitin with no internal lysine residues (K0-UBQ) revealed that higher molecular weight species above the monoubiquitin band (in monoubiquitination assay) are only present with wild-type ubiquitin, showing that these equate to short di/tri-ubiquitin chains rather than multiple monoubiquitination events (4.2).

However, previous data utilising lysine mutations suggested that lysine residues in the carboxyl-terminal of ELK-1 contribute more to protein stability than amino-terminal (ETS domain) residues, as a mutant lacking carboxyl-

terminal lysine residues (K130, K135, K230, K249, K253, K271, K312, K315, K392 and K427) was stabilised against wild-type ELK-1, which was not the case for a mutant lacking amino-terminal lysine residues (K35, K52, K59, K70, K75, K80 and K84) (Chow, PhD thesis, University of Nottingham, 2010). Furthermore, sELK-1, the neuronal isoform of ELK-1, which is inherently unstable and is partially stabilised in HEK293T cells by treatment with the proteasome inhibitor MG132, lacks both K35 and K52 (Evans et al., 2011). Polyubiquitination assays on ELK-1 mutants (with individual K35R, K52R and K59R mutations) also did not disrupt polyubiquitination (data not shown). All of this, coupled with the poor general coverage of the carboxyl-terminus of ELK-1 in MS/MS datasets (including no phosphopeptides pertaining to ELK-1 P-S383 despite strong signals *via* immunoblot), suggest that other ubiquitination sites important in proteasomal turnover of ELK-1 may have been missed due to incomplete sequence coverage.

8.2.1 Mechanisms governing subcellular localisation of ubiquitinated ELK-1

Subcellular fractionation of nuclear and cytoplasmic extracts of HEK293T cells transfected with His-ELK/HA-ubiquitin or His-ubiquitin/HA-ELK, followed by denaturing IMAC, clarified that both mono- and polyubiquitinated ELK-1 populations reside predominantly in the cytoplasm under steady-state conditions (5.1). This is despite the aforementioned evidence suggesting that ELK-1 monoubiquitination occurs in the nucleus in response to DNA binding

(Jurgen Handwerger, unpublished data). Given this, it follows that nuclear monoubiquitination of ELK-1 ultimately leads to its re-localisation to the cytoplasm. Whether this is due to the monoubiquitin mark actively promoting export (such as through recognition by UBD containing proteins or by exposing the NES in ELK-1) (Vanhoutte et al., 2001) or through impairing DNA-binding potential leading to removal from the nucleus (Evans et al., 2011), is not known at present. Nuclear export of proteins containing an NES is mediated through CRM1, which forms a complex with its cofactor RANBP3 and binds to the GTPase RAN and the NES on the target protein (Fornerod et al., 1997). The complex attaches to the nuclear pore complex *via* nucleoporins, and the target protein is exported to the cytoplasm following hydrolysis of RAN bound GTP to GDP (Askjaer et al., 1998).

Polyubiquitination of ELK-1 was almost entirely cytoplasmic, whereas monoubiquitinated ELK-1 was still clearly present in nuclear extracts. This could be because monoubiquitinated ELK-1 dynamically switches from nuclear to cytoplasmic compartments. Equally, monoubiquitinated ELK-1 transfer to the cytoplasm could be more open to polyubiquitination and proteasomal degradation, as is the case with p53 (M. Li et al., 2003). Cytoplasmic stability of ELK-1 is thought to be dependent on its ability to form dimers, possibly involving an amino-terminal dimerisation interface (DI) (amino acid residues 7-32) (Evans et al., 2011). In this model of ELK-1 proteasomal degradation, dimerisation-defective versions of ELK-1 reveal an unstructured cryptic degron

next to the B-domain, which could allow E3 ligase docking and UPS processing (Evans et al., 2011). The DI lies adjacent to the monoubiquitination acceptor K35, so it seems feasible that ELK-1 monoubiquitination could affect the formation of cytoplasmic dimers, which would destabilise ELK-1. This would explain why polyubiquitinated ELK-1 appears to be almost exclusively cytosolic under steady-state levels, as excess monoubiquitinated ELK-1 leaves the nucleus and is proteolysed. Equally, the opposite could be true, in that ELK-1 monoubiquitination could promote dimer formation, which would explain the difficulty in demonstrating ELK-1 dimers using recombinant protein (Evans et al., 2011). Additionally, polyubiquitin could be entirely independent of monoubiquitination, but still be restricted to the cytoplasm.

8.2.2 Mitogenic effects on ELK-1 ubiquitination

Another important difference between monoubiquitination and polyubiquitination of ELK-1 is in their regulation following mitogen treatment. Monoubiquitination is removed from ELK-1 after both acute (Chow, PhD thesis, University of Nottingham, 2010) and chronic (5.2) stimulation of the ERK cascade. In contrast, ELK-1 polyubiquitination appears to increase just 30 minutes after ERK cascade induction with TPA/serum (4.7). The loss of monoubiquitination could conceivably be due to chain extension into polyubiquitin chains (Figure 8-3A), although the same result was previously obtained when using K0-ubiquitin, so this seems unlikely (Chow, PhD thesis,

University of Nottingham, 2010). This suggests that mitogen stimulation results in the removal of monoubiquitination from ELK-1, while also potentiating the K48-linked polyubiquitination of ELK-1 possibly at the carboxyl-terminus (Figure 8-3B), promoting proteasomal degradation of ELK-1 *via* activation-dependent-destruction (Lipford et al., 2005).

A recent study found that ERK phosphorylates ELK-1 processively, proceeding through fast, intermediate and slow sites. Fast and intermediate site phosphorylation promotes ELK-1 activity, while slow sites act to inhibit this (Mylona et al., 2016). One plausible reason for this could be that slow sites act as phosphodegrons, promoting proteolysis of ELK-1 following a temporal delay after activation. However, there was no mention of ELK-1 stability varying in this study (Mylona et al., 2016). Moreover, in IMAC-purified His-ELK-1 samples (transfected into HEK293T cells), despite ELK-1-associated K48-linked polyubiquitin chains appearing 30 minutes after TPA/serum induction, there were no visible changes in ELK-1 protein levels by 60 minutes post-induction (4.7). It should also be noted that the monoubiquitination removal post-stimulation was with use of ectopic ubiquitin (5.2), whereas the increase in polyubiquitination was purely endogenous ubiquitin (4.7), meaning that direct comparison is not possible. Furthermore, immunoblotting for endogenous ubiquitin following IMAC proved challenging, with high background in control samples, although peptides pertaining to K48-linked polyubiquitin chains were seen in His-ELK-1 samples *via* MS/MS, and not in control samples (4.8).

Based on experiments involving proteasomal inhibition with MG132, ELK-1 exhibits relatively high stability and steady state levels in HEK293T cells, and is only marginally stabilised by proteasomal inhibition (although significantly, 7.2) compared to other tightly controlled transcription factors such as p53 (Gu et al., 2002; Evans et al., 2011). This suggests that proteasomal degradation is the not the major regulator of ELK-1 activity, pointing to other post-translational marks such as monoubiquitination, phosphorylation and SUMOylation (and their removal) as more efficacious regulators of ELK-1-driven transcription.

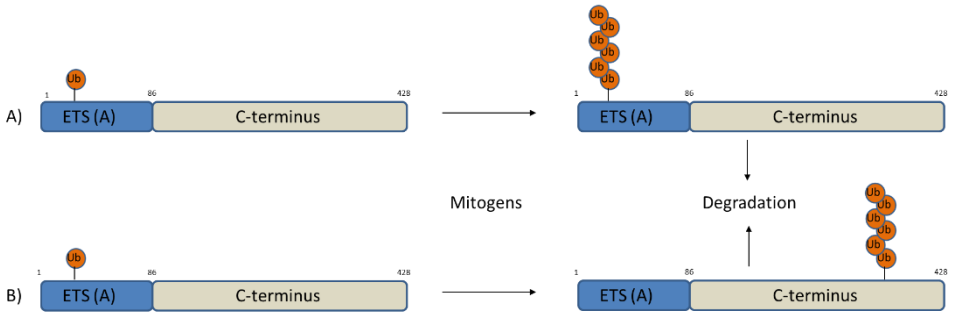

Figure 8-3: Possible routes of conversion from monoubiquitination to polyubiquitination of ELK-1 following mitogen stimulation. A) Monoubiquitinated ELK-1 targeted to the ETS domain is used as a scaffold for polyubiquitin chain extension *via* E3/E4 ligase. B) Monoubiquitinated ELK-1 is removed following mitogen stimulation by DUB, and polyubiquitin chain is conjugated to a separate carboxyl-terminal site by E3 ligase.

8.3 USP17 effects on ELK-1 activity

The disappearance of ELK-1 monoubiquitination upon mitogen stimulation even when formed with K0-ubiquitin suggested that ELK-1 may become deubiquitinated (Chow, PhD thesis, University of Nottingham, 2010). USP17 was shown to be a *bona fide* DUB of ELK-1, capable of removing both monoubiquitin and polyubiquitin chains (6.1). Despite this, USP17 had only a small effect on ELK-1 stability that appeared to be independent of catalytic activity (7.2). However, the ectopic expression of USP17 increased transcription of a panel of ELK-1 responsive genes (*CFOS*, *EGR1*, *EGR2*, *IER2*) and downstream markers of cell-cycle progression (*CCND1*) (Janice Saxton, unpublished data), while its endogenous depletion caused the opposite effect, leading to downregulation of *CFOS* and *EGR1* expression (7.1). This is strong evidence pointing to USP17 as a positive regulator of ELK-1 target gene transcription, and moreover, this appears not to be purely though protection of ELK-1 from UPS processing. USP17 has to date been mostly associated with protecting target proteins from proteasomal degradation through deubiquitination of polyubiquitin chains (Pereg et al., 2010), but can also have effects on targets independent of the proteasome, such as through the removal of non-proteolytic K63-linked polyubiquitin chains (Ramakrishna et al., 2011). Additionally, USP17 has also been shown to be capable of removing monoubiquitin marks from histone H2AX, which has important implications in the DNA damage response (Delgado-Diaz et al., 2014).

Other evidence also points to monoubiquitination as a negative regulator of ELK-1 transcriptional potency. Firstly, the removal of monoubiquitin after ERK cascade activation (5.2), coupled with the deubiquitination of ELK-1 by USP17 (6.1) promoting ELK-1 target gene activation (7.1) (Janice Saxton, unpublished data), points to a de-repression event co-occurring with ELK-1 activation. Secondly, a hypo-ubiquitinated ELK-1 mutant (K35R) increased activation compared with wild-type ELK-1 at the SRE (in the presence of hyperactive RAF259D) *via* reporter assay (Janice Saxton, unpublished data). This was also shown through qRT-PCR experiments, where hypo-ubiquitinated ELK-1 significantly increased *CFOS* expression against wild-type ELK-1 following induction of oestrogen-inducible version of active RAF-1 with Estradiol (Peter Shaw, Janice Saxton, unpublished data). Interestingly, the three ubiquitin modification sites in ELK-1 (K35, K52 and K59) are conserved across the TCFs, and USP17 is also capable of deubiquitinating both ELK-3 and ELK-4 (6.4). It therefore seems likely that ELK-3 and ELK-4 may undergo a similar regulatory process to ELK-1 involving monoubiquitination.

8.4 ELK-1 and USP17 cooperation in driving cell-cycle progression

HEK293T cells transfected with hypo-ubiquitinated ELK-1-mutant (K35R) cells grew significantly faster than those transfected with wild-type ELK-1 (7.5), showing direct effects on cell proliferation of increased ELK-1 transcriptional activity, caused by removing the dampening effects of monoubiquitination. The

importance of USP17 in proliferation is illustrated by the impairment of cell growth following its depletion in both HeLa (7.3) and HEK293T cells (7.4). Transcription of *USP17* is regulated in a cell cycle dependent manner, with higher levels of expression during late G1, where USP17 activity drives G1-S progression (McFarlane et al., 2010). Alongside this, USP17 catalytic activity is also regulated through the cell cycle, through phosphorylation by CDK4/6 (Liu et al., 2017). As yet, the only transcription factor implicated in regulating USP17 expression is Esrrb, which is important in self-renewal of mESCs and directly targets *Dub3* (mouse equivalent of *USP17*) and promotes its expression in these cells (van der Laan et al., 2013).

Hence, mitogens both induce USP17 expression and stimulate its activity to promote cell cycle progression, which it achieves through deubiquitination of a variety of substrates, notably CDC25A at the G1/S and G2/M checkpoints (Pereg et al., 2010). This also provides a rationale for the removal of monoubiquitin from ELK-1 after ERK cascade activation, which occurs independently of ELK-1 phosphorylation, as MAPK docking mutants (ΔD/FXLA) and phosphorylation accepter mutants (S383/9A) were still open to deubiquitination following ERK induction (5.4). Mitogen induction promotes USP17 expression (through an as yet unknown pathway) and activation (by CDK4/6 phosphorylation), triggering entry into the cell cycle and resulting in the deubiquitination and de-repression of ELK-1 (Liu et al., 2017). This occurs with concomitant phosphorylation by active ERK, potentiating ELK-1

transactivation and IEG expression (such as *CFOS*) and promoting cell-cycle progression (Figure 8-4). ELK-1 therefore represents the newest addition to the proliferatory substrates of USP17. Given that USP17 can also regulates RAS localisation through deubiquitination of RCE1, this gives two different points of control over the RAS-RAF-MEK-ERK-ELK-1 axis to drive forward IEG transcription following mitogenic signalling (Burrows et al., 2009; McFarlane et al., 2010). Ectopically-expressed USP17 increased basal levels of ERK phosphorylation in HEK293T cells (7.7), illustrating further that USP17 has regulatory targets upstream of ELK-1, and USP17 is thought to be a requirement for RAS signalling (McFarlane et al., 2010).

ERK cascade stimulation does not always result in cell cycle progression, and the strength and duration of the signal seem to be important determinants of this (Meloche et al., 1992). Sustained ERK activity has been suggested as a requirement for induction of *CCND1* through FOS family members to promote G1-S progression (Weber et al., 1997; Burch et al., 2004; Chambard et al., 2007). Additionally, ELK-1 deubiquitination may increase the pool of active ELK-1 to extend IEG expression and thus promote cell-cycle progression. Only a fraction of ELK-1 is monoubiquitinated, so USP17 activity would not be required immediately, but its expression at late G1 could drive transition to S-phase through removal of repressive monoubiquitin from ELK-1.

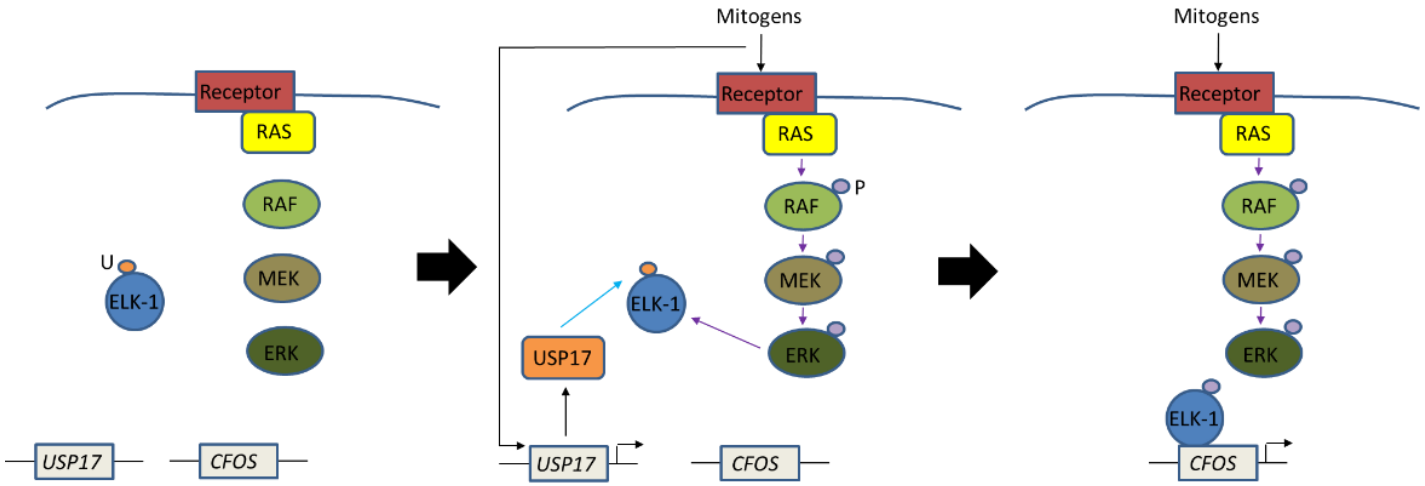

Figure 8-4: USP17 and ELK-1 involvement in cell-cycle progression. In unstimulated cells, ELK-1 is inactive and monoubiquitinated (U, orange circle), and *USP17* is not expressed. In response to mitogens, the ERK phosphorylation cascade is activated, leading to ELK-1 phosphorylation and transactivation (P, purple circle). *USP17* gene is expressed, through a currently unknown mechanism, which can be induced through growth stimulus or cytokines. USP17 removes monoubiquitin, de-repressing ELK-1 and allowing promoter binding and transcriptional activation of IEGs (such as *CFOS*), prompting progression of the cell cycle. Purple arrow -phosphorylation, blue arrow – deubiquitination.

Through the deubiquitination and stabilisation of CDC25A, USP17 also positively regulates its own activity, as CDC25A dephosphorylates CDK4/6, prompting CDK4/6-CyclinD mediated phosphorylation of USP17 (Iavarone & Massague, 1997; Liu et al., 2017) (Figure 8-5). ERK cascade activation leads to downstream *CCND1* (CyclinD) expression, ultimately resulting in Rb protein phosphorylation by CDK4/6-CyclinD, providing further positive feedback for G1-S progression (Woods et al., 1997; Chambard et al., 2007). It is worth noting that USP17 has also been implicated in regulation of the SIN3A HDAC-1/2 complex assembly and stability of HDAC2 individually (Ramakrishna et al., 2011; H. Song et al., 2015), both of which are recruited by DNA-bound ELK-1 to self-limit transcriptional output (S. Yang et al., 2001; S. Yang & Sharrocks, 2004). This could represent another route for USP17 regulation of ELK-1 activity.

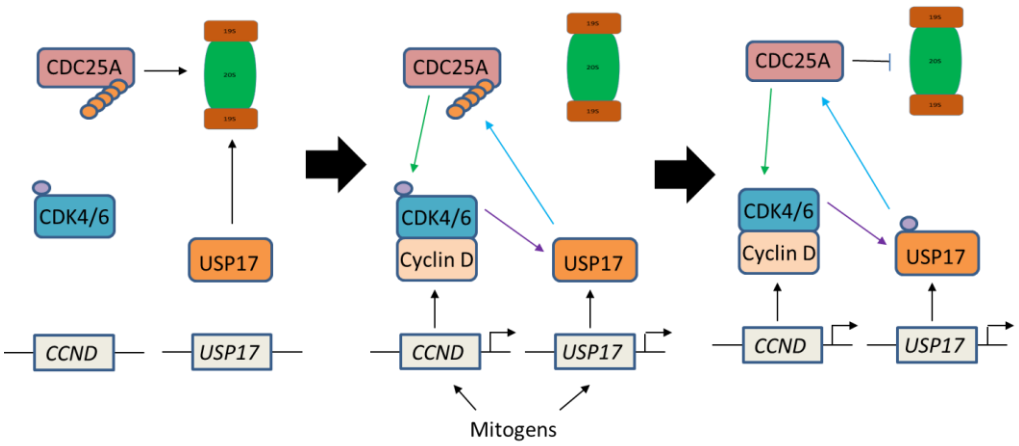

Figure 8-5: Regulation of USP17 activity/expression. In unstimulated cells, CDC25A and USP17 are readily polyubiquitinated (orange circles) and turned over by the 26S proteasome, *CCND1* and *USP17* genes are not expressed and CDK4/6 are phosphorylated (purple circles). Following mitogen induction, *CCND1* and *USP17* are expressed, producing CyclinD and USP17 respectively. USP17 deubiquitinates CDC25A, inhibiting its proteasomal degradation and allowing it to dephosphorylate CDK4/6. CDK4/6 forms an active complex with CyclinD and phosphorylates USP17, positively regulation its activity. Purple arrow – phosphorylation, green arrow – dephosphorylation, blue arrow -deubiquitination.

The importance of ELK-1-USP17 cooperation in the cell cycle is exemplified by the partial rescue of cell proliferation by hypo-ubiquitinated ELK-1 following USP17 knockdown (7.6). In this situation, the hypo-ubiquitinated mutant bypasses ELK-1 regulation by monoubiquitination, allowing IEG transcriptional

activation following phosphorylation that is unhampered by the repressive monoubiquitin mark. However, rescue is only partial due to the other USP17 substrates important in G1-S progression (e.g. RCE1 and CDC25A). Furthermore, as USP17 can deubiquitinate ELK-3 and ELK-4 in a similar manner, the inherent functional redundancies associated with the TCFs could mean in some cellular contexts that ELK-1 is dispensable for cell-cycle progression, although USP17 might still play a role (Boros et al., 2009B). However, ELK-1 depletion in HEK293T cells showed that ELK-1 is required for cell-cycle progression in this cell-line, as it resulted in a significant reduction in cell proliferation (7.4). Hence, both ELK-1 and USP17 have been shown to act in concert and serve as important regulators of the cell cycle.

8.5 Future work

8.5.1 Identity of ELK-1 E3 ligase(s)

Having confirmed that USP17 is a DUB for ELK-1, the question remained of the E3 ligase responsible for ubiquitinating ELK-1. It had been previously been reported that FBXO25 was responsible for polyubiquitinating ELK-1, promoting its proteasomal degradation (Teixeira et al., 2013). However, this is currently in doubt, as this data could not be reproduced, finding that despite interacting with ELK-1 through its established cryptic degron, FBXO25 had no effect on either ELK-1 polyubiquitination or stability (Franziska Gehringer, unpublished data). Equally, ELK-1 is readily polyubiquitinated in HEK293T cells, although

endogenous FBXO25 could not be detected in this cell line by immunoblot (data not shown). This shows that FBXO25 is certainly not the major E3 ligase responsible for ELK-1 in this cell line. Lastly, provisional experiments have suggested that FBXO25 was able to polyubiquitinate His-HAND1, as had been reported previously (Jang et al., 2011), but had no effect on His-ELK-1, further validating that FBXO25 is in fact not an E3 ligase for ELK-1 (Figure 8-6).

The search continues for the ELK-1 E3 ligase(s) for both monoubiquitination and polyubiquitination. It remains to be seen whether a single E3 ligase is capable of mediating both modifications, or whether these modifications are split between different E3 ligases. The evidence suggests the latter, as the polyubiquitination of ELK-1 appears likely to be targeted to the carboxyl-terminus whereas monoubiquitination is targeted to the amino-terminal ETS domain. However, the presence of short polyubiquitin chains seen in monoubiquitination assay means that polyubiquitination at K35, K52 and K59 cannot be ruled out (4.2). This could either occur through an E3 ligase monoubiquitinating ELK-1, followed by E4 activity by a different ligase to extend chains, or both monoubiquitination and polyubiquitination could be carried out by the same E3 ligase. Further work to complete the enzymatic network controlling the cycle of ELK-1 activation in response to mitogens is required.

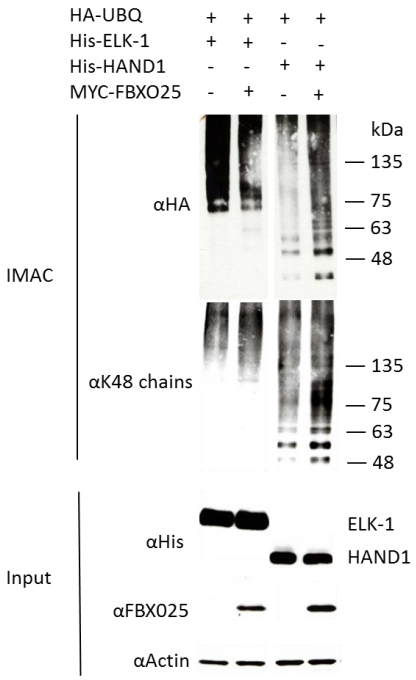

Figure 8-6: FBXO25 has no effect on ELK-1 polyubiquitination. HEK293T cells were transfected with HA-ubiquitin (UBQ) and either His-ELK or His-HAND1 with or without MYC-FBXO25 for 48 hours before harvesting. Top panel displays immunoblot for HA-tagged ubiquitin (HA and K48-linked chain antibodies) following denaturing IMAC. Bottom panels display input lysate with β-actin as a loading control.

8.5.2 Mechanism of monoubiquitination function and cross-talk with other post-translational modifications

This thesis has mostly focussed on the modification of ELK-1 by monoubiquitination, its reversal by USP17, and how this relates to its activation by phosphorylation. It has been clarified that monoubiquitination is a negative regulator of ELK-1 function, and that its removal by USP17 acts to de-repress ELK-1 function. However, the actual mechanism by which monoubiquitination transcriptionally silences ELK-1 is still uncertain. The efficacy of monoubiquitinated ELK-1 DNA binding needs to be assessed, and effects on subcellular localisation need to be clarified. Furthermore, ELK-1 is also SUMOylated, which mediates both repression and subcellular localisation (S. Yang & Sharrocks, 2004; Salinas et al., 2004). This has not been evaluated during this study, so it is unknown whether there is any cross-talk between SUMOylation and ubiquitination. Furthermore, MS/MS analyses revealed that ELK-1 is also open to acetylation, which targeted lysine residues that were also ubiquitination (K35) and SUMOylation (K254) sites (4.10). Although ELK-1 has previously been shown to associate with HATs (CBP/p300), acetylation of ELK-1 has not previously been reported (Janknecht & Nordheim, 1996; Nissen et al., 2001; Q. Li et al., 2003). It has however been suggested as a possible modification of ELK-1 based on HAT association (Nissen et al., 2001). This requires further work, to identify the role of acetylation and whether this actively antagonises ubiquitination/SUMOylation of ELK-1.

8.5.3 Other effects of ELK-1-USP17 cooperation on cellular processes

Focus on cellular outputs from USP17 deubiquitination of ELK-1 have been on proliferation. Through this, a model for the effects of USP17 and ELK-1 on cell proliferation following induction by mitogens has been proposed based on experiments carried out largely in HEK293T cells. The next step is to test this model in other biological contexts. ELK-1 has important functions in maintenance of stem cell pluripotency and self-renewal of hESCs (Goke et al., 2013). Dub3 also has a role in the self-renewal of mESCs, so looking into the relationship between USP17 and ELK-1 in the regulation of this would be interesting (van der Laan et al., 2013). Furthermore, dysregulated expression of ELK-1 and USP17 has been associated with the growth of several cancers, and hence it would be worth studying the effects of ELK-1 monoubiquitination on the cell cycle in tumour models. As drivers of cell proliferation, ELK-1 and USP17 could represent clinical targets for the treatment of cancers where their expression is elevated. Notably, WP1130 (Degrasyn) has recently been shown to bind to USP17 and inhibit its activity, and impair tumour growth in mice injected with breast cancer cells (Y. Wu et al., 2017). However, WP1130 is only semi-selective and is capable of inhibiting several other DUBs, including USP5, USP9x, USP14, and UCH37 (Kapuria et al., 2010).

Another potential avenue of investigation is cell migration. USP17 and ELK-1 are often linked to cancer metastasis and invasiveness through their effects on migration, and hence it would also be interesting to find out if functional overlap promotes this. Particularly, regulation of MMP expression is dependent on ELK-1 (Muddasani et al., 2007; Choi et al., 2011) and USP17 (S. Zhang et al., 2016), and USP17 has recently been implicated in the promotion of breast tumour metastasis *via* SNAIL-1 stabilisation through the deubiquitination of polyubiquitin chains (Y. Wu et al., 2017; Liu et al., 2017). SNAIL-1 is a transcription factor with important functions in promoting EMT, and ELK-1 has been shown to up-regulate its expression, increasing the migration and invasiveness of colorectal and breast cancers (Hsu et al., 2013; Smith et al., 2014; J. Zhao et al., 2017). This could represent another point of cooperation between USP17 and ELK-1 in the regulation of cell adhesion and migration.

8.6 Concluding statement

In conclusion, this study has revealed novel insights into the regulation of ELK-1 transcription, confirming monoubiquitination as another mechanism of control over ELK-1 through post-translational modification. ELK-1 can cycle between its active and inactive states through reversible phosphorylation and monoubiquitination respectively, which is required for cell-cycle progression and proliferation (Figure 8-7). Moreover, ELK-1 can also be polyubiquitinated, potentiating its proteasomal degradation, and both mono- and

polyubiquitination can be removed from ELK-1 *via* the deubiquitinating enzyme USP17. ELK-1 and USP17 function co-operatively, coordinated through diverse signalling mechanisms commensurate for concerted control over the cell cycle. These pathways culminate in regulated cellular responses, and place both USP17 and ELK-1 at the forefront of proliferation in response to mitogens.

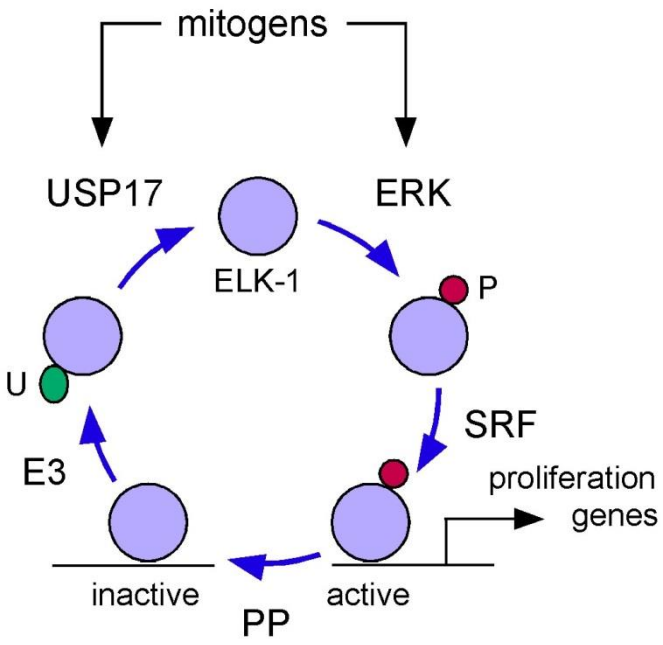

Figure 8-7: Regulatory cycle of ELK-1 activity. In response to mitogens, ELK-1 is deubiquitinated by USP17 and phosphorylated by ERK, rendering it active. It forms a ternary complex with SRF at the SRE and transcriptionally activates proliferation-inducing genes (IEGs such as *CFOS*). To inactivate ELK-1 following proliferation-induction, ELK-1 can be dephosphorylated by a protein phosphatase (PP) and monoubiquitinated by an E3 ligase. Taken from manuscript for (Ducker et al., 2017).

Professional Internships for PhD Students Reflection

Name of Organization

Sense about Science

Details of Placement

Contributed to morning newspaper meetings, reading tabloid newspapers and assessing the scientific articles for accuracy. Coordinated the plant science and energy panels, contacting experts to answer questions from the public in these areas. Edited answers for clarity and simplified them if necessary. Helped maintain the Sense about Science website in addition to those for the Ask for Evidence and AllTrials campaigns, in addition to producing and uploading content. Helped advertise and spread awareness for the John Maddox prize, and contacted learned organizations for nominations for the prize.

Placement Achievements

- "Standing up for Science" workshop - helped organize a workshop for early career researchers that gave insight into the perception of science in the media
- "Peer review: the nuts and bolts" workshop - also helped in the organisation of this meeting looking at peer review
- Attended a parliamentary links meeting focusing on Science after the EU referendum
- Attended award ceremony for 2016 John Maddox prize at the Royal Pharmaceutical Society

Skill development

My three-month internship at Sense about Science helped develop my IT skills, and particularly how to edit websites. I also developed my proofreading skills from working on the Plant science and Energy panels, and from editing a conference agenda. Spreading awareness of campaigns also helped me improve my communications skills. The placement highlighted the importance of public outreach and of communicating complex scientific ideas to the public in an approachable manner, something which I strive to uphold in any future scientific endeavours.

Appendices

DNA sequences of constructs produced in this study

A) pcDNA3.1 His-HAND1 (5′-3′)

GAATTCTCCAACATGAACCTCGTGGGCAGCTACGCACATCATCACCATCATCACCACTCACAC
CCGCCGCACCCCATGCTCCACGAACCCTTCCTGTTTGGCCCGGCCTCGCGTTGCCACCAGGAG
CGGCCTTACTTCCAGAGCTGGCTGCTGAGCCCGGCTGATGCTGCCCCAGATTTCCCTGCCGGC
GGGCCACCACCTACCACCGCAGTAGCAGCGGCTGCCTATGGTCCCGATGCCAGGCCGAGTCAG
AGCCCAGGTCGGCTGGAGGCTCTTGGAAGCCGCCTGCCCAAACGAAAAGGCTCAGGACCCAAG
AAGGAGAGGAGACGCACAGAGAGCATTAACAGCGCGTTCGCGGAGCTGCGTGAGTGCATCCCC
AATGTGCCCGCCGACACCAAGCTCTCCAAGATCAAGACTCTGCGCCTGGCTACCAGTTACATC
GCCTACTTGATGGACGTGCTGGCCAAGGATGCACAAGCAGGTGACCCCGAGGCCTTCAAGGCT
GAACTCAAAAAGACGGATGGCGGTCGCGAAAGCAAGCGGAAAAGGGAGTTGCCTCAGCAGCCC
GAAAGCTTCCCTCCTGCCTCGGGGCCCGGCGAGAAGAGGATTAAAGGGCGCACCGGCTGGCCT
CAGCAAGTCTGGGCGCTGGAGCTAAACCAGCACCATCACCATCACCATTAGGGCCC

GAATTC = EcoR1 site
ATG = Start codon
GGGCCC = Apa1/Bsp120I
CACCATCACCATCACCAT = His-tag
TAG = Stop codon

Untagged HAND1 had previously been cloned into pcDNA3.1 through EcoR1/Xho1 sites. His-tag was inserted at carboxyl-terminus through use of internal Apa1/Bsp120I sites in HAND1 and downstream Apa1/Bsp120I site in pcDNA3.1

B) pSUPER ELK sh#1 (5’-3’)

GATCCCCGGCCTTGCGGTACTACTATTTCAAGAGAATAGTAGTACCGCAAGGCCTTTTTA

GGCCTTGCGGTACTACTAT = Target sequence, sense
ATAGTAGTACCGCAAGGCC = Target sequence, antisense
TTCAAGAGA = Hairpin

C) pSUPER ELK sh#2 (5’-3’)

GATCCCCGCTTCCTACGCATACATTGTTCAAGAGACATGTATGCGTAGGAAGCTTTTTA

GCTTCCTACGCATACATTG = Target sequence, sense
CATGTATGCGTAGGAAGC = Target sequence, antisense
TTCAAGAGA = Hairpin

Annealed oligos were ligated into pSUPER through Bglii and Hindiii sites

References

Abdul Rehman, S. A., Kristariyanto, Y. A., Choi, S. Y., Nkosi, P. J., Weidlich, S., Labib, K., … Kulathu, Y. (2016). MINDY-1 Is a Member of an Evolutionarily Conserved and Structurally Distinct New Family of Deubiquitinating Enzymes. *Molecular Cell*, *63*(1), 146–155.

Agarwal, M. L., Agarwal, a, Taylor, W. R., & Stark, G. R. (1995). p53 controls both the G2/M and the G1 cell cycle checkpoints and mediates reversible growth arrest in human fibroblasts. *Proceedings of the National Academy of Sciences of the United States of America*, *92*(18), 8493–7.

Aillet, F., Lopitz-Otsoa, F., Egaña, I., Hjerpe, R., Fraser, P., Hay, R. T., … Lang, V. (2012). Heterologous SUMO-2/3-ubiquitin chains optimize IκBα degradation and NF-κB activity. *PloS One*, *7*(12), e51672.

Al-Shami, A., Jhaver, K. G., Vogel, P., Wilkins, C., Humphries, J., Davis, J. J., … Oravecz, T. (2010). Regulators of the proteasome pathway, Uch37 and Rpn13, play distinct roles in mouse development. *PLoS ONE*, *5*(10), e13654.

Alkan, C., Kidd, J. M., Marques-Bonet, T., Aksay, G., Antonacci, F., Hormozdiari, F., … Eichler, E. E. (2009). Personalized copy number and segmental duplication maps using next-generation sequencing. *Nature Genetics*, *41*(10), 1061–1067.

Allen, B. L., & Taatjes, D. J. (2015). The Mediator complex: a central integrator of transcription. *Nature Reviews. Molecular Cell Biology*, *16*(3), 155–166.

Angel, P., & Karin, M. (1991). The role of Jun, Fos and the AP-1 complex in cell-proliferation and transformation. *Biochim Biophys Acta*, *1072*(2–3), 129–57.

Askjaer, P., Jensen, T.H., Nilsson, J., Engelmeier, L,. & Kjems, J. (1998). The Specificity of the CRM1-Rev Nuclear Export Signal Interaction is Mediated by RanGTP. *The Journal of Biological Chemistry*, *273*(50), 33414-33422.

Atanassov, B. S., & Dent, S. Y. R. (2011). USP22 regulates cell proliferation by deubiquitinating the transcriptional regulator FBP1. *EMBO Reports*, *12*(9), 924–30.

Atanassov, B. S., Mohan, R. D., Lan, X., Kuang, X., Lu, Y., Lin, K., … Dent, S. Y. R. (2016). ATXN7L3 and ENY2 Coordinate Activity of Multiple H2B Deubiquitinases Important for Cellular Proliferation and Tumor Growth. *Molecular Cell*, *62*(4), 558–571.

Auble, D. T., & Brinckerhoff, C. E. (1991). The AP-1 Sequence Is Necessary but Not Sufficient for Phorbol Induction of Collagenase in Fibroblasts. *Biochemistry*, *30*(18), 4629–4635.

Bachmair, A., Finley, D., & Varshavsky, A. (1986). In vivo half-life of a protein is a function of its amino-terminal residue. *Science*, *234*(4773), 179–186.

Baek, K. H., Kim, M. S., Kim, Y. S., Shin, J. M., & Choi, H. K. (2004). DUB-1A, a Novel Deubiquitinating Enzyme Subfamily Member, Is Polyubiquitinated and Cytokine-inducible in B-lymphocytes. *Journal of Biological Chemistry*, *279*(4), 2368–2376.

Baek, K. H., Mondoux, M. A., Jaster, R., Fire-Levin, E., & D'Andrea, A. D.

(2001). DUB-2A, a new member of the DUB subfamily of hematopoietic deubiquitinating enzymes. *Blood*, *98*(3), 636–642.

Baeuerle, P. A., & Baltimoire, D. (1988). IkB: A Specific Inhibitor of the NFkB Transcription Factor. *Science*, *242*(4878), 540-6.

Basters, A., Geurink, P. P., Röcker, A., Witting, K. F., Hess, S., Semrau, M. S., … Ovaa, H. (2017). Structural basis for the specificity of USP18 towards ISG15. *Nat Struct Mol Biol 24*(3), 270–278.

Baumann, U., Fernández-Sáiz, V., Rudelius, M., Lemeer, S., Rad, R., Knorn, A.-M., … Bassermann, F. (2014). Disruption of the PRKCD–FBXO25–HAX-1 axis attenuates the apoptotic response and drives lymphomagenesis. *Nature Medicine*, *20*(12), 1401–1409.

Bhattacharya, S., Eckner, R., Grossman, S., Oldread, E., Arany, Z., D'Andrea, A., & Livingston, D. M. (1996). Cooperation of Stat2 and p300/CBP in signalling induced by interferon-α. *Nature*, 383, 344-7

Bienko, M., Green, C. M., Crosetto, N., Rudolf, F., Zapart, G., Coull, B., … Dikic, I. (2005). Ubiquitin-binding domains in Y-family polymerases regulate translesion synthesis. *Science*, *310*(5755), 1821–4.

Bienko, M., Green, C. M., Sabbioneda, S., Crosetto, N., Matic, I., Hibbert, R. G., … Dikic, I. (2010). Regulation of Translesion Synthesis DNA Polymerase η by Monoubiquitination. *Molecular Cell*, *37*(3), 396–407.

Bonnet, J., Devys, D., & Tora, L. (2014). Histone H2B ubiquitination: signaling not scrapping. *Drug Discovery Today Technologies*, *12*, e19-27.

Booy, E. P., Henson, E. S., & Gibson, S. B. (2011). Epidermal growth factor regulates Mcl-1 expression through the MAPK-Elk-1 signalling pathway contributing to cell survival in breast cancer. *Oncogene*, *30*(20), 2367–78.

Bornhorst, J., & Falke, J. (2000). Purification of Proteins Using Polyhistidine Affinity Tags. *Methods Enzymol*, *326*, 245–254.

Boros, J., Donaldson, I. J., Donnell, A. O., Boros, J., Donaldson, I. J., Donnell, A. O., … Sharrocks, A. D. (2009A). Elucidation of the ELK1 target gene network reveals a role in thecoordinate regulation of core components of the gene regulation machinery, *1*, 1963–1973.

Boros, J., O'Donnell, A., Donaldson, I. J., Kasza, A., Zeef, L., & Sharrocks, A. D. (2009B). Overlapping promoter targeting by Elk-1 and other divergent ETS-domain transcription factor family members. *Nucleic Acids Research*, *37*(22), 7368–7380.

Bouker, K. B., Skaar, T. C., Riggins, R. B., Harburger, D. S., Fernandez, D. R., Zwart, A., … Clarke, R. (2005). Interferon regulatory factor-1 (IRF-1) exhibits tumor suppressor activities in breast cancer associated with caspase activation and induction of apoptosis. *Carcinogenesis*, *26*(9), 1527–35.

Boulukos, K. E., Pognonec, P., Begue, A., Galibert, F., Gesquière, J. C., Stéhelin, D., & Ghysdael, J. (1988). Identification in chickens of an evolutionarily conserved cellular ets-2 gene (c-ets-2) encoding nuclear proteins related to the products of the c-ets proto-oncogene. *The EMBO Journal*, *7*(3), 697–705.

Boutet, S. C., Disatnik, M. H., Chan, L. S., Iori, K., & Rando, T. A. (2007). Regulation of Pax3 by Proteasomal Degradation of Monoubiquitinated Protein in Skeletal Muscle Progenitors. *Cell*, *130*(2), 349–362.

Boyartchuk, V. L. (1997). Modulation of Ras and a-Factor Function by Carboxyl-Terminal Proteolysis. *Science*, *275*(5307), 1796–1800.

Bridges, C. R., Tan, M.-C., Premarathne, S., Nanayakkara, D., Bellette, B., Zencak, D., … Wood, S. A. (2017). USP9X deubiquitylating enzyme maintains RAPTOR protein levels, mTORC1 signalling and proliferation in neural progenitors. *Scientific Reports*, *7*(391).

Buchwalter, G., Gross, C., & Wasylyk, B. (2005). The ternary complex factor net regulates cell migration through inhibition of PAI-1 expression. *Molecular and Cellular Biology*, *25*(24), 10853–10862.

Burch, P. M., Yuan, Z., Loonen, A., & Heintz, N. H. (2004). An extracellular signal-regulated kinase 1- and 2-dependent program of chromatin trafficking of c-Fos and Fra-1 is required for cyclin D1 expression during cell cycle reentry. *Molecular and Cellular Biology*, *24*(11), 4696–709.

Burrows, J. F., Kelvin, A. A., McFarlane, C., Burden, R. E., McGrattan, M. J., De La Vega, M., … Johnston, J. A. (2009). USP17 regulates Ras activation and cell proliferation by blocking RCE1 activity. *Journal of Biological Chemistry*, *284*(14), 9587–9595.

Burrows, J. F., McGrattan, M. J., & Johnston, J. A. (2005). The DUB/USP17 deubiquitinating enzymes, a multigene family within a tandemly repeated sequence. *Genomics*, *85*(4), 524–529.

Burrows, J. F., McGrattan, M. J., Rascle, A., Humbert, M., Baek, K. H., & Johnston, J. A. (2004). DUB-3, A Cytokine-inducible Deubiquitinating Enzyme That Blocks Proliferation. *Journal of Biological Chemistry*, *279*(14), 13993–14000.

Burrows, J. F., Scott, C. J., & Johnston, J. a. (2010). The DUB/USP17 deubiquitinating enzymes: a gene family within a tandemly repeated sequence, is also embedded within the copy number variable beta-defensin cluster. *BMC Genomics*, *11*, 250.

Cantin, G. T., Stevens, J. L., & Berk, A. J. (2003). Activation domain-mediator interactions promote transcription preinitiation complex assembly on promoter DNA. *Proceedings of the National Academy of Sciences of the United States of America*, *100*(21), 12003–8.

Cao, R., Wang, L., Wang, H., Xia, L., Erdjument-Bromage, H., Tempst, P., … Zhang, Y. (2002). Role of histone H3 lysine 27 methylation in Polycomb-group silencing. *Science (New York, N.Y.)*, *298*(5595), 1039–43.

Carter, S., Bischof, O., Dejean, A., & Vousden, K. H. (2007). C-terminal modifications regulate MDM2 dissociation and nuclear export of p53. *Nature Cell Biology*, *9*(4), 428–35.

Casar, B., Pinto, A., & Crespo, P. (2008). Essential Role of ERK Dimers in the Activation of Cytoplasmic but Not Nuclear Substrates by ERK-Scaffold Complexes. *Molecular Cell*, *31*(5), 708–721.

Casey, P. J., Solski, P. A., Der, C. J., & Buss, J. E. (1989). P21Ras Is Modified By a Farnesyl Isoprenoid. *Proceedings of the National Academy of Sciences of the United States of America*, *86*(21), 8323–8327.

Cavigelli, M., Dolfi, F., Claret, F. X., & Karin, M. (1995). Induction of c-fos expression through JNK-mediated TCF/Elk-1 phosphorylation. *The EMBO Journal*, *14*(23), 5957–64.

Cesari, F., Brecht, S., Vintersten, K., Vuong, L., Hofmann, M., Klingel, K., …

Nordheim, A. (2004). Mice deficient for the ets transcription factor elk-1 show normal immune responses and mildly impaired neuronal gene activation. *Molecular and Cellular Biology*, *24*(1), 294–305.

Chambard, J. C., Lefloch, R., Pouysségur, J., & Lenormand, P. (2007). ERK implication in cell cycle regulation. *Biochimica et Biophysica Acta - Molecular Cell Research*, *1773*(8), 1299–1310.

Chan, C. S., Rastelli, L., & Pirrotta, V. (1994). A Polycomb response element in the Ubx gene that determines an epigenetically inherited state of repression. *The EMBO Journal*, *13*(11), 2553–64.

Chanmee, T., Ontong, P., Mochizuki, N., Kongtawelert, P., Konno, K., & Itano, N. (2014). Excessive hyaluronan production promotes acquisition of cancer stem cell signatures through the coordinated regulation of twist and the transforming growth factor β (TGF-β)-snail signaling axis. *Journal of Biological Chemistry*, *289*(38), 26038–26056.

Chapman, R. S., Du, E. K., Lourenco, P. C., Tonner, E., Flint, D. J., Clarke, A. R., & Watson, C. J. (2000). A novel role for IRF-1 as a suppressor of apoptosis, 6386–6391.

Chardin, P., Camonis, J. H., Gale, N. W., Van Aelst, L., Schlessinger, J., Wigler, M. H., & Bar-Sagi, D. (1993). Human Sos 1: A guanine nucleotide exchange factor for Ras that bind to GRB2. *Science*, *260*(22), 1338–1343.

Chavrier, P., Janssen-Timmen, U., Mattéi, M. G., Zerial, M., Bravo, R., & Charnay, P. (1989). Structure, chromosome location, and expression of the mouse zinc finger gene Krox-20: multiple gene products and coregulation with the proto-oncogene c-fos. *Molecular and Cellular Biology*, *9*(2), 787–97.

Cheng, Y., Gao, W.-W., Tang, H.-M. V., Deng, J.-J., Wong, C.-M., Chan, C.-P., & Jin, D.-Y. (2016). β-TrCP-mediated ubiquitination and degradation of liver-enriched transcription factor CREB-H. *Scientific Reports*, *6*, 23938.

Chiu, R. K., Brun, J., Ramaekers, C., Theys, J., Weng, L., Lambin, P., … Wouters, B. G. (2006). Lysine 63-polyubiquitination guards against translesion synthesis-induced mutations. *PLoS Genetics*, *2*(7), 1070–1083.

Choi, B. D., Jeong, S. J., Guanlin, W., Park, J. J., Lim, D. S., Kim, B. H., … Jeong, M. J. (2011). Secretory leukocyte protease inhibitor is associated with MMP-2 and MMP-9 to promote migration and invasion in SNU638 gastric cancer cells. *International Journal of Molecular Medicine*, *28*(4), 527–534.

Chow, L., PhD Thesis, & University of Nottingham. (2010). The role of monoubiquitylation in the regulation of the transcription factor Elk-1.

Choy, E., Chiu, V. K., Silletti, J., Feoktistov, M., Morimoto, T., Michaelson, D., … Philips, M. R. (1999). Endomembrane trafficking of ras: The CAAX motif targets proteins to the ER and Golgi. *Cell*, *98*(1), 69–80.

Christy, B., & Nathans, D. (1989). Functional serum response elements upstream of the growth factor-inducible gene zif268. *Molecular and Cellular Biology*, *9*(11), 4889–95.

Chung, K. C., Gomes, I., Wang, D., Lau, L. F., & Rosner, M. R. (1998). Raf and fibroblast growth factor phosphorylate Elk1 and activate the serum response element of the immediate early gene pip92 by mitogen-activated

protein kinase-independent as well as -dependent signaling pathways. *Molecular and Cellular Biology*, *18*(4), 2272–81.

Chung, K. C., Kim, S. M., Rhang, S., Lau, L. F., Gomes, I., & Ahn, Y. S. (2000). Expression of immediate early gene pip92 during anisomycin-induced cell death is mediated by the JNK- and p38-dependent activation of Elk1. *European Journal of Biochemistry*, *267*(15), 4676–4684.

Ciechanover, A., & Ben-Saadon, R. (2004). N-terminal ubiquitination: More protein substrates join in. *Trends in Cell Biology*, *14*(3), 103–106.

Ciechanover, A., Heller, H., Elias, S., Haas, a L., & Hershko, A. (1980A). ATP-dependent conjugation of reticulocyte proteins with the polypeptide required for protein degradation. *Proceedings of the National Academy of Sciences of the United States of America*, *77*(3), 1365–1368.

Ciechanover, A., Elias, S., Heller, H., Ferber, S., & Hershko, A. (1980B). Characterization of the Heat- stable Polypeptide of the ATP- dependent Proteolytic System. *The Journal of Biological Chemistry*, *255*(16), 8–11.

Ciehanover, A., Hod, Y., & Hershko, A. (1978). A heat-stable polypeptide component of an ATP-dependent proteolytic system from reticulocytes. *Biochemical and Biophysical Research Communications*, *81*(4), 1100–1105.

Clague, M. J., Barsukov, I., Coulson, J. M., Liu, H., Rigden, D. J., & Urbé, S. (2013). Deubiquitylases from genes to organism. *Physiological Reviews*, *93*(3), 1289–315.

Costello, P., Nicolas, R., Willoughby, J., Wasylyk, B., Nordheim, A., & Treisman, R. (2010). Ternary complex factors SAP-1 and Elk-1, but not net, are functionally equivalent in thymocyte development. *Journal of Immunology*, *185*(2), 1082–92.

Craig, K. L., & Tyers, M. (1999). The F-box: A new motif for ubiquitin dependent proteolysis in cell cycle regulation and signal transduction. *Progress in Biophysics and Molecular Biology*, *72*(3), 299–328.

Crosas, B., Hanna, J., Kirkpatrick, D. S., Zhang, D. P., Tone, Y., Hathaway, N. A., … Finley, D. (2006). Ubiquitin Chains Are Remodeled at the Proteasome by Opposing Ubiquitin Ligase and Deubiquitinating Activities. *Cell*, *127*(7), 1401–1413.

Crowe, D. L., & Brown, T. N. (1999). Transcriptional inhibition of matrix metalloproteinase 9 (MMP-9) activity by a c-fos/estrogen receptor fusion protein is mediated by the proximal AP-1 site of the MMP-9 promoter and correlates with reduced tumor cell invasion. *Neoplasia*, *1*(4), 368–72.

Cruzalegui, F. H., Cano, E., & Treisman, R. (1999). ERK activation induces phosphorylation of Elk-1 at multiple S/T-P motifs to high stoichiometry. *Oncogene*, *18*(56), 7948–7957.

Cummins, J., & Vogelstein, B. (2004). HAUSP is required for p53 destabilization. *Cell Cycle*, 3(6), 689–692.

Czekay, R. P., Aertgeerts, K., Curriden, S. A., & Loskutoff, D. J. (2003). Plasminogen activator inhibitor-1 detaches cells from extracellular matrices by inactivating integrins. *Journal of Cell Biology*, *160*(5), 781–791.

Dalton, S., & Treisman, R. (1992). Characterization of SAP-1, a protein recruited by serum response factor to the c-fos serum response element.

Cell, *68*(3), 597–612.

De Bosscher, K., Hill, C. S., & Nicolás, F. J. (2004). Molecular and functional consequences of Smad4 C-terminal missense mutations in colorectal tumour cells. *The Biochemical Journal*, *379*(Pt 1), 209–216.

De La Vega, M., Burrows, J. F., McFarlane, C., Govender, U., Scott, C. J., & Johnston, J. A. (2010). The deubiquitinating enzyme USP17 blocks N-Ras membrane trafficking and activation but leaves K-Ras unaffected. *Journal of Biological Chemistry*, *285*(16), 12028–12036.

de la Vega, M., Kelvin, A. A., Dunican, D. J., McFarlane, C., Burrows, J. F., Jaworski, J., … Johnston, J. A. (2011). The deubiquitinating enzyme USP17 is essential for GTPase subcellular localization and cell motility. *Nature Communications*, *2*, 259.

de Taisne, C., Gegonne, A., Stehelin, D., Bernheim, A., & Berger, R. (1984). Chromosomal localization of the human proto-oncogene c-ets. *Nature*, *310*, 581–583.

Degnan, B. M., Degnan, S. M., Nagamura, T., & Morse, D. E. (1993). The ets multigene family is conserved througout the Metazoa. *Nucleic Acids Res.*, *21*(15), 3479–3484.

Delgado-Diaz, M. R., Martin, Y., Berg, A., Freire, R., & Smits, V. A. J. (2014). Dub3 controls DNA damage signalling by direct deubiquitination of H2AX. *Molecular Oncology*, *8*(5), 884–893.

Dephoure, N., Zhou, C., Villén, J., Beausoleil, S. a, Bakalarski, C. E., Elledge, S. J., & Gygi, S. P. (2008). A quantitative atlas of mitotic phosphorylation. *Proceedings of the National Academy of Sciences of the United States of America*, *105*(31), 10762–10767.

Dhillon, A. S., Meikle, S., Peyssonnaux, C., Grindlay, J., Kaiser, C., Steen, H., … Eyche, A. (2003). A Raf-1 Mutant That Dissociates MEK / Extracellular Signal-Regulated Kinase Activation from Malignant Transformation and Differentiation but Not Proliferation. *Society*, *23*(6), 1983–1993.

Dimova, N. V, Hathaway, N. A., Lee, B., & Kirkpatrick, D. S. (2012). APC/C-mediated multiple monoubiquitination provides an alternative degradation signal for cyclin B1, *14*(2), 168–176.

Doil, C., Mailand, N., Bekker-Jensen, S., Menard, P., Larsen, D. H., Pepperkok, R., … Lukas, C. (2009). RNF168 Binds and Amplifies Ubiquitin Conjugates on Damaged Chromosomes to Allow Accumulation of Repair Proteins. *Cell*, *136*(3), 435–446.

Dong, B., Horowitz, D. S., Kobayashi, R., & Krainer, A. R. (1993). Purification and cDNA cloning of HeLa cell p54nrb, a nuclear protein with two RNA recognition motifs and extensive homology to human splicing factor PSF and Drosophila NONA/BJ6. *Nucleic Acids Research*, *21*(17), 4085–4092.

Dornan, D., Wertz, I., Shimizu, H., Arnott, D., Koeppen, H., & Dixit, V. M. (2004). The ubiquitin ligase COP1 is a critical negative regulator of p53. Nature *429*(6987), 86-92.

Drewett, V., Muller, S., Goodall, J., & Shaw, P. E. (2000). Dimer Formation by Ternary Complex Factor ELK-1. *Journal of Biological Chemistry*, *275*(3), 1757–1762.

Ducker, C., Chow, L., Saxton, J., Handwerger, J., Layfield, R., & Shaw, P. (2017). USP17-mediated de-ubiquitylation of ELK-1 potentiates mitogen-

dependent gene expression and cell proliferation. Manuscript.
Dupont, S., Mamidi, A., Cordenonsi, M., Montagner, M., Zacchigna, L., Adorno, M., … Piccolo, S. (2009). FAM/USP9x, a Deubiquitinating Enzyme Essential for TGF?? Signaling, Controls Smad4 Monoubiquitination. *Cell*, *136*(1), 123–135.
Dupont, S., Zacchigna, L., Cordenonsi, M., Soligo, S., Adorno, M., Rugge, M., & Piccolo, S. (2005). Germ-layer specification and control of cell growth by ectodermin, a Smad4 ubiquitin ligase. *Cell*, *121*(1), 87–99.
Eddins, M. J., Varadan, R., Fushman, D., Pickart, C. M., & Wolberger, C. (2007). Crystal Structure and Solution NMR Studies of Lys48-linked Tetraubiquitin at Neutral pH. *Journal of Molecular Biology*, *367*(1), 204–211.
Esnault, C., Gualdrini, F., Horswell, S., Kelly, G., Stewart, A., East, P., … Treisman, R. (2017). ERK-Induced Activation of TCF Family of SRF Cofactors Initiates a Chromatin Modification Cascade Associated with Transcription. *Molecular Cell*, *65*(6), 1081–1095.
Esser, C., Scheffner, M., & Höhfeld, J. (2005). The chaperone-associated ubiquitin ligase CHIP is able to target p53 for proteasomal degradation. *The Journal of Biological Chemistry*, *280*(29), 27443–8.
Evanko, S. P., & Wight, T. N. (1999). Intracellular Localization of Hyaluronan in Proliferating Cells. *Journal of Histochemistry & Cytochemistry*, *47*(10), 1331–1341.
Evans, E. L., Saxton, J., Shelton, S. J., Begitt, A., Holliday, N. D., Hipskind, R. a, & Shaw, P. E. (2011). Dimer formation and conformational flexibility ensure cytoplasmic stability and nuclear accumulation of Elk-1. *Nucleic Acids Research*, *39*(15), 6390–402.
Faesen, A. C., Dirac, A. M. G., Shanmugham, A., Ovaa, H., Perrakis, A., & Sixma, T. K. (2011). Mechanism of USP7/HAUSP activation by its C-Terminal ubiquitin-like domain and allosteric regulation by GMP-synthetase. *Molecular Cell*, *44*(1), 147–159.
Faggiano, S., Menon, R. P., Kelly, G. P., Todi, S. V, Scaglione, K. M., Konarev, P. V, … Pastore, A. (2015). Allosteric regulation of deubiquitylase activity through ubiquitination. *Frontiers in Molecular Biosciences*, *2*(2).
Fan, C.-M., & Maniatis, T. (1991). Generation of p50 subunit of NF-kB by processing of p105 through an ATP-dependent pathway. *Nature*, *354*, 395–398.
Fang, S., Jensen, J. P., Ludwig, R. L., Vousden, K. H., & Weissman, A. M. (2000). Mdm2 is a RING finger-dependent ubiquitin protein ligase for itself and p53. *Journal of Biological Chemistry*, *275*(12), 8945–8951.
Fantz, D. A., Jacobs, D., Glossip, D., & Kornfeld, K. (2001). Docking Sites on Substrate Proteins Direct Extracellular Signal-regulated Kinase to Phosphorylate Specific Residues. *Journal of Biological Chemistry*, *276*(29), 27256–27265.
Fernández-Montalván, A., Bouwmeester, T., Joberty, G., Mader, R., Mahnke, M., Pierrat, B., … Gerhartz, B. (2007). Biochemical characterization of USP7 reveals post-translational modification sites and structural requirements for substrate processing and subcellular localization. *FEBS Journal*, *274*(16), 4256–4270.

Firulli, B. A., Howard, M. J., Mcdaid, J. R., Mcilreavey, L., Dionne, K. M., Centonze, V. E., … Antonio, S. (2003). PKA , PKC , and the Protein Phosphatase 2A Influence HAND Factor Function : A Mechanism for Tissue-Specific Transcriptional Regulation, *12(5)*, 1225–1237.

Fischle, W., Wang, Y., Jacobs, S. a, Kim, Y., Allis, C. D., & Khorasanizadeh, S. (2003). Molecular basis for the discrimination of repressive methyl-lysine marks in histone H3 by Polycomb and HP1 chromodomains. *Genes & Development*, *17*(15), 1870–81.

Fisher, R., Mavrothalassitis, G., Kondoh, A., & Papas, T. (1991). High-affinity DNA-protein interactions of the cellular ETS1 protein: the determination of the ETS binding motif. *Oncogene*, *6*, 2249–2254.

Fornerod, M., Ohno, M., Yoshida, M., & Mattaj, I. W. (1997). CRM1 is an Export Receptor for Leucine-Rich Nuclear Export Signals. *Cell*, *90*(6), 1051-1060.

Fridman, J. S., & Lowe, S. W. (2003). Control of apoptosis by p53. *Oncogene*, *22*(56), 9030–40.

Fuchs, G., Shema, E., Vesterman, R., Kotler, E., Wolchinsky, Z., Wilder, S., … Oren, M. (2012). RNF20 and USP44 Regulate Stem Cell Differentiation by Modulating H2B Monoubiquitylation. *Molecular Cell*, *46*(5), 662–673.

Fuchs, S. Y., Xie, B., Adler, V., Fried, V. A., Davis, R. J., & Ronai, Z. (1997). C-jun NH2-terminal kinases target the ubiquitination of their associated transcription factors. *Journal of Biological Chemistry*, *272*(51), 32163–32168.

Galbraith, M. D., Saxton, J., Li, L., Shelton, S. J., Zhang, H., Espinosa, J. M., & Shaw, P. E. (2013). ERK phosphorylation of MED14 in promoter complexes during mitogen-induced gene activation by Elk-1. *Nucleic Acids Research*, *41*(22), 10241–53.

Garnett, M. J., Rana, S., Paterson, H., Barford, D., & Marais, R. (2005). Wild-type and mutant B-RAF activate C-RAF through distinct mechanisms involving heterodimerization. *Molecular Cell*, *20*(6), 963–969.

Ghosh, S., Gifford, a M., Riviere, L. R., Tempst, P., Nolan, G. P., & Baltimore, D. (1990). Cloning of the p50 DNA binding subunit of NF-kappa B: homology to rel and dorsal. *Cell*, *62*(5), 1019–29.

Ghysdael, J., Gegonne, a, Pognonec, P., Dernis, D., Leprince, D., & Stehelin, D. (1986). Identification and preferential expression in thymic and bursal lymphocytes of a c-ets oncogene-encoded Mr 54,000 cytoplasmic protein. *Proceedings of the National Academy of Sciences of the United States of America*, *83*(6), 1714–8.

Gille, H., Kortenjann, M., Thomae, O., Moomaw, C., Slaughterl, C., Cobb, M., & Shaw, P. E. (1995A). ERK phosphorylation potentiates Elk-1-mediated ternary complex formation and transactivation. *EMBO Journal*, *14*(5), 951–962.

Gille, H., Strahl, T., & Shaw, P. E. (1995B). Activation of ternary complex factor Elk-1 by stress-activated protein kinases. *Current Biology*, *5*, 1191–1200.

Gille, H., Sharrocks, A., & Shaw, P. (1992). Phosphorylation of transcription factor P62TCF by MAP Kinase stimulates ternary complex-formation at C-FOS promoter. *Nature*, *358*(6385), 414–417.

Giovane, A., Pintzas, A., Maira, S. M., Sobieszczuk, P., & Wasylyk, B. (1994). Net, a new ets transcription factor that is activated by Ras. *Genes and Development*, *8*(13), 1502–1513.

Glickman, M. H., & Ciechanover, A. (2002). The ubiquitin-proteasome proteolytic pathway: destruction for the sake of construction. *Physiological Reviews*, *82*(2), 373–428.

Goke, J., Chan, Y. S., Yan, J., Vingron, M., & Ng, H. H. (2013). Genome-wide kinase-chromatin interactions reveal the regulatory network of ERK signaling in human embryonic stem cells. *Mol Cell*, *50*(6), 844–855.

Goldstein, G., Scheid, M., Hammerling, U., Schlesinger, D. H., Niall, H. D., & Boyse, E. A. (1975). Isolation of a polypeptide that has lymphocyte-differentiating properties and is probably represented universally in living cells. *Proceedings of the National Academy of Sciences of the United States of America*, *72*(1), 11–5.

Gondo, Y., Okada, T., Matsuyama, N., Saitoh, Y., Yanagisawa, Y., & Ikeda, J. E. (1998). Human megasatellite DNA RS447: copy-number polymorphisms and interspecies conservation. *Genomics*, *54*(1), 39–49.

Greenberg, M. E., & Ziff, E. B. (1984). Stimulation of 3T3 cells induces transcription of the c-fos proto-oncogene. *Nature*, *311*(5985), 433–438.

Grice, G. L., & Nathan, J. A. (2016). The recognition of ubiquitinated proteins by the proteasome. *Cellular and Molecular Life Sciences*, *73*(18), 3497–3506.

Grosstessner-Hain, K., Hegemann, B., Novatchkova, M., Rameseder, J., Joughin, B. A., Hudecz, O., … Mechtler, K. (2011). Quantitative Phospho-proteomics to Investigate the Polo-like Kinase 1-Dependent Phospho-proteome. *Molecular & Cellular Proteomics*, *10*(11), M111.008540.

Gu, J., Kawai, H., Nie, L., Kitao, H., Wiederschain, D., Jochemsen, A. G., … Yuan, Z. M. (2002). Mutual dependence of MDM2 and MDMX in their functional inactivation of p53. *Journal of Biological Chemistry*, *277*(22), 19251–19254.

Gualdrini, F., Esnault, C., Horswell, S., Stewart, A., Matthews, N., & Treisman, R. (2016). SRF Co-factors Control the Balance between Cell Proliferation and Contractility. *Molecular Cell*, *64*(6), 1048–1061.

Guan, J., Yu, S., & Zheng, X. (2017). NEDDylation antagonizes ubiquitination of proliferating cell nuclear antigen and regulates the recruitment of polymerase η in response to oxidative DNA damage. *Protein & Cell*. s13238-017-0455-x

Guha, M., O'Connell, M. A., Pawlinski, R., Hollis, A., McGovern, P., Yan, S. F., … Mackman, N. (2001). Lipopolysaccharide activation of the MEK-ERK1/2 pathway in human monocytic cells mediates tissue factor and tumor necrosis factor α expression by inducing Elk-1 phosphorylation and Egr-1 expression. *Blood*, *98*(5), 1429–1439.

Hassler, M., & Richmond, T. J. (2001). The B-box dominates SAP-1-SRF interactions in the structure of the ternary complex. *EMBO Journal*, *20*(12), 3018–3028.

Hatakeyama, S., Kitagawa, M., Nakayama, K., Shirane, M., Matsumoto, M., Hattori, K., … Good, R. A. (1999). Ubiquitin-dependent degradation of IkappaBalpha is mediated by a ubiquitin ligase Skp1/Cul 1/F-box protein

FWD1. *Proc Natl Acad Sci USA*, *96*(7), 3859–63.
Heride, C., Urbé, S., & Clague, M. J. (2014). Ubiquitin code assembly and disassembly. *Current Biology*, *24*(6), R215–R220.
Hernández-Pérez, S., Cabrera, E., Salido, E., Lim, M., Reid, L., Lakhani, S. R., … Freire, R. (2017). DUB3 and USP7 de-ubiquitinating enzymes control replication inhibitor Geminin: molecular characterization and associations with breast cancer. *Oncogene*, (2016), 6(33), 4802-4809.
Hershko, A., Ciechanover, A., Heller, H., Haas, A. L., & Rose, I. A. (1980). Proposed role of ATP in protein breakdown: conjugation of protein with multiple chains of the polypeptide of ATP-dependent proteolysis. *Proceedings of the National Academy of Sciences of the United States of America*, *77*(4), 1783–6.
Hershko, A., Heller, H., Elias, S., & Ciechanover, A. (1983). Components of Ubiquitin-Protein Ligase System. *The Journal of Biological Chemistry*, *258*(13), 8206–8214.
Hipskind, R. A., Baccarini, M., & Nordheim, A. (1994). Transient activation of RAF-1, MEK, and ERK2 coincides kinetically with ternary complex factor phosphorylation and immediate-early gene promoter activity in vivo. *Molecular and Cellular Biology*, *14*(9), 6219–31.
Hipskind, R. A., Rao, V. N., Mueller, C. G., Reddy, E. S., & Nordheim, A. (1991). Ets-related protein Elk-1 is homologous to the c-fos regulatory factor p62TCF. *Nature*, *354*(6354), 531–4.
Hjerpe, R., Aillet, F., Lopitz-Otsoa, F., Lang, V., England, P., & Rodriguez, M. S. (2009). Efficient protection and isolation of ubiquitylated proteins using tandem ubiquitin-binding entities. *EMBO Reports*, *10*(11), 1250–8.
Hjortland, N. M., & Mesecar, A. D. (2016). Steady-state kinetic studies reveal that the anti-cancer target Ubiquitin-Specific Protease 17 (USP17) is a highly efficient deubiquitinating enzyme. *Archives of Biochemistry and Biophysics*, *612*, 35–45.
Hodge, C., Liao, J., Stofega, M., Guan, K., Carter-Su, C., & Schwartz, J. (1998). Growth Hormone Stimulates Phosphorylation and Activation of Elk-1 and Expression of c-fos, egr-1, andjunB through Activation of Extracellular Signal-regulated Kinases 1 and 2. *Journal of Biological Chemistry*, *273*(47), 31327–31336.
Hoege, C., Pfander, B., Moldovan, G.-L., Pyrowolakis, G., & Jentsch, S. (2002). RAD6-dependent DNA repair is linked to modification of PCNA by ubiquitin and SUMO. *Nature*, *419*(6903), 135–141.
Hofmann, K., & Bucher, P. (1996). The UBA domain: A sequence motif present in multiple enzyme classes of the ubiquitination pathway. *Trends in Biochemical Sciences*, *21*(5), 172–173.
Homan, C. C., Kumar, R., Nguyen, L. S., Haan, E., Raymond, F. L., Abidi, F., … Jolly, L. A. (2014). Mutations in USP9X are associated with x-linked intellectual disability and disrupt neuronal cell migration and growth. *American Journal of Human Genetics*, *94*(3), 470–478.
Hsu, Y.-L., Hou, M.-F., Kuo, P.-L., Huang, Y.-F., & Tsai, E.-M. (2013). Breast tumor-associated osteoblast-derived CXCL5 increases cancer progression by ERK/MSK1/Elk-1/Snail signaling pathway. *Oncogene*, *32*(37), 4436–4447.

Hu, M., Chen, H., Han, C., Lan, J., Xu, Y., Li, C., … Lou, M. (2016). Neuroscience Letters Expression and functional implications of USP17 in glioma. *Neuroscience Letters*, *616*, 125–131.

Hu, M., Li, P., Li, M., Li, W., Yao, T., Wu, J. W., … Shi, Y. (2002). Crystal structure of a UBP-family deubiquitinating enzyme in isolation and in complex with ubiquitin aldehyde. *Cell*, *111*(7), 1041–1054.

Hu, M., Li, P., Song, L., Jeffrey, P. D., Chenova, T. A., Wilkinson, K. D., … Shi, Y. (2005). Structure and mechanisms of the proteasome-associated deubiquitinating enzyme USP14. *The EMBO Journal*, *24*(21), 3747–56.

Hurley, J., Lee, S., & Prag, G. (2006). Ubiquitin-binding domains. *Journal of Biological Chemistry*, *399*, 361–372.

Hussain, S., Zhang, Y., & Galardy, P. J. (2009). DUBs and cancer: The role of deubiquitinating enzymes as oncogenes, non-oncogenes and tumor suppressors. *Cell Cycle*, *8*(11), 1688–1697.

Hwang, C., Shemorry, A., & Varshavsky, A. (2010). N-Terminal Acetylation of Cellular Proteins Creates Specific Degradation Signals. *Science*, *327*(5968), 973–977.

Iavarone, A., & Massague, J. (1997). Repression of the CDK activator Cdc25A and cell-cycle arrest by cytokine TGF-beta in cells lacking the CDK inhibitor p15., *387*, 417–422.

Ishizuka, T., & Lazar, M. a. (2003). The N-CoR/histone deacetylase 3 complex is required for repression by thyroid hormone receptor. *Molecular and Cellular Biology*, *23*(15), 5122–31.

Ito, A., Kawaguchi, Y., Lai, C. H., Kovacs, J. J., Higashimoto, Y., Appella, E., & Yao, T. P. (2002). MDM2-HDAC1-mediated deacetylation of p53 is required for its degradation. *EMBO Journal*, *21*(22), 6236–6245.

Ito, a, Lai, C. H., Zhao, X., Saito, S., Hamilton, M. H., Appella, E., & Yao, T. P. (2001). p300/CBP-mediated p53 acetylation is commonly induced by p53-activating agents and inhibited by MDM2. *The EMBO Journal*, *20*(6), 1331–40.

Jacobs, D., Glossip, D., Xing, H., Muslin, A. J., & Kornfeld, K. (1999). Multiple docking sites on substrate proteins form a modular system that mediates recognition by ERK MAP kinase. *Genes and Development*, *13*(2), 163–175.

Jang, J. W., Lee, W. Y., Lee, J. H., Moon, S. H., Kim, C. H., & Chung, H. M. (2011). A novel Fbxo25 acts as an E3 ligase for destructing cardiac specific transcription factors. *Biochemical and Biophysical Research Communications*, *410*(2), 183–188.

Janknecht, R., Ernst, W. H., Pingoud, V., & Nordheim, a. (1993). Activation of ternary complex factor Elk-1 by MAP kinases. *The EMBO Journal*, *12*(13), 5097–104.

Janknecht, R., & Nordheim, A. (1992). Elk-1 protein domains required for direct and SRF-assisted DNA-binding. *Nucleic Acids Research*, *20*(13), 3317–3324.

Janknecht, R., & Nordheim, A. (1996). MAP kinase-dependent transcriptional coactivation by ELK-1 and its cofactor CBP. *Biochemical and Biophysical research communications*, *228*(3), 831–837.

Janknecht, R., Zinck, R., & Ernst, W. (1994). Functional dissection of the

transcription factor ELK-1. *Oncogene*, *9*(4), 1273–1278.
Joerger, C., & Fersht, R. (2007). Structure-function-rescue: the diverse nature of common p53 cancer mutants. *Oncogene*, *26*(15), 2226–42.
Joo, H.-Y., Zhai, L., Yang, C., Nie, S., Erdjument-Bromage, H., Tempst, P., … Wang, H. (2007). Regulation of cell cycle progression and gene expression by H2A deubiquitination. *Nature*, *449*(7165), 1068–1072.
Kaltschmidt, B., Kaltschmidt, C., Hofmann, T. G., Hehner, S. P., Dröge, W., & Schmitz, M. L. (2000). The pro- or anti-apoptotic function of NF-kappaB is determined by the nature of the apoptotic stimulus. *European Journal of Biochemistry / FEBS*, *267*(12), 3828–35.
Kannouche, P. L., Wing, J., & Lehmann, A. R. (2004). Interaction of human DNA polymerase eta with monoubiquitinated PCNA: A possible mechanism for the polymerase switch in response to DNA damage. *Molecular Cell*, *14*(4), 491–500.
Kapuria, V., Perterson, L. F., Fang, D., Bornmann, W. G., Talpaz, M., & Donato, N.J. (2010). Deubiquitinase Inhibition by Small-Molecule WP1130 Triggers Aggresome Formation and Tumor Cell Apoptosis. *Cancer Research*, *70*(22), 9265-9276.
Karim, F., Urness, L., Thummel, C., Klemsz, M., & McKercher, S. (1990). The ETS-domaln: a new DNA-binding motif that recognizes a purine-rich core DNA sequence. *Genes and Development*, *4*, 1452–1453.
Kasza, A., Wyrzykowska, P., Horwacik, I., Tymoszuk, P., Mizgalska, D., Palmer, K., … Jura, J. (2010). Transcription factors Elk-1 and SRF are engaged in IL1-dependent regulation of ZC3H12A expression. *BMC Mol Biol*, 11(14).
Kawahara, T., Shareef, H. K., Aljarah, A. K., Ide, H., Li, Y., Kashiwagi, E., … Miyamoto, H. (2015). ELK1 is up-regulated by androgen in bladder cancer cells and promotes tumor progression. *Oncotarget*, *6*(30), 29860–76.
Khaminets, A., Behl, C., & Dikic, I. (2016). Ubiquitin-Dependent And Independent Signals In Selective Autophagy. *Trends in Cell Biology*, *26*(1), 6–16.
Khokhlatchev, A. V., Canagarajah, B., Wilsbacher, J., Robinson, M., Atkinson, M., Goldsmith, E., & Cobb, M. H. (1998). Phosphorylation of the MAP kinase ERK2 promotes its homodimerization and nuclear translocation. *Cell*, *93*(4), 605–615.
Khoronenkova, S. V., Dianova, I. I., Ternette, N., Kessler, B. M., Parsons, J. L., & Dianov, G. L. D. (2012). ATM-Dependent Downregulation of USP7/HAUSP by PPM1G Activates p53 Response to DNA Damage. *Molecular Cell*, *45*(6), 801–813.
Kim, J., D'Annibale, S., Magliozzi, R., Low, T. Y., Jansen, P., Shaltiel, I. a, … Guardavaccaro, D. (2014). USP17- and SCFβTrCP-Regulated Degradation of DEC1 Controls the DNA Damage Response. *Molecular and Cellular Biology*, *34*(22), 4177–85.
Kim, P. K. M., Armstrong, M., Liu, Y., Yan, P., Bucher, B., Zuckerbraun, B. S., … Yim, J. H. (2004). IRF-1 expression induces apoptosis and inhibits tumor growth in mouse mammary cancer cells in vitro and in vivo. *Oncogene*, *23*(5), 1125–35.
Koegl, M., Hoppe, T., Schlenker, S., Ulrich, H. D., Mayer, T. U., & Jentsch, S.

(1999). A novel ubiquitination factor, E4, is involved in multiubiquitin chain assembly. *Cell*, *96*(5), 635–44.

Komander, D. (2009). The emerging complexity of protein ubiquitination. *Biochemical Society Transactions*, *37*(Pt 5), 937–53.

Komander, D., Reyes-Turcu, F., Licchesi, J. D. F., Odenwaelder, P., Wilkinson, K. D., & Barford, D. (2009A). Molecular discrimination of structurally equivalent Lys 63-linked and linear polyubiquitin chains. *EMBO Reports*, *10*(5), 466–473.

Komander, D., Clague, M. J., & Urbé, S. (2009B). Breaking the chains: structure and function of the deubiquitinases. *Nature Reviews. Molecular Cell Biology*, *10*(8), 550–563.

Komander, D., & Rape, M. (2012). The ubiquitin code. *Annual Review of Biochemistry*, *81*, 203–29.

Koyano, F., Okatsu, K., Kosako, H., Tamura, Y., Go, E., Kimura, M., … Matsuda, N. (2014). Ubiquitin is phosphorylated by PINK1 to activate parkin. *Nature*, *510*(7503), 162–166.

Kravtsova-Ivantsiv, Y., Cohen, S., & Ciechanover, A. (2010). Modification by Single Ubiquitin Moieties Rather Than Polyubiquitination Is Sufficient for Proteasomal Processing of the p105 NF-κB Precursor. *Adv Exp Med Biol*, *691*, 95-106.

Kubbutat, M., Jones, S., & Vousden, K. (1997). Regulation of p53 stability by Mdm2. *Nature*, *387*(6630), 299–303.

Lan, X., Atanassov, B. S., Li, W., Zhang, Y., Florens, L., Mohan, R. D., … Dent, S. Y. R. (2016). USP44 Is an Integral Component of N-CoR that Contributes to Gene Repression by Deubiquitinating Histone H2B. *Cell Reports*, *17*(9), 2382–2393.

Landré, V., Pion, E., Narayan, V., Xirodimas, D. P., & Ball, K. L. (2013). DNA-binding regulates site-specific ubiquitination of IRF-1. *The Biochemical Journal*, *449*(3), 707–17.

Latinkić, B. V., & Lau, L. F. (1994). Transcriptional activation of the immediate early gene pip92 by serum growth factors requires both Ets and CArG-like elements. *Journal of Biological Chemistry*, *269*(37), 23163–23170.

Lawrence, T. (2009). The nuclear factor NF-kappaB pathway in inflammation. *Cold Spring Harbor Perspectives in Biology*, *1*(6), a001651.

Lazarou, M., Sliter, D. A., Kane, L. A., Sarraf, S. A., Wang, C., Burman, J. L., … Youle, R. J. (2015). The ubiquitin kinase PINK1 recruits autophagy receptors to induce mitophagy. *Nature*, *524*(7565), 309–314.

Lee, B., Lee, M. J., Park, S., Oh, D., Elsasser, S., Chen, P., … Finley, D. (2010). Enhancement of Proteasome Activity by a Small-Molecule Inhibitor of Usp14, *467*(7312), 179–184.

Leevers, S. J., & Marshall, C. J. (1992). Activation of extracellular signal-regulated kinase, ERK2, by p21ras oncoprotein. *The EMBO Journal*, *11*(2), 569–74.

Leggett, D. S., Hanna, J., Borodovsky, A., Crosas, B., Schmidt, M., Baker, R. T., … Finley, D. (2002). Multiple associated proteins regulate proteasome structure and function. *Molecular Cell*, *10*(3), 495–507.

Leissner, P., Verjat, T., Bachelot, T., Paye, M., Krause, A., Puisieux, A., & Mougin, B. (2006). Prognostic significance of urokinase plasminogen

activator and plasminogen activator inhibitor-1 mRNA expression in lymph node- and hormone receptor-positive breast cancer. *BMC Cancer*, *6*, 216.

Lemon, B., & Tjian, R. (2000). Orchestrated response: A symphony of transcription factors for gene control. *Genes and Development*, *14*(20), 2551–2569.

Leprince, D., Gegonne, A., Coll, J., de Taisne, C., Schneeberger, A., Lagrou, C., & Stehelin, D. (1983). A putative second cell-derived oncogene of the avian leukaemia retrovirus E26. *Nature*, *306*(5941), 395–397.

Li, B., Hu, Q., Xu, R., Ren, H., Fei, E., Chen, D., & Wang, G. (2012). Hax-1 is rapidly degraded by the proteasome dependent on its PEST sequence. *BMC Cell Biology*, *13*(1), 20.

Li, M., Brooks, C. L., Wu-Baer, F., Chen, D., Baer, R., & Gu, W. (2003). Mono- versus polyubiquitination: differential control of p53 fate by Mdm2. *Science*, *302*(5652), 1972–5.

Li, Q. J., Yang, S. H., Maeda, Y., Sladek, F. M., Sharrocks, A. D., & Martins-Green, M. (2003). MAP kinase phosphorylation-dependent activation of Elk-1 leads to activation of the co-activator p300. *EMBO Journal*, *22*(2), 281–291.

Lidke, D. S., Huang, F., Post, J. N., Rieger, B., Wilsbacher, J., Thomas, J. L., … Lenormand, P. (2010). ERK nuclear translocation is dimerization-independent but controlled by the rate of phosphorylation. *Journal of Biological Chemistry*, *285*(5), 3092–3102.

Lilienbaum, A. (2013). Relationship between the proteasomal system and autophagy. *International Journal of Biochemistry and Molecular Biology*, *4*(1), 1–26.

Lin, S., Chung, L., Lamoth, B., Rajashankar, K., Lu, M., Lo, Y., … Wu, H. (2008). Molecular Basis for the Unique De-ubiquitinating Activity of the NF-κB Inhibitor A20, *376*(2), 526–540.

Lin, Z., Yang, H., Kong, Q., Li, J., Lee, S. M., Gao, B., … Fang, D. (2012). USP22 Antagonizes p53 Transcriptional Activation by Deubiquitinating Sirt1 to Suppress Cell Apoptosis and Is Required for Mouse Embryonic Development. *Molecular Cell*, *46*(4), 484–494.

Ling, Y., Lakey, J. H., Roberts, C. E., & Sharrocks, A. D. (1997). Molecular characterization of the B-box protein-protein interaction motif of the ETS-domain transcription factor Elk-1. *EMBO Journal*, *16*(9), 2431–2440.

Ling, Y., West, A. G., Roberts, E. C., Lakey, J. H., & Sharrocks, A. D. (1998). Interaction of Transcription Factors with Serum Response Factor, *273*(17), 10506–10514.

Lipford, J. R., Smith, G. T., Chi, Y., & Deshaies, R. J. (2005). A putative stimulatory role for activator turnover in gene expression. *Nature*, *438*(7064), 113–6.

Liu, T., Yu, J., Deng, M., Yin, Y., Zhang, H., Luo, K., … Lou, Z. (2017). CDK4/6-dependent activation of DUB3 regulates cancer metastasis through SNAIL1. *Nature Communications*, *8*, 13923.

Livneh, I., Kravtsova-Ivantsiv, Y., Braten, O., Kwon, Y. T., & Ciechanover, A. (2017). Monoubiquitination joins polyubiquitination as an esteemed proteasomal targeting signal. *BioEssays*, *39*(6), 1–7.

Low, T., & Goldstein, A. (1979). The Chemistry and Biology of Thermolysin, *254*(3), 987–995.

Lu, S., Nie, J., Luan, Q., Feng, Q., Xiao, Q., Chang, Z., … Yang, Z. (2011). Phosphorylation of the twist1-family basic helix-loop-helix transcription factors is involved in pathological cardiac remodeling. *PLoS ONE*, *6*(4).

MacKichan, M. L., Logeat, F., & Israel, A. (1996). Phosphorylation of p105 PEST Sequences via a Redox-insensitive Pathway Up-regulates Processing to p50 NF-kappaB. *Journal of Biological Chemistry*, *271*(11), 6084–6091.

Mahmoodzadeh, S., Dworatzek, E., Fritschka, S., Pham, T. H., & Regitz-Zagrosek, V. (2010). 17β-Estradiol inhibits matrix metalloproteinase-2 transcription via MAP kinase in fibroblasts. *Cardiovascular Research*, *85*(4), 719–728.

Marais, R., Wynne, J., & Treisman, R. (1993). The SRF accessory protein Elk-1 contains a growth factor-regulated transcriptional activation domain. *Cell*, *73*(2), 381–93.

Marchenko, N. D., Wolff, S., Erster, S., Becker, K., & Moll, U. M. (2007). Monoubiquitylation promotes mitochondrial p53 translocation. *The EMBO Journal*, *26*(4), 923–934.

Margolis, B., & Skolnik, E. Y. (1994). Activation of Ras by receptor tyrosine kinases. *Journal of the American Society of Nephrology : JASN*, *5*(6), 1288–1299.

Masutani, H., Magnaghi-Jaulin, L., Ait-Si-Ali, S., Groisman, R., Robin, P., & Harel-Bellan, A. (1997). Activation of the c-fos SRE through SAP-1a. *Oncogene*, *15*(14), 1661–1669.

Matsuda, N. (2016). Phospho-ubiquitin: Upending the PINK-Parkin-ubiquitin cascade. *Journal of Biochemistry*, *159*(4), 379–385.

McFadden, D. G. (2004). The Hand1 and Hand2 transcription factors regulate expansion of the embryonic cardiac ventricles in a gene dosage-dependent manner. *Development*, *132*(1), 189–201.

McFarlane, C., Kelvin, A. A., De La Vega, M., Govender, U., Scott, C. J., Burrows, J. F., & Johnston, J. A. (2010). The deubiquitinating enzyme USP17 is highly expressed in tumor biopsies, is cell cycle regulated, and is required for G1-S progression. *Cancer Research*, *70*(8), 3329–3339.

McFarlane, C., McFarlane, S., Paul, I., Arthur, K., Scheaff, M., Kerr, K., … Johnston, J. A. (2013). The deubiquitinating enzyme USP17 is associated with non-small cell lung cancer (NSCLC) recurrence and metastasis. *Oncotarget*, *4*(10), 1836–43.

Mehić, M., de Sa, V. K., Hebestreit, S., Heldin, C.-H., & Heldin, P. (2017). The deubiquitinating enzymes USP4 and USP17 target hyaluronan synthase 2 and differentially affect its function. *Oncogenesis*, *6*(6), e348.

Meloche, S., Seuwen, K., Pagès, G., & Pouysségur, J. (1992). Biphasic and synergistic activation of p44mapk (ERK1) by growth factors: correlation between late phase activation and mitogenicity. *Molecular Endocrinology*, *6*(5), 845–54.

Metzger, M. B., Hristova, V. a, & Weissman, A. M. (2012). HECT and RING finger families of E3 ubiquitin ligases at a glance. *Journal of Cell Science*, *125*(Pt 3), 531–7.

Meulmeester, E., Maurice, M. M., Boutell, C., Teunisse, A. F. A. S., Ovaa, H.,

Abraham, T. E., … Jochemsen, A. G. (2005). Loss of HAUSP-mediated deubiquitination contributes to DNA damage-induced destabilization of Hdmx and Hdm2. *Molecular Cell*, *18*(5), 565–576.

Meyer, H., & Rape, M. (2014). Enhanced protein degradation by branched ubiquitin chains. *Cell*, *157*(4), 910–21.

Meyer, R. D., Srinivasan, S., Singh, A. J., Mahoney, J. E., Gharahassanlou, K. R., & Rahimi, N. (2011). PEST Motif Serine and Tyrosine Phosphorylation Controls Vascular Endothelial Growth Factor Receptor 2 Stability and Downregulation. *Molecular and Cellular Biology*, *31*(10), 2010–2025.

Minty, A., & Kedes, L. (1986). Upstream regions of the human cardiac actin gene that modulate its transcription in muscle cells: presence of an evolutionarily conserved repeated motif. *Molecular and Cellular Biology*, *6*(6), 2125–2136.

Miyamotot, S., Makit, M., Schmittt, M. J., & Vermat, I. M. (1994). Tumor necrosis factor a-induced phosphorylation of IKBa is a signal for its degradation but not dissociation from NF-KB, *91*, 12740–12744.

Mo, Y., Vaessen, B., & Johnston, K. (2000). Structure of the Elk-1 – DNA complex reveals how DNA- distal residues affect ETS domain recognition of DNA. *Nature Structural Biology*, *7*(4), 3–8.

Mo, Y., Vaessen, B., Johnston, K., & Marmorstein, R. (1998). Structures of SAP-1 bound to DNA targets from the E74 and c-fos promoters: insights into DNA sequence discrimination by Ets proteins. *Molecular Cell*, *2*(2), 201–212.

Mosmann, T. (1983). Rapid colorimetric assay for cellular growth and survival: Application to proliferation and cytotoxicity assays. *J Immunol Methods*, *65*, 55–63.

Motegi, A., Liaw, H.-J., Lee, K.-Y., Roest, H. P., Maas, A., Wu, X., … Myung, K. (2008). Polyubiquitination of proliferating cell nuclear antigen by HLTF and SHPRH prevents genomic instability from stalled replication forks. *Proceedings of the National Academy of Sciences of the United States of America*, *105*(34), 12411–12416.

Muddasani, P., Norman, J. C., Ellman, M., Van Wijnen, A. J., & Im, H. J. (2007). Basic fibroblast growth factor activates the MAPK and NFκB pathways that converge on Elk-1 to control production of matrix metalloproteinase-13 by human adult articular chondrocytes. *Journal of Biological Chemistry*, *282*(43), 31409–31421.

Mueller, C. G., & Nordheim, a. (1991). A protein domain conserved between yeast MCM1 and human SRF directs ternary complex formation. *The EMBO Journal*, *10*(13), 4219–4229.

Müller, R., Bravo, R., Burckhardt, J., & Curran, T. (1984). Induction of c-fos gene and protein by growth factors precedes activation of c-myc. *Nature*, *312*(5996), 716–20.

Muratani, M., & Tansey, W. P. (2003). How the ubiquitin-proteasome system controls transcription. *Nature Reviews. Molecular Cell Biology*, *4*(3), 192–201.

Mylona, A., Theillet, F.-X., Foster, C., Cheng, T. M., Miralles, F., Bates, P. A., … Treisman, R. (2016). Opposing effects of Elk-1 multisite phosphorylation shape its response to ERK activation. *Science*, *354*(6309),

233–237.
Narayan, V., Pion, E., Landré, V., Müller, P., & Ball, K. L. (2011). Docking-dependent ubiquitination of the interferon regulatory factor-1 tumor suppressor protein by the ubiquitin ligase CHIP. *The Journal of Biological Chemistry*, *286*(1), 607–19.
Nentwich, O., Dingwell, K. S., Nordheim, A., & Smith, J. C. (2009). Downstream of FGF during mesoderm formation in Xenopus: The roles of Elk-1 and Egr-1. *Developmental Biology*, *336*(2), 313–326.
Nguyen, A., Burack, W. R., Stock, J. L., Kortum, R., Chaika, O. V, Afkarian, M., … Shaw, A. S. (2002). Kinase suppressor of Ras (KSR) is a scaffold which facilitates mitogen-activated protein kinase activation in vivo. *Molecular and Cellular Biology*, *22*(9), 3035–45.
Nguyen, H. T., Kugler, J. M., & Cohen, S. M. (2017). DUB3 deubiquitylating enzymes regulate Hippo pathway activity by regulating the stability of ITCH, LATS and AMOT proteins. *PLoS ONE*, *12*(1), 1–15.
Ni, Y., Tao, L., Chen, C., Song, H., Li, Z., Gao, Y., … Li, B. (2015). The deubiquitinase USP17 regulates the stability and nuclear function of IL-33. *International Journal of Molecular Sciences*, *16*(11), 27956–27966.
Nielsen, M. L., Vermeulen, M., Bonaldi, T., Cox, J., Moroder, L., & Mann, M. (2008). Iodoacetamide-induced artifact mimics ubiquitination in mass spectrometry. *Nature Methods*, *5*(6), 459–460.
Nilsson, J., Yekezare, M., Minshull, J., & Pines, J. (2008). The APC/C maintains the spindle assembly checkpoint by targeting Cdc20 for destruction. *Nat Cell Biol*, *10*(12), 1411–1420.
Nissen, L. J., Gelly, J. C., & Hipskind, R. A. (2001). Induction-independent Recruitment of CREB-binding Protein to the c-fos Serum Response Element through Interactions between the Bromodomain and Elk-1. *Journal of Biological Chemistry*, *276*(7), 5213–5221.
Nolan, G. P., Ghosh, S., Tempst, P., & Baltimore, D. (1991). DNA binding and IKB Inhibition of the Cloned p65 Subunit of NF-KB , a rel-related pepetide. *Cell*, *64*, 961–969.
Norman, C., Runswick, M., Pollock, R., & Treisman, R. (1988). Isolation and properties of cDNA clones encoding SRF, a transcription factor that binds to the c-fos serum response element. *Cell*, *55*(6), 989–1003.
Nunn, M., Seeburg, P. H., Moscovici, C., & H., D. P. (1983). Tripartite structure of the avian erythroblastosis virus E26 transforming gene. *Nature*, *306*, 391–395.
Ohtake, F., Saeki, Y., Sakamoto, K., Ohtake, K., Nishikawa, H., Tsuchiya, H., … Kanno, J. (2015). Ubiquitin acetylation inhibits polyubiquitin chain elongation. *EMBO Reports*, *16*(2), 192–201.
Okada, T., Gondo, Y., Goto, J., Kanazawa, I., Hadano, S., & Ikeda, J. E. (2002). Unstable transmission of the RS447 human megasatellite tandem repetitive sequence that contains the USP17 deubiquitinating enzyme gene. *Human Genetics*, *110*(4), 302–313.
Olsen, J. V, & Mann, M. (2013). Status of large-scale analysis of post-translational modifications by mass spectrometry. *Molecular & Cellular Proteomics : MCP*, *12*(12), 3444–52.
Otto, J. C., Kim, E., Young, S. G., & Casey, P. J. (1999). Cloning and

Characterization of a Mammalian Prenyl protein-specific protease. *The Journal of Biological Chemistry*, 8379–8382.

Palombella, V. J., Rando, O. J., Goldberg, A. L., & Maniatis, T. (1994). The Ubiquitin-Proteasome Pathway Is Required for Processing the NF-KB1 Precursor Protein and the Activation of NF-KB. *Cell*, *78*, 773–785.

Pan, H., Sheng, J. Z., Tang, L., Zhu, R., Zhou, T. H., & Huang, H. F. (2008). Increased expression of c-fos protein associated with increased matrix metalloproteinase-9 protein expression in the endometrium of endometriotic patients. *Fertility and Sterility*, *90*(4), 1000–1007.

Pankiv, S., Clausen, T. H., Lamark, T., Brech, A., Bruun, J. A., Outzen, H., … Johansen, T. (2007). p62/SQSTM1 binds directly to Atg8/LC3 to facilitate degradation of ubiquitinated protein aggregates by autophagy. *Journal of Biological Chemistry*, *282*(33), 24131–24145.

Parker, J. L., & Ulrich, H. D. (2009). Mechanistic analysis of PCNA poly-ubiquitylation by the ubiquitin protein ligases Rad18 and Rad5. *The EMBO Journal*, *28*(23), 3657–3666.

Patki, M., Chari, V., Sivakumaran, S., Gonit, M., Trumbly, R., & Ratnam, M. (2013). The ETS domain transcription factor ELK1 directs a critical component of growth signaling by the androgen receptor in prostate cancer cells. *Journal of Biological Chemistry*, *288*(16), 11047–11065.

Paulson, M., Pisharody, S., Pan, L., Guadagno, S., Mui, A. L., David, E., & Levy, D. E. (1999). Stat Protein Transactivation Domains Recruit p300 / CBP through Widely Divergent Sequences Stat Protein Transactivation Domains Recruit p300 / CBP through Widely Divergent Sequences, *274*(36), 25343–25349.

Pereg, Y., Liu, B. Y., O'Rourke, K. M., Sagolla, M., Dey, A., Komuves, L., … Dixit, V. M. (2010). Ubiquitin hydrolase Dub3 promotes oncogenic transformation by stabilizing Cdc25A. *Nature Cell Biology*, *12*(4), 400–406.

Pfander, B., Moldovan, G.-L., Sacher, M., Hoege, C., & Jentsch, S. (2005). SUMO-modified PCNA recruits Srs2 to prevent recombination during S phase. *Nature*, *436*(July), 17–22.

Pickart, C. M., & Eddins, M. J. (2004). Ubiquitin: structures, functions, mechanisms. *Biochimica et Biophysica Acta*, *1695*(1–3), 55–72.

Potu, H., Peterson, L. F., Kandarpa, M., Pal, A., Sun, H., Durham, A., … Donato, N. J. (2017). Usp9x regulates Ets-1 ubiquitination and stability to control NRAS expression and tumorigenicity in melanoma. *Nature Communications*, *8*, 14449.

Price, M. A., Rogers, A. E., & Treisman, R. (1995). Comparative analysis of the ternary complex factors Elk-1, SAP-1a and SAP-2 (ERP/NET). *The EMBO Journal*, *14*(11), 2589–601.

Raasi, S., & Pickart, C. M. (2003). Rad23 ubiquitin-associated domains (UBA) inhibit 26 S proteasome-catalyzed proteolysis by sequestering lysine 48-linked polyubiquitin chains. *Journal of Biological Chemistry*, *278*(11), 8951–8959.

Raingeaud, J., Whitmarsh, A. J., Barrett, T., Dérijard, B., & Davis, R. J. (1996). MKK3- and MKK6-regulated gene expression is mediated by the p38 mitogen-activated protein kinase signal transduction pathway. *Mol Cell*

Biol, *16*(3), 1247–1255.
Ramakrishna, S., Suresh, B., Lee, E. J., Lee, H. J., Ahn, W. S., & Baek, K. H. (2011). Lys-63-specific deubiquitination of SDS3 by USP17 regulates HDAC activity. *Journal of Biological Chemistry*, *286*(12), 10505–10514.
Rao, V. N., Huebner, K. A. Y., Isobe, M., Ar-rushdi, A., Croce, C. M., & Reddy, E. S. P. (1989). ELK, tissue-specific ets-related genes on chromosomes X and 14 near translocation breakpoints, *244*(4900), 66–70.
Rao, V. N., Papas, T. S., & Reddy, E. S. (1987). Erg, a Human Ets-Related Gene on Chromosome 21: Alternative Splicing, Polyadenylation, and Translation. *Science*, *237*(4815), 635–639.
Rechsteiner, M., & Rogers, S. W. (1996). PEST sequences and regulation by proteolysis. *Trends in Biochemical Sciences*, *21*(7), 267–271.
Reddy, E. S., Rao, V. N., & Papas, T. S. (1987). The erg gene : A human gene related to the ets oncogene. *Proceedings of the National Academy of Sciences of the United States of America*, *84*(17), 6131–6135.
Reits, E. a, Benham, a M., Plougastel, B., Neefjes, J., & Trowsdale, J. (1997). Dynamics of proteasome distribution in living cells. *The EMBO Journal*, *16*(20), 6087–94.
Reyes-Turcu, F. E., Horton, J. R., Mullally, J. E., Heroux, A., Cheng, X., & Wilkinson, K. D. (2006). The Ubiquitin Binding Domain ZnF UBP Recognizes the C-Terminal Diglycine Motif of Unanchored Ubiquitin. *Cell*, *124*(6), 1197–1208.
Rosati, R., Patki, M., Chari, V., Dakshnamurthy, S., McFall, T., Saxton, J., … Ratnam, M. (2016). The amino-terminal domain of the androgen receptor co-opts extracellular signal-regulated kinase (ERK) docking sites in ELK1 protein to induce sustained gene activation that supports prostate cancer cell growth. *Journal of Biological Chemistry*, *291*(50), 25983–25998.
Roskoski, R. (2012). MEK1/2 dual-specificity protein kinases: Structure and regulation. *Biochemical and Biophysical Research Communications*, *417*(1), 5–10.
Sadowski, I., Ma, J., Triezenberg, S., & Ptashne, M. (1988). GAL4-VP16 is an unusually potent transcriptional activator. *Nature*, *335*(6190), 563-4.
Saitoh, Y., Miyamoto, N., Okada, T., Gondo, Y., Showguchi-Miyata, J., Hadano, S., & Ikeda, J. E. (2000). The RS447 human megasatellite tandem repetitive sequence encodes a novel deubiquitinating enzyme with a functional promoter. *Genomics*, *67*(3), 291–300.
Salinas, S., Briançon-Marjollet, A., Bossis, G., Lopez, M.-A., Piechaczyk, M., Jariel-Encontre, I., … Hipskind, R. a. (2004). SUMOylation regulates nucleo-cytoplasmic shuttling of Elk-1. *The Journal of Cell Biology*, *165*(6), 767–73.
Sato, Y., Yoshikawa, A., Yamagata, A., Mimura, H., Yamashita, M., Ookata, K., … Fukai, S. (2008). Structural basis for specific cleavage of Lys 63-linked polyubiquitin chains. *Nature*, *455*(7211), 358–362.
Saxton, J., Ferjentsik, Z., Ducker, C., Johnson, A. D., & Shaw, P. E. (2016). Stepwise evolution of Elk-1 in early deuterostomes. *FEBS Journal*, *283*(6), 1025–1038.
Schlesinger, D. H., Goldstein, G., & Niall, H. D. (1975). The complete amino acid sequence of ubiquitin, an adenylate cyclase stimulating polypeptide

probably universal in living cells. *Biochemistry*, *14*(10), 2214–2218.
Schwarz-Sommer, Z., Huijser, P., Nacken, W., Saedler, H., & Sommer, H. (1990). Genetic Control of Flower Development by Homeotic Genes in Antirrhinum majus. *Science*, *250*(4983), 931–6.
Schwickart, M., Huang, X., Lill, J. R., Liu, J., Ferrando, R., French, D. M., … Dixit, V. M. (2010). Deubiquitinase USP9X stabilizes MCL1 and promotes tumour cell survival. *Nature*, *463*(7277), 103–7.
Scott, D., Oldham, N. J., Strachan, J., Searle, M. S., & Layfield, R. (2015). Ubiquitin-binding domains: Mechanisms of ubiquitin recognition and use as tools to investigate ubiquitin-modified proteomes. *Proteomics*, *15*(5–6), 844–861.
Sgambato, V., Pages, C., Rogard, M., Besson, M. J., & Caboche, J. (1998). Extracellular signal-regulated kinase (ERK) controls immediate early gene induction on corticostriatal stimulation. *J Neurosci*, *18*(21), 8814–8825.
Shao, N., Chai, Y., Cui, J. Q., Wang, N., Aysola, K., Reddy, E. S., & Rao, V. N. (1998). Induction of apoptosis by Elk-1 and deltaElk-1 proteins. *Oncogene*, *17*(4), 527–32.
Sharrocks, A. D. (1995). ERK2/p42 MAP kinase stimulates both autonomous and SRF-dependent DNA binding by Elk-1. *FEBS Letters*, *368*(1), 77–80.
Shaw, P. (1992). Ternary Complex-formation over the C-FOS serum response element - P62(TCF) exhibits dual component specificity with contacts to DNA and an extended structure in the DNA-binding domain of P67(SRF). *EMBO Journal*, *11*(8), 3011–3019.
Shaw, P. E., Schröter, H., & Nordheim, A. (1989). The ability of a ternary complex to form over the serum response element correlates with serum inducibility of the human c-fos promoter. *Cell*, *56*(4), 563–572.
Shi, D., Pop, M., Kulikov, R., Love, I., Kung, A., & Grossman, S. (2009). CBP and p300 are cytoplasmic E4 polyubiquitin ligases for p53. *PNAS*, *106*(40), 16275–16280.
Shin, J.-M., Yoo, K.-J., Kim, M.-S., Kim, D., & Baek, K.-H. (2006). Hyaluronan- and RNA-binding deubiquitinating enzymes of USP17 family members associated with cell viability. *BMC Genomics*, *7*, 292.
Shore, P., & Sharrocks, A. D. (1994). The Transcription Factors Elk-1 and Serum Response Factor Interact by Direct Protein-Protein Contacts Mediated by a Short Region of Elk-1, *14*(5), 3283–3291.
Shore, P., & Sharrocks, a D. (1995). The ETS-domain transcription factors Elk-1 and SAP-1 exhibit differential DNA binding specificities. *Nucleic Acids Research*, *23*(22), 4698–4706.
Shore, P., Whitmarsh, A. J., Bhaskaran, R., Davis, R. J., Waltho, J. P., & Sharrocks, A. D. (1996). Determinants of DNA-binding specificity of ETS-domain transcription factors. *Molecular and Cellular Biology*, *16*(7), 3338–49.
Smith, B. N., Burton, L. J., Henderson, V., Randle, D. D., Morton, D. J., Smith, B. A., … Odero-Marah, V. A. (2014). Snail promotes epithelial mesenchymal transition in breast cancer cells in part via activation of nuclear ERK2. *PLoS ONE*, *9*(8).
Song, C., Liu, W., & Li, J. (2017). USP17 is upregulated in osteosarcoma and promotes cell proliferation , metastasis , and epithelial – mesenchymal

transition through stabilizing SMAD4, (29).
Song, H., Tao, L., Chen, C., Pan, L., Hao, J., Ni, Y., … Shi, G. (2015). USP17-mediated deubiquitination and stabilization of HDAC2 in cigarette smoke extract-induced inflammation. *International Journal of Clinical and Experimental Pathology*, *8*(9), 10707–10715.
Spratt, D. E., Walden, H., & Shaw, G. S. (2014). RBR E3 ubiquitin ligases: new structures, new insights, new questions. *Biochemical Journal*, *458*(3), 421–437.
Stankovic-Valentin, N., Deltour, S., Seeler, J., Pinte, S., Vergoten, G., Guérardel, C., … Leprince, D. (2007). An acetylation/deacetylation-SUMOylation switch through a phylogenetically conserved psiKXEP motif in the tumor suppressor HIC1 regulates transcriptional repression activity. *Molecular and Cellular Biology*, *27*(7), 2661–75.
Stegmeier, F., Rape, M., Draviam, V. M., Nalepa, G., Sowa, M. E., Ang, X. L., … Elledge, S. J. (2007). Anaphase initiation is regulated by antagonistic ubiquitination and deubiquitination activities. *Nature*, *446*(7138), 876–881.
Stevens, J. L. (2002). Transcription Control by E1A and MAP Kinase Pathway via Sur2 Mediator Subunit. *Science*, *296*(5568), 755–758. https://doi.org/10.1126/science.1068943
Strachan, J., Roach, L., Sokratous, K., Tooth, D., Long, J., Garner, T. P., … Layfield, R. (2012). Insights into the Molecular Composition of Endogenous Unanchored Polyubiquitin Chains. *J Proteome Res*, *11*(3), 1969-80
Tarpey, P. S., Smith, R., Pleasance, E., Whibley, A., Edkins, S., Hardy, C., … Esch, H. Van. (2009). A systematic, large-scale resequencing screen of X-chromosome coding exons in mental retardation. *Nature Genetics*, *41*(5), 535–543.
Teixeira, F. R., Manfiolli, A. O., Soares, C. S., Baqui, M. M. a, Koide, T., & Gomes, M. D. (2013). The F-box protein FBXO25 promotes the proteasome-dependent degradation of ELK-1 protein. *The Journal of Biological Chemistry*, *288*(39), 28152–62.
Teixeira, F. R., Manfiolli, A. O., Vieira, N. A., Medeiros, A. C., Coelho, P. de O., Santiago Guimarães, D., … Gomes, M. D. (2017). FBXO25 regulates MAPK signaling pathway through inhibition of ERK1/2 phosphorylation. *Archives of Biochemistry and Biophysics*, *621*, 38–45.
Therrien, M., Chang, H. C., Solomon, N. M., Karim, F. D., Wassarman, D. a, & Rubin, G. M. (1995). KSR, a novel protein kinase required for RAS signal transduction. *Cell*, *83*(6), 879–888.
Thurston, T. L. M., Ryzhakov, G., Bloor, S., von Muhlinen, N., & Randow, F. (2009). The TBK1 adaptor and autophagy receptor NDP52 restricts the proliferation of ubiquitin-coated bacteria. *Nature Immunology*, *10*(11), 1215–1221.
Townsend, K. J., Zhou, P., Qian, L., Bieszczad, C. K., Lowrey, C. H., Yen, A., & Craig, R. W. (1999). Regulation of MCL1 through a serum response factor/elk-1-mediated mechanism links expression of a viability-promoting member of the BCL2 family to the induction of hematopoietic cell differentiation. *Journal of Biological Chemistry*, *274*(3), 1801–1813.
Treisman, R., Marais, R., & Wynne, J. (1992). Spatial flexibility in ternary

complexes between SRF and its accessory proteins. *The EMBO Journal*, *11*(12), 4631–40.

Ueda, Y., Hirai, S. I., Osada, S. I., Suzuki, A., Mizuno, K., & Ohno, S. (1996). Protein kinase C activates the MEK-ERK pathway in a manner independent of Ras and dependent on Raf. *Journal of Biological Chemistry*, *271*(38), 23512–23519.

Uht, R. M., Amos, S., Martin, P. M., Riggan, a E., & Hussaini, I. M. (2007). The protein kinase C-eta isoform induces proliferation in glioblastoma cell lines through an ERK/Elk-1 pathway. *Oncogene*, *26*(20), 2885–93.

Urness, L. D., & Thummel, C. S. (1990). Molecular interactions within the ecdysone regulatory hierarchy: DNA binding properties of the Drosophila ecdysone-inducible E74A protein. *Cell*, *63*(1), 47–61.

Valouev, A., Johnson, D. S., Sundquist, A., Medina, C., Anton, E., Batzoglou, S., … Sidow, A. (2008). Genome-wide analysis of transcription factor binding sites based on ChIP-Seq data. *Nature Methods*, *5*(9), 829–834.

vanderLaan, S., Tsanov, N., Crozet, C., & Maiorano, D. (2013). High Dub3 Expression in Mouse ESCs Couples the G1/S Checkpoint to Pluripotency. *Molecular Cell*, *52*(3), 366–379.

Vanhoutte, P., Nissen, J. L., Brugg, B., Gaspera, B. D., Besson, M. J., Hipskind, R. a, & Caboche, J. (2001). Opposing roles of Elk-1 and its brain-specific isoform, short Elk-1, in nerve growth factor-induced PC12 differentiation. *The Journal of Biological Chemistry*, *276*(7), 5189–96.

Varshavsky, A. (1991). Naming a targeting signal. *Cell*, *64*(1), 13–15.

Varshavsky, A. (2011). The N-end rule pathway and regulation by proteolysis. *Protein Science*, *20*(8), 1298–1345.

Verma, S., Dixit, R., & Pandey, K. C. (2016). Cysteine proteases: Modes of activation and future prospects as pharmacological targets. *Frontiers in Pharmacology*, *7*, 1–12.

Vickers, E. R., Kasza, A., Kurnaz, I. A., Seifert, A., Zeef, L. A. H., Donnell, A. O., … Sharrocks, A. D. (2004). Ternary Complex Factor-Serum Response Factor Complex-Regulated Gene Activity Is Required for Cellular Proliferation and Inhibition of Apoptotic Cell Death. *American Society for Microbiology*, *24*(23), 10340–10351.

Vijaykumar, S., Bugg, C., & Cook, W. (1987). Structure of Ubiquitin refined at 1.8 A resolution. *Journal of Molecular Biology*, *194*(3), 531–544.

Vitari, A. C., Leong, K. G., Newton, K., Yee, C., O'Rourke, K., Liu, J., … Dixit, V. M. (2011). COP1 is a tumour suppressor that causes degradation of ETS transcription factors. *Nature*, *474*(7351), 403–6.

Wan, M., Tang, Y., Tytler, E. M., Lu, C., Jin, B., Vickers, S. M., … Cao, X. (2004). Smad4 Protein Stability Is Regulated by Ubiquitin Ligase SCF β-TrCP1. *Journal of Biological Chemistry*, *279*(15), 14484–14487.

Wang, G., Balamotis, M. A., Stevens, J. L., Yamaguchi, Y., Handa, H., & Berk, A. J. (2005). Mediator requirement for both recruitment and postrecruitment steps in transcription initiation. *Molecular Cell*, *17*(5), 683–694.

Wang, S., Kollipara, R. K., Srivastava, N., Li, R., Ravindranathan, P., Hernandez, E., … Kittler, R. (2014). Ablation of the oncogenic transcription factor ERG by deubiquitinase inhibition in prostate cancer.

Proc Natl Acad Sci U S A, *111*(11), 4251–4256.
Wang, W., Huang, L., Huang, Y., Yin, J., Berk, A. J., Friedman, J. M., & Wang, G. (2009). Mediator MED23 links insulin signaling to the adipogenesis transcription cascade. *Developmental Cell*, *16*(5), 764–71.
Wang, W., Yao, X., Huang, Y., Hu, X., Liu, R., Hou, D., … Wang, G. (2013). Mediator MED23 regulates basal transcription in vivo via an interaction with P-TEFb. *Transcription*, *4*(1), 39–51.
Wang, X., Herr, R. A., Chua, W. J., Lybarger, L., Wiertz, E. J. H. J., & Hansen, T. H. (2007). Ubiquitination of serine, threonine, or lysine residues on the cytoplasmic tail can induce ERAD of MHC-I by viral E3 ligase mK3. *Journal of Cell Biology*, *177*(4), 613–624.
Wang, X., Herr, R. A., & Hansen, T. H. (2012). Ubiquitination of substrates by esterification. *Traffic*, *13*(1), 19–24.
Wang, Z., Bishop, E. P., & Burke, P. A. (2011). Expression profile analysis of the inflammatory response regulated by hepatocyte nuclear factor 4α. *BMC Genomics*, *12*(Il), 128.
Wang, Z., Wang, D., Hockemeyer, D., McAnally, J., Nordheim, A., & Olson, E. (2004). Myocardin and ternary complex factors compete for SRF to control smooth muscle gene expression. *Nature*, *428*, 185–189.
Watson, D. K., McWilliams-Smith, M. J., Nunn, M. F., Duesberg, P. H., O'Brien, S. J., & Papas, T. S. (1985). The ets sequence from the transforming gene of avian erythroblastosis virus, E26, has unique domains on human chromosomes 11 and 21: both loci are transcriptionally active. *Proceedings of the National Academy of Sciences of the United States of America*, *82*(21), 7294–8.
Watson, D. K., McWilliams, M. J., Lapis, P., Lautenberger, J. a, Schweinfest, C. W., & Papas, T. S. (1988). Mammalian ets-1 and ets-2 genes encode highly conserved proteins. *Proceedings of the National Academy of Sciences of the United States of America*, *85*, 7862–7866.
Weber, J. D., Raben, D. M., Phillips, P. J., & Baldassare, J. J. (1997). Sustained activation of extracellular-signal-regulated kinase 1 (ERK1) is required for the continued expression of cyclin D1 in G1 phase. *The Biochemical Journal*, *326 (Pt 1)*, 61–8.
Wellbrock, C., Karasarides, M., & Marais, R. (2004). The RAF proteins take centre stage. *Nature Reviews Molecular Cell Biology*, *5*(11), 875–885.
Wells, A. (1999). EGF receptor. *The International Journal of Biochemistry & Cell Biology*, *31*(6), 637–643.
Wertz, I. E., O'Rourke, K. M., Zhou, H., Eby, M., Aravind, L., Seshagiri, S., … Dixit, V. M. (2004). De-ubiquitination and ubiquitin ligase domains of A20 downregulate NF-κB signalling. *Nature*, *430*(7000), 694–699.
Whitmarsh, A. J., Shore, P., Sharrocks, A. D., & Davis, R. J. (1995). Integration of MAP kinase signal transduction pathways at the serum response element. *Science*, *269*(5222), 403–7.
Wild, P., Farhan, H., McEwan, D. G., Wagner, S., Rogov, V. V., Brady, N. R., … Dikic, I. (2011). Phosphorylation of the Autophagy Receptor Optineurin Restricts Salmonella Growth. *Science*, *333*(6039), 228–233.
Wilkinson, K. D., Tashayev, V. L., O'Connor, L. B., Larsen, C. N., Kasperek, E., & Pickart, C. M. (1995). Metabolism of the Polyubiquitin Degradation

Signal: Structure, Mechanism, and Role of Isopeptidase T. *Biochemistry*, *34*(44), 14535–14546.

Willems, A. R., Goh, T., Taylor, L., Chernushevich, I., Shevchenko, A., & Tyers, M. (1999). SCF ubiquitin protein ligases and phosphorylation-dependent proteolysis. *Philosophical Transactions of the Royal Society of London. Series B, Biological Sciences*, *354*(1389), 1533–50.

Woods, D., Parry, D., Cherwinski, H., Bosch, E., Lees, E., & McMahon, M. (1997). Raf-induced proliferation or cell cycle arrest is determined by the level of Raf activity with arrest mediated by p21Cip1. *Molecular and Cellular Biology*, *17*(9), 5598–611.

Wortzel, I., & Seger, R. (2011). The ERK Cascade: Distinct Functions within Various Subcellular Organelles. *Genes & Cancer*, *2*(3), 195–209.

Wu, X., Bayle, J. H., Olson, D., & Levine, a J. (1993). The p53-mdm-2 autoregulatory feedback loop. *Genes & Development*, *7*(7a), 1126–1132.

Wu, Y., Wang, Y., Lin, Y., Liu, Y., Wang, Y., Jia, J., … Zhou, B. P. (2017). Dub3 inhibition suppresses breast cancer invasion and metastasis by promoting Snail1 degradation. *Nature Communications*, *8*, 14228.

Wyrzykowska, P., Stalińska, K., Wawro, M., Kochan, J., & Kasza, A. (2010). Epidermal growth factor regulates PAI-1 expression via activation of the transcription factor Elk-1. *Biochimica et Biophysica Acta*, *1799*(9), 616–21.

Xiong, J., Wang, Y., Gong, Z., Liu, J., & Li, W. (2014). Identification of a functional nuclear localization signal within the human USP22 protein. *Biochemical and Biophysical Research Communications*, *449*(1), 14–18.

Xu, G., Paige, J., & Jaffrey, S. (2010). Global analysis of lysine ubiquitination by ubiquitin remnant immunoaffinty profiling. *Natural Biotechnology*, *28*(8), 868–873.

Xu, P., Duong, D. M., Seyfried, N. T., Cheng, D., Xie, Y., Robert, J., … Peng, J. (2009). Quantitative Proteomics Reveals the Function of Unconventional Ubiquitin Chains in Proteasomal Degradation. *Cell*, *137*(1), 133–145.

Yada, M., Hatakeyama, S., Kamura, T., Nishiyama, M., Tsunematsu, R., Imaki, H., … Nakayama, K. I. (2004). Phosphorylation-dependent degradation of c-Myc is mediated by the F-box protein Fbw7. *Embo Journal*, *23*(10), 2116–2125.

Yang, S.-H., Bumpass, D. C., Perkins, N. D., & Sharrocks, A. D. (2002). The ETS domain transcription factor Elk-1 contains a novel class of repression domain. *Molecular and Cellular Biology*, *22*(14), 5036–46.

Yang, S.-H., Jaffray, E., Hay, R. T., & Sharrocks, A. D. (2003). Dynamic interplay of the SUMO and ERK pathways in regulating Elk-1 transcriptional activity. *Molecular Cell*, *12*(1), 63–74.

Yang, S.-H., & Sharrocks, A. D. (2005). PIASx acts as an Elk-1 coactivator by facilitating derepression. *The EMBO Journal*, *24*(12), 2161–2171.

Yang, S. H., & Sharrocks, A. D. (2004). SUMO promotes HDAC-mediated transcriptional repression. *Molecular Cell*, *13*(4), 611–617.

Yang, S. H., Shore, P., Willingham, N., Lakey, J. H., & Sharrocks, A. D. (1999). The mechanism of phosphorylation-inducible activation of the ETS-domain transcription factor Elk-1. *EMBO Journal*, *18*(20), 5666–5674.

Yang, S. H., Vickers, E., Brehm, a, Kouzarides, T., & Sharrocks, a D. (2001).

Temporal recruitment of the mSin3A-histone deacetylase corepressor complex to the ETS domain transcription factor Elk-1. *Molecular and Cellular Biology*, *21*(8), 2802–14.

Yang, S. H., Yates, P. R., Whitmarsh, A. J., Davis, R. J., & Sharrocks, A. D. (1998A). The Elk-1 ETS-domain transcription factor contains a mitogen-activated protein kinase targeting motif. *Molecular and Cellular Biology*, *18*(2), 710–20.

Yang, S. H., Whitmarsh, A. J., Davis, R. J., & Sharrocks, A. D. (1998B). Differential targeting of MAP kinases to the ETS-domain transcription factor Elk-1. *EMBO Journal*, *17*(6), 1740–1749.

Yang, X., Zhao, M., Xia, M., Liu, Y., Yan, J., Ji, H., & Wang, G. (2012). Selective requirement for Mediator MED23 in Ras-active lung cancer. *Proceedings of the National Academy of Sciences*, *109*(41), E2813–E2822.

Ye, Y., Scheel, H., Hofmann, K., & Komander, D. (2009). Dissection of USP catalytic domains reveals five common insertion points. *Molecular bioSystems*, *5*, 1797–1808.

Zhang, C., Lu, J., Zhang, Q.-W., Zhao, W., Guo, J.-H., Liu, S.-L., … Gao, F.-H. (2016). USP7 promotes cell proliferation through the stabilization of Ki-67 protein in non-small cell lung cancer cells. *The International Journal of Biochemistry & Cell Biology*, *79*, 209–221.

Zhang, H. M., Li, L., Papadopoulou, N., Hodgson, G., Evans, E., Galbraith, M., … Shaw, P. E. (2008). Mitogen-induced recruitment of ERK and MSK to SRE promoter complexes by ternary complex factor Elk-1. *Nucleic Acids Research*, *36*(8), 2594–2607.

Zhang, P., Kong, F., Deng, X., Yu, Y., Hou, C., Liang, T., & Zhu, L. (2017). MicroRNA-326 suppresses the proliferation, migration and invasion of cervical cancer cells by targeting ELK1. *Oncology Letters*, 2949–2956.

Zhang, S., Yuan, J., & Zheng, R. (2016). Suppression of Ubiquitin-Specific Peptidase 17 (USP17) Inhibits Tumorigenesis and Invasion in Non-Small Cell Lung Cancer Cells, *24*(1158), 263–269.

Zhang, X., Varthi, M., Sykes, S., Phillips, C., Warzecha, C., Zhu, W., … McMahon, S. (2008). The putative cancer stem cell marker USP22 is a subunit of the human SAGA complex required for activator-driven transcription and cell cycle progression. *Molecular Cell*, *18*(29), 102–111.

Zhang, Y. (2003). Transcriptional regulation by histone ubiquitination and deubiquitination. *Genes & Development*, *17*(22), 2733–40.

Zhang, Y., van Deursen, J., & Galardy, P. J. (2011). Overexpression of ubiquitin specific protease 44 (USP44) induces chromosomal instability and is frequently observed in human T-Cell leukemia. *PLoS ONE*, *6*(8).

Zhao, J., Ou, B., Han, D., Wang, P., Zong, Y., Zhu, C., … Lu, A. (2017). Tumor-derived CXCL5 promotes human colorectal cancer metastasis through activation of the ERK/Elk-1/Snail and AKT/GSK3β/β-catenin pathways. *Molecular Cancer*, *16*(1), 70.

Zhao, Y., Lang, G., Ito, S., Bonnet, J., Metzger, E., Sawatsubashi, S., … Devys, D. (2008). A TFTC/STAGA Module Mediates Histone H2A and H2B Deubiquitination, Coactivates Nuclear Receptors, and Counteracts Heterochromatin Silencing. *Molecular Cell*, *29*(1), 92–101.

Zhou, L., Azfer, A., Niu, J., Graham, S., Choudhury, M., Adamski, F. M., …

Kolattukudy, P. E. (2006). Monocyte chemoattractant protein-1 induces a novel transcription factor that causes cardiac myocyte apoptosis and ventricular dysfunction. *Circulation Research*, *98*(9), 1177–85.

Zhou, Y., Romero-Campero, F. J., Gómez-Zambrano, Á., Turck, F., & Calonje, M. (2017). H2A monoubiquitination in Arabidopsis thaliana is generally independent of LHP1 and PRC2 activity. *Genome Biology*, *18*(1), 69.

Zhu, Q., Sharma, N., He, J., Wani, G., & Wani, A. A. (2015). USP7 deubiquitinase promotes ubiquitin-dependent DNA damage signaling by stabilizing RNF168. *Cell Cycle*, *14*(9), 1413–1425.

Zhu, Y., Lambert, K., Corless, C., Copeland, N. G., Gilbert, D. J., Jenkins, N. A., & D'Andrea, A. D. (1997). DUB-2 is a member of a novel family of cytokine-inducible deubiquitinating enzymes. *Journal of Biological Chemistry*, *272*(1), 51–57.

Zhu, Y., Pless, M., Inhorn, R., Mathey-Prevot, B., & D'Andrea, a D. (1996). The murine DUB-1 gene is specifically induced by the betac subunit of interleukin-3 receptor. *Molecular and Cellular Biology*, *16*(9), 4808–17.